

AD-A038 299

ILLINOIS UNIV AT URBANA-CHAMPAIGN DEPT OF ELECTRICAL --ETC F/G 17/2.1  
TECHNIQUES OF DETERMINING IONOSPHERIC STRUCTURE FROM OBLIQUE RA--ETC(U)  
DEC 76 N N RAO, K C YEH, M Y YOUAKIM

F19628-75-C-0088

UNCLASSIFIED

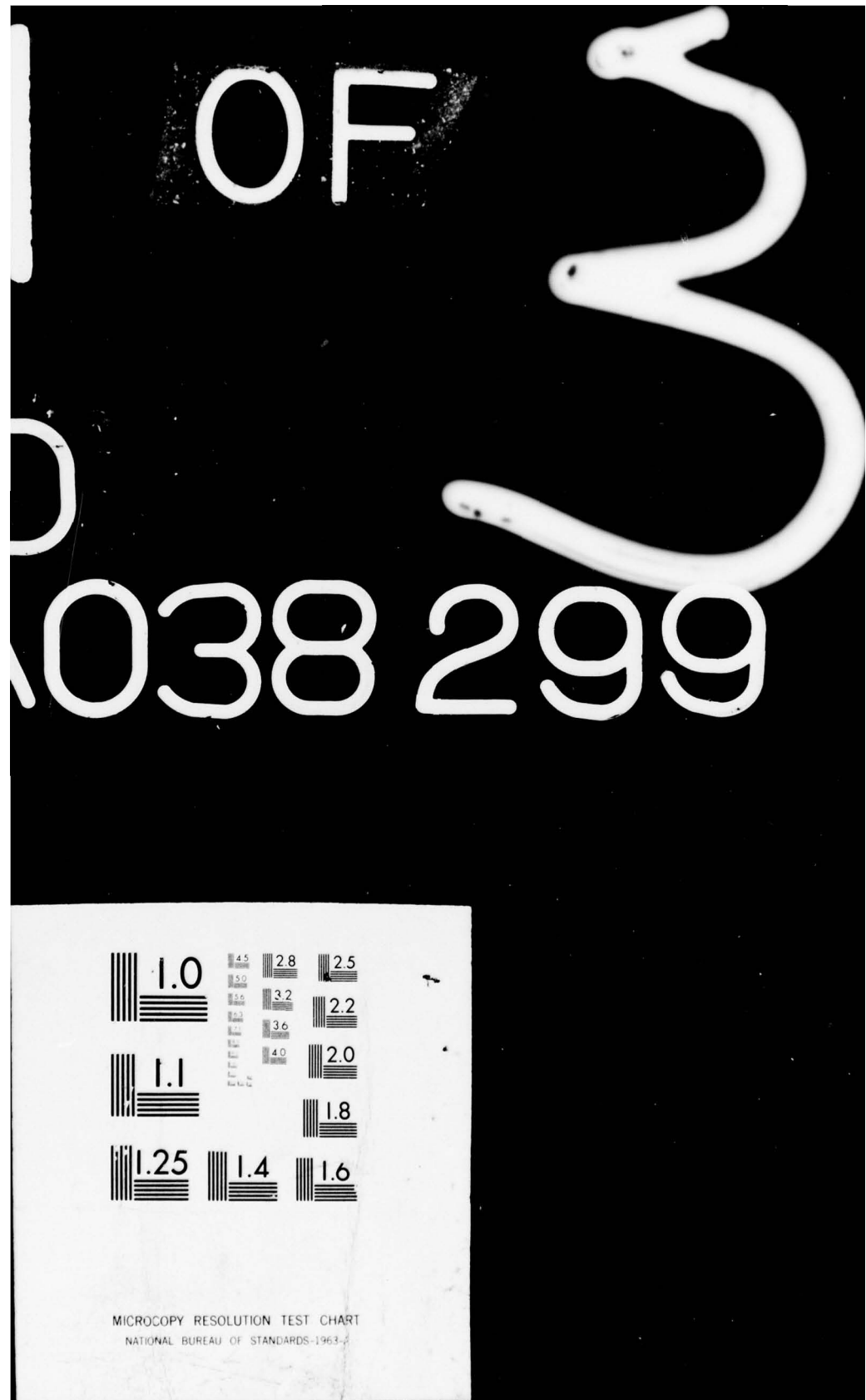
UILU-ENG-76-2559

RADC-TR-76-401

NL

1 OF 3  
AD  
A038 299





ADA 038299

RADC-TR-76-401  
Final Technical Report  
December 1976

12



TECHNIQUES OF DETERMINING IONOSPHERIC STRUCTURE  
FROM OBLIQUE RADIO PROPAGATION MEASUREMENTS

Ionosphere Radio Laboratory  
Department of Electrical Engineering  
University of Illinois at Urbana-Champaign

Approved for public release; distribution unlimited.

ROME AIR DEVELOPMENT CENTER  
AIR FORCE SYSTEMS COMMAND  
GRIFFISS AIR FORCE BASE, NEW YORK 13441

DDC FILE COPY  
No. \_\_\_\_\_  
DDC

AIR FORCE (1) MARCH 9, 1977--280

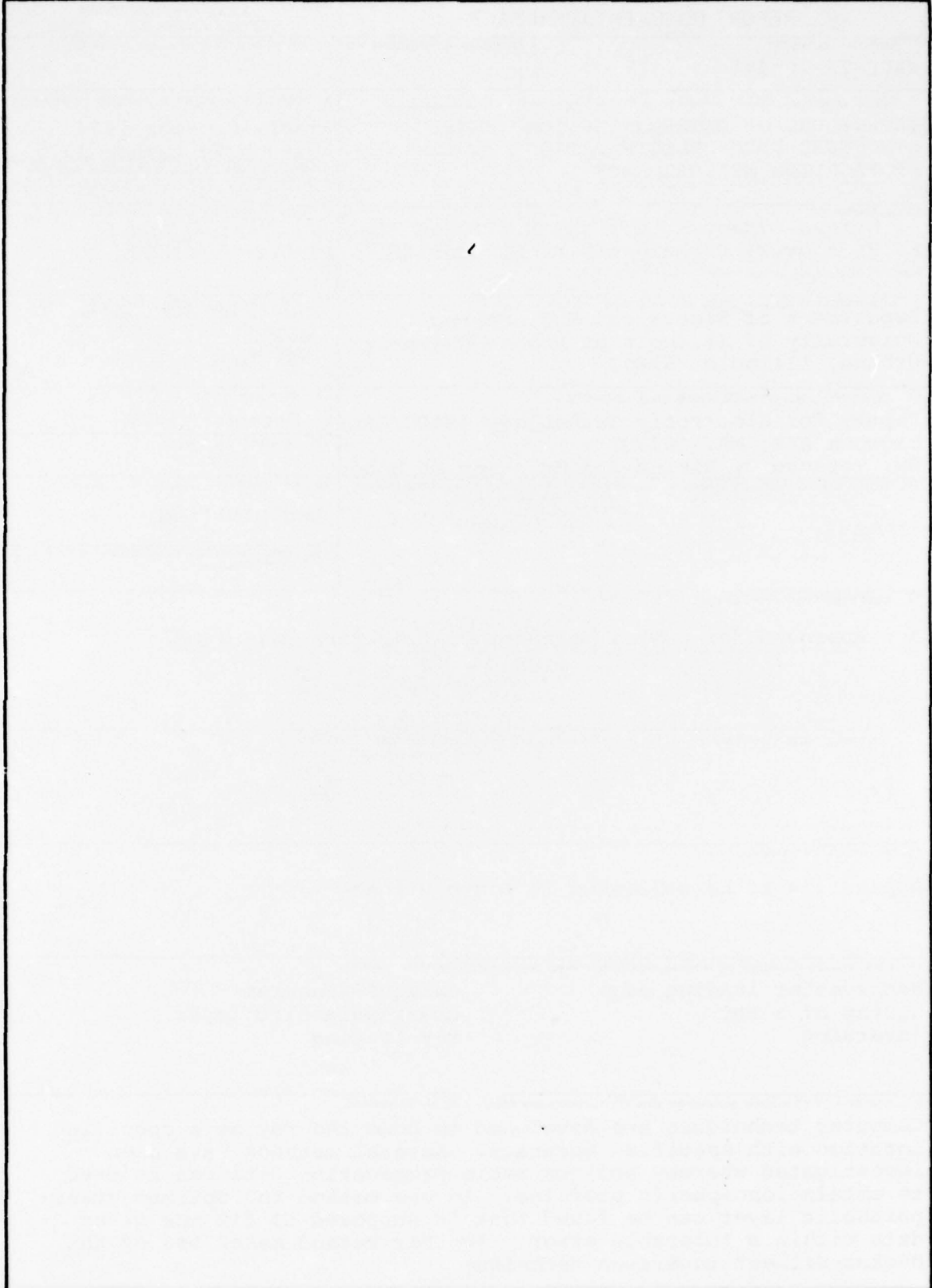
APR 15 1977  
REPRODUCED FOR  
THE USE OF THE  
U.S. AIR FORCE  
BY THE  
U.S. AIR FORCE  
LIBRARIES  
AND  
DOCUMENTATION  
CENTERS

Qualified requesters may obtain additional copies from  
the Defense Documentation Center. All others should  
apply to the National Technical Information Service.

Unclassified

**SECURITY CLASSIFICATION OF THIS PAGE (When Data Entered)**

SECURITY CLASSIFICATION OF THIS PAGE(When Data Entered)



SECURITY CLASSIFICATION OF THIS PAGE(When Data Entered)

## EVALUATION

F19628-75-C-0088 - University of Illinois

1. This report is the Final Report on this contract, covering two fiscal years work on the development of mathematical techniques for inversion of oblique ionograms.
  2. The work reported is significant from both scientific and applied viewpoints and represents a major contribution to the subject. The techniques developed can and will be applied to the propagation management of operational OTH radars and have other potential applications in HF radio propagation research and technology.

TERENCE J. ELKINS  
Contract Monitor  
Ionospheric Radio Physics Branch  
Electromagnetic Sciences Division

AC	1	1	1
ATIS	1	1	1
INFO	1	1	1
DEPARTURE	1	1	1
ARRIVAL	1	1	1
BY	1	1	1
DISTRIBUTION/AVAILABILITY	1	1	1
DIS.	1	1	1

A

## ACKNOWLEDGMENT

We would like to thank our contract monitors Dr. Terence J. Elkins and Mr. Ming S. Wong for providing us with the ray tracing program and the Air Force model ionosphere, based on which we have carried out our computations. The expert typing is the work of Mrs. Linda Houston.

The financial support of this work was provided by Rome Air Development Center, Deputy for Electronic Technology (ETEI), L G Hanscom Air Force Base, MA., under Contract F19628-75-C0088.

## TABLE OF CONTENTS

	Page
1. Introduction . . . . .	1
2. Homing of the Ray . . . . .	4
2.1 Introduction . . . . .	4
2.2 Ground-to-ground homing . . . . .	5
2.2.1 General description . . . . .	5
2.2.2 Approximate elevation angle - single layer ionosphere . . . . .	8
2.2.3 Approximate elevation angle - multiple layer ionosphere . . . . .	16
2.2.4 Refinement of the elevation angle . . . . .	17
2.2.5 Group path homing . . . . .	23
2.2.6 Examples and Discussion . . . . .	24
2.3 Ground-Satellite homing . . . . .	37
2.3.1 Approximate elevation angle . . . . .	37
2.3.2 Refinement of the elevation angle . . . . .	41
2.3.3 Examples and Discussion . . . . .	43
2.4 Minimum Group path . . . . .	49
2.4.1 Chopping technique . . . . .	49
2.4.2 Examples . . . . .	53
2.5 Computer programs . . . . .	55
2.5.1 General description . . . . .	55
2.5.2 Program listings . . . . .	65
2.6 Discussion . . . . .	66
3. Analysis of Oblique Propagation Data . . . . .	68
3.1 Introduction . . . . .	68
3.1.1 Point-to-point oblique ionograms . . . . .	68
3.1.2 Backscatter leading edge . . . . .	70
3.2 The Quasi-parabolic Layer . . . . .	73
3.2.1 The earth-concentric quasi-parabolic layer . . . . .	74
3.2.2 The eccentric quasi-parabolic layer . . . . .	76
3.3 Inversion of point-to-point oblique ionograms . . . . .	83
3.3.1 Sensitivity analysis . . . . .	83
3.3.2 Determination of initial set of parameters . . . . .	89
3.3.3 Inversion of synthesized oblique ionograms . . . . .	92
3.3.4 Inversion of experimental oblique ionograms . . . . .	102
3.4 Inversion of backscatter leading edge . . . . .	108
3.4.1 Basic inversion technique . . . . .	108
3.4.2 Inversion of synthesized QP layer data . . . . .	113
3.4.3 Inversion of synthesized data involving horizontal gradients . . . . .	118

## TABLE OF CONTENTS CONT.

	Page
3.4.4 Inversion of synthesized data for three-dimensional ionosphere. . . . .	127
3.4.5 Application of the backscatter inversion technique . . . . .	133
3.5 General consideration of the inversion problem. . . . .	155
3.6 Conclusions. . . . .	156
4. Recommendations for Future Work . . . . .	157
Appendix 1. . . . .	159
Appendix 2. . . . .	208
Appendix 3. . . . .	211
Appendix 4. . . . .	249
References. . . . .	265

## LIST OF FIGURES

Figure		Page
2.1	Idealized sketch showing the nature of ground distance dependence on the elevation angle of once reflected ray from a single layer ionosphere . . . . .	6
2.2	Sketch showing the geometry of the reflected ray. . . . .	9
2.3	Earth geometry for finding the coordinates of the midpoint. . . . .	10
2.4	Sketch showing the ground distance - elevation angle curve for a four-layer ionosphere . . . . .	18
2.5	Sketch illustrating the homing in azimuth. . .	22
2.6	Example 1 illustrating the ground-to-ground homing using the Air Force supplied model ionosphere. The example shows how the initial elevation is determined. . . . .	26
2.7	Continuation of the example shown in Fig. 2.6 This shows the refinement procedure in ground distance and azimuth homing using 3D ray tracing . . . . .	27
2.8	Example 2 illustrating the ground-to-ground homing for rays reflected from a two-layer ionosphere. Note that for a ground range of 1039.36 km, three approximate solutions (indicated by circle A, circle B and circle C) in the elevation angle exist in this case. .	29
2.9	Continuation of Example 2 shown in Fig. 2.8 illustrating the ground distance homing for circle A and circle C using 3D ray tracing. . .	31
2.10	Continuation of Example 2 illustrating azimuthal correction for final homing of the ray on the receiver . . . . .	32
2.11	Computed initial group path versus elevation angle curve for Example 3. For a specified group path of 2654.08 km two solutions are indicated . . . . .	33
2.12	Continuation of Example 3 illustrating group path homing for two rays. . . . .	35

Figure		Page
2.13	Sketch showing the geometry of ground-satellite homing. . . . .	38
2.14	Sketch showing the geometry of satellite-ground homing . . . . .	39
2.15	Earth geometry for finding the optical elevation angle . . . . .	42
2.16	Example illustrating ground-to-satellite homing. The plot shows ground distance between the transmitter and the sub-satellite point versus the elevation angle for successive iterations using 3D ray tracing at three frequencies 90 MHz, 170 MHz and 250 MHz . . . . .	44
2.17	Continuation of example shown in Fig. 2.16 illustrating that no azimuthal correction is needed for homing at all three frequencies. . . . .	46
2.18	Example illustrating satellite-to-ground homing for three radio frequencies 70 MHz, 140 MHz and 210 MHz. . . . .	47
2.19	Continuation of example shown in Fig. 2.18 illustrating that no azimuthal correction is needed for homing at all three frequencies. . . . .	48
2.20	Sketch showing the general behavior of group path versus elevation angle curve . .	51
2.21	Sketch illustrating three possibilities for purpose of finding the minimum group path ray. . . . .	52
2.22	Example illustrating the steps in finding the minimum group path ray in a group path versus elevation angle plot. Note the index shifting, equal chopping and final location of the minimum group path to within the tolerance . . . . .	56
2.23	Another example illustrating the steps in finding the minimum group path ray. . . . .	57
3.1a	Ray paths for point-to-point oblique ionograms at different frequencies. . . . .	69

Figure		Page
3.1b	Typical shape of one-hop trace for point-to-point oblique ionogram . . . . .	69
3.2a	Ray paths for backscattered rays at one frequency . . . . .	71
3.2b	Showing that the leading edge of a backscatter ionogram is the tangent curve to a continuum of point-to-point oblique ionograms . . . . .	71
3.3	The eccentric quasi-parabolic model with its defining parameters . . . . .	78
3.4	The geometry for computing gradients as a function of $\omega_t$ , D . . . . .	80
3.5	Peak height gradient as a function of D and $\omega_t$ . . . . .	82
3.6	Effect of the $f_c$ (critical frequency parameter (in MHz) . . . . .	84
3.7	Effect of changing $h_0$ ; the layer base-height (in km) . . . . .	85
3.8	Effect of changing the layer semi-thickness $y_m$ (in km) . . . . .	86
3.9	Effect of changing the D parameter (in km) . . .	87
3.10	Effect of varying the $\omega_t$ parameter (in degrees) . . . . .	88
3.11	Determining an initial set of parameters. . .	91
3.12	Inverting numerically synthesized data. . .	95
3.13	Synthesized oblique ionograms for Range=1111.7 km and $\omega_t = 0^\circ$ . The parameter D is successively changed by 500 km. For each D, the remaining three parameters are adjusted so as to force the curve through the three points marked by X. The parameters for the two extreme curves are given above . . . . .	96

Figure		Page
3.14	Technique for the inversion of real data. The first three data points are adjusted so that the technique in Section 3.3.3 can be employed for minimizing $(\Delta f_4)^2 +$ $(\Delta f_5)^2$ . . . . .	100
3.15	Method of steepest descent for inverting actual data . . . . .	103
3.16	Graphical illustration of the least sum- squared error method of backscatter iono- gram leading-edge inversion for a Q-P ionosphere. . . . .	110
3.17	Nominal electron density profile. . . . .	121
3.18	Reconstruction of ground range. . . . .	135
3.19	Limitations of information contained in data.	136
3.20	Interpolation procedure . . . . .	140
3.21	Block diagram of steps involved in backscatter leading edge inversion and application. . . .	141
A.3.1	Flow chart for main program . . . . .	233
A.3.2	Flow chart for subroutine FUNCT . . . . .	234
A.3.3.a	Flow chart for subroutine BACKS3 (continued next figure) . . . . .	235
A.3.3.b	Flow chart for subroutine BACKS3 (continuation of Fig. A.3.3.a) . . . . .	236
A.3.4.a	Flow chart for subroutine FSTDFS (continued on next figure) . . . . .	237
A.3.4.b	Flow chart for subroutine FSTDFS (continuation of Fig. A.3.4.a) . . . . .	238
A.3.5	Flow chart for subroutine DCAL. . . . .	239
A.3.6	Flow chart for special functions (square root, log, and $\cos^{-1}$ ) . . . . .	240
A.3.7	Sequence of data cards. . . . .	241

## LIST OF TABLES

Table		Page
3.1	Inversion of synthesized oblique ionograms using the technique in section 3.3.3 . . . . .	98
3.2	Inversion of real oblique ionograms, using the technique in section 3.3.3 . . . . .	101
3.3(a)	Inversion of an actual ionogram. . . . .	106
3.3(b)	Inversion of an actual ionogram. . . . .	107
3.4	Synthesized noisy backscatter ionogram leading edge data inversion assuming a spherical earth-concentric quasi-parabolic ionosphere model . . . . .	114
3.5	Noisy backscatter leading edge synthesis assuming earth-centered Q-P ionosphere $r_b = 6570$ km, $r_m = 6720$ km, and $f_c = 7.0$ MHz . . . . .	116
3.6	Results of Inversion of the data in Table 3.4, using various numbers of points in E. . . . . . . . . . .	117
3.7	Inversion of synthesized backscatter leading edge data for an eccentric quasiparabolic layer . . . . . . . . .	119
3.8	Group path (km) to leading edge of backscatter ionogram for various linear tilts and gradients. . . . . . . . . . .	122
3.9	Ground range (km). . . . . . . . . . .	123
3.10	Height of maximum plasma frequency ( $h_m F_2$ ) (kilometers) . . . . . . . . . . .	124
3.11	Base height of ionosphere (km) . . . . . . .	125
3.12	Critical frequency ( $f_o F_2$ ) (in MHz) . . . . .	126
3.13	Results of inversion of simulated backscatter ionogram data. . . . . . . . .	128
3.14	Computed minimum group path data and other propagation parameters for transmitter location of $40^\circ N$ , $175^\circ W$ , and $330^\circ$ azimuth. . . . .	130

Table	Page
3.15	Same as Table 3.14 except for 358° azimuth . . 131
3.16	Computed QP layer parameter values and the corresponding ground ranges for 330° azimuth . . . . . 132
3.17	Same as Table 3.16, except for 358° azimuth . . . . . 132
3.18	Group path and ground range versus elevation angle for 16 MHz and for 340° azimuth, using the originally assumed model . . . . . 137
3.19	Same as Table 3.18 except using computed ionosphere . . . . . 137
3.20	Same as Table 3.18 except using the simplified ionospheric model. . . . . 142
3.21	The effect of varying $r_b$ initial estimate upon inversion of group path into ground range (untilted ionosphere) . . . . . 144
3.22	The effect of varying the initial estimate of critical frequency upon inversion of group path into ground range (untilted ionosphere) . . . . . 146
3.23	The effect of varying layer semithickness upon inversion of group path to ground range (untilted ionosphere) . . . . . 147
3.24	The effect of the initial estimate of $r_b$ (radius to ionospheric base) upon the inversion of group path into ground range . . . . . 148
3.25	The effect of initial estimate of critical frequency ( $f_c$ ) upon inversion . . . . . 149
3.26	The effect of initial estimate of $r_m$ upon inversion of group path into ground range. Program was allowed to go 40 iterations in computing QPP . . . . . 150
3.27	The effect of varying the layer semithickness upon the inversion of group path to ground range . . . . . 151
3.28	The effect of initial estimate of $r_m$ upon inversion of group path into ground range. Program was allowed to go 80 iterations in fitting QPP. . . . . 153

Table	Page
3.29 Variance resulting from different values of $r_m$ as affected by iteration number . . . . .	154

## 1. INTRODUCTION

The use of pulse sounding as an experimental technique in the investigation of the ionosphere can be traced back to Breit and Tuve (1926). These authors invented such a technique to prove the existence of the ionosphere. Modern reviews of these early endeavors can be found in Waynick (1974) and Booker (1974). The improved electronic technology after the Second World War stimulated interest in the possibility of computing the electron density profiles from pulse sounding data whose carrier frequency was swept. While the major emphasis has been towards inverting the vertical sounding data for electron density profiles, there have also been sporadic attempts to devise techniques of obtaining ionospheric structure from oblique sounding data. Our work, reported here, is concerned with this later problem.

Mathematically, the group delay measured experimentally is a nonlinear functional of the electron density profile. As such this is very difficult to solve. Fortunately, for vertical incidence case with the geomagnetic field ignored, the integral can be cast in the form of a convolution integral known as Abel's integral equation which can then be solved, for example, by Laplace transform (Manning, 1947). Once the geomagnetic field effect is introduced or when the propagation path becomes oblique, the convolution integral property is destroyed. The problem becomes much more difficult. The methods that have been devised in the literature are almost all numerical. Ours is no exception. In this connection, the capability of homing the ray at a specified

location with specified tolerance must be established first. This is the subject of Chapter 2. In ray homing we are interested in three configurations: ground-to-ground homing via a reflection from the ionosphere, ground-to-satellite homing via transmission through the ionosphere and satellite-to-ground homing also via transmission through the ionosphere. In each case, the homing is achieved through an iterative procedure whereby the ray lands at a point successively closer to the given location. Several examples are also given to illustrate the method used. The inversion of backscatter ionograms utilizes the values of the minimum group path computed for a given ionospheric profile. It is therefore desirable to have the capability of computing the minimum group path. A chopping method is used to achieve this and two examples are given to illustrate the procedure involved. In order to achieve these capabilities, the Air Force supplied three-dimensional ray tracing program and the associated electron density model are augmented by seven subroutines. These subroutines are fully described and documented with computer listings.

The major objective of this research is to investigate methods whereby oblique radio propagation data can be used to obtain ionospheric profiles. This is contained in Chapter 3. There exist in practice two kinds of oblique propagation data: point-to-point oblique ionograms and backscatter leading edges. The nature of these data and their intuitive limitations are discussed in section 3.1. In many ionospheric propagation studies, the quasi-parabolic layer has been found to give adequate accuracy. Further, such a layer has a relatively small number of parameters (3, consisting of critical frequency, base

height of the ionosphere and the semi-thickness) and, in many cases, the desired expressions can be evaluated analytically. For this reason our inversion is based on finding the optimum quasi-parabolic layer that fits the given data within a tolerable error. After some discussion of the nature and properties of the quasi-parabolic layer in section 3.2, we go directly to the inversion problem. The inversion of a point-to-point oblique ionogram is discussed first (section 3.3), which is then followed by a discussion of backscatter leading edge (section 3.4). The results are given in terms of graphs and tables. In addition to approaches discussed in 3.3 and 3.4, we have also looked into the inversion problem from general considerations (section 3.5 and Appendix 4). This inversion method makes use of the Backus-Gilbert technique and seems to be very promising. Finally, the report is concluded in Chapter 4 with recommendations for future research.

## 2. HOMING OF THE RAY

### 2.1 Introduction

Homing of the ray is the main objective of this chapter. Our study deals with the modification of the three dimensional ray tracing program to incorporate the homing features for ground-to-ground, ground-to-satellite, and satellite-to-ground propagation.

Homing of the ray to the required location can be obtained through an iterative procedure by homing first to the ground distance for a fixed value of the azimuthal angle. If the ground distance homing is successful the azimuthal angle of the transmitted ray is then corrected next. This type of iteration requires back and forth transfer from homing in ground distance to homing in azimuthal angle. The iteration stops when the errors are smaller than the prescribed values.

For each of the three configurations studied we present a detailed development of the technique applied to achieve homing of the ray together with some examples. Difficulties encountered during the course of the study are also pointed out. In section 2.2 we discuss the ground-to-ground homing procedure for a single and multiple layer ionosphere. The ground-to-satellite and satellite-to-ground configurations together with examples to illustrate the homing technique are presented in section 2.3. In section 2.4 we discuss the chopping method utilized in finding the minimum group path for a given transmitter location, azimuthal angle, and oblique frequency. A listing of the computer programs developed under this study together with their description is included in section 2.5. Finally, in section 2.6 we discuss the current

accomplishments and outline suggestions towards future improvement and possible additions to the three dimensional ray tracing program.

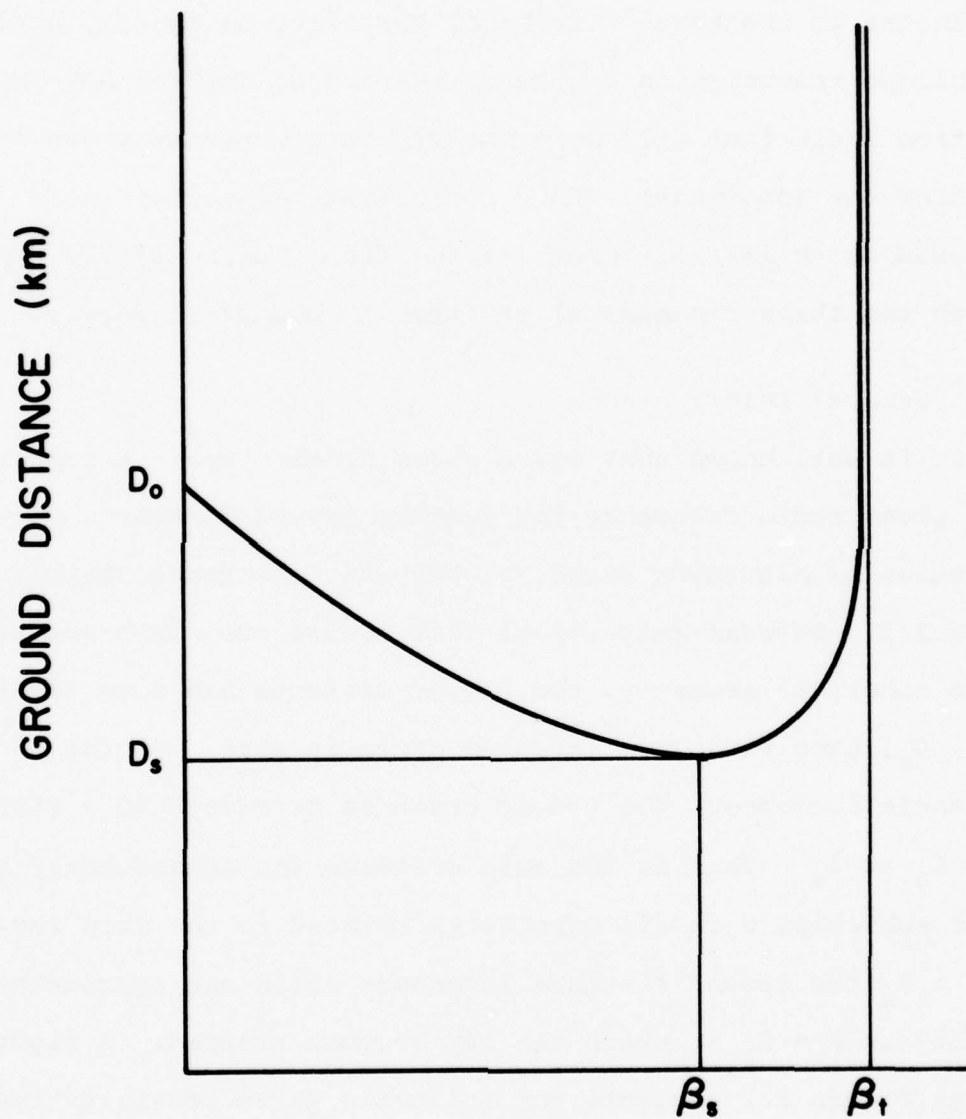
## 2.2 Ground-to-Ground Homing

The ground-to-ground homing is the most involved configuration of the homing study. Given the transmitter and receiver coordinates on the Earth's surface, the electron density profile, the oblique transmission frequency we find an initial approximate elevation angle that will home the ray to the receiver via reflection from the ionosphere. This approximate elevation angle is then used as an initial input for the final homing of the ray through the three dimensional ray tracing computer program.

### 2.2.1 General Description

It is well known that for a given single-layer ionosphere and a given radio frequency the one-hop ground distance,  $D$ , as a function of elevation angle,  $\beta$ , has the dependence sketched in Figure 2.1. Several features of this figure are worth noting. Due to spherical geometry, the ground distance has some finite value,  $D_0$ , even when the elevation angle is zero. As the elevation angle increases, the ground distance decreases to a minimum value  $D_s$  at  $\beta_s$ . This is the skip distance and consequently the use of subscript s on all quantities related to the skip ray. For  $\beta > \beta_s$  the ground distance increases again and approaches to infinity at  $\beta = \beta_t$  at which the ray becomes trapped. A figure such as Figure 2.1 suggests the following three possibilities:

- i) For  $D < D_s$  the observer is in the shadow region and no ray can reach the observer via reflection from the ionosphere.



### ELEVATION ANGLE (DEGREES)

Figure 2.1. Idealized sketch showing the nature of ground distance dependence on the elevation angle of once reflected ray from a single layer ionosphere.

- ii) For  $D_0 < D < D_s$  the observer is in the illuminated region within which a low ray and a high ray (Pedersen ray) can reach the observer.
- iii) For  $D > D_0$  the low ray is cut off by the earth shadow and only the high ray can reach the observer. Generally, the high ray with an elevation angle  $\beta$  near  $\beta_t$  is very much de-focussed and is very sensitive to elevation angles and small changes in the ionospheric model.

Based upon the above observations, we outline the procedure to obtain an approximate homing elevation angle. This approximate angle is then refined through utilization of the three dimensional ray tracing program.

The given ionosphere at the midpoint of the transmitter and receiver is approximated by segments of a second degree polynomial which for the  $i^{th}$  segment has the form

$$N_i(r) = a_i + \frac{b_i}{r} + \frac{c_i}{r^2} \quad r_{i-1} \leq r \leq r_i \quad (2.1)$$

The coefficients are chosen by fitting to the given ionospheric model and making sure that both the density and its derivatives are continuous in going from segment to segment. Using the electron density profile given by (2.1) we find analytic expressions for the ground distance (range)  $D$  and the virtual path (group path)  $P'$ . Since the trapped rays are known to have ray apogee slightly below the peak of the layer and since the high rays are very sensitive near  $\beta_t$  we let the ray apogee occur at the ionospheric peak as an approximation and find the penetration angle  $\beta_p$ . In general  $\beta_p$  so found is slightly less than  $\beta_t$ . Then, from the range

of elevation angles we calculate the corresponding ground distances and group paths through the analytical expressions, thus generating a table of elevation angles versus ground distance and group path. The ground distance between the transmitter and receiver is compared with the tabulated ground distances. If  $D < D_s$  there is no solution; if  $D = D_s$  there is possibly one solution; if  $D_s < D < D_o$  there are two solutions; and  $D > D_o$  there is one solution. The solutions, if they exist, are found by linear interpolation. Once the solutions are found, the approximate elevation angles serve as the initial input in the ray tracing program to eventually home the ray.

#### 2.2.2 Approximate Elevation Angle-Single Layer Ionosphere

The geometry of the ground-to-ground homing problem is shown in Figure 2.2. We assume that the transmitter and receiver coordinates are given in geographic east longitude and north latitude. The ground distance,  $D_{TR}$ , between the transmitter and receiver is given by

$$D_{TR} = r_0 \gamma \quad (2.2)$$

where  $r_0$  is the earth radius in km and  $\gamma$  is the angle subtended at the earth center between the transmitter and receiver. Applying the cosine law of spherical trigonometry to Figure 2.3, angle  $\gamma$  is

$$\gamma = \cos^{-1} [\cos \theta_T \cos \theta_R + \sin \theta_T \sin \theta_R \cos (\phi_T - \phi_R)] \quad (2.3)$$

where  $\theta_T$ ,  $\theta_R$  are the colatitudes,  $\phi_T$ ,  $\phi_R$  are the longitudes of

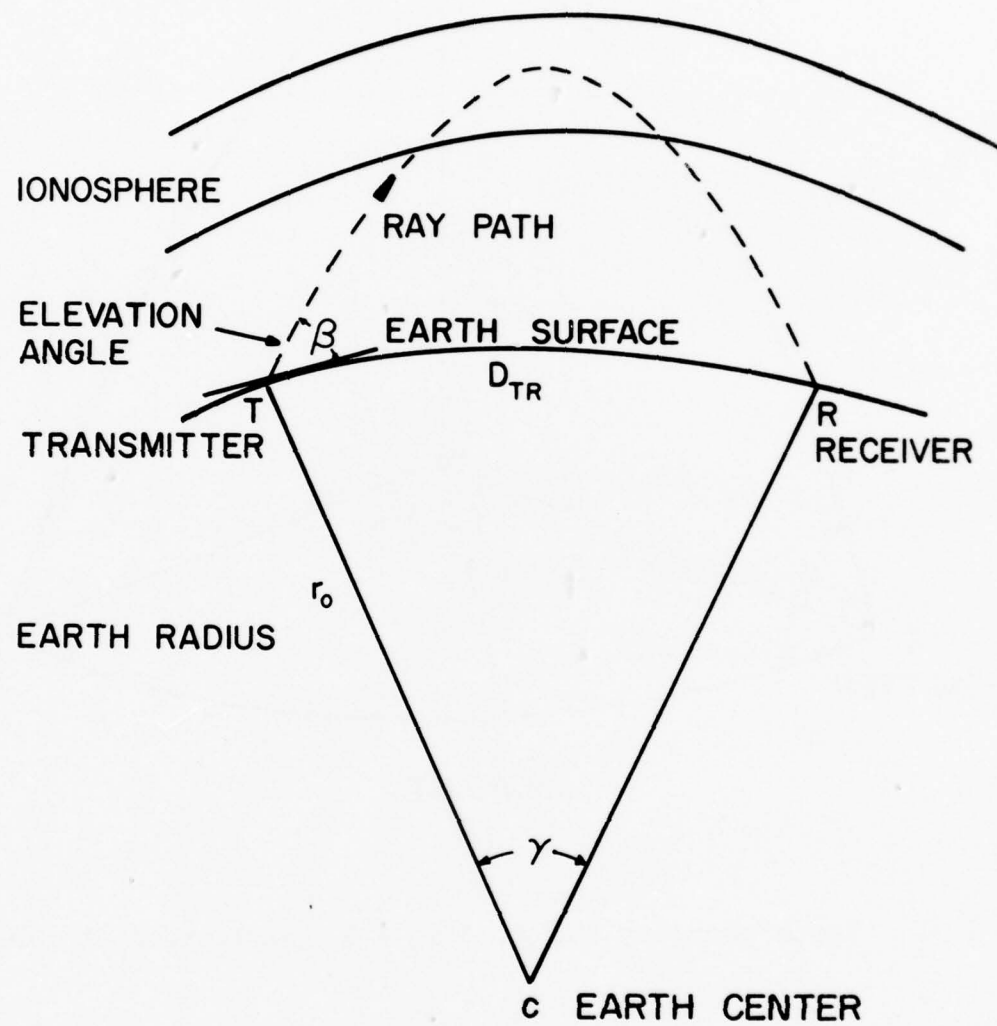


Figure 2.2. Sketch showing the geometry of the reflected ray.

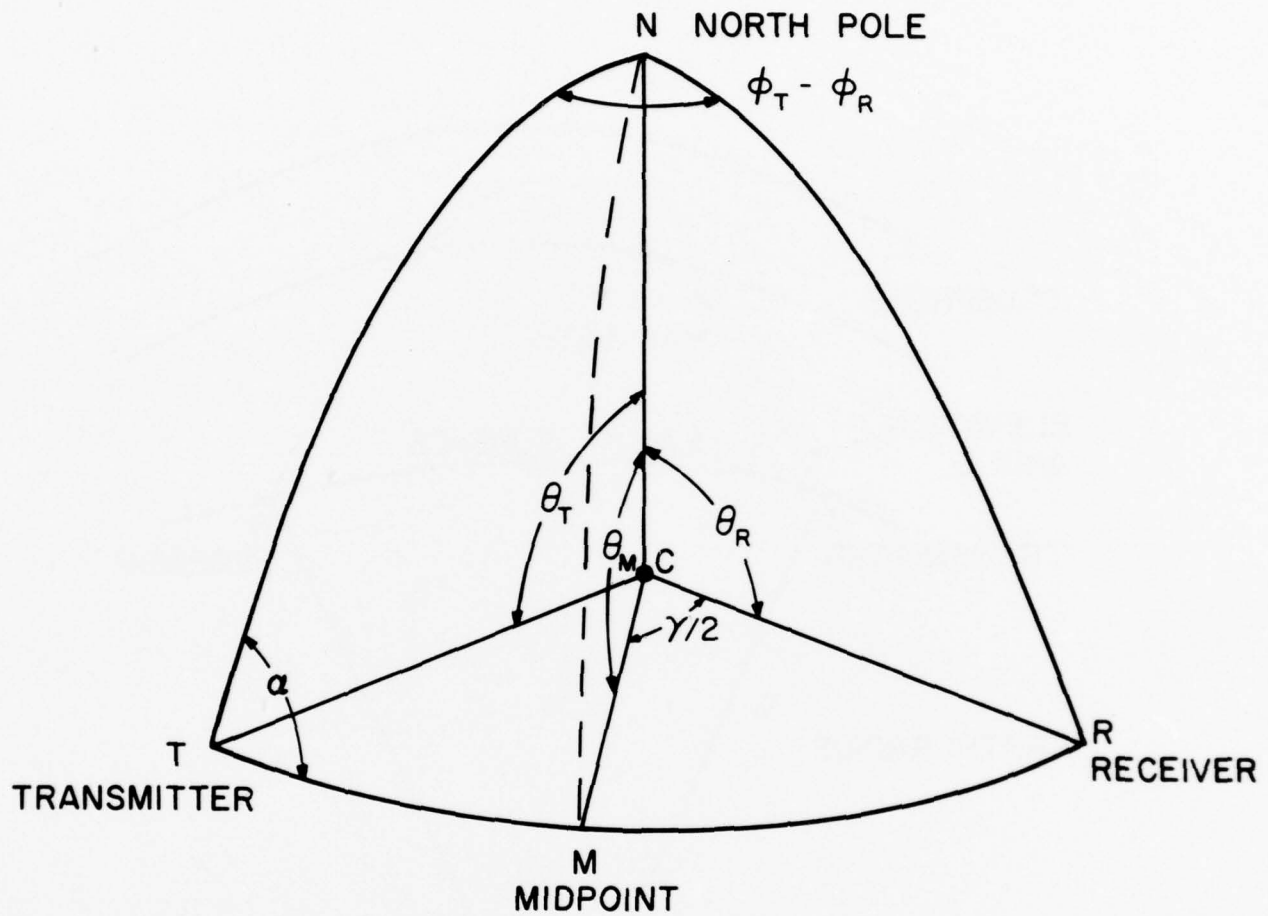


Figure 2.3. Earth geometry for finding the coordinates of the midpoint.

the transmitter and receiver respectively. The coordinates of the midpoint between the transmitter and receiver are then found through the application of the sine and cosine laws of spherical trigonometry to Figure 2.3. From Figure 2.3, the azimuthal angle of the receiver as viewed from the transmitter is

$$\alpha = \sin^{-1} [\sin (\phi_T - \phi_R) \sin \theta_R / \sin \gamma] \quad (2.4)$$

The colatitude of the midpoint, M, is

$$\theta_M = \cos^{-1} [\cos \theta_T \cos \frac{\gamma}{2} + \sin \theta_T \sin \frac{\gamma}{2} \cos \alpha] \quad (2.5)$$

The relative longitude of the midpoint M with respect to the transmitter longitude,  $\delta\phi_M$ , is given by

$$\delta\phi_M = \sin^{-1} [\sin \alpha \sin \frac{\gamma}{2} / \sin \theta_M] \quad (2.6)$$

The exact longitude of the midpoint M is found by adding or subtracting the relative longitude  $\delta\phi_M$  from the transmitter longitude  $\phi_T$ , i.e.

$$\phi_M = \phi_T \pm \delta\phi_M \quad (2.7)$$

If the receiver is located east of the transmitter the positive sign is used otherwise the negative sign is applied. The coordinates of the midpoint thus found are compared with the coordinates of the grid points at which ionospheric models are given. The profile corresponding to the grid point having the smallest difference in coordinates is chosen to represent the profile at the midpoint of the path.

The midpoint profile selected in this manner is approximated by segments of a second degree polynomial which for the  $i^{\text{th}}$  segment has the form given by (2.1). The coefficients in equation (2.1) are found by making sure that both the density and its derivatives are continuous in going from one segment to another. Each segment value corresponds to the height increment dictated by the composite ionospheric profile. Utilizing equation (2.1) we find analytical expressions for the ground distance  $D$  and the group path  $P'$ . Neglecting the effects of the Earth's magnetic field and collisions, the ground distance and the group path can be expressed in the form

$$D = 2 \int_{r_0}^{r_t} \frac{r_0^2 \cos \beta_0 dr}{r[r^2 \mu^2 - r_0^2 \cos^2 \beta_0]^{\frac{1}{2}}} \quad (2.8)$$

and

$$P' = 2 \int_{r_0}^{r_t} \frac{r dr}{[r^2 \mu^2 - r_0^2 \cos^2 \beta_0]^{\frac{1}{2}}} \quad (2.9)$$

where  $r_t$  is the radial distance from the Earth center to ray apogee,  $\beta_0$  is the ray elevation angle, and  $\mu$  is the refractive index of the medium. The refractive index  $\mu$  and the plasma frequency  $f_p$  are related through

$$\mu^2 = 1 - (f_p/f)^2 \quad (2.10)$$

Since the density  $N$  is proportional to the square of the plasma frequency, we can substitute (2.1) in (2.10) to obtain

$$\mu_i^2 = 1 - \frac{1}{f^2} \left( \frac{a_i + b_i}{r} + \frac{g_i}{r^2} \right) \quad (2.11)$$

Through substitution of (11) in (8) and (9), the ground distance and the group path can be written in the form

$$D = D_o + \sum_{i=1}^n D_i + D_f \quad (2.12a)$$

and

$$P' = P'_o + \sum_{i=1}^n P'_i + P'_f \quad (2.12b)$$

The terms  $D_o$  and  $P'_o$  in (2.12) are evaluated from the earth surface up to the base of the composite ionospheric profile. The terms  $\sum_{i=1}^n D_i$  and  $\sum_{i=1}^n P'_i$  are evaluated from the base of the composite profile up to layer  $n$  just below the layer containing the reflection height. The last terms  $D_f$  and  $P'_f$  are the contributions from the top of the  $n^{th}$  layer up to the reflection height of the ray. Explicitly, the terms in (2.12) are

$$D_o = 2r_o [\cos^{-1} \left( \frac{r_o \cos \beta_o}{r_b} \right) - \beta_o] \quad (2.13a)$$

$$P'_o = 2r_o [\sqrt{(r_b/r_o)^2 - \cos^2 \beta_o} - \sin \beta_o] \quad (2.13b)$$

$$D_i = 2 \int_{r_i}^{r_{i+1}} \frac{r_o^2 \cos \beta_o dr}{[A_i r^2 + B_i r + G_i]^{\frac{1}{2}}} \quad i=1, 2, \dots, n \quad (2.14a)$$

$$P'_i = 2 \int_{r_i}^{r_{i+1}} \frac{r dr}{[A_i r^2 + B_i r + G_i]^{\frac{1}{2}}} \quad i=1, 2, \dots, n \quad (2.14b)$$

and

$$D_f = 2 \int_{r_n}^{r_t} \frac{r_0^2 \cos \beta_0 dr}{[A_n r^2 + B_n r + G_n]^{\frac{1}{2}}} \quad (2.15a)$$

$$P'_f = 2 \int_{r_n}^{r_t} \frac{r dr}{[A_n r^2 + B_n r + G_n]^{\frac{1}{2}}} \quad (2.15b)$$

where  $r_b$  is the base radius of the composite ionospheric profile, and

$$\begin{aligned} A_i &= 1 - a_i/f^2 \\ B_i &= b_i/f^2 \\ G_i &= g_i/f^2 - r_0^2 \cos^2 \beta_0 \end{aligned} \quad (2.16)$$

Analytical expressions for the integrals in (2.14) and (2.15) are readily available from standard integral tables. The resulting analytical expressions together with (2.13) are programmed on the computer under subroutine FITT. Given the elevation angle  $\beta_0$ , the oblique frequency  $f$ , and the density profile  $N$ , the subroutine FITT calculates the corresponding ground distance and group path.

Since we are seeking all possible homing solutions, we need to generate a table of ground distances versus elevation angles corresponding to the midpoint density profile. Due to the sensitivity of the trapping angle to changes in the ionospheric model we take the penetration angle  $\beta_p$  as the maximum elevation angle possible. The penetration angle  $\beta_p$  is the solution of the equation

$$r_{\max}^2 \mu^2 - r_0^2 \cos^2 \beta_p = 0 \quad (2.17)$$

Therefore,  $\beta_p$  is given by

$$\beta_p = \cos^{-1} \left\{ \frac{r_{\max}}{r_0} [1 - (f_c/f)^2]^{1/2} \right\} \quad (2.18)$$

and the range of elevation angles is

$$0 \leq \beta \leq \beta_p \quad (2.19)$$

The interval in (2.19) is subdivided into 50 subintervals of elevation angles. For each of the resulting 51 elevation angles the ground distance and the group path are computed through subroutine FITT. The generated values of ground distance and group path together with their corresponding elevation angles are assembled in a table. The table is then scanned to locate the two successive entries within which the ground distance between the transmitter and receiver is located. For each pair of entries thus found we perform linear interpolation to locate a possible homing solution within a specified tolerance. We assume that the ground distance and the elevation angle within the two entries are linearly related through

$$D = a + b\beta \quad (2.20)$$

Starting with the two entries of ground distances and their corresponding elevation angles the coefficients  $a$  and  $b$  are found and a new elevation angle and ground distance are computed. A comparison test is then carried out between the new ground distance and the exact ground distance,  $D_{TR}$ . If the difference is

larger than the specified ground distance tolerance,  $\delta D$ , then the procedure of calculating the coefficients in (2.20) utilizing the two closest values of ground distances to  $D_{TR}$  and their corresponding elevation angles is repeated until  $|D - D_{TR}| \leq \delta D$ . The number of interpolations is limited to ten (10) trials for finding the approximate elevation angle, otherwise homing of the ray is said to be not possible. The specified ground distance tolerance,  $\delta D$ , is an input parameter in W(387) of the ray tracing program.

Every possible homing solution of elevation angles is assembled in a table. Then, through the three-dimensional ray tracing program these elevation angles are refined to obtain the corresponding true elevation angles that will home the ray. In some cases true elevation angles are not possible. In either situation a message is printed to show whether or not a homing solution has been achieved. The complete procedure described in this section is simulated on the computer under subroutine HOME.

### 2.2.3 Approximate Elevation Angle - Multiple Layer Ionosphere

In a single layer ionosphere there are at most two approximate initial elevation angles, one for the low ray and the other for the high ray. In a multiple layer ionosphere, the number of approximate initial elevation angles depends upon the number of layers in the given ionospheric profile. The approximate elevation angle solutions are designated by first layer low or high ray, second layer low or high ray, third layer low or high ray, and fourth layer low or high ray. In our study we selected four as the highest number of layers. This restriction could be removed

with minor modifications on the computer code in subroutine HOME.

Whether the given ionospheric profile is single or a multi-layered one, the procedure of finding the approximate elevation angle is the same as the one described in section 2.2.2. The computer code does not differentiate between single and multi-layered profiles and it is written for a four-layered ionosphere. A sample of the ground distance versus elevation angle curve for a four-layered ionosphere is shown in Figure 2.4.

#### 2.2.4 Refinement of the Elevation Angle

Thus far we have discussed the computation of the approximate elevation angles. In this section we focus our attention on the procedure to refine these approximate elevation angles through actual ray tracing.

Let the exact ground distance between the transmitter and receiver be  $D_{TR}$ . Then starting with one of the tabulated approximate elevation angles,  $\beta_1$ , we trace one ray through the given ionospheric model utilizing the three dimensional ray tracing program. The ground distance corresponding to  $\beta_1$  is  $D_1$ . Utilizing the table of ground distances and elevation angles generated in the previous section we increment or decrement elevation angle  $\beta_1$ . The value and sign of the increment depends on the relative location of  $D_1$  with respect to  $D_{TR}$  in the ground distance versus elevation angle table. With the new elevation angle  $\beta_2$  we compute  $D_2$  through the ray tracing program. The ground distance,  $D_{TR}$ , must then be located either above  $D_1$  and  $D_2$ , below  $D_1$  and  $D_2$ , or in between  $D_1$  and  $D_2$ . For the cases where  $D_{TR}$  is above or below  $D_1$  and  $D_2$  the elevation angles and their corresponding ground

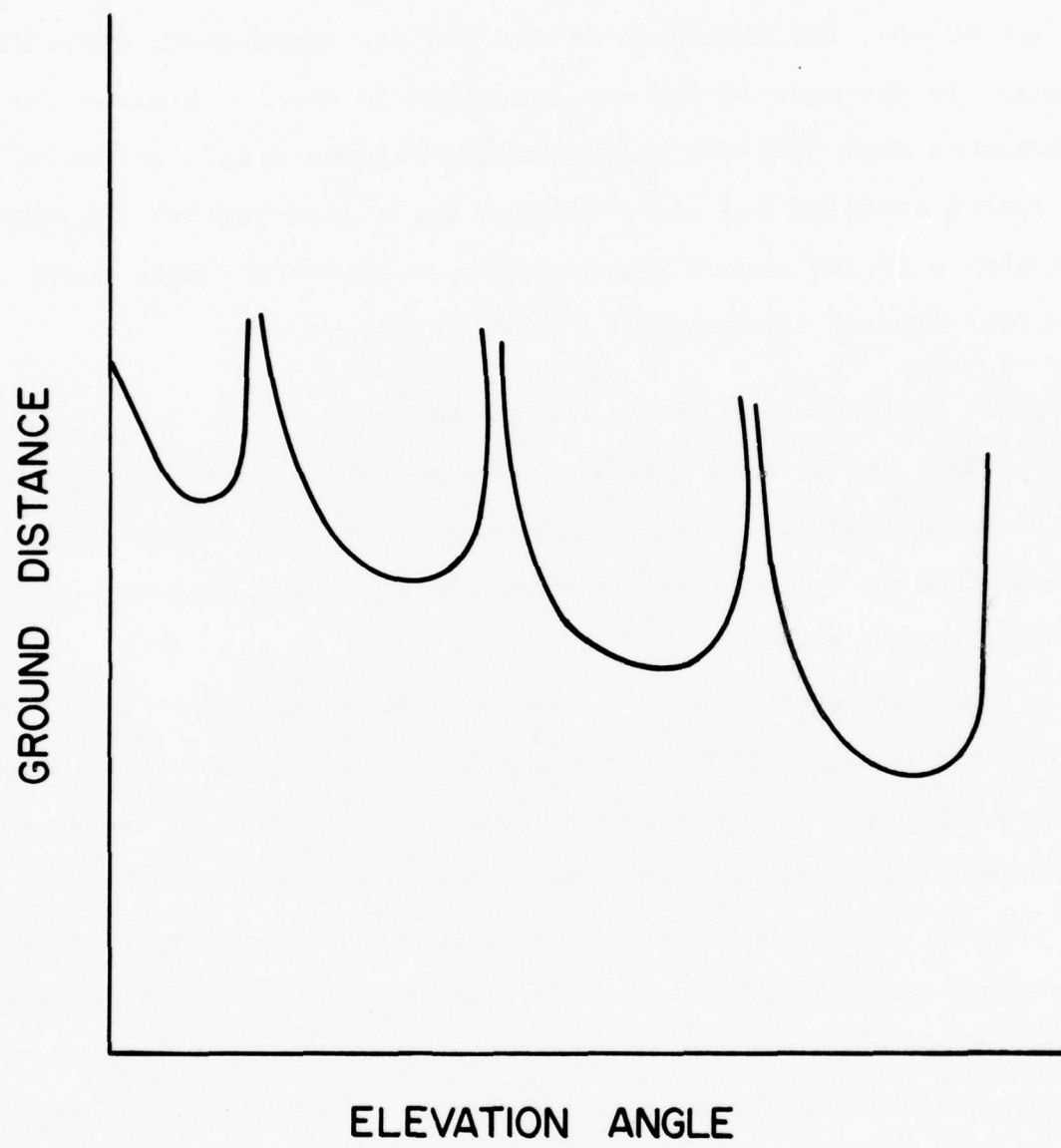


Figure 2.4. Sketch showing the ground distance - elevation angle curve for a four-layer ionosphere.

distances are adjusted through linear interpolation in accordance with equation (2.20) until  $D_{TR}$  is either located between  $D_1$  and  $D_2$  or such a condition cannot be achieved. In the latter situation the elevation angle found through (2.20) lies outside the range of elevation angles set for the ray in a multiple layer ionosphere. In the event that  $D_{TR}$  cannot be located between  $D_1$  and  $D_2$ , homing of the ray cannot be accomplished and one of the statements 'High angle ray' or 'Discontinuity in the ray traced range - Beta curve or range too close to the skip distance' is printed from subroutine ADJUST.

Let us assume that we can locate  $D_{TR}$  between  $D_1$  and  $D_2$  then we can find  $\beta_3$  through linear interpolation on  $\beta_1$ ,  $D_1$ ,  $\beta_2$  and  $D_2$ . With  $\beta_3$  we calculate a new ground distance  $D_3$ . If the difference between  $D_{TR}$  and  $D_3$  is less than a specified ground distance tolerance, then  $\beta_3$  is the desired homing elevation angle except for azimuthal angle corrections. The ground distance tolerance,  $\delta D$ , is an input parameter and is specified in W(387). However, if the difference between  $D_{TR}$  and  $D_3$  is greater than  $\delta D$  then we need to correct for the ground distance discrepancy. Since the dependence of the ground distance on the elevation angle is known to be nonlinear, we let

$$D_i = a_0 + a_1 \beta_i + a_2 \beta_i^2 \quad i=1,2,3 \quad (2.21)$$

The coefficients  $a_0$ ,  $a_1$ , and  $a_2$  are computed by inverting the matrix resulting from the substitution of ground distances  $D_1$ ,  $D_2$ ,  $D_3$  and their corresponding elevation angles  $\beta_1$ ,  $\beta_2$ ,  $\beta_3$ . The new elevation angle is then given by

$$\beta_{\pm} = \frac{1}{2a_2} [-a_1 \pm \sqrt{a_1^2 - 4a_2(a_0 - D_{TR})}] \quad (2.22)$$

If the quantity under the radical sign in (2.22) is negative, then we cannot find an elevation angle and an appropriate message is printed. Equation (2.22) yields two solutions,  $\beta_+$  and  $\beta_-$ . In order to decide whether  $\beta_+$  or  $\beta_-$  is the desired elevation angle we set up the following criterion. First, we take the absolute differences between  $D_{TR}$  and  $D_1$ ,  $D_2$ ,  $D_3$  and the resulting three difference values are compared with each other. The elevation angle  $\beta_1$ ,  $\beta_2$ , or  $\beta_3$  corresponding to the smallest difference is then selected. The elevation angles  $\beta_+$  and  $\beta_-$  are then compared with the selected elevation angle. The one yielding the smaller difference is chosen as the new elevation angle i.e.  $\beta_4 = \beta_+$  or  $\beta_4 = \beta_-$ . With  $\beta_4$  we trace another ray and find  $D_4$ . If the difference between  $D_{TR}$  and  $D_4$  is within the specified tolerance  $\delta D$ , then  $\beta_4$  is the homing angle except for possible azimuthal corrections. However, if the difference between  $D_{TR}$  and  $D_4$  is the largest difference then we cannot home the ray and the message 'Discontinuity in the ray traced range-beta curve or range too close to the skip distance' or 'High angle ray' is printed. On the other hand, if  $D_4$  is closer to  $D_{TR}$  than any or all of  $D_1$ ,  $D_2$ ,  $D_3$  then the ground distance  $D_1$ ,  $D_2$ , or  $D_3$  yielding the largest absolute difference with  $D_{TR}$  is replaced by  $D_4$  and its corresponding elevation angle by  $\beta_4$ . The procedure starting with equation (2.21) is repeated to find a new elevation angle and a new ground distance. The comparison steps are carried out until the ground distance tolerance criterion is met or a message is printed. The number of allowable tries to find the homing angle is controlled

by an input parameter in W(386).

Once the ground distance tolerance criterion is satisfied a first order elevation angle that will home the ray to the receiver is said to be found except for possible azimuthal deviation correction. The azimuthal deviation is defined as the difference between azimuth of the computed receiving point from the transmitter and the azimuth of the intended receiving point from the transmitter. If the azimuthal deviation of the ray is within the calculated azimuthal tolerance,  $\delta A$ , the homing of the ray is completed. Otherwise, the azimuth of transmission has to be corrected in order to satisfy the azimuthal tolerance condition. The azimuthal tolerance,  $\delta A$ , is computed with the help of Figure 2.5. In Figure 2.5, we show the transmitter T, the receiver R, the computed receiver  $R'$ , and the angles  $\gamma_1$ ,  $\gamma_2$ ,  $\gamma_3$  subtended at the earth center opposite arcs TR, TR', and RR' or  $\delta D$  respectively. Applying the cosine law to the spherical triangle TRR' we obtain

$$\cos \gamma_3 = \cos \gamma_1 \cos \gamma_2 + \sin \gamma_1 \sin \gamma_2 \cos \delta A \quad (2.23)$$

If we let  $\gamma_1 = \gamma_2 = D_{TR}/r_o$  and  $\gamma_3 = \delta D/r_o$ , then

$$\cos \delta A = [\cos (\delta D/r_o) - \cos^2 (D_{TR}/r_o)] / \sin^2 (D_{TR}/r_o) \quad (2.24)$$

Since  $\delta D$  is much smaller than  $r_o$ , the argument of the cosine function,  $\delta D/r_o$  is very small. Expanding this term and retaining two terms of the expansion, (2.24) takes the form

$$\cos \delta A \approx 1 - \frac{1}{2} \left[ \frac{\delta D}{r_o \sin(D_{TR}/r_o)} \right]^2 \quad (2.25)$$

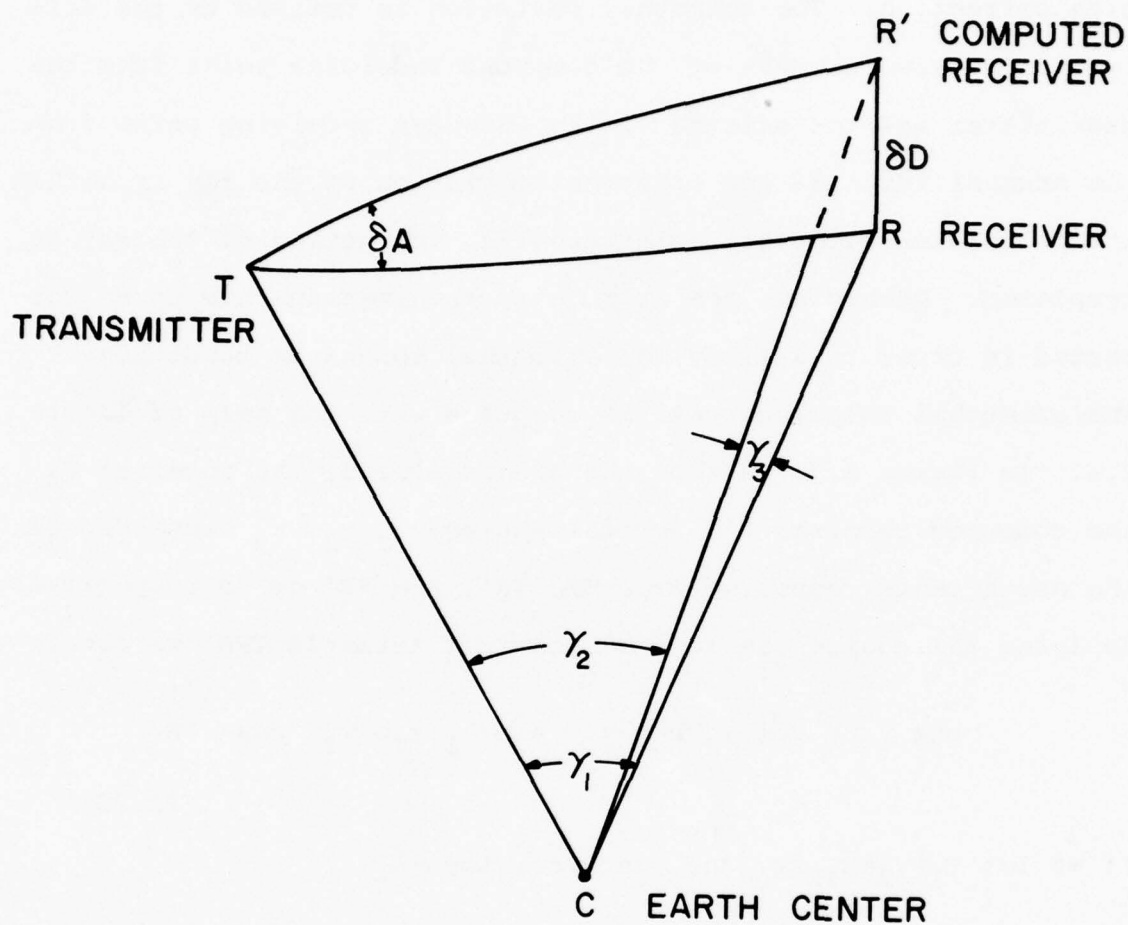


Figure 2.5. Sketch illustrating the homing in azimuth.

Since the azimuthal tolerance  $\delta A$  is also small, we expand the left hand side of (2.25) retaining two terms of the expansion. The resulting expression for  $\delta A$  is

$$\delta A \approx \frac{\delta D}{r_0 \sin(D_{TR}/r_0)} \quad (2.26)$$

For each ray homed in ground distance a comparison test is performed between the ray azimuth and the computed transmitter-receiver azimuth. If the ray azimuthal deviation is within the azimuthal tolerance  $\delta A$  then homing is achieved and control is transferred to another activity within the ray tracing program. However, if the ray azimuthal deviation is larger than  $\delta A$  we adjust the azimuth of transmission by the amount of the ray azimuthal deviation. With a new azimuth of transmission and the same elevation angle we repeat the complete procedure of ground distance homing and find a new homing angle. The ray azimuthal deviation corresponding to this new homing angle is then compared to the azimuthal tolerance,  $\delta A$ . The above steps are repeated until both ground distance tolerance and azimuthal tolerance criteria are satisfied or a message is printed.

#### 2.2.5 Group Path Homing

The capabilities of the three-dimensional ray tracing program was extended to include homing of the group path. The procedure described in the ground-to-ground homing case is also used for the group path homing. The only difference being in the parameters supplied to the ray tracing program through the W-array data input.

The parameters needed to perform group path homing are the transmitter coordinates, the azimuthal angle of transmission, the oblique frequency of transmission and the value of the homed in group path. The homed in group path is supplied through W(394). In the event that group path homing is not desired, then W(394) should be set to zero. An example of group path homing is discussed in the next section.

#### 2.2.6 Examples and Discussion

In the preceding section we discussed in detail the technique through which the ground-to-ground homing of the ray is achieved. In order to illustrate the homing procedure we present three examples. The first example is for a single layer ionosphere, the second example is for a two layered ionosphere, and the third example is for group path homing. In all cases the ray is traced through the Air Force supplied ionospheric model. This model gives the electron density profile on a geomagnetic longitude-geomagnetic colatitude grid spanning from  $-130^{\circ}$ E to  $-110^{\circ}$ E in geomagnetic longitude and  $0^{\circ}$  to  $54^{\circ}$  in geomagnetic colatitude. The increments in longitude, colatitude and height are  $5^{\circ}$ ,  $3^{\circ}$  and 10 km respectively. The base height in all cases is 90 km extending upward to 600 km. Note that these increments are very coarse for accurate ray tracing even with careful interpolation routines. This causes some difficulty as discussed later.

##### Example 1. Single Layer Ionosphere

Let the transmitter and receiver geographic coordinates be located at ( $125^{\circ}$ W,  $78^{\circ}$ N) and ( $185^{\circ}$ W,  $56^{\circ}$ N) respectively. For this

configuration the ground distance  $D_{TR} = 3296.55$  km and the azimuthal angle of transmission is 258.2 degrees. Since the ionospheric profile grid points are given in geomagnetic coordinates we transform the transmitter and receiver geographic coordinates to obtain colatitudes of 10.81658 and 40.06548 degrees and longitudes of 114.47052 and 128.20226 degrees east. Utilizing equations (2.4), (2.5), and (2.7) the geographic and geomagnetic coordinates of the midpoint are found to be (-169.81, 69.18) longitude and latitude, (-125.12, 25.33) longitude and colatitude respectively. A comparison between the geomagnetic coordinates of the midpoint and the given ionospheric profile results in the selection of the density profile located at (-125.0, 24.0). For an oblique frequency of transmission of 20 MHz equation (2.18) yields the penetration angle of 14.236 degrees. Then, the interval of elevation angles from zero to 14.236 degrees is divided into 50 intervals. For each of the 51 resulting elevation angles the ground distance and group path are calculated through equations (2.13), (2.14), (2.15) and (2.16) utilizing the density profile of the midpoint located at (-125.0, 24.0). The result of this calculation is shown in Figure 2.6. For the specified ground distance tolerance of 5 km, figure 6 shows that the approximate initial elevation angle was found to be 3.312 degrees.

Figure 2.7 shows the steps taken in the refinement procedure and the eventual homing of the ray. The top portion of Figure 2.7 displays the ground distance versus elevation angle homing steps. The figure shows that the ray is homed in ground distance in the 5th step. However, the bottom portion of the figure also shows

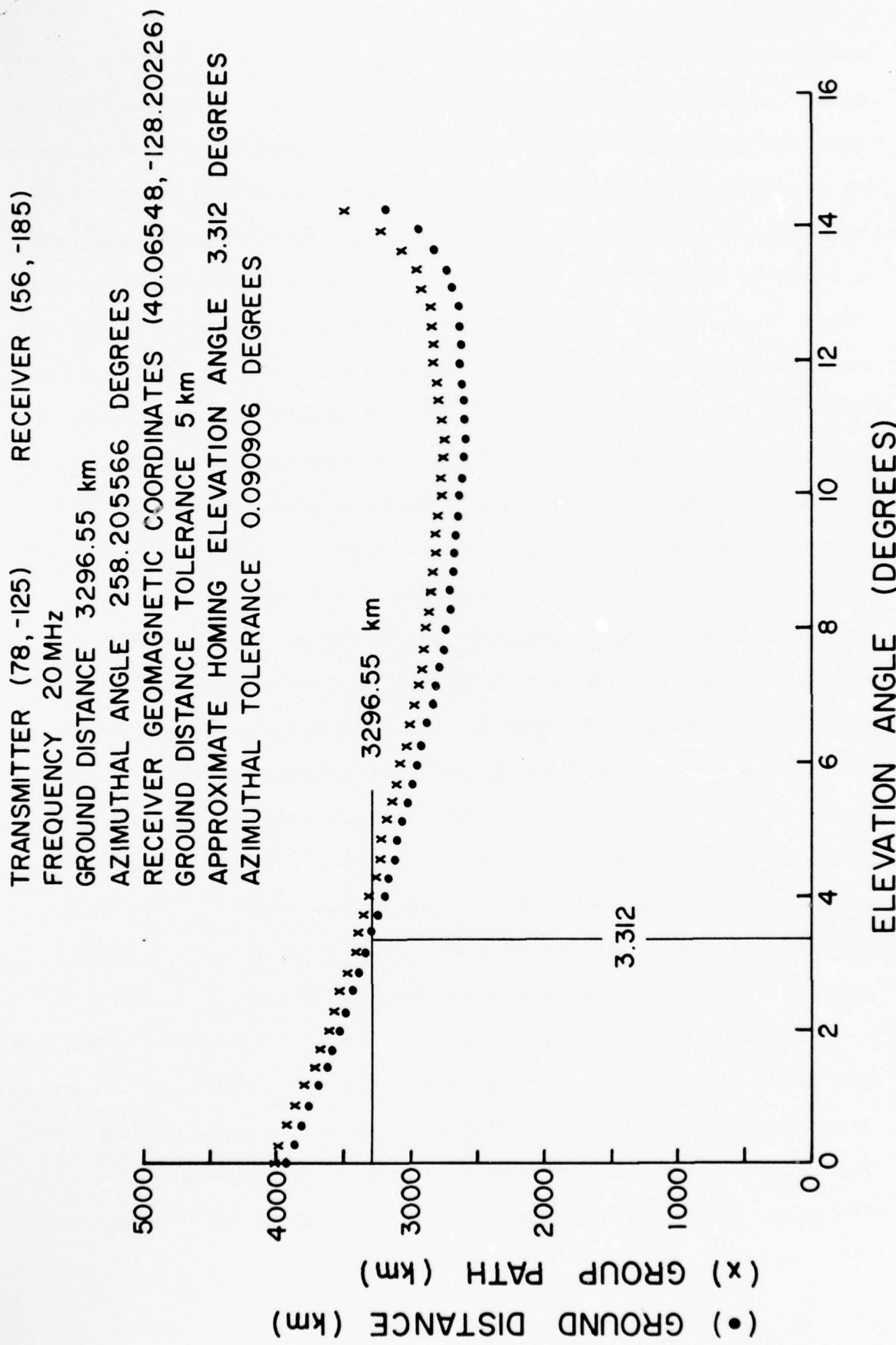


Figure 2.6. Example 1 illustrating the ground-to-ground homing using the Air Force supplied model ionosphere. The example shows how the initial elevation is determined.

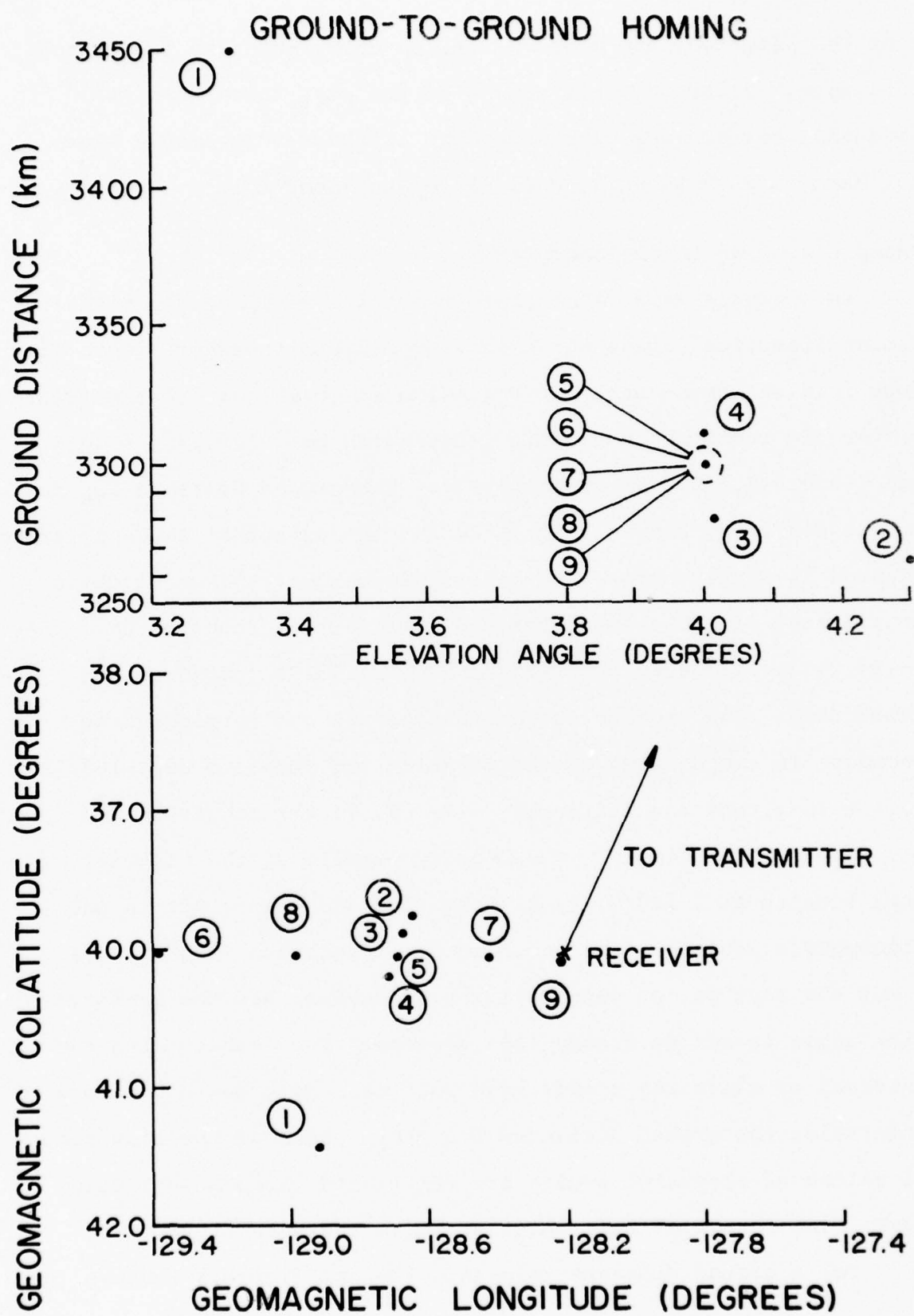


Figure 2.7. Continuation of the example shown in Fig. 2.6. This shows the refinement procedure in ground distance and azimuth homing using 3D ray tracing.

that the azimuthal angle of the ray is not within the calculated tolerance. Prior to final homing of the ray, there were four azimuthal corrections with no ground distance adjustments since for each azimuth the ground distance was homed in.

#### Example 2. Two Layer Ionosphere

In a single layer ionosphere there are at most two initial homing elevation angles while in a two layer ionosphere there are four initial homing angles. Following example 1 we let the transmitter and receiver geographic coordinates be ( $-175.0^{\circ}\text{E}$ ,  $68.0^{\circ}\text{N}$ ) and ( $-150.0^{\circ}\text{E}$ ,  $72.0^{\circ}\text{N}$ ) respectively. The ground distance  $D_{\text{TR}}$  for such a configuration is 1039.36 km and the azimuthal angle of transmission is 53.51 degrees. Upon transformation, the geomagnetic coordinates of the transmitter and receiver are found to be (-127.7972, 27.21986) and (-114.25255, 19.5317) longitude and colatitude. The geographic coordinates and the corresponding geomagnetic coordinates of the midpoint are found to be (-163.72, 70.43) longitude and latitude, (-122.09, 23.22) longitude and colatitude respectively. The density profile at the midpoint is then located at (-120.0, 24.0) longitude and colatitude in the ionospheric profile. For an oblique transmission frequency of 7 MHz the rays do not penetrate the ionosphere and the penetration angle is set to ninety (90) degrees. Upon subdividing the interval of elevation angles from zero to ninety degrees into 50 intervals, the ground distances and group paths of the resulting 51 values of elevation angles are calculated through subroutine FITT. The result of this calculation is shown in Figure 2.8.

For a ground distance tolerance  $\delta D=2$  km Figure 2.8 shows that

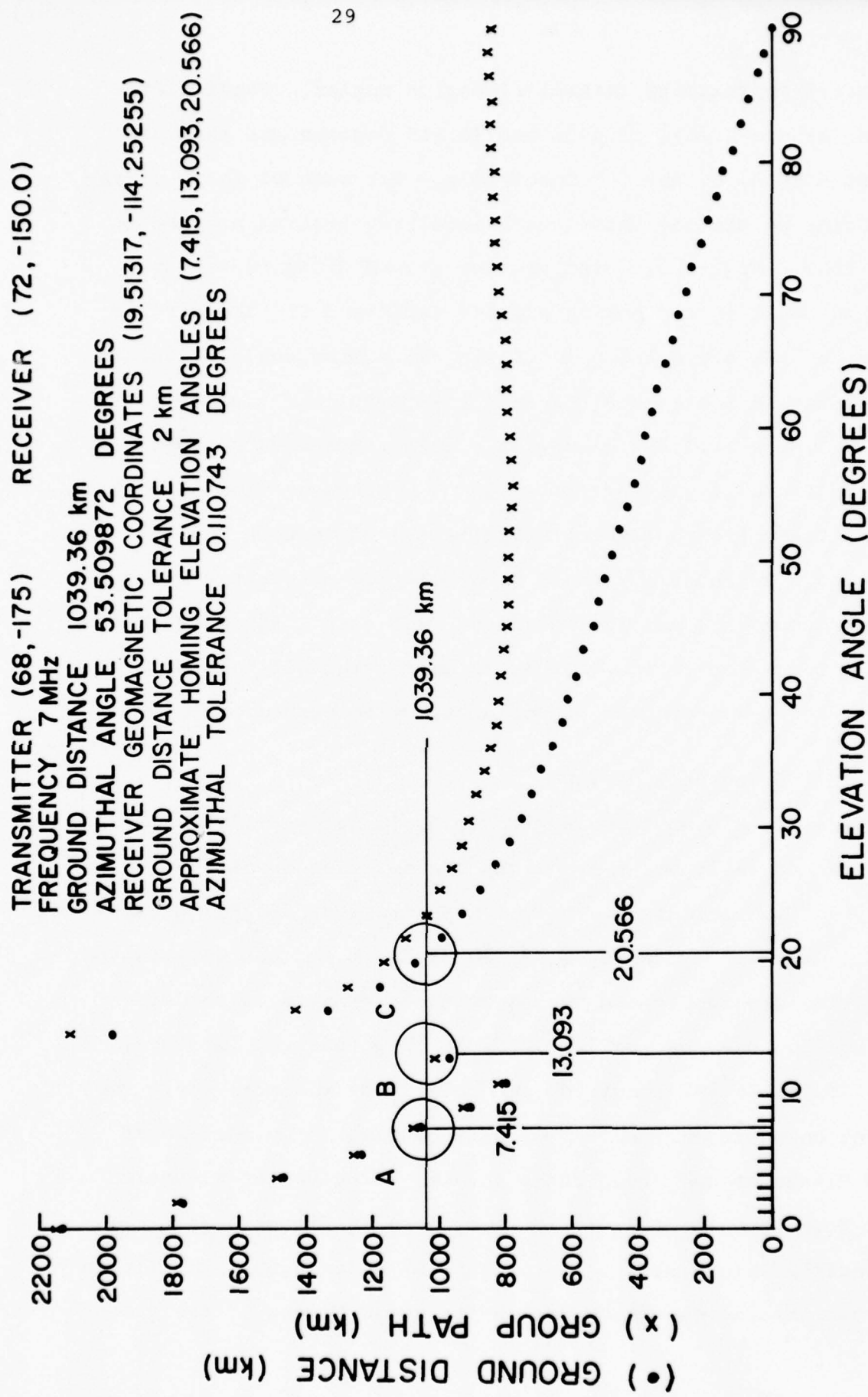


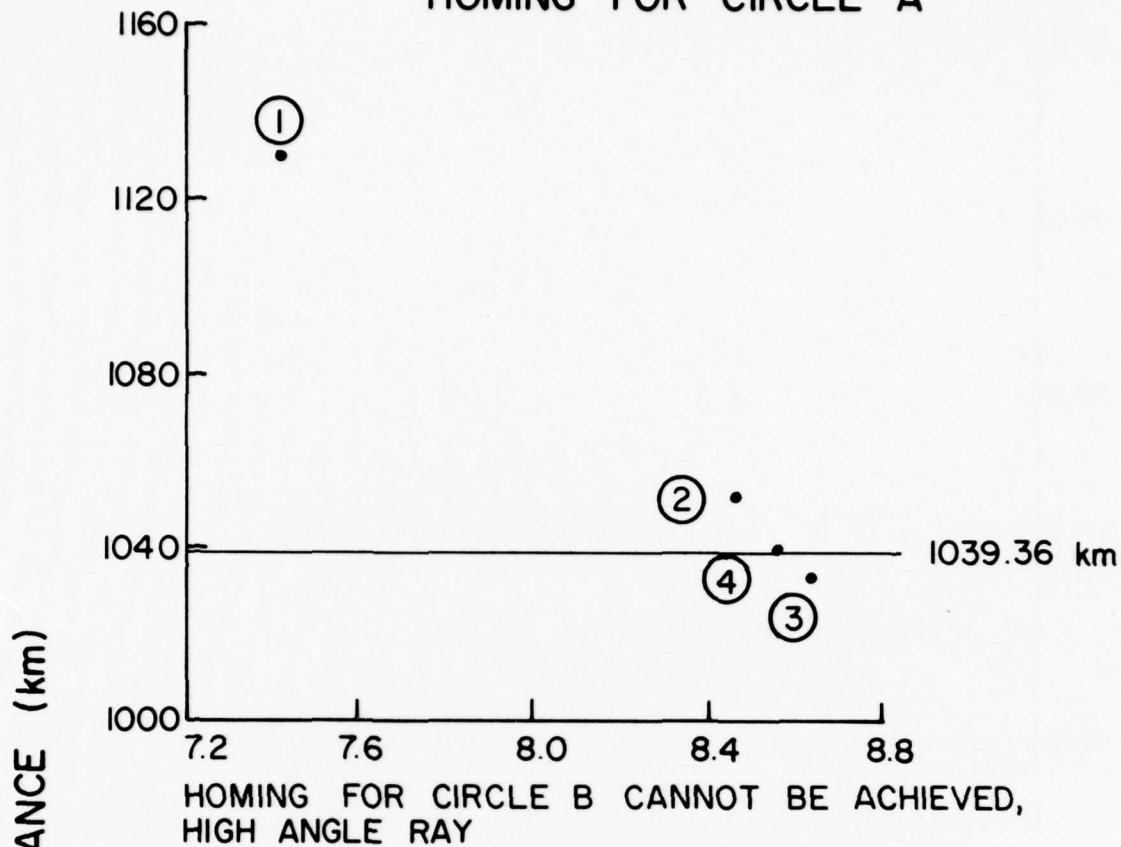
Figure 2.8. Example 2 illustrating the ground-to-ground homing for rays reflected from a two-layer ionosphere. Note that for a ground range of 1039.36 km, three approximate solutions (indicated by circle A, circle B and circle C) in the elevation angle exist in this case.

there are 3 approximate initial elevation angles. These elevation angles are 7.415, 13.093, and 20.566 degrees and they are designated by A, B, and C respectively. For each of these elevation angles we use the three dimensional ray tracing program to refine them. Figure 2.9 displays the ground distance versus elevation angle in the homing process for A and C. The circled numbers are the steps taken to obtain the homing angle. Homing for B cannot be achieved since it corresponds to a high angle ray. In Figure 2.10 the geomagnetic colatitude versus geomagnetic longitude is plotted for A and C. For case A the azimuthal angle of transmission does not require any correction and the homing angle is found by linear interpolation on steps 2 and 3 without recourse to matrix inversion. For case C the azimuthal angle is corrected twice in order to meet azimuthal tolerance criterion corresponding to ground distance tolerance of 2 km.

#### Example 3. Group Path Homing

Using the transmitter geographic coordinates (-150.0, 78.0) longitude and latitude, the oblique transmission frequency of 12 MHz, and the azimuthal angle of transmission of 209.4 degrees we calculated the coordinates of the midpoint and the penetration angle. The geographic and geomagnetic coordinates of the midpoint are found to be (-164.97, 66.86) longitude and latitude, and (-119.04, 26.59) longitude and colatitude respectively. The penetration angle is found to be 38.9 degrees. The calculated ground distances and group paths for the 51 values of elevation angles from zero to 38.9 degrees are shown in Figure 2.11. For the specified group path value of 2654.08 km in W(394) the figure shows two initial elevation angles for which homing of the group

## HOMING FOR CIRCLE A



## HOMING FOR CIRCLE C

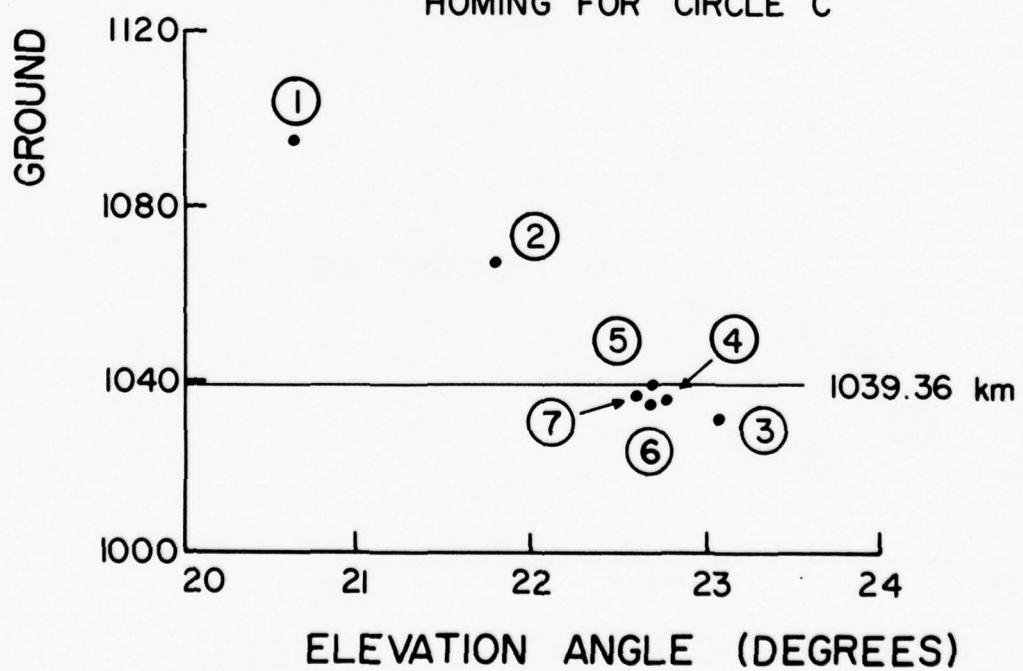
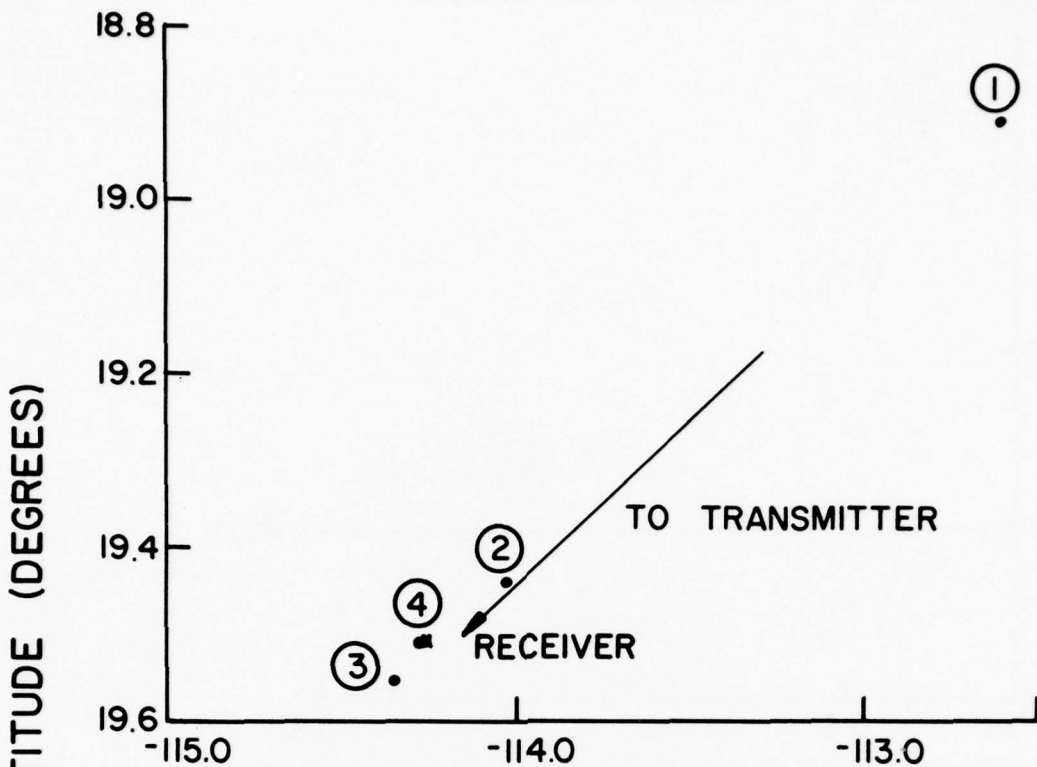
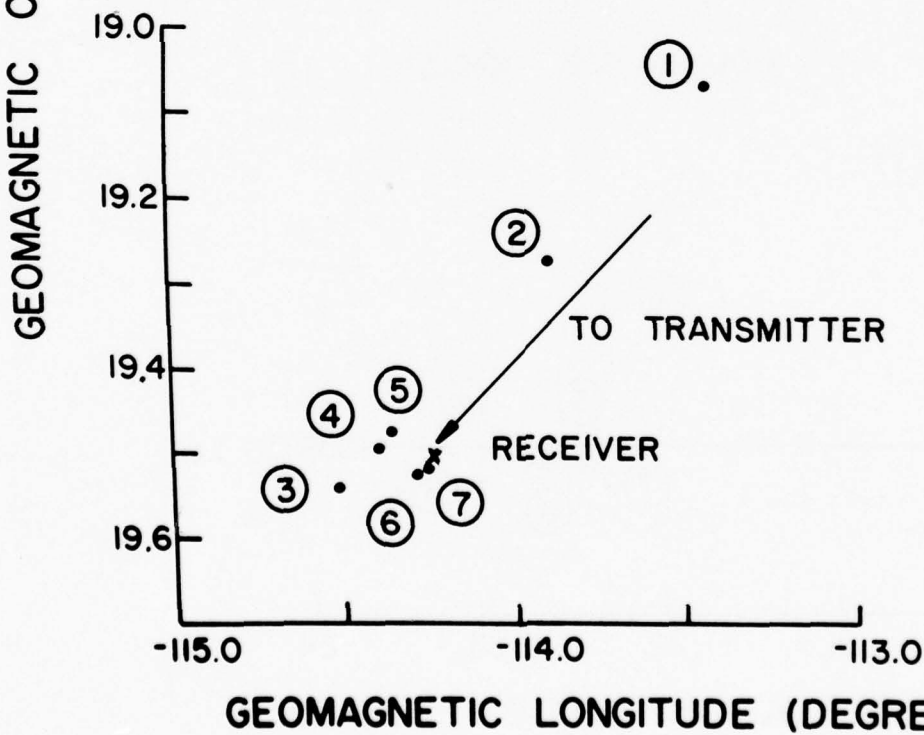


Figure 2.9. Continuation of Example 2 shown in Fig. 2.8 illustrating the ground distance homing for circle A and circle C using 3D ray tracing.

## HOMING FOR CIRCLE A



HOMING FOR CIRCLE B CANNOT BE ACHIEVED, HIGH ANGLE RAY  
HOMING FOR CIRCLE C



GEOMAGNETIC LONGITUDE (DEGREES)

Figure 2.10. Continuation of Example 2 illustrating azimuthal correction for final homing of the ray on the receiver.

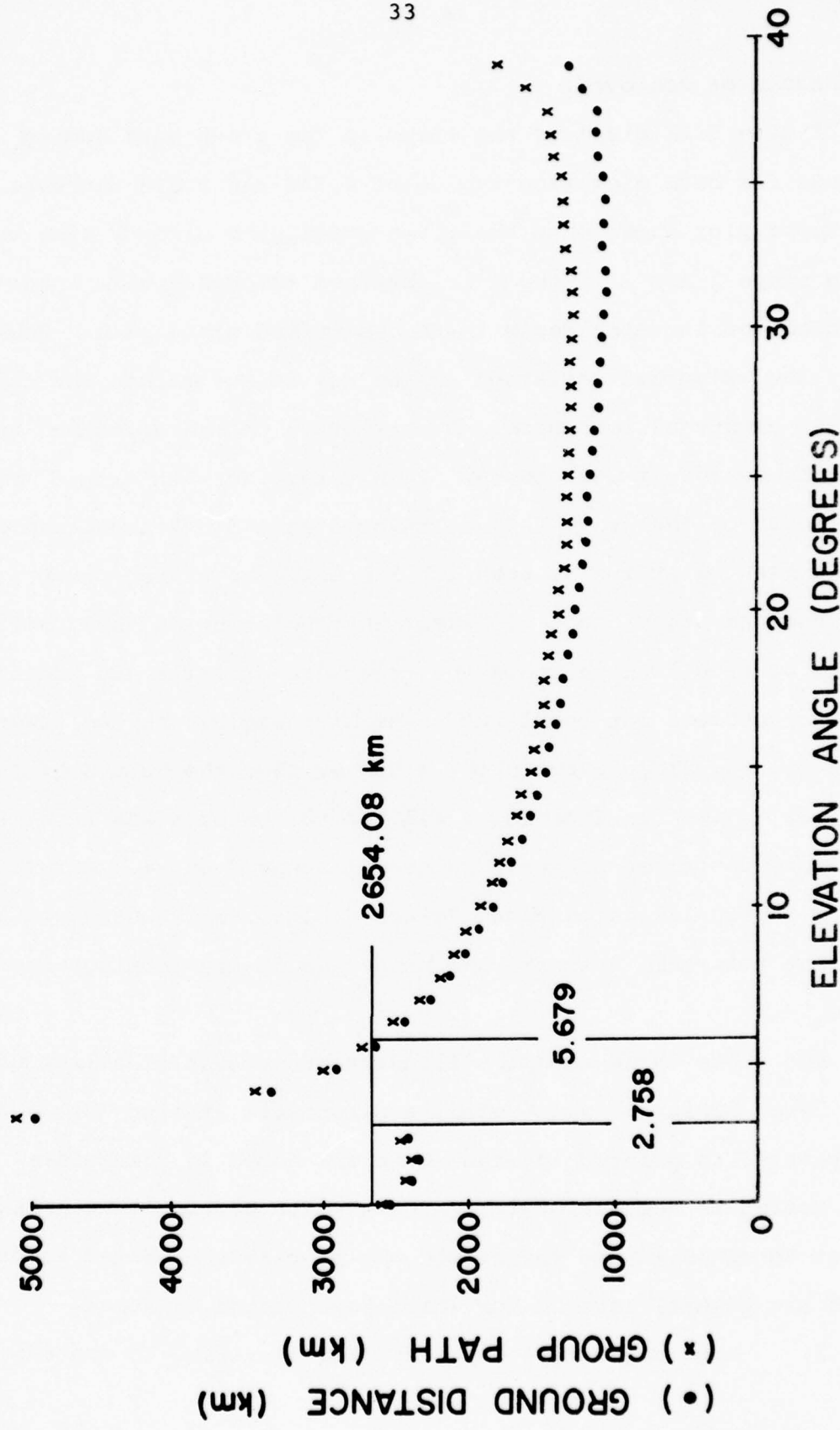


Figure 2.11. Computed initial group path versus elevation angle curve for Example 3.  
For a specified group path of 2654.08 km two solutions are indicated.

path could be achieved.

Figure 2.12 displays the steps in the group path homing process for both elevation angles of 2.758 and 5.679 degrees. The upper plot shows that the given group path already lies between steps 2 and 3. Step 4 is obtained through linear interpolation and it coincides with the specified group path. However, the azimuthal deviation of the ray is not within the calculated azimuthal tolerance. A correction on the azimuthal angle of transmission yields step 5. Then, starting with step 5 and using increments of the previously calculated ground distances and elevation angles we arrive at step 6. Since the specified group path lies between steps 5 and 6, linear interpolation on them yields values of step 7 which meets the tolerance criteria and homing is thus complete for the first layer high angle. In the lower graph the specified group path is higher than the values of steps 1, 2, 3, 4, and 5. Therefore, all the values of steps 1, 2, 4, and 5 are discarded and only values of steps 3 and 6 are retained. Linear interpolation on these values yields step 7 which satisfies the tolerance criteria and hence the desired homing elevation angle.

The above three examples illustrated successful homing of the ray. When homing is successful, a diagnostic stating that homing is achieved is printed together with the homed in parameters. When homing is not successful, a diagnostic stating that homing cannot be achieved and the reason why it cannot be homed is printed. There are several reasons for which rays cannot be homed.

- i) high angle rays which are too sensitive to ionospheric

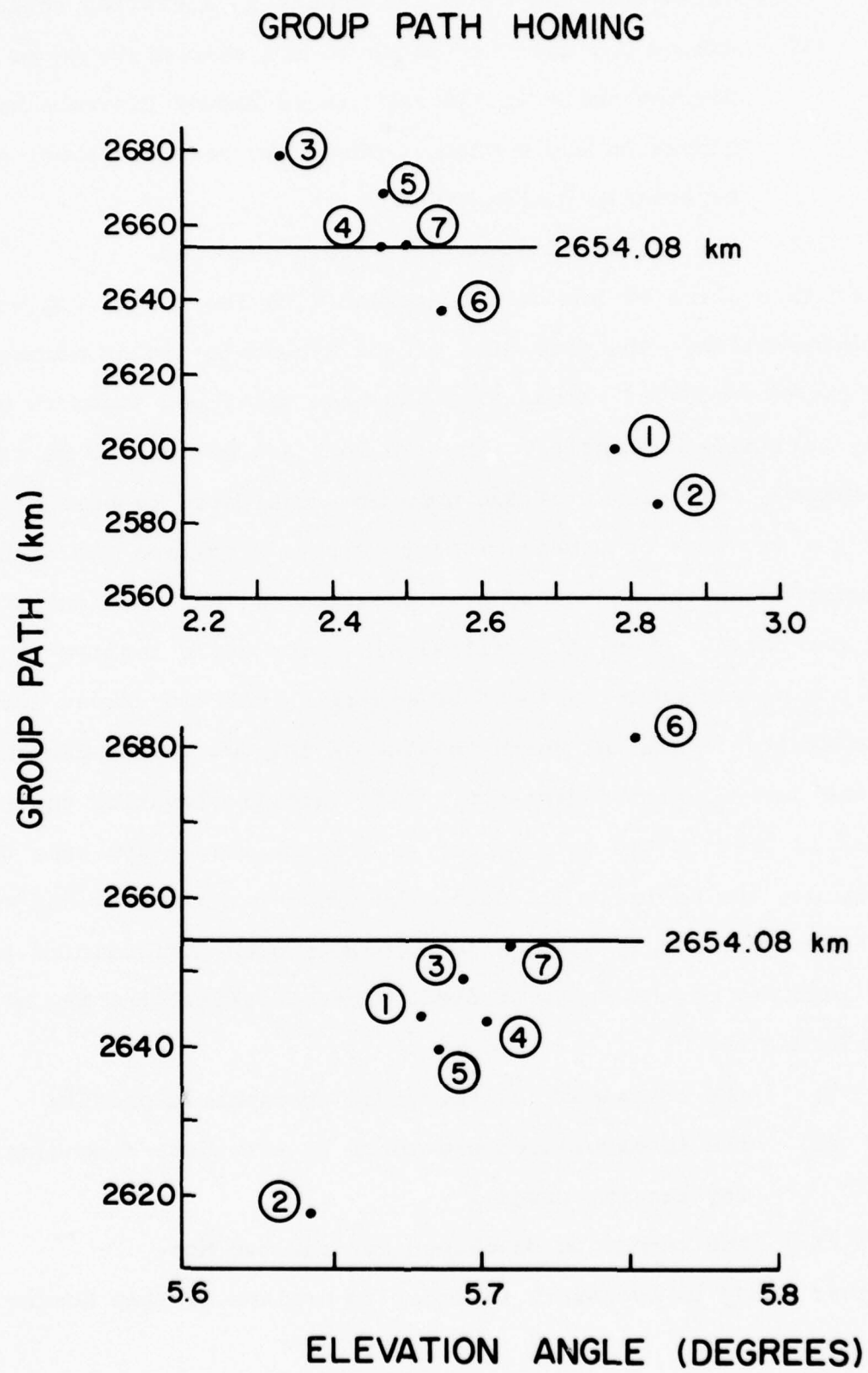


Figure 2.12. Continuation of Example 3 illustrating group path homing for two rays.

parameters and small increments in elevation angles.

- ii) ground distance too close to the skip distance or discontinuity in the ray traced ground distance versus elevation angle curve. These two reasons cannot be separately distinguished.

- iii) the specified number of trials exceeded.

Up to this point we are only concerned with the single hop mode of propagation. The extension of the ground-to-ground homing to the two-hop mode of propagation has been tried and found to be only partially successful. The two hops are assumed to be similar or mixed. Initially, the two hops are considered to be similar and the two sets of ground distance versus elevation angle curves corresponding to the ionospheric profiles at the two midpoints are generated. Then, the initial elevation angle required in the homing procedure is found by searching the two curves for an elevation angle for which the sum of the two ground distances is the desired ground distance. This initial elevation angle if found is used in the same manner as for the single hop case to carry out the homing. Utilizing the above technique we had success in homing for a few cases while we encountered difficulties in the majority of the cases studied. These difficulties may be attributed to

- i) the coarseness of the given ionospheric profile
- ii) the interpolation procedure in the three-dimensional ray tracing program
- iii) the technique developed for the two hop.

Further study is necessary in order to achieve two-hop homing.

### 2.3 Ground-Satellite Homing

When the transmission frequency is much higher than the critical frequency of the given ionospheric profile the ray penetrates the ionosphere. The geometries of the two possible configurations are shown in Figures 2.13 and 2.14. In Figure 2.13 the transmitter is below the receiver and the configuration is called ground-to-satellite homing. The satellite-to-ground homing configuration is shown in Figure 2.14. In either case our objective is to home the ray to the receiver within a specified ground distance tolerance and a computed azimuthal tolerance. The following discussion is applicable to either configuration.

#### 2.3.1 Approximate Elevation Angle

We assume that the transmitter and receiver coordinates are given in east longitude and latitude north in degrees and their heights above the earth surface in km. Then, to a first approximation we calculate the initial or approximate elevation angle for a straight line path between the transmitter and receiver.

Let  $\theta_T$ ,  $\theta_R$ ,  $\phi_T$ ,  $\phi_R$  be the transmitter and receiver colatitudes and longitudes respectively. Compute the cartesian coordinates of the transmitter and receiver through the transformation

$$\begin{aligned}x &= r \sin \theta \cos \phi \\y &= r \sin \theta \sin \phi \\z &= r \cos \theta\end{aligned}\tag{2.27}$$

where  $r=r_0+h$  and  $h$  is the height of the transmitter or receiver above the earth surface. From Figures 2.13 and 2.14, the vectors

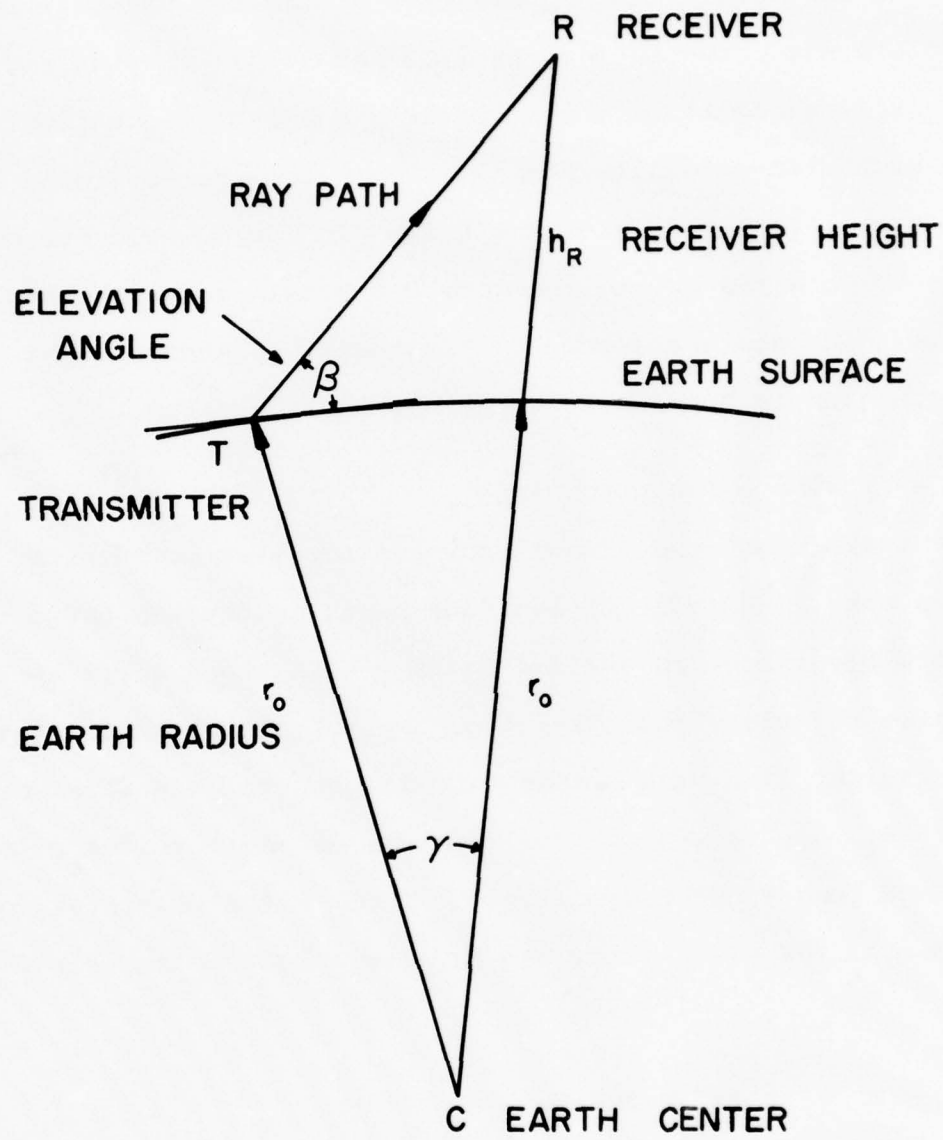


Figure 2.13. Sketch showing the geometry of ground-satellite homing.

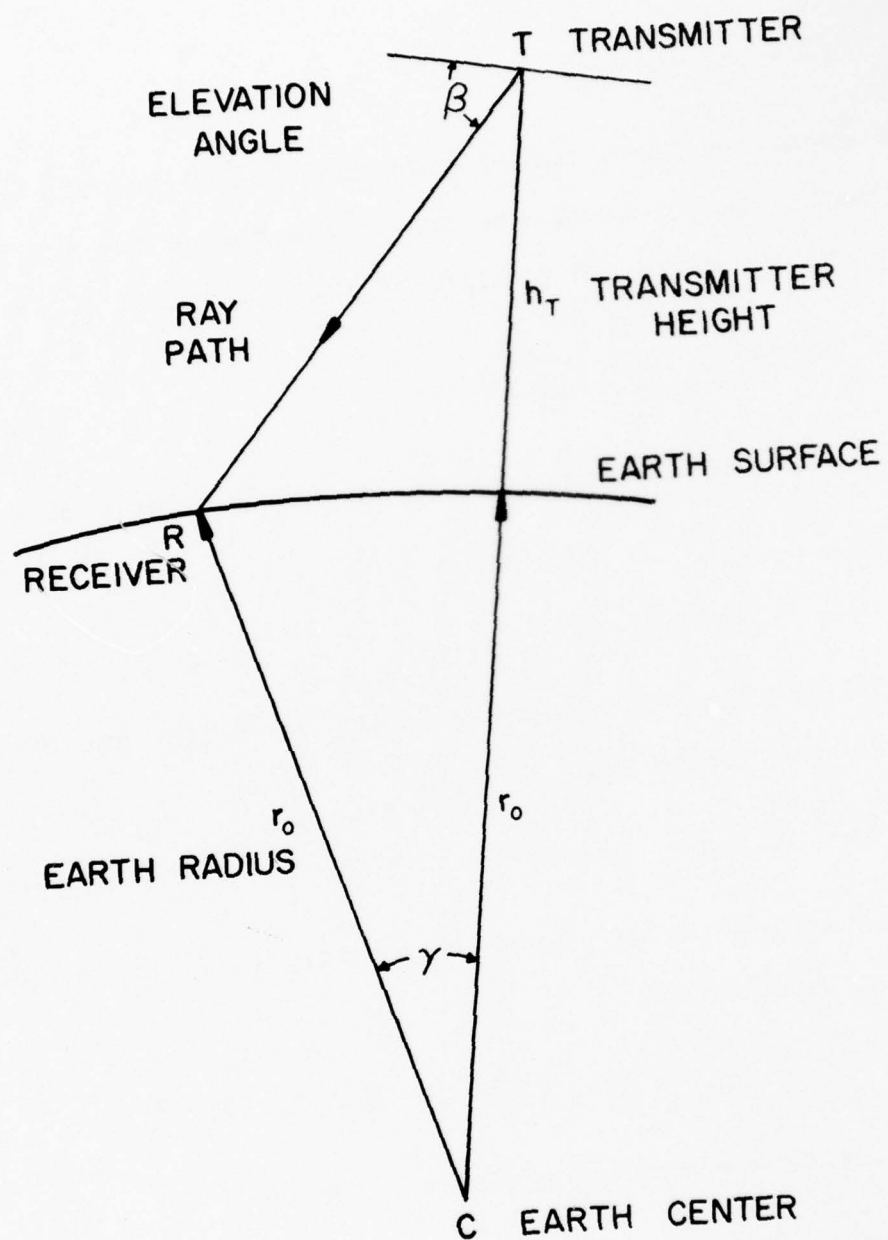


Figure 2.14. Sketch showing the geometry of satellite-ground homing.

$\vec{CT}$  and  $\vec{CR}$  are given by

$$\vec{CT} = x_T \hat{i} + y_T \hat{j} + z_T \hat{k} \quad (2.28)$$

$$\vec{CR} = x_R \hat{i} + y_R \hat{j} + z_R \hat{k}$$

Then the ground distance  $D_{TR}$  between the transmitter and receiver can be found either through the use of the cosine law equation (2.3) or by taking the dot product of the vectors in (2.28), i.e.

$$\gamma = \cos^{-1} \left[ \frac{\vec{CT} \cdot \vec{CR}}{|\vec{CT}| |\vec{CR}|} \right] \quad (2.29)$$

The ground distance  $D_{TR}$  projected at the transmitter radius is given by

$$D_{TR} = (r_o + h_T) \gamma \quad (2.30)$$

In order to find the elevation angle, we define the straight line path by the vector  $\vec{TR}$ ,

$$\vec{TR} = \vec{CR} - \vec{CT} \quad (2.31)$$

Applying the cosine law of plane trigonometry to triangle CTR, angle CTR is found to be

$$\chi_{CTR} = \cos^{-1} [ (|\vec{TR}|^2 + |\vec{CT}|^2 - |\vec{CR}|^2) / 2 |\vec{TR}| |\vec{CT}| ] \quad (2.32)$$

and the approximate elevation angle is given by

$$\beta = \chi_{CTR} - \pi/2 \quad (2.33)$$

In the ground-to-satellite case  $\beta$  is positive while in the satellite-to-ground case  $\beta$  is negative. The above procedure is pro-

grammed in subroutine HOMES.

### 2.3.2 Refinement of the Elevation Angle

In section 2.2.3 we presented in detail the steps used to refine the approximate elevation angle for the ground-to-ground configuration. The refinement of the elevation angle for both the ground-to-satellite and satellite-to-ground is basically the same as that of the ground-to-ground case except for the initial elevation angle increment. The computer code of ADJUST is used for all three configurations. The initial elevation angle increment is only used once upon entry into routine ADJUST.

Starting with the known value  $\beta_1 = \beta$  of the approximate straight line path between the transmitter and receiver we trace one ray and obtain the ground distance  $D_1$ . In order to find a new elevation angle  $\beta_2$  we assume a plane earth geometry and consider the equivalent triangle TRA in Figure 2.15. In this figure, T is the transmitter, R is the equivalent receiver, which, when a perpendicular line is dropped on RC from T, is a distance D km away and which is h km above the foot of the perpendicular point A as shown in Figure 2.15. From triangle TRA, the approximate elevation angle  $\tilde{\beta}$  is given by

$$\tan \tilde{\beta} = h/D \quad (2.34)$$

Differentiating both sides of the equation and solving for the approximate initial increment in  $\tilde{\beta}$  we obtain the relation

$$\delta \tilde{\beta} \approx \sin \tilde{\beta} \cos \tilde{\beta} \delta D/D \quad (2.35)$$

where  $\beta = \beta_1$ ,  $\delta D = D_{TR} - D_1$ , and  $D = D_{TR}$ . Then, with an elevation angle

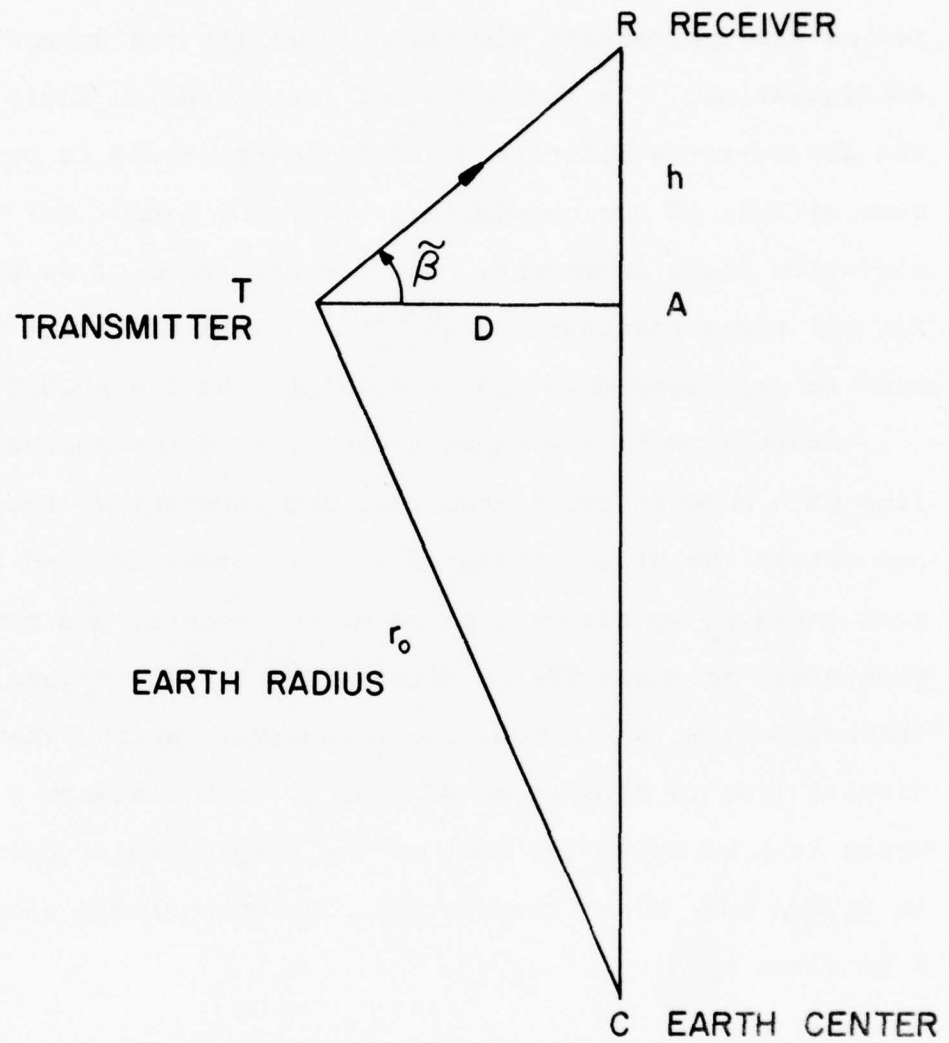


Figure 2.15. Earth geometry for finding the optical elevation angle.

$\beta_2 = \beta_1 + \delta\beta$  we proceed in the same manner as that described in section 2.2.3 to find the true homing elevation angle.

### 2.3.3 Examples and Discussion

In order to illustrate our homing technique we present two examples, one for ground-to-satellite and the other for the satellite-to-ground case. In both examples we studied the homing technique for the different oblique frequencies. The initial elevation angle is independent of the frequency of transmission. Since the straight line path approximation approaches the true path for high frequencies we expect the initial elevation angle to be very close to the true homing elevation angle.

#### Example 1. Ground-to-satellite.

Let the transmitter and receiver geographic coordinates be (-165.0, 72.0) and (-170.0, 56.0) longitude and latitude respectively. Also, let the transmitter and receiver heights above the earth surface be 0.0 and 560.0 km respectively. Then, for such a configuration the ground distance at the transmitter radius is 1793.97 km, the azimuthal angle of transmission is 190.1 degrees, and the initial approximate elevation angle is 8.475. The oblique transmission frequencies considered for this example were 90, 170, and 250 MHz. For each of these frequencies and starting with an elevation angle of 8.475 degrees we utilize the ray tracing program through subroutine ADJUST. The result of the calculation is presented in Figure 2.16. From Figure 2.16 we note that as the frequency gets higher the number of steps needed to achieve homing decreases. We also note that neither matrix

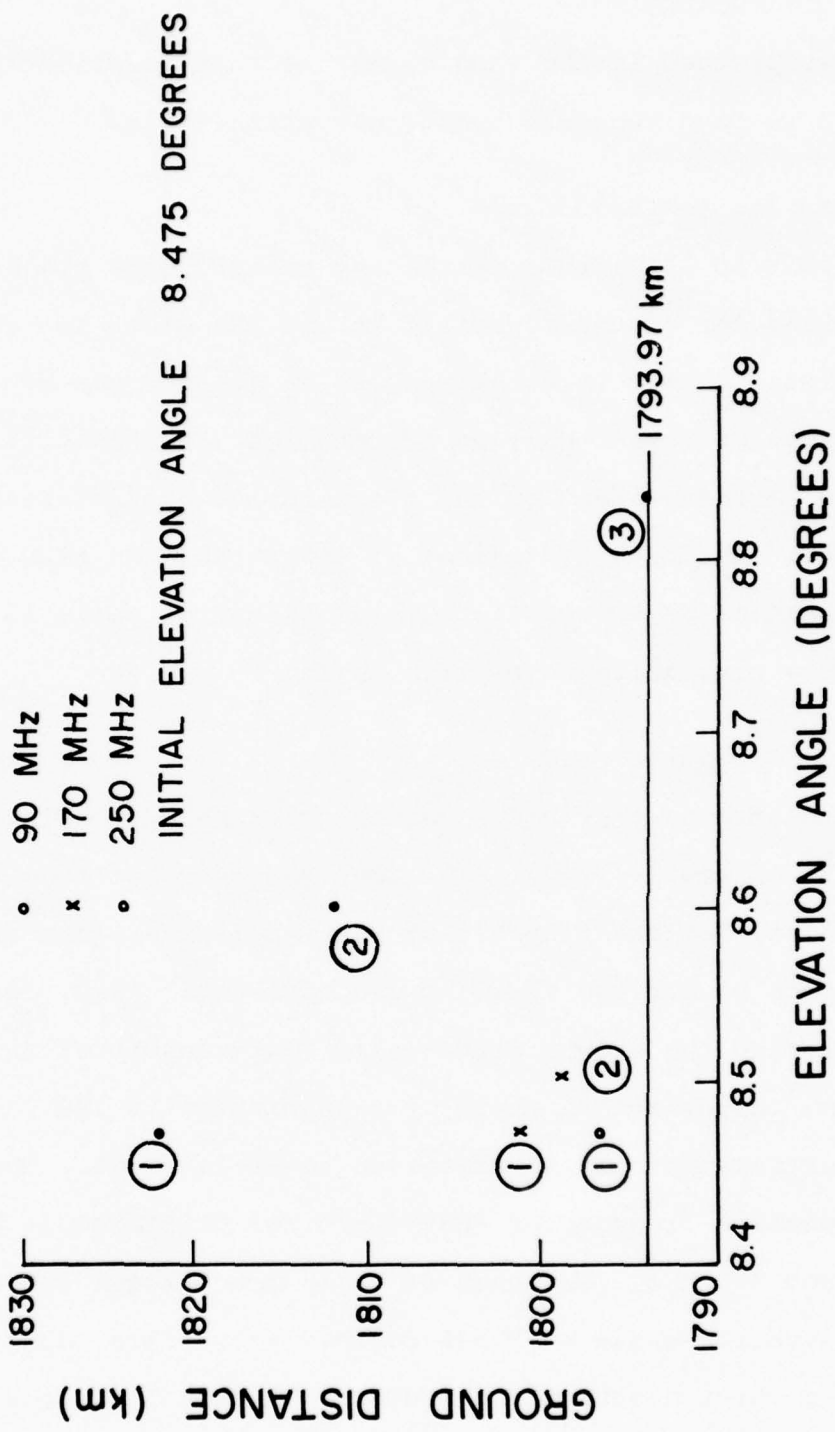


Figure 2.16. Example illustrating ground-to-satellite homing. The plot shows ground distance between the transmitter and the sub-satellite point versus the elevation angle for successive iterations using 3D ray tracing at three frequencies 90 MHz, 170 MHz and 250 MHz.

Figure 2.16.

inversion nor linear interpolation is needed to achieve homing for all three frequencies. In Figure 2.17 the geomagnetic colatitude is plotted versus the geomagnetic longitude to show the homing steps for the three frequencies. For all frequencies the figure shows that no azimuthal correction is needed.

#### Example 2. Satellite-to-ground

For this example we let the transmitter and receiver be located at (-150.0, 78.0) and (-165.0, 60.0) longitude and latitude respectively. We also let the transmitter and receiver heights above the earth surface be at 550 and 0.0 km. For these geographic coordinates the ground distance at the transmitter radius is 2251.96 km, the azimuthal angle of transmission is 203.87 degrees, and the initial approximate elevation angle is -23.472 degrees. For each of the oblique frequencies 70, 140, and 210 MHz we used routine ADJUST to find the homing elevation angle. Figure 2.18 shows the ground distance versus the elevation for all frequencies together with the number of steps needed to achieve homing. For the 70 and 140 MHz it takes 4 steps while for 210 MHz only 3 steps are needed. One linear interpolation and one matrix inversion are required for the 70 and 140 MHz while one linear interpolation is carried out for 210 MHz. Figure 2.19 displays the geomagnetic colatitude versus geomagnetic longitude for the three frequencies. This figure shows the number of steps along the azimuth of transmission for each frequency. Homing for all frequencies is achieved without azimuthal corrections.

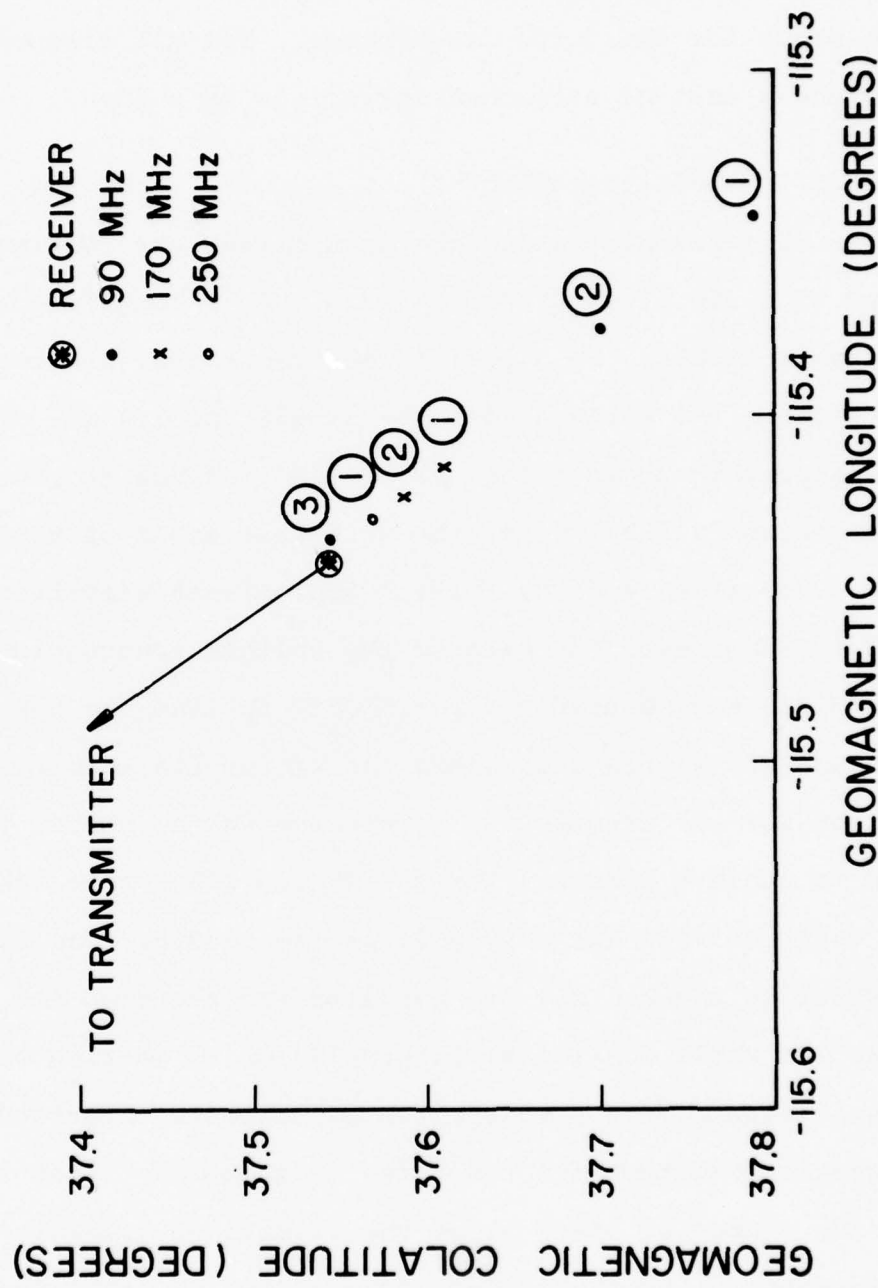


Figure 2.17. Continuation of example shown in Fig. 2.16 illustrating that no azimuthal correction is needed for homing at all three frequencies.

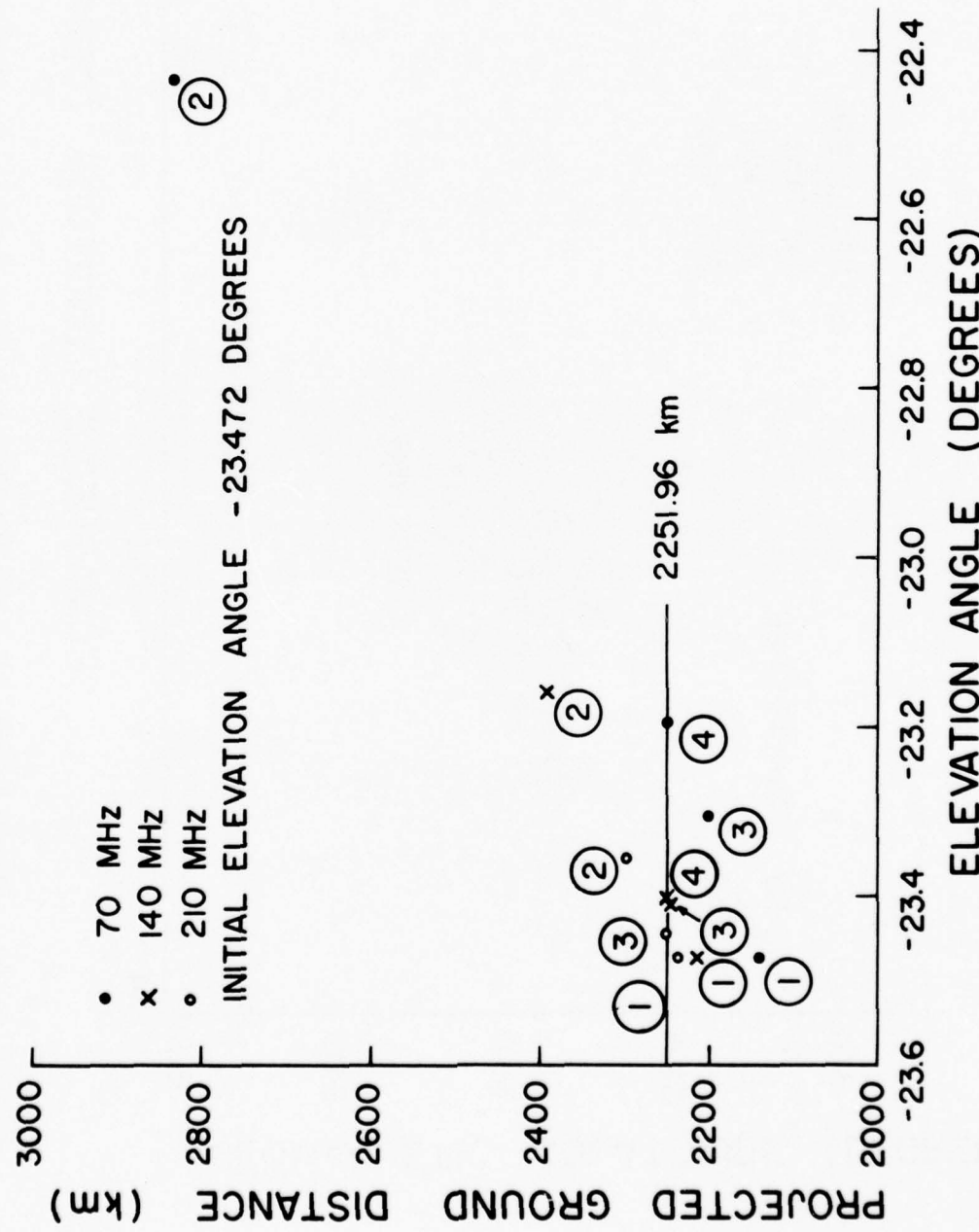


Figure 2.18. Example illustrating satellite-to-ground homing for three radio frequencies 70 MHz, 140 MHz, and 210 MHz.

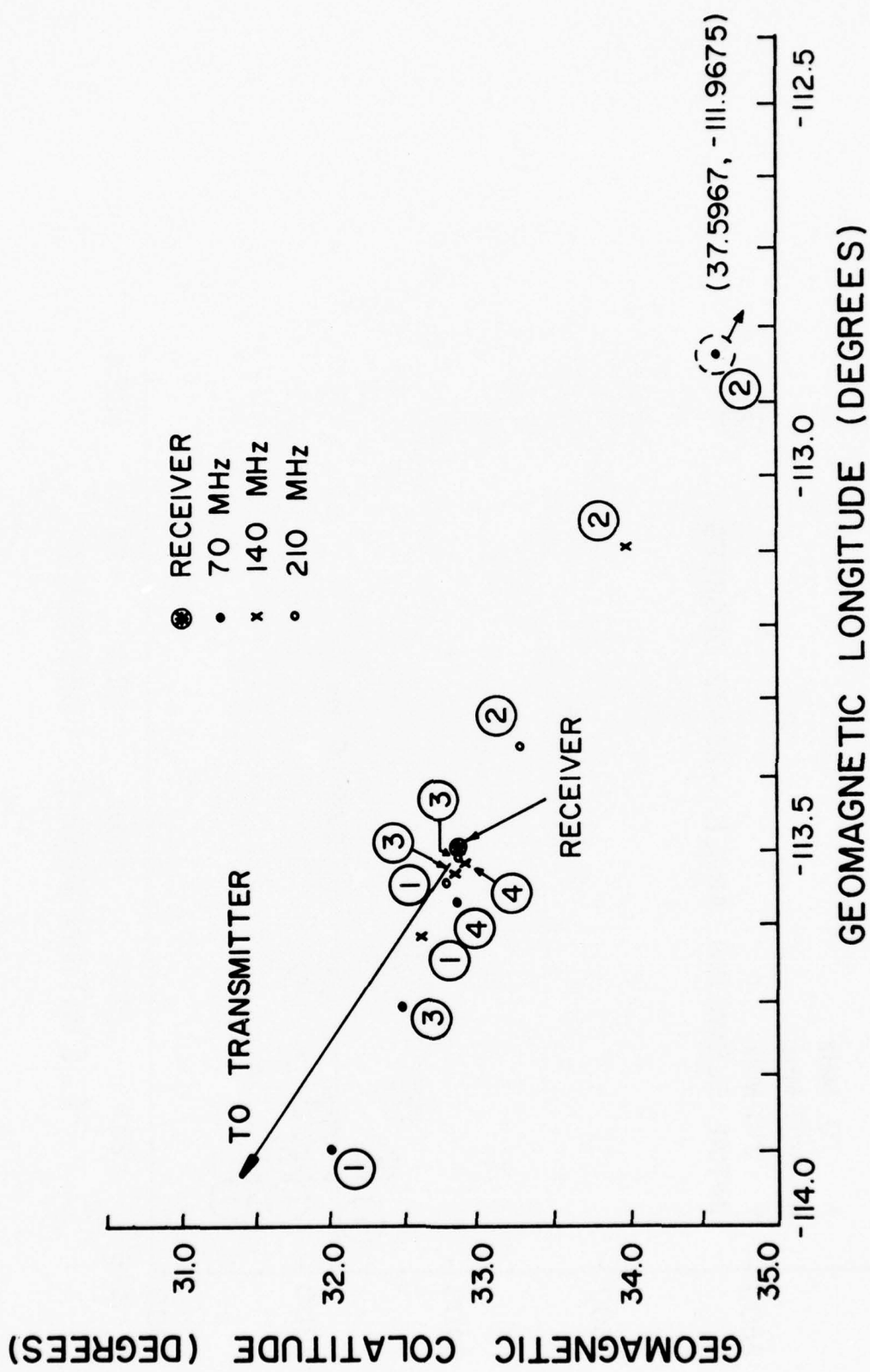


Figure 2.19. Continuation of example shows in Fig. 2.18 illustrating that no azimuthal correction is needed for homing at all three frequencies.

## 2.4 Minimum Group Path

The technique of backscatter ionogram inversion utilizes the values of the minimum group path computed for the given ionospheric profile. Therefore, it is necessary to extend the ray tracing program to include the numerical computation of the minimum group path. The complete method is documented in subroutine GROUP M.

### 2.4.1 The Chopping Method

We assume that the transmitter location, the ionospheric model, the oblique transmission frequency, and the azimuthal angle are given. In addition, the minimum group path tolerance  $\delta P'$  is also specified. At the present, the minimum group path tolerance is internally specified with a value of 1 km. With the known transmitter coordinates we can select the closest ionospheric model and find an approximate penetration angle  $\beta_p$ . This approximate angle is found through equation (18). Utilizing the ray tracing program and the given ionosphere we correct the approximate penetration angle until  $\beta_1$  is just below the penetration condition. Since  $\beta_p$  is approximate we could encounter two main possibilities; either  $\beta_p$  is larger or smaller than the true penetration angle. Very seldom  $\beta_p$  will be equal to the true penetration angle and this situation is included in the cases where  $\beta_p$  is larger or smaller. For the case where  $\beta_p$  is larger than the true penetration angle we successively decrement  $\beta_p$  by one percent i.e.  $\beta_{pi} = 0.99\beta_{pi-1}$ ,  $i=1,2,3,\dots$ , and obtain  $\beta_1$  just below  $\beta_p$ . While in the case where  $\beta_p$  is smaller we successively increment  $\beta_p$  by five percent i.e.  $\beta_{pi} = 1.05\beta_{pi-1}$ ,  $i=1,2,3,\dots$  until the

ray penetrates the ionosphere and then we successively decrement  $\beta_p$  by one percent and obtain  $\beta_1$  just below  $\beta_p$ .

Associated with  $\beta_1$  is a group path  $P'_1$ . In order to locate the minimum group path we need three points along the group path versus elevation angle curve. The general behavior of this curve is shown in Figure 2.20. Define  $\beta_2$  and  $\beta_3$  as ninety five (95) and ninety (90) percent of  $\beta_1$  and generate their corresponding group path values  $P'_2$  and  $P'_3$  through ray tracing. A comparison test is then performed on  $P'_1$ ,  $P'_2$ , and  $P'_3$ . If  $P'_1 > P'_2 > P'_3$  as in Figure 2.21a we discard  $\beta_1$  and  $P'_1$ , shift indices backward and calculate a new  $\beta_3$  equal to ninety five (95) percent of the old  $\beta_3$ . With the new  $\beta_3$  we generate a new group path  $P'_3$ . On the other hand, if  $P'_1 < P'_2 < P'_3$  as in Figure 2.21b we discard  $\beta_3$  and  $P'_3$ , shift indices forward and calculate a new  $\beta_1$  equal to 105 percent of the old  $\beta_1$ . With this new  $\beta_1$  we generate a new group path  $P'_1$ . In either case we repeat the comparison tests on  $P'_1$ ,  $P'_2$ , and  $P'_3$  until the condition  $P'_1 > P'_2$  and  $P'_3 > P'_2$  is satisfied.

Let us assume that we finally arrive at the situation depicted in Figure 2.21c where the condition  $P'_1 > P'_2$  and  $P'_3 > P'_2$  is satisfied. Then, in order to decide whether the minimum group path has been found or not we consider the following steps;

Step 1. Utilizing the chopping technique we take  $\beta_4$  and  $\beta_5$  at the mid point of the intervals  $\beta_1$ ,  $\beta_2$  and  $\beta_2$ ,  $\beta_3$  respectively. Tracing two rays with  $\beta_4$  and  $\beta_5$  we obtain two group paths  $P'_4$  and  $P'_5$ .

Step 2. If  $|P'_5 - P'_2| > \delta P'$  then we transfer to actions taken in step 3; otherwise, we have arrived at the minimum group path and a decision is made to select the

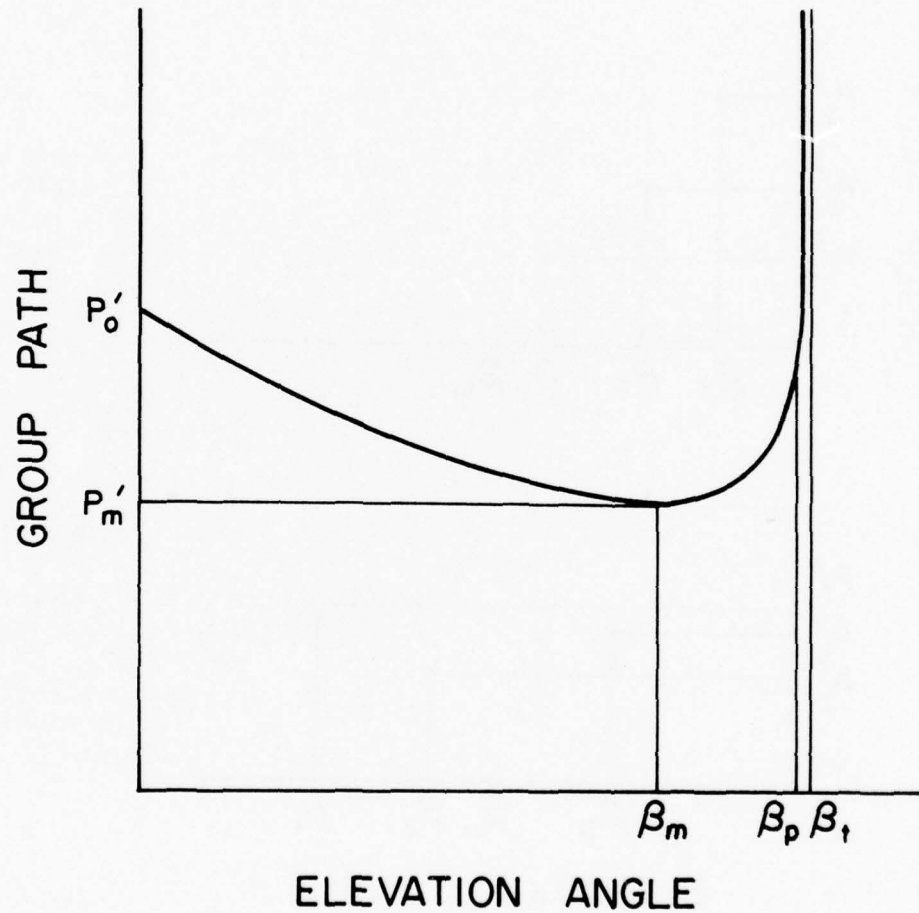


Figure 2.20. Sketch showing the general behavior of group path versus elevation angle curve.

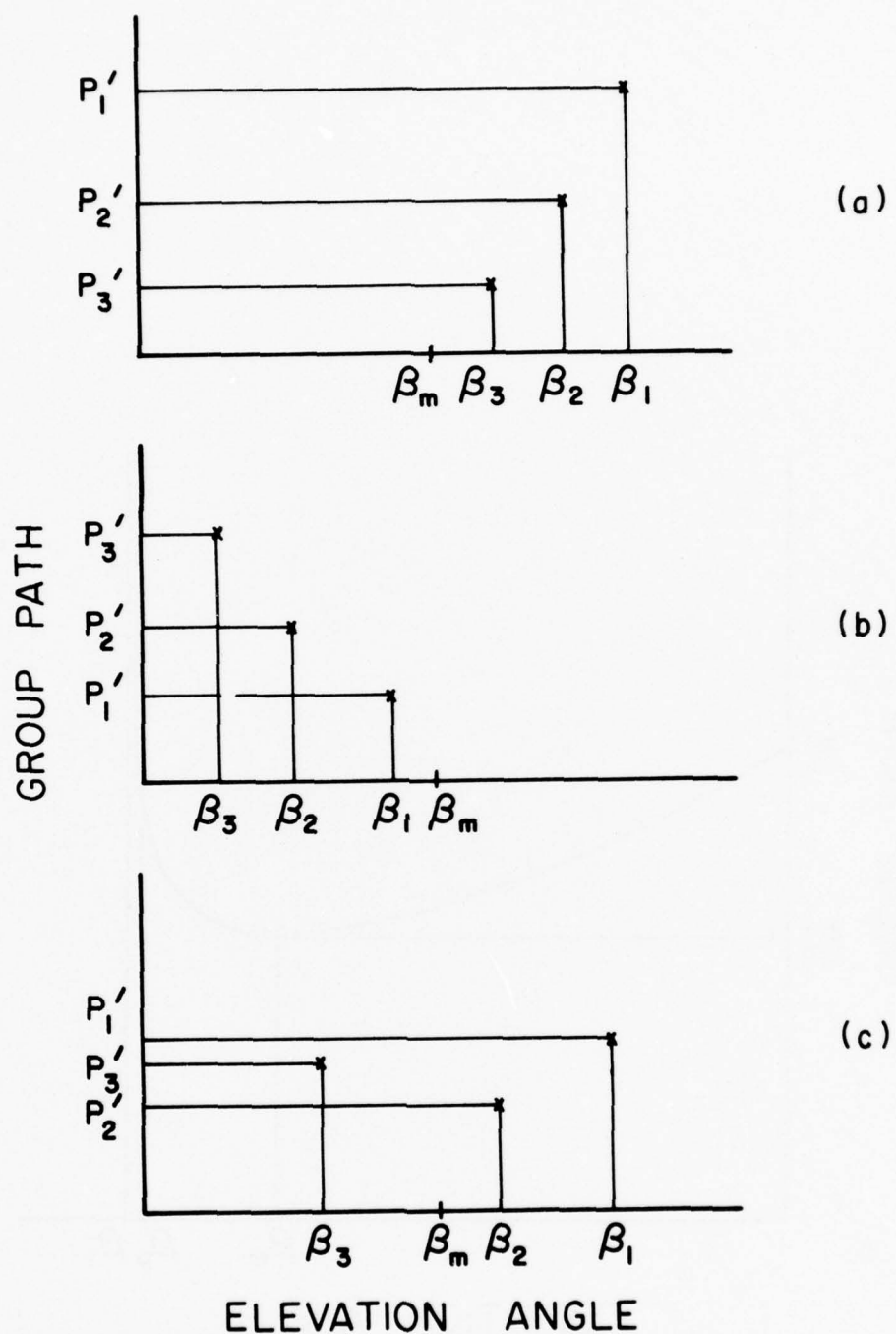


Figure 2.21. Sketch illustrating three possibilities for purpose of finding the minimum group path ray.

smallest of  $P'_2$ ,  $P'_4$ , and  $P'_5$ .

Step 3. If  $P'_5 > P'_2$  then we concentrate on actions taken in step 4. For  $P'_5 < P'_2$ , the interval given by  $P'_3 > P'_5$  and  $P'_2 > P'_5$  is our main concern. In this interval we replace the values of  $\beta_1$ ,  $\beta_2$ ,  $P'_1$ ,  $P'_2$  by the values  $\beta_2$ ,  $\beta_5$ ,  $P'_2$ ,  $P'_5$  respectively and start over from step 1.

Step 4. If  $|P'_4 - P'_2| > \delta P'$  then we transfer to actions taken in step 5. Otherwise, we have arrived at the minimum group path and a decision is made to select the smaller of  $P'_2$  and  $P'_4$ .

Step 5. If  $P'_4 > P'_2$  then we concentrate on the interval given by  $P'_5 > P'_2$  and  $P'_4 > P'_2$  and replace the values of  $\beta_1$ ,  $\beta_3$ ,  $P'_1$ ,  $P'_3$  by the values  $\beta_5$ ,  $\beta_4$ ,  $P'_5$ ,  $P'_4$  respectively. Otherwise, our main concern is the interval given by  $P'_2 > P'_4$  and  $P'_1 > P'_4$ . In this interval we replace the values  $\beta_2$ ,  $\beta_3$ ,  $P'_2$ ,  $P'_3$  by the values  $\beta_4$ ,  $\beta_2$ ,  $P'_4$ ,  $P'_2$  respectively. In either case we transfer to step 1 and start over again.

Once the minimum group path is found, control is transferred to the main program to perform a prescheduled activity in accordance with the input data through the W array.

#### 2.4.2 Examples

In order to illustrate the technique of finding the minimum group path we present two examples. Both examples are derived from the same transmitter location at -175 and 40 degrees geographic longitude and latitude respectively. In the first example the azimuthal angle of transmission is 330 degrees and the oblique

frequency of transmission is 12 MHz, while in the second example the azimuthal angle and the oblique frequency are 308 degrees and 10 MHz respectively.

Example 1.

For an oblique frequency of 12 MHz the penetration angle from equation (2.18) is found to be 52.91 degrees. Starting with  $\beta_1 = 52.9$  we generate the group path  $P'_1$  through ray tracing. Following the discussion in section 2.4.1 we take 95 and 90 percent of  $\beta_1$  and define them as  $\beta_2$  and  $\beta_3$ . The values of  $\beta_2$  and  $\beta_3$  then are given by 50.26 and 47.62 degrees. The corresponding group path values  $P'_2$  and  $P'_3$  are found to be 1077.37 and 1022.81 km. Since  $P'_1 > P'_2 > P'_3$  we discard  $\beta_1$  and  $P'_1$  and shift the indices backward to obtain  $\beta_1 = 50.26$ ,  $P'_1 = 1077.37$ ,  $\beta_2 = 47.62$  and  $P'_2 = 1022.81$ . Taking 95% of 47.62 degrees we generate  $\beta_3 = 45.24$  and its corresponding group path  $P'_3 = 995.86$ . From the values thus known we still have  $P'_1 > P'_2 > P'_3$ . Discarding  $\beta_1$  and  $P'_1$ , taking 95% of 45.24 degrees we obtain the following three sets of values,  $\beta_1 = 47.62$ ,  $P'_1 = 1022.81$ ,  $\beta_2 = 45.24$ ,  $P'_2 = 995.86$ ,  $\beta_3 = 42.98$ ,  $P'_3 = 981.11$ . Since the condition  $P'_1 > P'_2 > P'_3$  is still satisfied we carry out the same operations as above and arrive at the values  $\beta_1 = 45.25$ ,  $P'_1 = 995.86$ ,  $\beta_2 = 42.98$ ,  $P'_2 = 981.11$ ,  $\beta_3 = 40.83$ ,  $P'_3 = 973.56$ . Comparison of the group path values reveal that  $P'_1 > P'_2 > P'_3$  is the prevailing condition. Therefore, the next set of values are  $\beta_1 = 42.98$ ,  $P'_1 = 981.11$ ,  $\beta_2 = 40.83$ ,  $P'_2 = 973.56$ ,  $\beta_3 = 38.79$ ,  $P'_3 = 973.17$ . Since the condition  $P'_1 > P'_2 > P'_3$  is satisfied we carry out the calculations once more and arrive at the situation given by the values  $\beta_1 = 40.83$ ,  $P'_1 = 973.56$ ,  $\beta_2 = 38.79$ ,  $P'_2 = 973.17$ ,  $\beta_3 = 36.85$ ,  $P'_3 = 976.87$ . An examination

of the group path values shows that the condition  $P'_1 > P'_2$  and  $P'_3 > P'_2$  is satisfied. Following the chopping method steps we find  $\beta_4$  and  $\beta_5$  at the midpoint of the intervals  $\beta_1$ ,  $\beta_2$ , and  $\beta_2$ ,  $\beta_3$ , respectively. With the values of  $\beta_4 = 39.81$  and  $\beta_5 = 37.82$  we find the group path values  $P'_4 = 972.60$  and  $P'_5 = 974.07$ . Going to step 2 of the chopping method we find that  $|P'_5 - P'_2| > \delta P' = 1$ . Therefore, we find the minimum group path, it is either  $P'_2$ ,  $P'_4$  or  $P'_5$  whichever is the smallest. In this case the minimum group path is given by  $P'_4 = 972.60$  and the elevation angle is  $\beta_4 = 39.81$ . Figure 2.22 shows the group path versus elevation angle for the values generated under this example. The test sequence and indices shifting is also displayed on the graph.

#### Example 2.

In this example we use an azimuthal angle of 308 degrees and an oblique frequency of 10 MHz. The result of the calculation, testing and the value of the minimum group path are displayed in Figure 2.23. The circled numbers beside each point is the sequence calculation number. The table in the figure presents the sequence of operations performed before converging on the minimum group path value. In this example also the chopping technique is applied only once to achieve the final result.

### 2.5 Computer Programs

During the course of the study we augmented the 3D ray tracing program with six subroutines. They are discussed in the following.

#### 2.5.1 General Description

For each of these subprograms we will be presenting

AZIMUTHAL ANGLE 330 DEGREES  
 OBLIQUE FREQUENCY 12 MHz  
 GROUP PATH TOLERANCE 1 km

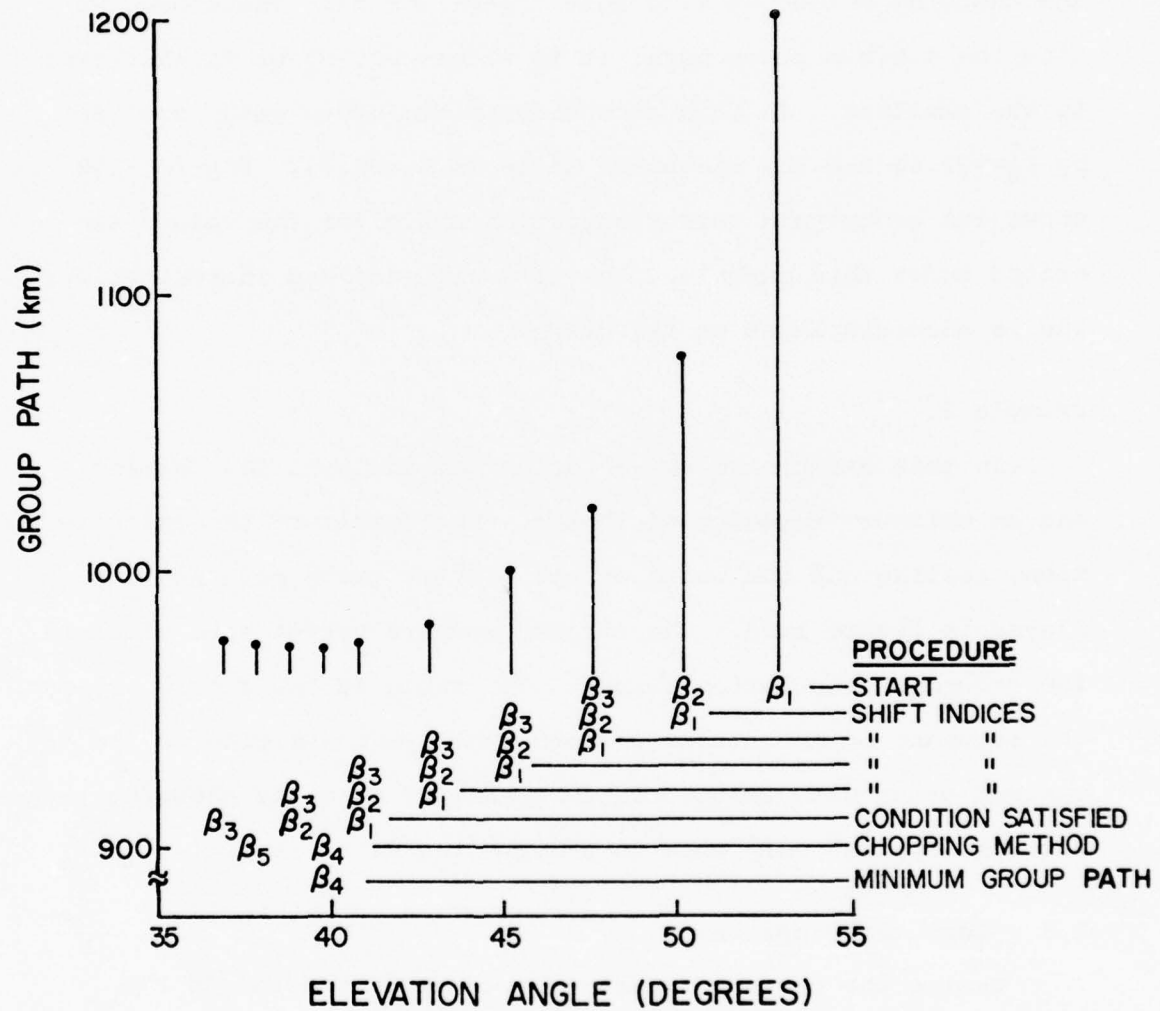


Figure 2.22. Example illustrating the steps in finding the minimum group path ray in a group path versus elevation angle plot. Note the index shifting, equal chopping and final location of the minimum group path to within the tolerance.

AZIMUTHAL ANGLE 308 DEGREES  
 OBLIQUE FREQUENCY 10 MHz  
 GROUP PATH TOLERANCE 1 km

#	$\beta_1$	$\beta_2$	$\beta_3$	$P'_1$	$P'_2$	$P'_3$	$\beta_4$	$\beta_5$	$P'_4$	$P'_5$
1	78.28	74.36	70.45	948.38	899.78	862.87	-	-	-	-
2	74.36	70.45	66.93	899.78	862.87	837.53	-	-	-	-
3	70.45	66.93	63.58	862.87	837.53	819.36	-	-	-	-
4	66.93	63.58	60.40	837.53	819.36	806.67	-	-	-	-
5	63.58	60.40	57.38	819.36	806.67	798.30	-	-	-	-
6	60.40	57.38	54.51	806.67	798.30	793.28	-	-	-	-
7	57.38	54.51	51.79	798.30	793.28	791.73	-	-	-	-
8	54.51	51.79	49.20	793.28	791.73	793.19	53.15	50.49	792.50	791.83
9	-	51.79	-	-	791.73	-	-	-	-	-

GRUOP PATH (km)

950

900

850

800

750

40 45 50 55 60 65 70 75 80

ELEVATION ANGLE (DEGREES)

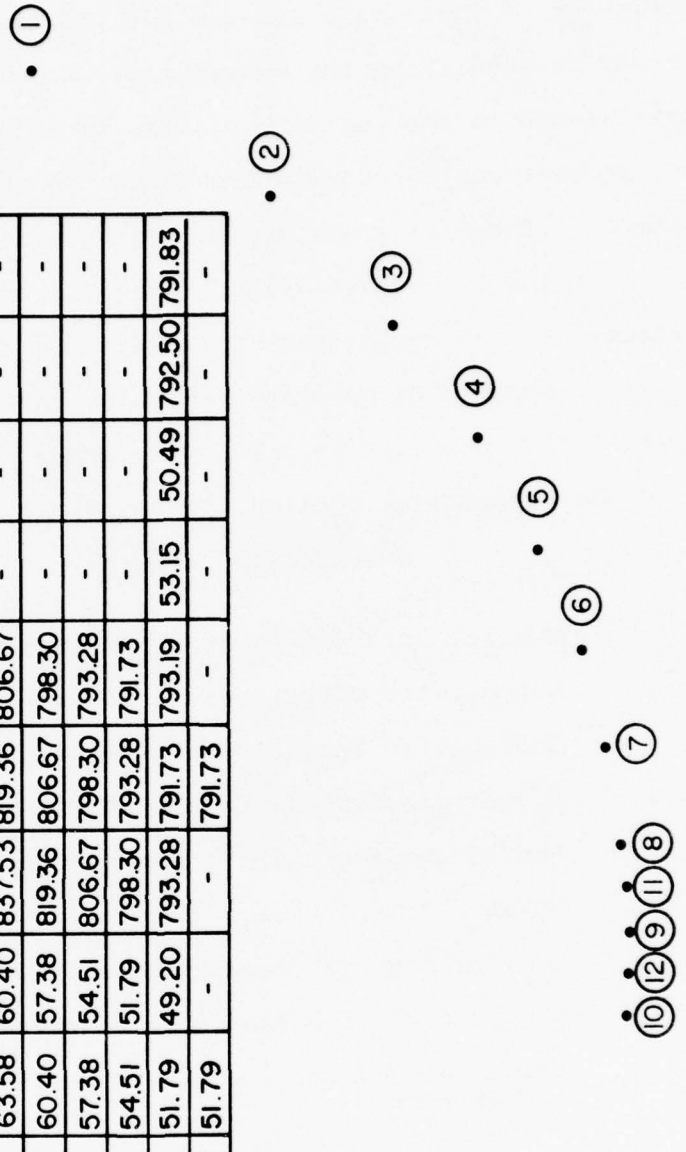


Figure 2.23. Another example illustrating the steps in finding the minimum group path ray.

a description of their main purpose and the functions they perform.

Prior to describing the subprograms we present a list of the controls needed to successfully run the three dimensional ray tracing program for the homing cases and the minimum group path calculation. These controls are either internal or external allocations in the already existing W-array input data. The internal allocations are equivalence statements in the subprograms and there is no need to specify them. The external allocations are specified by the user in the input data of the W-array. The internal and external allocations of the W-array are:

W	Description	Internal (In) External (Ex)
371	Control used for penetration conditions	(In)
372	Geomagnetic colatitude of the ray	(In)
373	Geomagnetic longitude of the ray	(In)
374	Local azimuthal deviation of the ray	(In)
375	Radial distance to the transmitter	(In)
376	ALPHA	(In)
377	THO, geomagnetic colatitude of transmitter	(In)
378	PHO, geomagnetic longitude of transmitter	(In)
379	Azimuthal deviation of the ray at the transmitter	(In)
0	regular ray tracing	
1	ground-to-ground homing	
380	2 ground-to-satellite or satellite-to-ground homing	(Ex)
3	minimum group path	
381	Geographic East longitude of receiver in degrees	(Ex)
382	Geographic latitude north of receiver in degrees	(Ex)

383	Height of the ray above the earth surface	(In)
384	Ground distance computed in PRINTR	(In)
385	Ground distance computed from the geometry of the problem	(In)
386	Maximum number of iterations for finding the approximate elevation angle	(Ex)
387	The tolerance allowed between the ground distance in W(385) and calculated ground distance	(Ex)
389	Penetration angle used in homing	(In)
390	Height of the bottom of the ionosphere above earth	(Ex)
391	Maximum height of the ionosphere above earth	(Ex)
393	0 utilizes the given ionospheric profile 1 generates a new ionospheric profile based upon the given quasi-parabolic parameters	(Ex)
394	Value of the group path used in the group path homing	(Ex)

#### Subroutine HOME

##### Purpose:

The HOME subroutine calculates the initial approximate elevation angle in the ground-to-ground homing for the ground distance and the group path.

##### Description:

The HOME routine calculates several parameters and generates tables prior to obtaining the final result of initial approximate elevation angles. The azimuthal angle of transmission and the exact ground distance are computed from the given transmitter and receiver coordinates. The midpoint between the transmitter and receiver is found and the electron density profile at this midpoint is extracted from the given ionospheric profile. With

the critical frequency of the midpoint profile and the given oblique frequency of transmission the penetration angle is computed from equation (2.18). Then, the elevation angle interval from zero to this penetration angle is subdivided into 50 intervals thus generating 51 values of elevation angles. For each value of elevation angle in the interval a ground distance and a group path value are calculated from the analytical expressions for a quasi-parabolic density profile. These analytical expressions are programmed in subroutine FITT. Through this procedure a table of elevation angles, ground distances, and group paths is assembled.

The exact ground distance is then compared to the ground distance values in the table. If the exact ground distance is lower or higher than the ground distances in the table, then no approximate elevation angles can be found. However, if the exact ground distance is located between two ground distances in the table, we interpolate linearly to find an approximate elevation angle. Since there might be more than one homing solution we scan through the table and locate all possible elevation angles.

The HOME subroutine is capable of storing approximate elevation angles for a four layered ionosphere. In addition, this subroutine has been mainly written for the single hop mode of propagation. The two hop mixed mode of propagation is already included as described in section 2.2.6.

#### Subroutine HOMES

##### Purpose:

The HOMES subroutine calculates the initial approximate ele-

vation angle for a straight line path in the ground-to-satellite and the satellite-to-ground configurations.

Description:

Given the transmitter and receiver coordinates and the oblique transmission frequency subroutine HOMES computes the azimuthal angle of transmission and the ground distance projected at the transmitter radius. Assuming a straight line path between the transmitter and receiver, the approximate elevation angle is found from the triangle in the plane containing the transmitter, the receiver, and the earth center.

Subroutine FITT

Purpose:

Given an elevation angle routine FITT calculates the corresponding ground distance and group path from analytical expressions for a quasi-parabolic density profile.

Description:

Utilizing the analytical expression given by equations (2.13) - (2.16), the electron density profile at the midpoint of the path between the transmitter and receiver, and the oblique frequency of transmission, subroutine FITT computes the ground distance and the group path for a specified elevation angle. The contributions of ground distances and group paths are added up from the transmitter height up to the ray reflection height. The integration step corresponds to the height increment of the electron density profile at the midpoint.

**Subroutine RAYINT****Purpose:**

Routine RAYINT initializes the ray parameters before any actual ray tracing is performed.

**Description:**

The code in subroutine RAYINT is extracted from the main subprogram of the ray tracing program to enable the homing and minimum group path procedures to function independently from the main program. With a specified elevation and azimuthal angles this subroutine initializes the ray parameters prior to tracing the ray via subroutine TRACE.

**Subroutine ADJUST****Purpose:**

The ADJUST subroutine takes the approximate elevation angles for any of the three configurations, ground-to-ground, ground-to-satellite, or satellite-to-ground and modifies them through the ray tracing program to achieve homing.

**Description:**

Utilizing the initial elevation angle a ray is traced in the ionospheric profile to obtain a ground distance value. Then, the initial elevation angle is incremented or decremented by a small amount depending upon the configuration under consideration. In the ground-to-ground case the initial increment or decrement is found from the table assembled in subroutine HOME, while in the other two cases the initial increment or decrement is found from equation (2.35). Adjusting the initial elevation angle by the initial increment or decrement we obtain a new elevation angle

and a corresponding ground distance through ray tracing. The objective is to locate the exact ground distance between the ground distances of the traced rays. Sometimes, the rays are homed without further calculations and at other times we cannot locate the exact ground distance between the ground distances obtained through ray tracing at which point a message is printed. Let us assume that the exact ground distance lies between the two ground distances obtained from ray tracing. With the two values of elevation angles and their corresponding ground distances we interpolate linearly and find a third elevation angle. Utilizing this third elevation angle we trace another ray to obtain the ground distance. If the ray is not homed in yet, we have three elevation angles and their ground distances. Since the variation between ground distance and elevation angle is nonlinear we fit a second degree polynominal in elevation angle and invert the resulting matrix to find a new elevation angle that will eventually home the ray.

With this elevation angle we trace a ray and find the ground distance. A comparison test on the ground distances will reveal whether or not homing is achieved. In the event that homing is not achieved, the procedure of fitting the second degree polynomial is repeated utilizing the closest three ground distances to the exact ground distance and their corresponding elevation angles. Then, either homing is achieved and no further calculations are needed, or the above procedure is repeated to attain homing. Homing may not be achieved due to discontinuities in the ray-traced ground distance versus elevation angle curve, high angle ray, or that the maximum number of specified trials to find

an elevation angle have been exceeded.

Subroutine GROUPM

Purpose:

Subroutine GROUPM calculates the minimum group path for given transmitter coordinates, azimuthal angle of transmission and an oblique transmission frequency.

Description:

With the given transmitter coordinates, the closest density profile is selected from the composite ionospheric profile. From the knowledge of the critical frequency of the selected profile and the oblique frequency of transmission, the penetration angle is computed through equation (2.18). Then, starting with this penetration angle we initialize the ray parameters and trace a ray through the given ionosphere. If the ray penetrates the ionosphere we decrement the elevation angle (penetration angle) by one percent and trace another ray. This procedure is repeated until the ray is reflected and a value for the group path is obtained. There, we take 95 or 90 percent of the resulting elevation angle thus generating two new elevation angles. With these two new elevation angles we trace two rays to obtain their corresponding group path values. The three values of elevation angles and their corresponding group paths describe a curve. This curve may assume three shapes, sloping to the left (most common), sloping to the right (rare) or concave upwards. In the cases where the curve is sloping to the right or left we increment or decrement the elevation angle and trace rays until the shape of the curve is concave upward. For this shape the values

of the group paths are compared with each other to test for the minimum value within a specified 1 km tolerance.

Let us assume that we did not attain the minimum group path value, then we subdivide the two intervals in the curve and obtain two elevation angles, one in each interval, thus generating two additional intervals. Through ray tracing we obtain two values of group paths corresponding to the two new elevation angles. A test is performed between the five group path values and the largest two are discarded retaining only three values and their corresponding elevation angles. Through repeated application of this procedure we converge on the minimum group path value with the specified tolerance of 1 km. This tolerance is imbeded in the subroutine and could be changed to any desired value.

#### 2.5.2 Program Listings

A complete listing of all the programs discussed in this section is given in Appendix 1.

## 2.6 Discussion

We have modified the three dimensional ray tracing program to include the homing features for ground-to-ground, ground-to-satellite, and satellite-to-ground configurations. In addition, the ray tracing program has been augmented by a chopping technique to find the minimum group path. In the preceding sections we presented in detail the approach and methods utilized in the homing of the ray together with representative examples. We also outlined the purpose and description of each computer subprogram added to the originally supplied AFCRL three dimensional ray tracing program.

The results of our homing approach for the one hop mode of propagation show that homing is almost always achieved provided the input parameters are correctly entered through the input data. We say almost since there are situations where homing of the ray may not be possible. During the course of our study we came across three situations in the ground-to-ground case whereby homing might not be possible. These three situations are

- i) high angle ray
- ii) ground distance too close to the skip distance or discontinuity in the ray traced ground distance versus elevation angle curve.
- iii) number of tries to find an elevation angle is exceeded.

A preliminary investigation of the two mixed hop mode of propagation has been initiated and the technique has been implemented in the HOME subroutine. The application of our technique to achieve homing is only partially successful; the ray was homed in for a few cases while for the majority of the cases tested we

encountered difficulties in homing of the ray. These difficulties may be attributed to the following reasons:

- i) the coarseness of the given ionospheric profile
- ii) the interpolation procedure used in the ray tracing program
- iii) the technique applied to the two hop mode

Through further research, the true nature of the problem could be pinpointed and if need be a sophisticated homing technique for the multi-hop mode of propagation can be developed.

Aside from the homing problems, we have also incorporated a chopping method to find the minimum group path. The results of such a method are quite evident from the examples presented in section 2.4.2. For all the cases studied we have been successful in finding the minimum group path within the specified tolerance. The number of steps needed to obtain the minimum group path decreases as the frequency of transmission gets higher. Once we arrive at the condition whereby the variation of group path versus elevation angle curve is concave upward, the convergence of the chopping method is very fast.

From the results presented in this report and other examples derived from the techniques used in homing of the ray and finding the minimum group path it is quite evident that we have been successful in achieving our objective. The difficulties encountered during the course of this study could be overcome through modification and refinement of the ray tracing program and the ionospheric profile. Such modification and refinement can only be achieved through further research.

## 3. ANALYSIS OF OBLIQUE PROPAGATION DATA

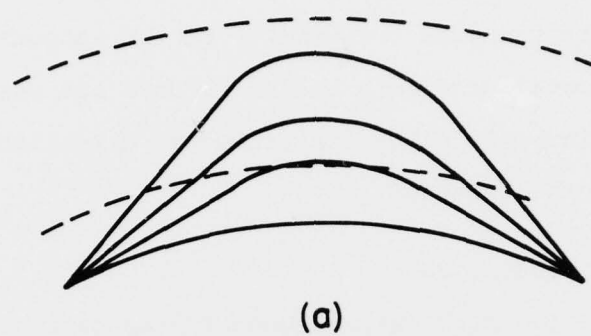
## 3.1 Introduction

The goal of this investigation is to devise techniques for inverting h.f. oblique radio propagation data for ionospheric models with horizontal gradients. There are two kinds of oblique propagation data: (a) Point-to-point oblique ionograms, and (b) Backscatter leading edge. In this section, we shall consider briefly the nature of these two types of data and discuss qualitatively their capabilities and limitations in providing information concerning ionospheric models with horizontal gradients.

## 3.1.1 Point-to-Point Oblique Ionograms

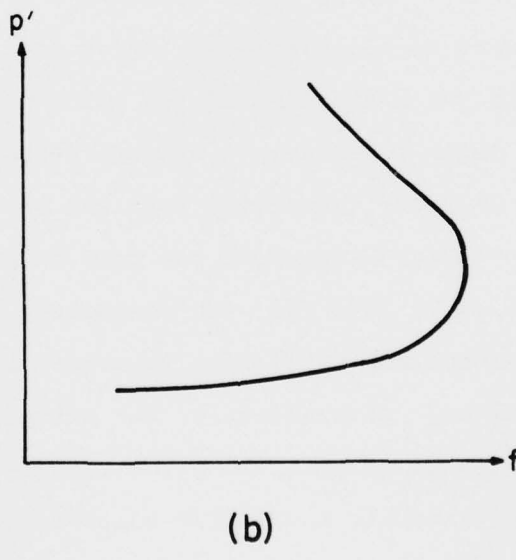
These are traces of group path ( $P'$ ) versus frequency ( $f$ ) for oblique propagation between two fixed points separated by some distance. Since the end points of the propagation path are fixed, the reflection points of the rays lie in the neighborhood of the midpoint between the transmitter (T) and receiver (R) for the one-hop mode of propagation, irrespective of the frequency, as shown in Fig. 3.1(a). Similarly, for multiple-hop mode of propagation, reflection for each hop occurs in the neighborhood of a single location, for all frequencies capable of propagating in that mode. A typical shape of the oblique ionogram trace for the one-hop mode is shown in Fig. 3.1(b).

It can be easily conjectured from Fig. 3.1(a) that a one-hop mode oblique ionogram is capable of providing an equivalent vertical profile of electron density valid near the midpoint between the transmitter and the receiver, but is not by itself too useful for deriving the horizontal gradients of electron density. How-



(a)

Figure 3.1a. Ray paths for point-to-point oblique ionograms at different frequencies.



(b)

Figure 3.1b. Typical shape of one-hop trace for point-to-point oblique ionogram.

ever, for a particular assumed model with horizontal gradients near the midpoint, it is in principle possible to deduce the parameters so as to achieve a best fit with the experimental ionogram. The use of a two-hop mode trace in addition to the one-hop mode trace would increase the utility of the ionogram for deriving the horizontal gradients but still does not permit their determination continuously along the azimuthal direction from the transmitter to the receiver.

### 3.1.2 Backscatter Leading Edge

In the case of the backscatter mode of propagation, the transmitter and the receiver are located at about the same location and the time delay of the transmitted signal backscattered from the ground and then received at the receiver is measured as a function of frequency. For a given frequency, many returns are possible corresponding to all elevation angles of transmission and reception within the bandwidths of the transmitting and receiving antennas. There is however a minimum value for the time delay which occurs near the transition from the low angle ray mode of propagation to the high angle ray mode of propagation, as shown in Fig. 3.2(a). Thus for each frequency, a continuum of backscattered returns beginning with the minimum time delay return will be received. Alternatively, the situation can be thought of as a continuum of point-to-point oblique ionograms corresponding to continuously increasing values of ground range of the backscatter location away from the transmitter. Such a continuum of oblique ionograms is shown in Fig. 3.2(b). The tangent curve to these ionograms is the "backscatter leading

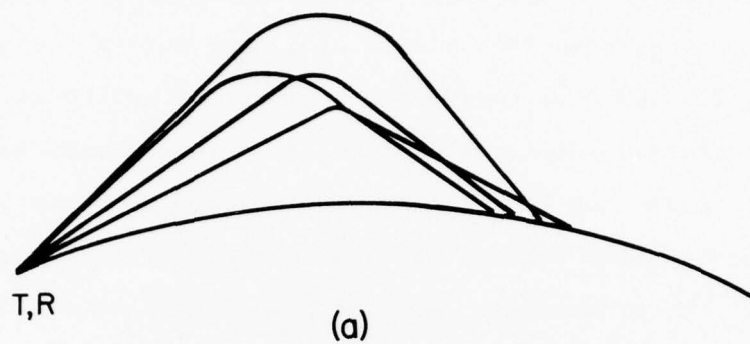


Figure 3.2a. Ray paths for backscattered rays at one frequency.

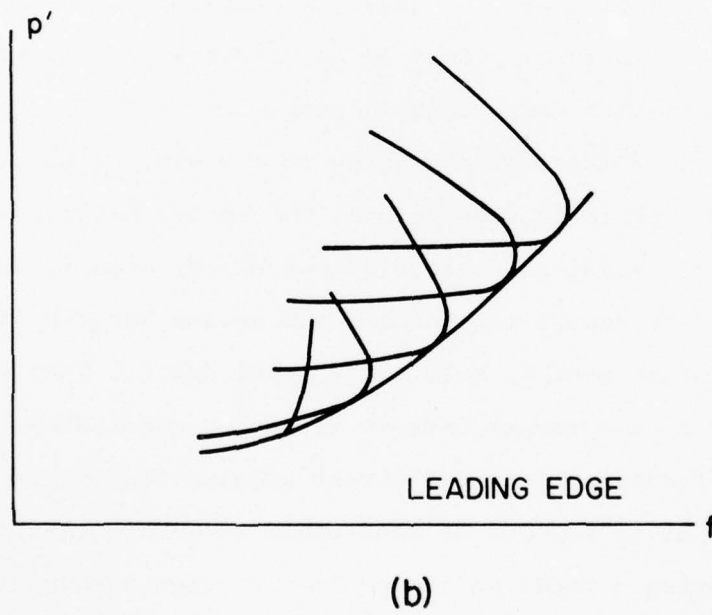


Figure 3.2b. Showing that the leading edge of a backscatter ionogram is the tangent curve to a continuum of point-to-point oblique ionograms.

edge", and is generally the only useful portion of the backscatter ionogram since all the other returns cannot be distinguished from one another, except in the case of high resolution ionograms.

It can now be seen from Fig. 3.2(b) that points along the backscatter leading edge correspond to rays reflecting at continuously increasing distant locations from the transmitter. Hence in principle the backscatter leading edge contains information concerning the horizontal gradients of electron density outward from the transmitter location along the azimuthal direction corresponding to the backscatter ionogram. However to obtain a vertical profile of electron density at any given location, a minimum number of points along an ionogram are required. For example, a quasi-parabolic profile requires a minimum of three points. If we consider three points on the backscatter leading edge, we must select them very close to each other in order to obtain the vertical profile corresponding to a given location. On the other hand, for three such points, the apogee heights of reflection for the corresponding rays do not differ significantly. Hence to increase the separation between the apogee heights of reflection, the points must be selected farther apart. Thus it becomes necessary to compromise between these two conflicting requirements. A further point of interest arising from these requirements is that it may not be profitable to invert the leading edge by employing a model which requires a large number of parameters to describe its vertical profile. This observation is augmented by the fact that simulated backscatter leading edge data using three-dimensional ray tracing indicates that the apogee heights of rays corresponding to points on the leading

edge lie within a narrow range of values. This also makes it impossible for the backscatter leading edge to provide the vertical profile above the maximum apogee height. However, as will be pointed out later, this is not a limitation insofar as the application of the leading edge data is concerned, although it may be a limitation for the purpose of obtaining the complete ionospheric structure up to the layer peak.

Thus in this introductory section, we point out that while the point-to-point oblique ionograms are capable of providing the vertical profile near the midpoint between the transmitter and the receiver, they are not too useful for obtaining horizontal gradients over wide ranges of distance along the line from the transmitter to the receiver. On the other hand, the backscatter leading edge, while unable to provide the vertical profiles above certain heights, is useful for deducing the horizontal gradients over wide ranges of distance along the azimuthal direction from the transmitter corresponding to the backscatter ionogram.

### 3.2 The Quasi-Parabolic Layer

Since the primary purpose of this investigation is to devise techniques capable of yielding the horizontal gradients of electron density, it can be seen from the discussion in the previous section that it becomes necessary to attach more importance to the backscatter leading edge data than to the point-to-point oblique ionogram data. Hence for selecting a model, the limitation of the leading edge data need to be considered. In view of this, an ionospheric model requiring a small number of parameters to

define its vertical profile is more suitable. Such a model, which is also amenable to analytical solution for the ray path parameters, as compared to numerical ray tracing, is the quasi-parabolic layer model. Hence this section is devoted to the quasi-parabolic layer.

### 3.2.1 The Earth Concentric Quasi-Parabolic Layer

The quasi-parabolic layer is defined by the variation of electron density  $N_e$  with the radial distance  $r$  from the center of the earth as given by

$$N_e(r) = \begin{cases} N_m [1 - \left(\frac{r-r_m}{y_m}\right)^2 \left(\frac{r_b}{r}\right)^2] & \text{for } r_b < r < r_m \left(\frac{r_b}{r_b-y_m}\right) \\ 0 & \text{otherwise} \end{cases}$$
(3.1)

where

$N_m = f_c^2 / 80.6$  = maximum value of electron density

$f_c$  = critical frequency

$r_m$  = value of  $r$  at which  $N_e$  is equal to  $N_m$

$r_b$  = value of  $r$  at the base of the layer

$y_m = r_m - r_b$  = semithickness of the layer

The slight modification over the parabolic model, which is defined by ignoring the factor  $(r_b/r)^2$  in (3.1), enables the derivation of exact closed form expressions for the ray path parameters for the quasi-parabolic layer (Croft and Hoogasian, 1968), by application of Bouguer's rule for ray tracing in a spherically symmetric layer. For a signal of frequency  $f$  and elevation angle

of transmission  $\beta$ , these expressions for the ground range  $R$ , and group path  $P'$  are given as follows (Rao, 1974; Rao, 1975):

$$R = 2r_0 \left\{ (\gamma - \beta) - \frac{F r_0 \cos \beta}{2\sqrt{C}} \ln \frac{Ur_b^2}{W^2} \right\} \quad (3.2)$$

$$P' = 2(1 - \frac{F^2}{A}) r_b \sin \gamma - 2r_0 \sin \beta - \frac{BF}{2A^2} \ln \frac{U}{V^2} \quad (3.3)$$

where

$$\begin{aligned} F &= f/f_c \\ \gamma &= \cos^{-1} \left( \frac{r_0 \cos \beta}{r_b} \right) = \text{elevation angle at the base} \\ &\quad \text{of the layer} \end{aligned}$$

$r_0$  = radius of the earth

$U = B^2 - 4AC$

$V = 2Ar_b + B + 2r_b F\sqrt{A} \sin \gamma$

$W = 2\sqrt{C} Fr_b \sin \gamma + 2C + Br_b$

$A = F^2 - 1 + (r_b/y_m)^2$

$B = -2r_m r_b^2 / y_m^2$

$C = \left( \frac{r_b r_m}{y_m} \right)^2 - F^2 r_0^2 \cos^2 \beta$

To find the minimum group path, which is equal to the minimum time delay times the velocity of light in free space, we first note that for a given frequency and for a given set of layer parameters, the elevation angle of transmission corresponding to the minimum group path ray is given by the solution of the equation

$$\begin{aligned}\frac{\partial P'}{\partial \beta} &= 2 \left(1 - \frac{F^2}{A} + \frac{BF^2}{AV}\right) r_0 \sin \beta \cos \gamma \\ &\quad - 2 \left(1 - \frac{2BF^3 r_0 \sin \beta}{\sqrt{A} U}\right) r_0 \cos \beta \\ &= 0\end{aligned}\tag{3.4}$$

Recognizing that  $\partial P'/\partial \beta$  varies continuously from a large negative value near zero elevation angle to a large positive value near maximum elevation angle corresponding to penetration of the ray through the layer, we can solve (3.4) for  $\beta$  in an iterative manner. The penetration condition occurs for the ray apogee radius equal to  $-B/2A$  and hence for the elevation angle of transmission given by

$$\beta_p = \cos^{-1} \left\{ \frac{1}{Fr_0} \left[ \left( \frac{r_b r_m}{y_m} \right)^2 - \frac{B^2}{4A} \right]^{\frac{1}{2}} \right\}\tag{3.5}$$

Thus starting with values of  $\beta$  near zero and  $\beta_p$ , the value of  $\beta$  for which  $\partial P'/\partial \beta$  is a small specified value can be found in an iterative manner. Substitution of this value of  $\beta$  in (3.2) then gives the value of the minimum group path,  $P'_{\min}$ .

In the formulation of the procedures for inversion of the point-to-point oblique ionograms and backscatter leading edges for quasi-parabolic layer parameter, we will find later that the partial derivatives of  $R$  and  $P'$  with respect to the layer parameters are required. Expressions for these quantities, which can be easily derived from (3.2) and (3.3) are given in the appendix.

### 3.2.2 The Eccentric Quasi-Parabolic Layer

In papers by Rao (1968, 1973), the ionospheric layer has

been assumed to be still spherical but eccentric with respect to the earth. Figure 3.3 shows the geometry pertinent to such a layer with its center  $C'$  displaced by vector  $\vec{D}$  from the earth's center  $C$ . Assuming quasi-parabolic distribution of electrons in the eccentric layer, the spherical geometry of the system with respect to its own center enables us to use the formulas for the concentric case (Section 3.2.1) with some additional computations introduced by Rao (1968). Thus the eccentric quasi-parabolic layer model, which permits the existence of gradients in the electron density, is completely defined by the following six parameters:

- $f_c$  : critical frequency of the layer
- $h_o$  : vertical distance between the base of the ionosphere and the surface of earth along vector  $\vec{D}$
- $y_m$  : semi-thickness of the layer
- $D$  : the distance between the centers of the earth and the ionosphere
- $w_t$  : the angle between the displacement vector  $\vec{D}$  and the radius of earth through the transmitter
- $\alpha$  : an angle pertinent to the azimuthal angle of transmission

For simplicity, we assume no gradient lateral to the transmission path ( $\alpha = 0$ ) and the model is then defined by the first five parameters. The consideration of non zero  $\alpha$  will not affect the presented techniques and will only add an additional dimension to the problem.

It is essential to have a feel for the type and amount of

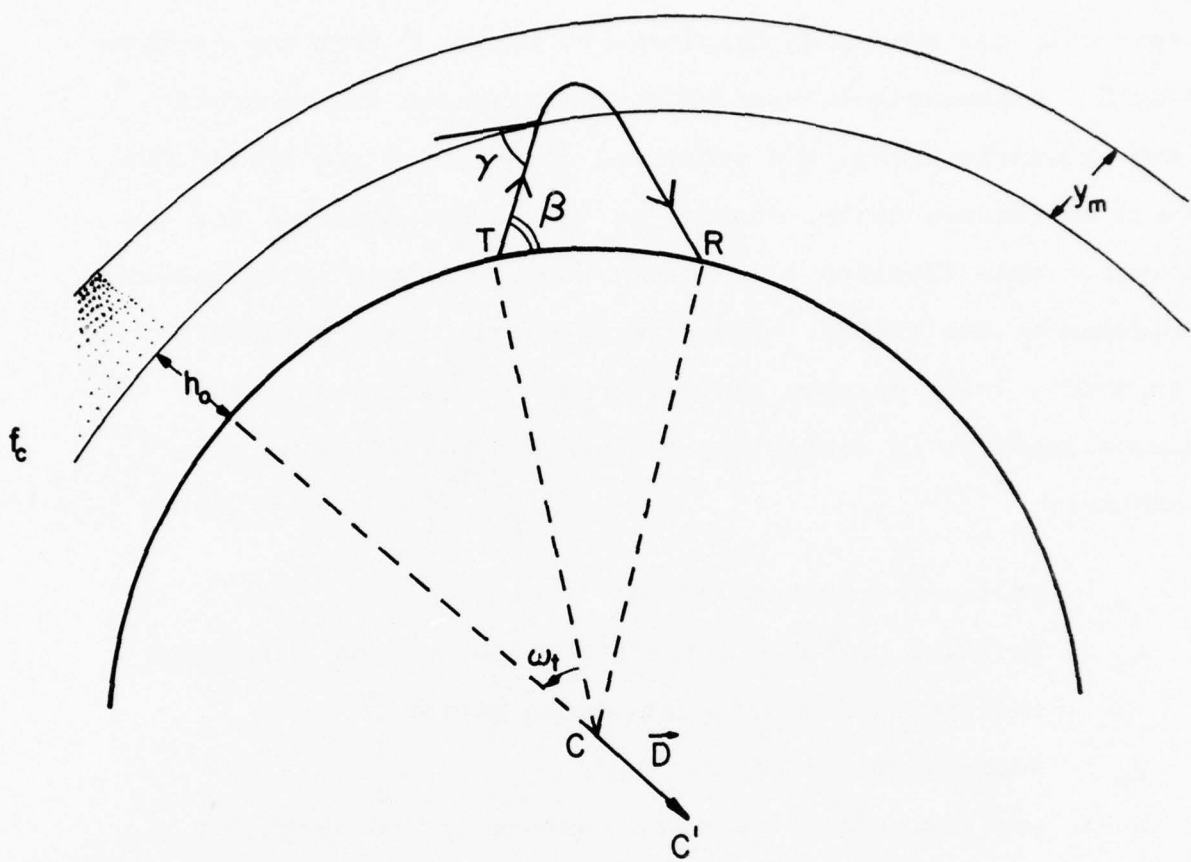


Figure 3.3. The eccentric quasi-parabolic layer with its defining parameters.

the gradients introduced by  $D$  and  $\omega_t$  parameters of the eccentric layer. To accomplish this, we must make a few simplifying assumptions and approximations. The geometry of Figure 3.3 suggests that we have gradients in the base and peak heights of the layer. To obtain realistic relative values for these two gradients, we will assume that the base height of the layer above the transmitter be a constant value for all cases. In Figure 3.4,  $T$  and  $R$  are the locations of the transmitter and the receiver with  $M$  and  $\theta_0$  being the location and the angle of their mid-point. The base heights of the layer above  $T$  and  $R$  are denoted by  $h'_0$  and  $h''_0$ . Expressions can now be derived for the gradients at angle  $\theta_0$  (approximately where the reflection takes place).

The equation of the base-height circle can be written as

$$(x + D \cos \omega_t)^2 + (y + D \sin \omega_t)^2 = D^2 + (r_0 + h'_0)^2 + 2D(r_0 + h'_0) \cos \omega_t \quad (3.6)$$

Writting (3.6) in polar coordinates, we get

$$r^2 + 2rD[\cos(\theta - \omega_t)] = (r_0 + h'_0)^2 + 2D(r_0 + h'_0) \cos \omega_t \quad (3.7)$$

Differentiating 3.7 with respect to  $\theta$ , we have

$$2r \frac{\partial r}{\partial \theta} + 2D \frac{\partial r}{\partial \theta} \cos(\theta - \omega_t) - 2Dr \sin(\theta - \omega_t) = 0$$

$$\left. \frac{\partial r}{\partial \theta} \right|_{\theta=\theta_0} = \frac{D \sin(\theta_0 - \omega_t)}{1 + \frac{D}{r'} \cos(\theta_0 - \omega_t)} \quad (3.8)$$

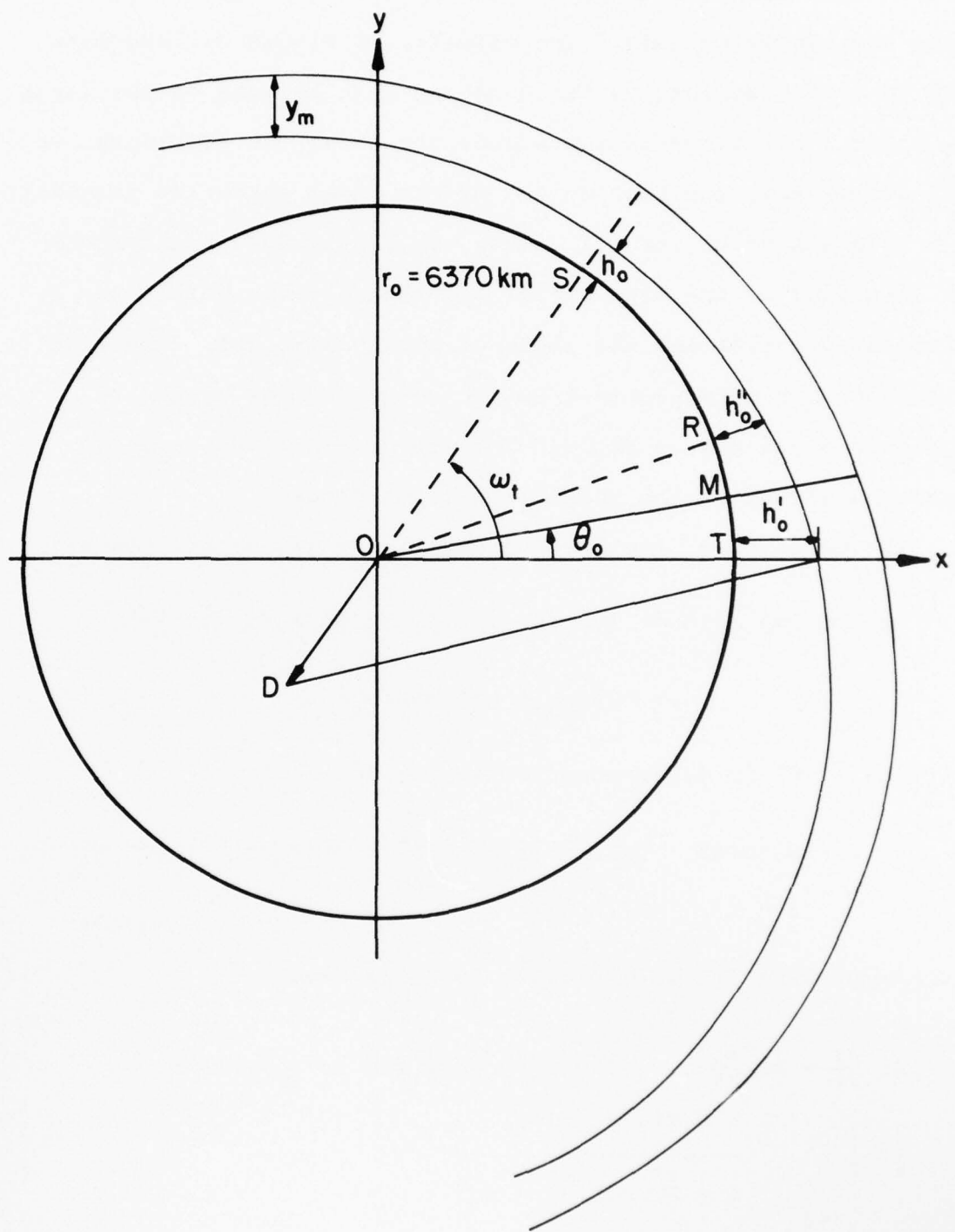


Figure 3.4. The geometry for computing gradients as a function of  $\omega_t$ ,  $D$ .

where

$$r' = r_0 + h'_0 \quad \text{for the base height gradient}$$

$$r' = r_0 + h'_0 + y_m \quad \text{for the peak height gradient.}$$

Since, in general  $r_0 \gg h'_0$  and  $y_m$ , we can assume that the gradient is equal for both base and peak heights ( $r' \approx r_0$ ).

As a typical example, let us assume  $\text{TOR} = 10^\circ$  corresponding to a ground range of  $R = 1111.8 \text{ km}$  ( $\theta_0 = 5^\circ$ ). The gradient given by (3.8) is evaluated for several values of  $D$  and  $\omega_t$  and Fig. 3.5 shows the peak height gradient ( $r' = 6370 + 150 + 200 = 6720 \text{ km}$ ) as a function of  $D$  for several values of  $\omega_t$ . Figure 3.5 also shows the forbidden regions, characterized by the ionosphere going underground at the receiver. This happens when the gradients are large, forcing the base height of the layer to be less than zero above the receiver ( $h''_0 < 0$ ). The quantity  $h''_0$  can be derived by solving (3.7) for  $r$  and setting  $\theta = 2\theta_0$ . Thus

$$r_0 + h''_0 = -D \cos(2\theta_0 - \omega_t)$$

$$+ \sqrt{D^2 \cos^2(2\theta_0 - \omega_t) + (r_0 + h'_0)^2 + 2D(r_0 + h'_0) \cos \omega_t}$$

(3.9)

The above equation can also be used to set an upper limit for  $h''_0$  as well as a lower limit. This will result in a usable region on Fig. 3.5 for the values of  $D$  and  $\omega_t$ .

AD-A038 299

ILLINOIS UNIV AT URBANA-CHAMPAIGN DEPT OF ELECTRICAL --ETC F/G 17/2.1  
TECHNIQUES OF DETERMINING IONOSPHERIC STRUCTURE FROM OBLIQUE RA--ETC(U)  
DEC 76 N N RAO, K C YEH, M Y YOUAKIM

F19628-75-C-0088

UNCLASSIFIED

2 OF 3  
AD  
A038 299

UILU-ENG-76-2559

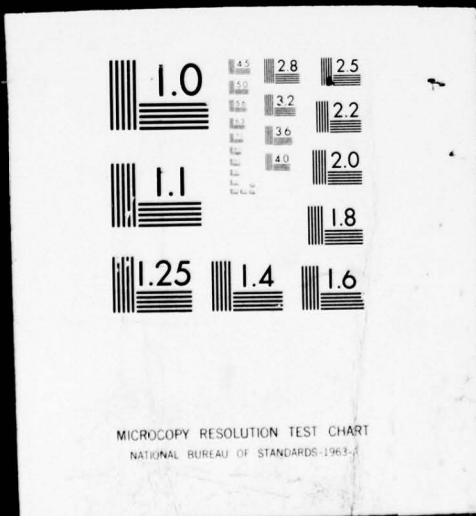
RADC-TR-76-401

NL



2 OF 3

AD  
A038 299



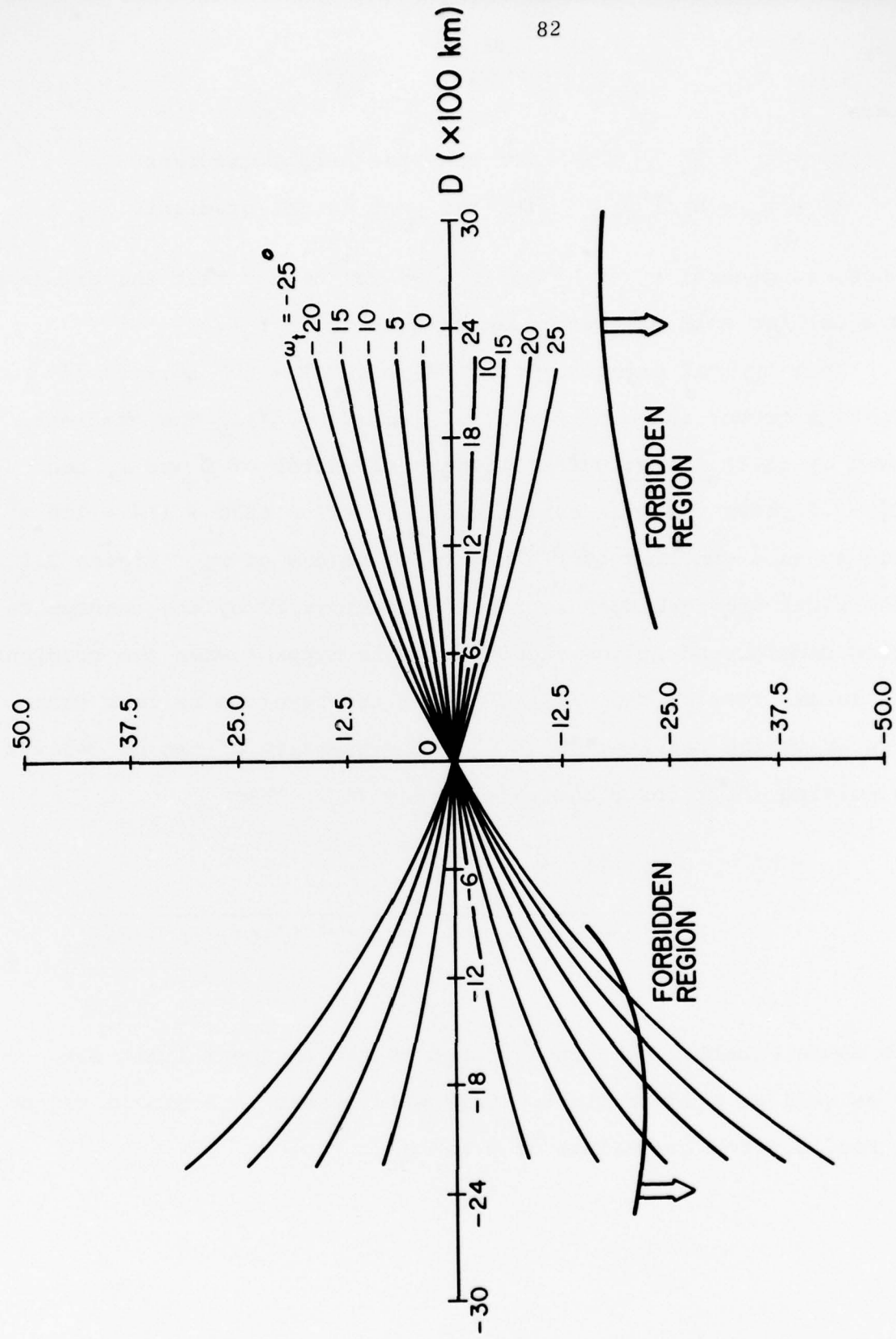


Figure 3.5. Peak height gradient as a function of  $D$  and  $\omega_t$ .

### 3.3 Inversion of Point-to-Point Oblique Ionograms

In this section, we report our investigation of techniques for inversion of point-to-point oblique ionograms. The inversion of such ionograms for earth-concentric ionospheric layers already exist in the literature. Hence, we consider here their inversion to a layer with horizontal gradients, and in particular the eccentric quasi-parabolic layer discussed in Sec. 3.2.2.

#### 3.3.1 Sensitivity Analysis

First we need to explore the individual behavior of the five parameters of the eccentric Q-P layer model with respect to numerically synthesized oblique ionograms, so that we can devise an efficient numerical procedure for inverting a given oblique ionogram to the model's parameters. In Figs. 3.6-3.10, four of the five parameters are held constant, with the fifth varying over a small range, and the resulting oblique ionograms are plotted. Investigation of these graphs shows that small changes in  $f_c$ ,  $h_0$ , and  $y_m$  parameters have a relatively linear effect on their respective ionograms, that is, the curves are shifted by a similar amount for equal changes in each of the three parameters. However, for changes in the gradient parameters ( $\omega_t$ , D), the shifted ionograms actually tend to converge to a certain curve and do not demonstrate the linear behavior associated with the variation of the first three parameters.

The above conclusion can also be verified from the geometric point of view. Since  $\omega_t$  is a periodic variable, the constructed ionograms will not be linearly shifted as the  $\omega_t$  parameter is increased. Also the constructed ionograms can be very insensi-

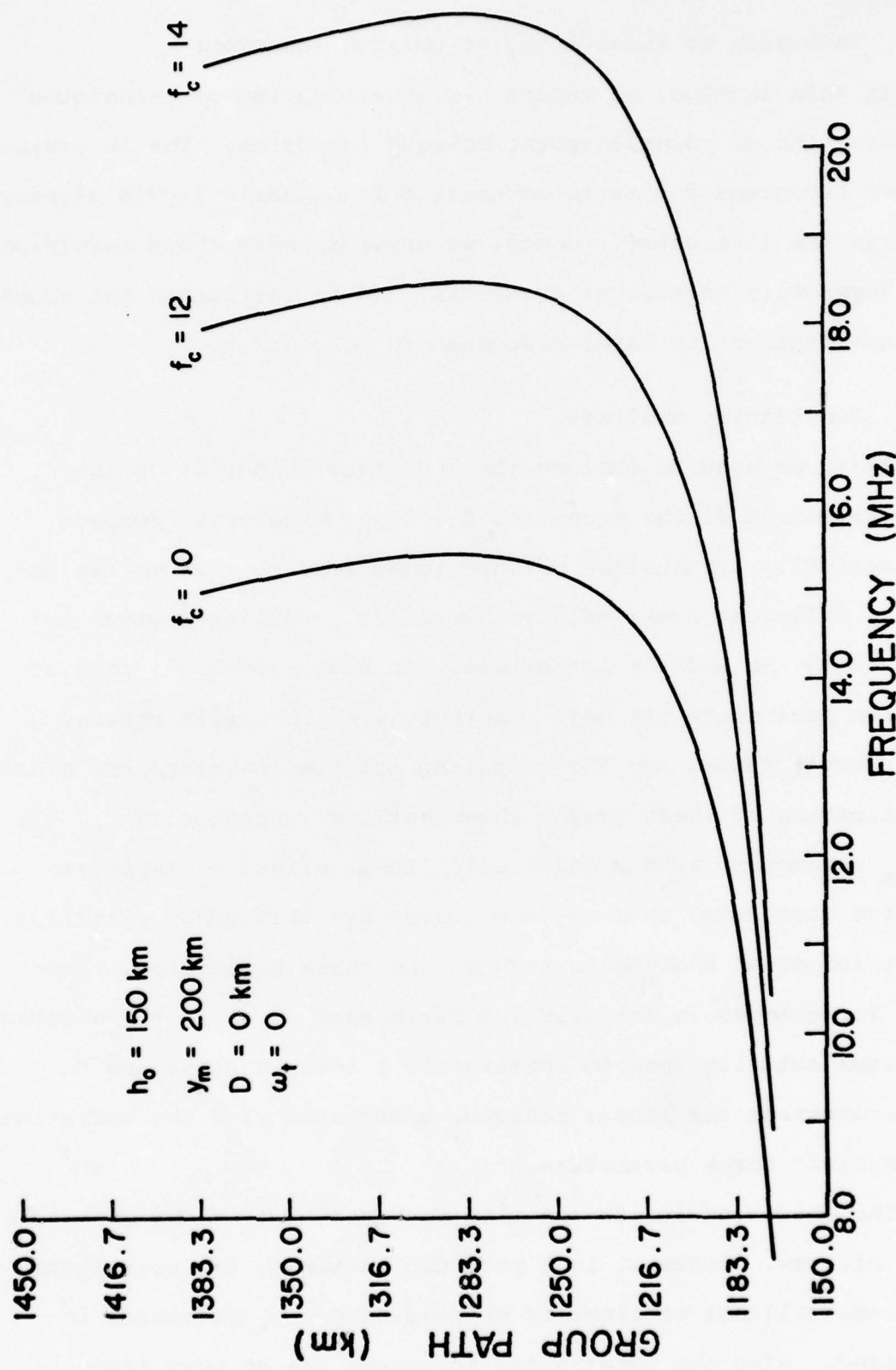


Figure 3.6. Effect of changing the  $f_c$  (critical frequency) parameter (in MHz).

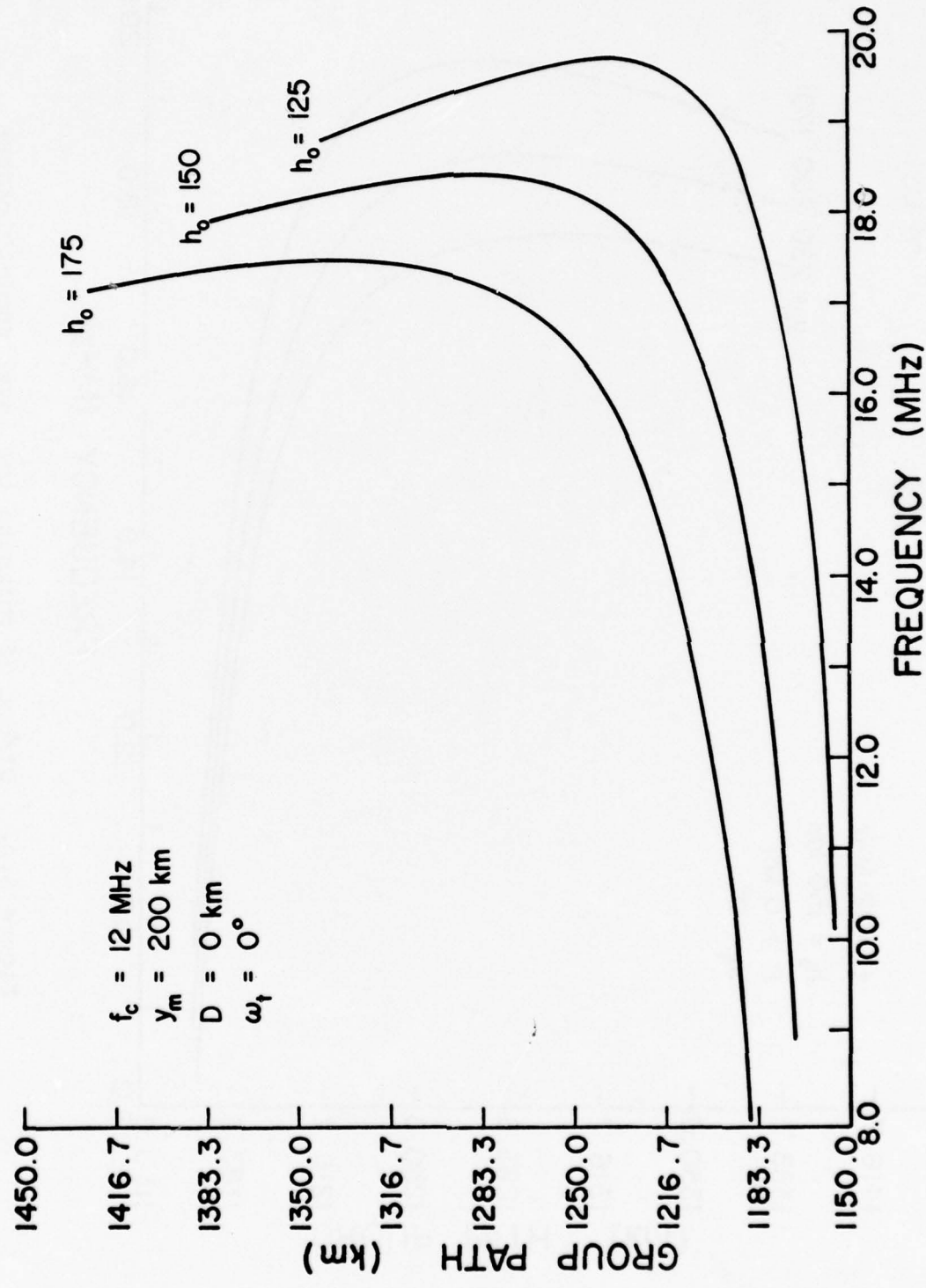


Figure 3.7. Effect of changing  $h_o$ ; the layer base-height  
(in km).

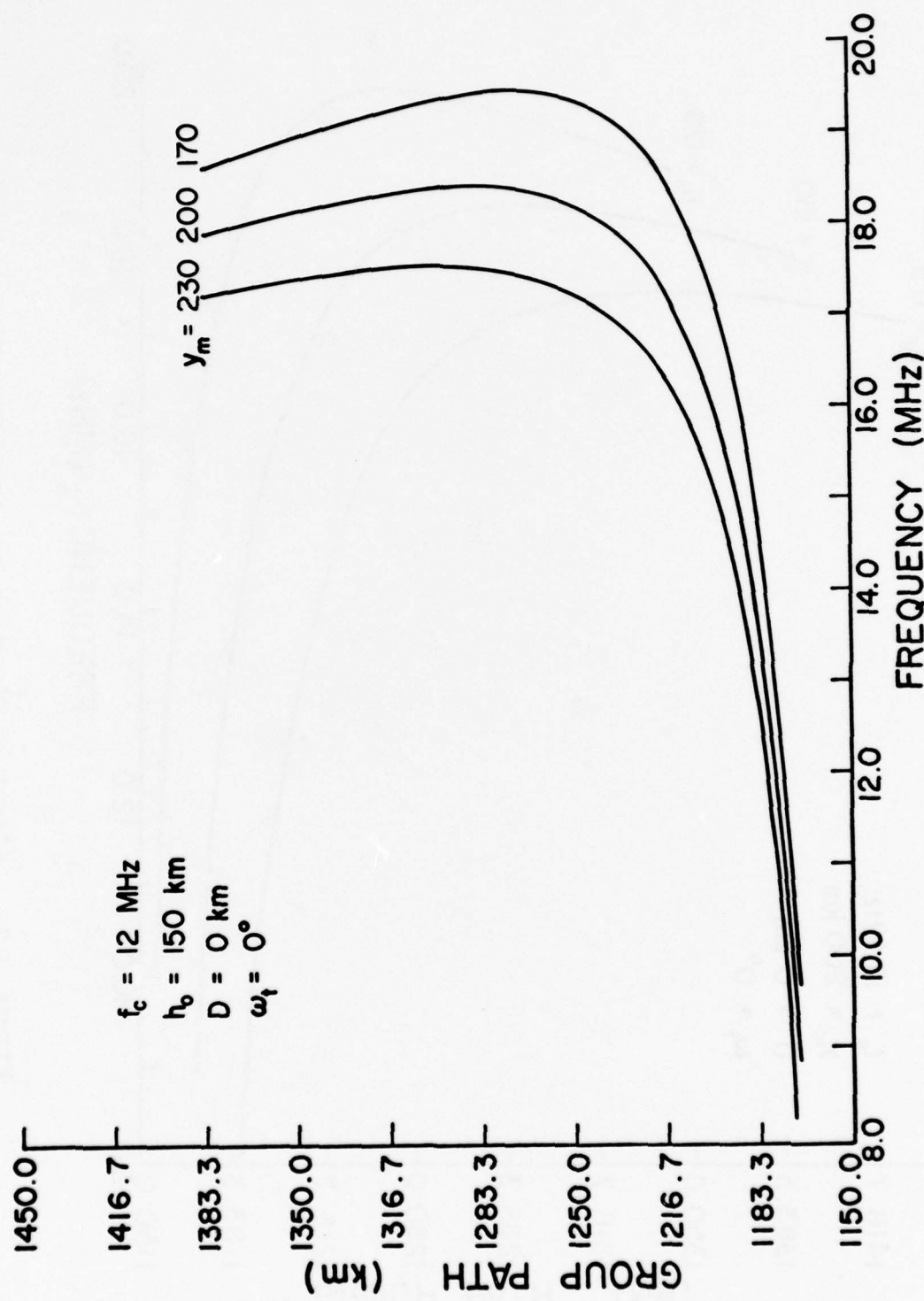


Figure 3.8. Effect of changing the layer semi-thickness  $y_m$  (in km).

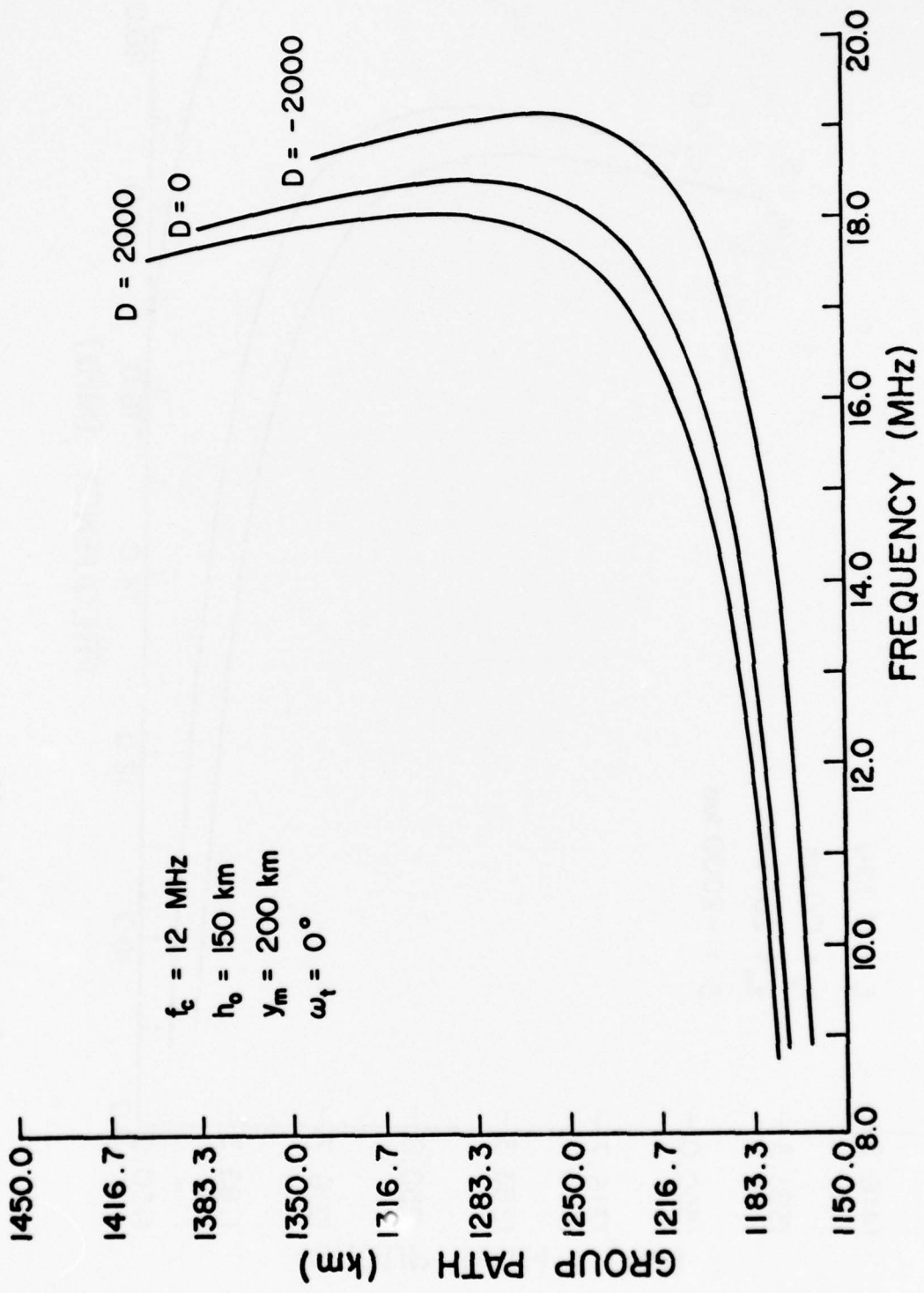


Figure 3.9. Effect of changing the D parameter (in km).

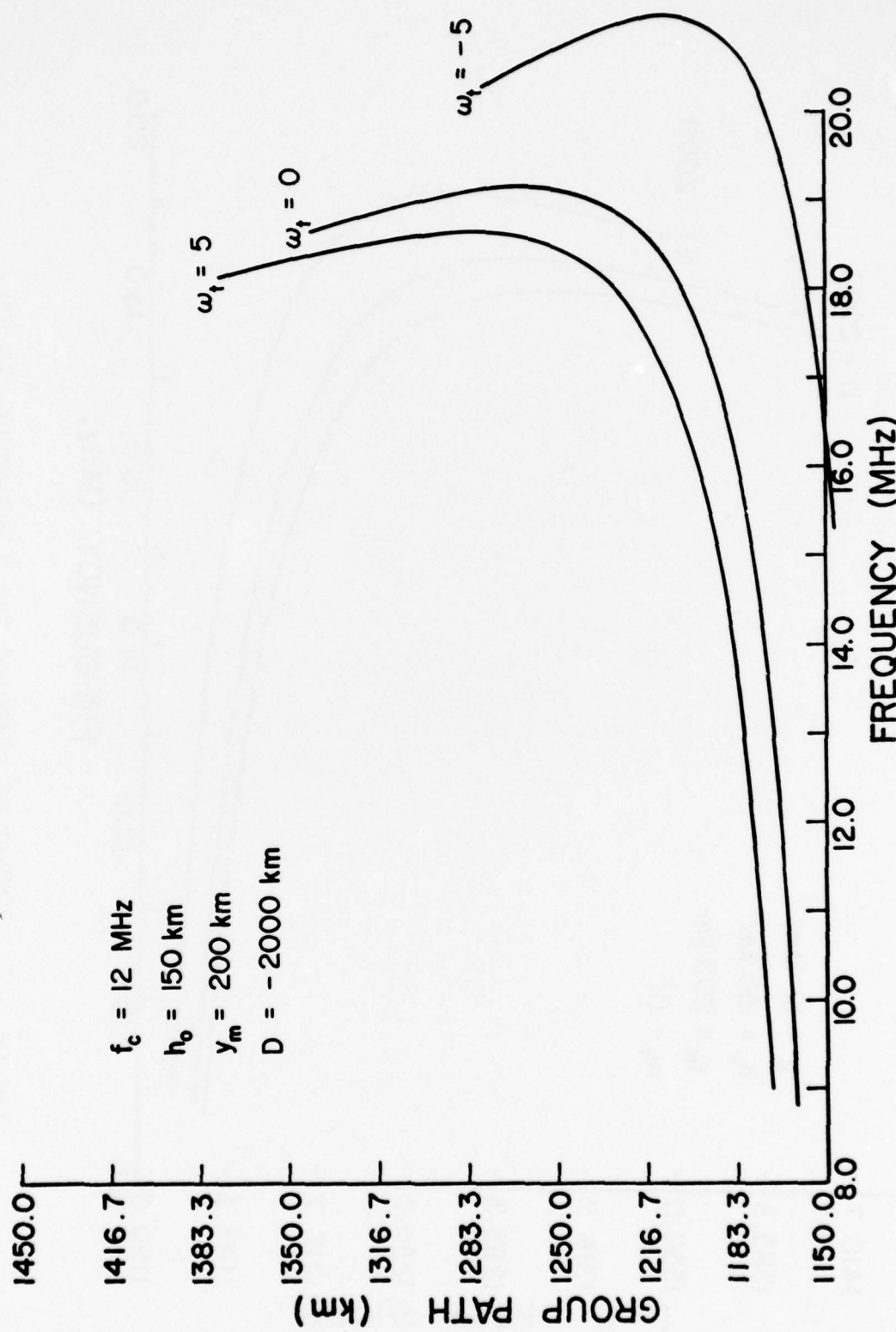


Figure 3.10. Effect of varying the  $\omega_t$  parameter (in degrees).

tive to changes in  $D$  for large values of  $D$  (the layer approaches a plane slab) and be highly sensitive for negative  $D$  values. These facts tend to suggest that most standard numerical procedures have the potential for inverting for the  $f_c$ ,  $h_0$ , and  $y_m$  parameters, but could easily encounter convergence problems when the gradient parameters are introduced.

Rao (1975) successfully inverted an oblique ionogram, using three data points, to the three defining parameters of a concentric quasi-parabolic layer using Newton's iterative technique (this procedure is described and used in Section 3.3.3). An attempt to extend this attractive technique to include two more parameters,  $D$  and  $\omega_t$ , failed because of convergence problems caused by the nonlinear behavior with respect to the gradient parameters. These observations suggest that a slower and more controllable technique is needed to converge to the final solution.

### 3.3.2 Determination of Initial Set of Parameters

In every complex numerical convergence procedure, it is essential to have a reasonable set of approximate starting values in order to be able to converge to the desired solution. In the present problem we have five data points (frequency-group path pairs) corresponding to five rays with frequencies  $f_i$ , group paths  $P'_i$  and all having a constant range  $R$ . It is desired to find a set of parameters and five elevation angles  $\beta_i$ , so that the reflection of each ray (with frequency  $f_i$  and approximate elevation angle  $\beta_i$ ) is ensured with small errors in their corresponding group paths and range.

A concentric layer is a practical choice for initial approximation, thus assuming  $D = \omega_t = 0$ . Using the geometry of Fig. 3.11(a) and applying Martyn's theorem, we can derive approximate expressions for  $\gamma_i$ , the angle of ray at the reflection point and then  $\beta_i$ , the elevation angle:

$$\gamma_i = \sin^{-1} \left[ \frac{r_o}{P'_i} \sin \left( \frac{R}{2r_o} \right) \right] \quad (3.10a)$$

$$\beta_i = \pi/2 - \gamma_i - R/2r_o. \quad (3.10b)$$

The critical frequency  $f_c$  is chosen to be equal to the highest ray frequency ( $f_5$ ) to ensure the reflection of all five rays by the modelled ionosphere. Since the zero frequency ray (with group path  $P'_o$ ), reflects from the base of the layer, the geometry of Fig. 3.11(a) can be used for determining the initial base height  $h_o$ . A linear interpolation of two data points (preferably in the lower frequency region) is made to find an approximate value for  $P'_o$  [Fig. 3.11(b)] and then by using the simple geometry of Figure 3.11(a),  $h_o$  is determined:

$$P'_o = P'_1 - \left[ \frac{P'_2 - P'_1}{f_2 - f_1} \right] f_1 \quad (3.11)$$

$$h_o = r_o \cos(R/2r_o) + \sqrt{\frac{P'_o}{4} - r_o^2 \sin^2(R/2r_o) - r_o}. \quad (3.12)$$

Initial value of  $y_m$  is not as critical as the other two parameters, we will simply use a physical constraint. Here, we have chosen  $y_m = 300 - h_o$  (in kilometers). Using these sets of approximate starting values, we are now ready to consider techniques in order

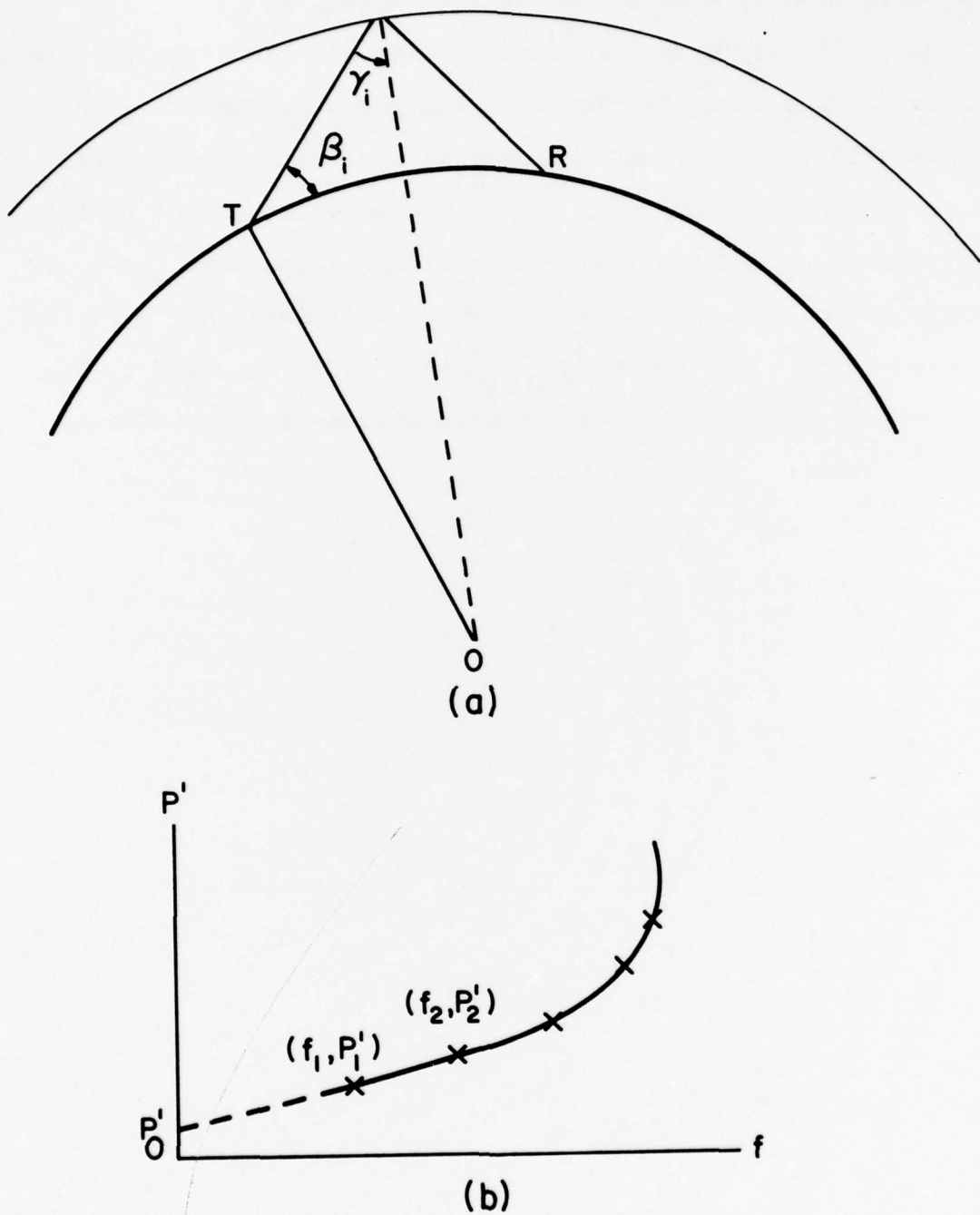


Figure 3.11. Determining an initial set of parameters.

for the solution to converge to an optimal set of parameters.

### 3.3.3 Inversion of Synthesized Oblique Ionograms

Rao (1975) employed a version of Newton's technique in order to invert a concentric Q-P layer in its three parameters. In each iteration, this procedure requires evaluating the partial derivatives of the group path and the range with respect to the three parameters and three elevation angles (subscript  $i = 1, 2, 3$  refers to the data point used). The matrix equation (3.13) is then used to find the required increments in  $f_c$ ,  $h_o$ , and  $r_m$  and the three elevation angles and then update these quantities as shown in (3.14):

$$\begin{bmatrix}
 \Delta f_c \\
 \Delta h_o \\
 \Delta Y_m \\
 \Delta \beta_1 \\
 \Delta \beta_2 \\
 \Delta \beta_3
 \end{bmatrix} = \begin{bmatrix}
 \left( \frac{\partial P'}{\partial f_c} \right)_1 & \left( \frac{\partial P'}{\partial h_o} \right)_1 & \left( \frac{\partial P'}{\partial Y_m} \right)_1 & \left( \frac{\partial P'}{\partial \beta} \right)_1 & 0 & 0 \\
 \left( \frac{\partial P'}{\partial f_c} \right)_2 & \left( \frac{\partial P'}{\partial h_o} \right)_2 & \left( \frac{\partial P'}{\partial Y_m} \right)_2 & 0 & \left( \frac{\partial P'}{\partial \beta} \right)_2 & 0 \\
 \left( \frac{\partial P'}{\partial f_c} \right)_3 & \left( \frac{\partial P'}{\partial h_o} \right)_3 & \left( \frac{\partial P'}{\partial Y_m} \right)_3 & 0 & 0 & \left( \frac{\partial P'}{\partial \beta} \right)_3 \\
 \left( \frac{\partial R}{\partial f_c} \right)_1 & \left( \frac{\partial R}{\partial h_o} \right)_1 & \left( \frac{\partial R}{\partial Y_m} \right)_1 & \left( \frac{\partial R}{\partial \beta} \right)_1 & 0 & 0 \\
 \left( \frac{\partial R}{\partial f_c} \right)_2 & \left( \frac{\partial R}{\partial h_o} \right)_2 & \left( \frac{\partial R}{\partial Y_m} \right)_2 & 0 & \left( \frac{\partial R}{\partial \beta} \right)_2 & 0 \\
 \left( \frac{\partial R}{\partial f_c} \right)_3 & \left( \frac{\partial R}{\partial h_o} \right)_3 & \left( \frac{\partial R}{\partial Y_m} \right)_3 & 0 & 0 & \left( \frac{\partial R}{\partial \beta} \right)_3
 \end{bmatrix}^{-1} \begin{bmatrix}
 \Delta P'_1 \\
 \Delta P'_2 \\
 \Delta P'_3 \\
 \Delta R_1 \\
 \Delta R_2 \\
 \Delta R_3
 \end{bmatrix} \quad (3.13)$$

$$\left. \begin{aligned}
 [f_c]_{\text{new}} &= [f_c]_{\text{old}} + \Delta f_c \\
 [h_o]_{\text{new}} &= [h_o]_{\text{old}} + \Delta h_o \\
 \dots & \\
 \dots &
 \end{aligned} \right\} \quad (3.14)$$

where  $\Delta P_i^!$  and  $\Delta R_i$  are defined to be the differences between the actual and the computed values of group path and range using the latest values of the parameters.

The iteration in (3.14) is repeated until the errors in the group path and range satisfy a given convergence condition. As mentioned in Section 3.3.1, our attempt to extend this convenient technique to include two more parameters,  $D$  and  $\omega_t$ , failed to result in a stable procedure. However, by employing a bisection search on  $D$  and  $\omega_t$ , and repeating the iteration for every change in these two parameters, the procedure becomes stable. Fig. 3.12 contains the flow chart for such a technique, and for simplicity, it only optimizes  $D$  with  $\omega_t$  constant. This technique can also be demonstrated graphically in Fig. 3.13. Several oblique ionograms are synthesized for different values of the  $D$  parameter, satisfying three common data points at all times (step 3.14 is repeated for every value of  $D$ ). It is clear that by selecting the fourth and the fifth data point in the high frequency region of the ionograms, which is the most sensitive region with respect to the gradient parameters, a bisection search can be used to optimize the values of  $D$  and  $\omega_t$ .

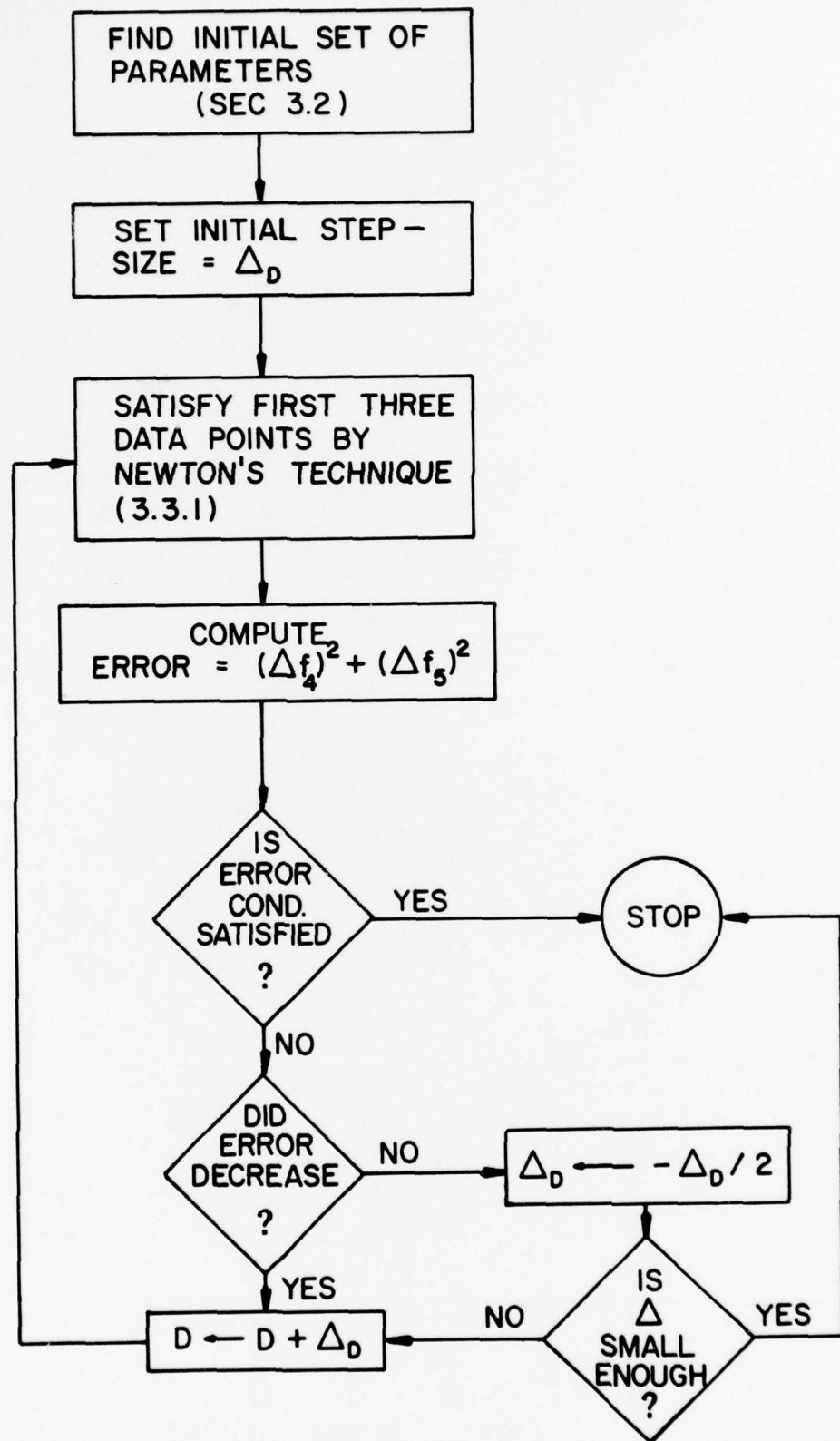


Figure 3.12. Inverting numerically synthesized data.

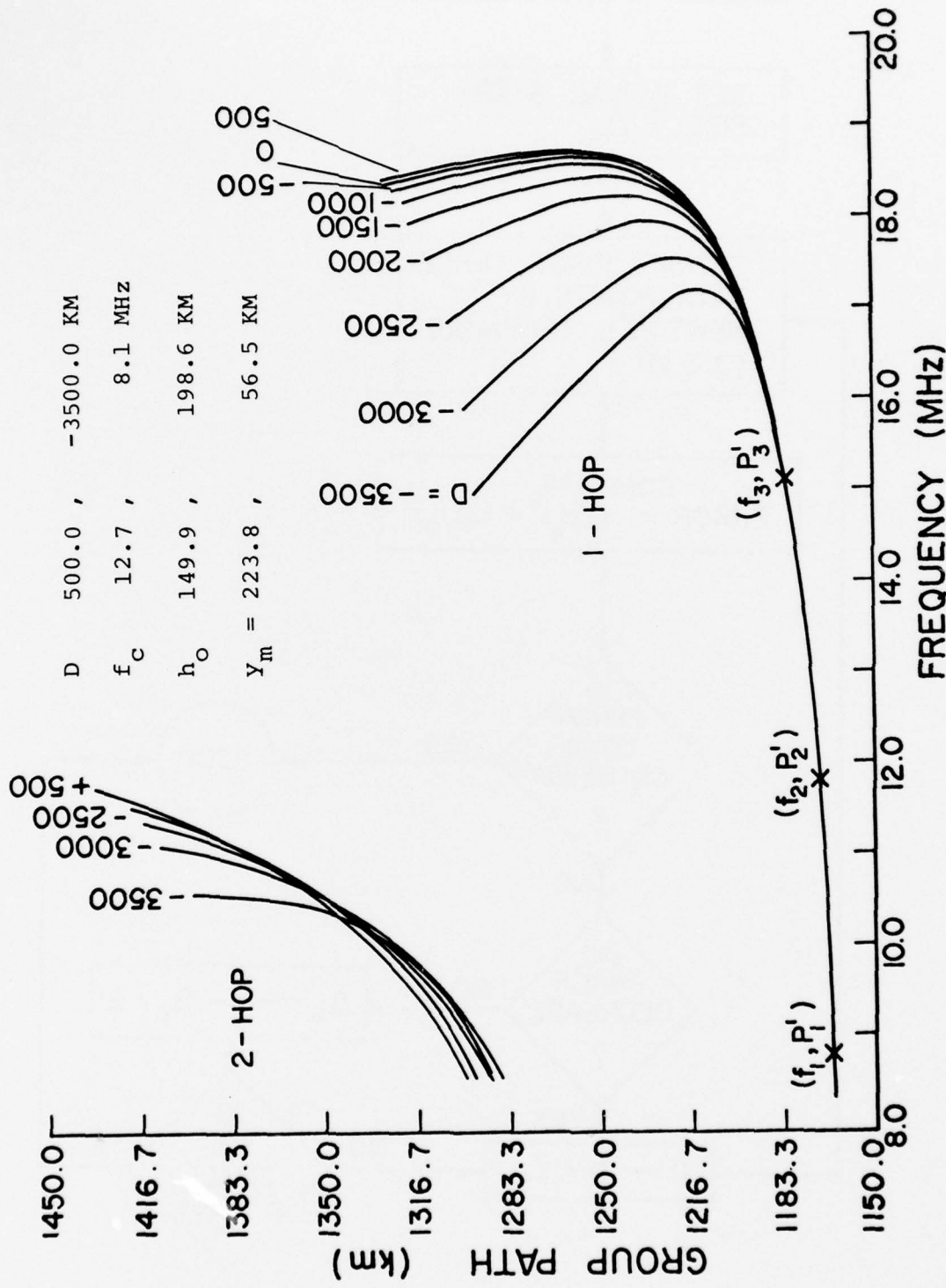


Figure 3.13. Synthesized oblique ionograms for Range = 1111.7 km and  $\omega_t = 0^\circ$ . The parameter  $D$  is successively changed by 500 km. For each  $D$ , the remaining three parameters are adjusted so as to force the curve through the three points marked by X. The parameters for the two extreme curves are given above.

The error function used for the bisection search was initially proposed to be:

$$\text{Error} = (\Delta P'_4)^2 + (\Delta P'_5)^2 . \quad (3.15)$$

However, as apparent from Fig. 3.13, for a given set of parameters, a ray with frequency  $f_i$  might penetrate the ionosphere making  $\Delta P'_i$  approach infinity. This problem can be solved by considering the ray with group path  $P'_i$  and finding the error in its frequency  $\Delta f_i$  (this value is always finite). Based on this explanation, the final error function used in the inversion technique is chosen to be:

$$\text{Error} = (\Delta f_4)^2 + (\Delta f_5)^2 . \quad (3.16)$$

It is important to note that  $\Delta f_i$  ( $i = 4, 5$ ) is defined to be the frequency deviation of the modelled ray, from the actual data value, which has its group path equal to  $P'_i$  and the range equal to  $R$  (the elevation angle  $\beta_i$  is adjusted so that the error in range vanishes). This technique is completely programmed and simulated on an IBM-360 digital computer, and Table 3.1 contains an example in which a numerically synthesized oblique ionogram is inverted with excellent accuracy to the model's parameters.

TABLE 3.1. Inversion of Synthesized Oblique Ionograms  
Using the Technique in Section 3.3.3

Model parameters:  $f_c = 12$  MHz  
 $h_o = 150$  km  
 $y_m = 100$  km  
 $D = -2000$  km  
 $\omega_t = 0$   
Range = 1111.8 km

Synthesized data points used:

i	1	2	3	4	5
$f_i$	12.23	19.03	22.10	23.57	24.15 MHz
$P'_i$	1161.3	1173.1	1186.3	1200.9	1217.2 km

Inversion results:

	$f_c$ MHz	$h_o$ km	$y_m$ km	D km	$\omega_t$ deg	$\Delta f_4^2 + \Delta f_5^2$ (MHz) <sup>2</sup>
1st iteration	13.07	136.4	125.3	0	0	.031
2nd iteration	12.96	138.5	123.5	-500	0	.026
3rd iteration	12.78	141.3	119.6	-1000	0	.018
4th iteration	12.48	144.9	112.3	-1500	0	.0081
5th iteration	11.99	150.0	99.89	-2000	0	.00004

Since Newton's technique attempts to converge the error to zero, problems can be encountered in case of real data because of the finite errors involved in the final solution. In order to adapt this technique for inversion of real data, a steepest descent method (discussed in detail later in Section 3.3.4) is employed to find an optimal set of starting parameters for three of our data points. Then the group paths of the three rays were computed using the parameters and used to replace the original group path values (Fig. 3.14). These adjusted data points are indeed well behaved and we can continue our procedure as before for minimizing  $(\Delta f_4)^2 + (\Delta f_5)^2$ . Table 3.2 contains a numerical example for this technique; it must be noted that in this example the fourth and the fifth data points are chosen in the nearly horizontal region of the ionogram, therefore making  $\Delta f_4$ ,  $\Delta f_5$  correspond to a much smaller error in group paths  $(\Delta P'_4, \Delta P'_5)$ .

Because of the two-step optimization involved in inverting real oblique ionograms, the final result is not guaranteed to be optimum. In fact, different combinations of the real data points used in the inversion procedure tend to converge to different sets of parameters (in that case, the combination with the least amount of error is the final solution). Even though the technique converges quite rapidly in the synthesized data case, the computation time becomes an order of magnitude larger for the real data case, which could be considered undesirable.

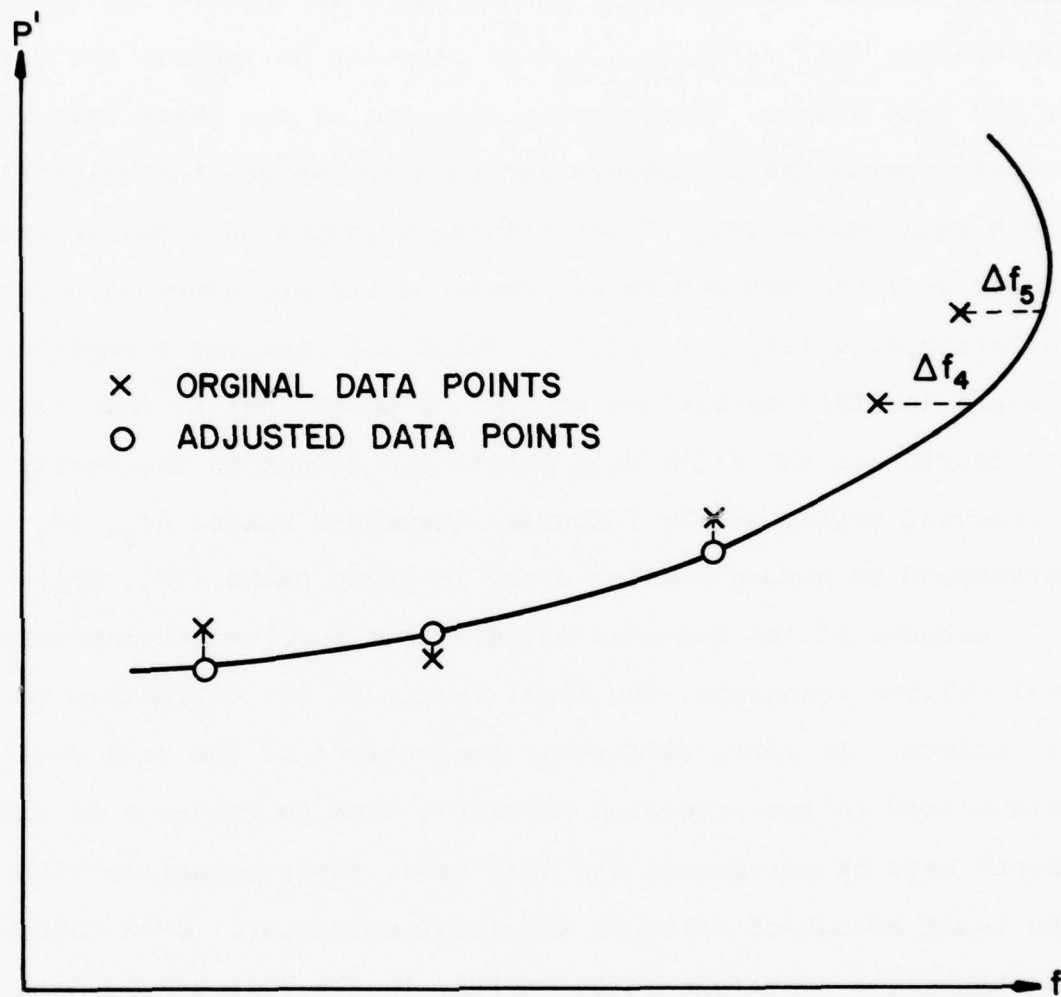


Figure 3.14. A technique for the inversion of real data. The first three data points are adjusted so that the technique in Section 3.3.3 can be employed for minimizing  $(\Delta f_4)^2 + (\Delta f_5)^2$ .

TABLE 3.2. Inversion of Real Oblique Ionograms,  
Using the Technique in Section 3.3.3

Range = 1421.5 km

Frequency, MHz	14	18	22	16	20
actual ( $P'$ ) km	1532.0	1540.4	1556.1	1528.5	1539.0
adjusted ( $P'$ ) km (after steepest descent)	1527.0	1530.3	1559.4	same	same

Parameters	$f_c$ MHz	$h_o$ km	$y_m$ km	D km	$\omega_t$ deg	$(\Delta f_4)^2 + (\Delta f_5)^2$ (MHz) <sup>2</sup>
Iteration #1	12.87	236.7	74.2	0	0	26.8
Iteration #2	12.73	244.6	72.1	-1000	0	27.4
Iteration #3	12.80	240.3	73.3	-500	0	26.6
.	.	.	.	.	.	.
.	.	.	.	.	.	.
.	.	.	.	.	.	.
Iteration #7	12.82	239.2	73.5	-375	0	26.2

Based on the controllable convergence behavior of the steepest descent method, a different approach to the inversion of real data is proposed and discussed in detail in the following section.

### 3.3.4 Inversion of Experimental Oblique Ionograms

Actual oblique ionograms are not smooth and nicely behaved as the numerically generated ones. In fact, one can frequently find discontinuities, and other peculiarities on the plots of actual data. Ideal zero error cannot be accomplished when actual data points are used, requiring the optimization of the error function to a minimum value.

It is convenient to approximate the gradient, in the actual data case, by using only one parameter. Referring back to Fig. 3.5, it is apparent that a wide range of gradients can be obtained by holding  $\omega_t$  at a reasonable value and varying D. In the examples to follow,  $\omega_t = 0$  is chosen not only to span a wide range of gradient values by varying D, but also to force  $h_0$  to represent the actual base height value of the layer above the transmitter. The steepest descent method, with its controlled step size is an ideal choice for simultaneous inversion of the remaining four parameters. Figure 3.10 outlines the procedure in a simple flow chart.

Since, in fact, we are finding a best fit curve through the data points, we need not be limited to using five points, and obviously the more data points used the more descriptive the model will be. The error function is chosen to be:

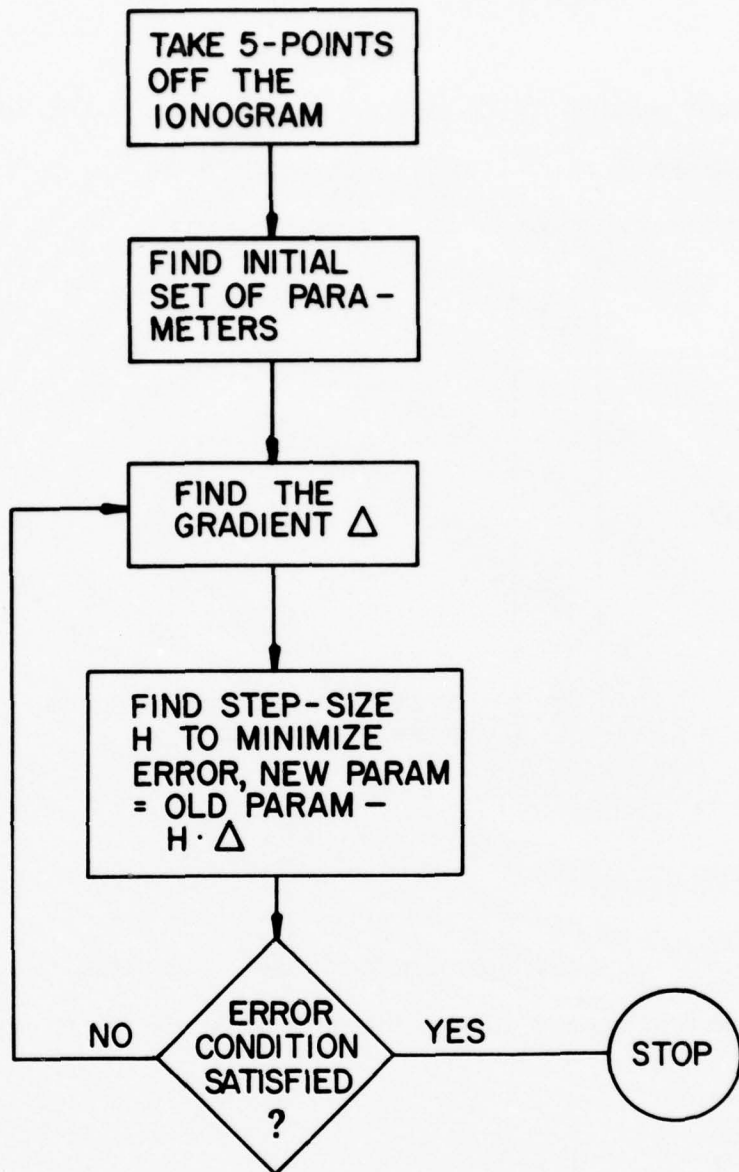


Figure 3.15. Method of steepest descent for inverting actual data.

$$E = \sum_{i=1}^N (\Delta P_i')^2$$

where  $N$  is the number of data points and  $\Delta P_i'$  is the error in the  $i^{th}$  group path as defined in Section 3.3.

The gradient vector  $\Delta$  is defined to be:

$$[\Delta] = \begin{bmatrix} \frac{\partial f_c}{\partial E} \\ \frac{\partial h_o}{\partial E} \\ \frac{\partial y_m}{\partial E} \\ \frac{\partial D}{\partial E} \end{bmatrix} \quad \text{Evaluated at the current parameter values}$$

The theory of steepest descent uses the fact that continuous functions decrease along the negative of their gradient.

Thus

$$\text{New } \begin{bmatrix} f_c \\ h_o \\ y_m \\ D \end{bmatrix} = \text{Old } \begin{bmatrix} f_c \\ h_o \\ y_m \\ D \end{bmatrix} - H \times [\Delta]$$

where  $H$  is a positive scalar step size. For this iteration to be most efficient, we like to choose an  $H$  such that the resultant error function from the new parameter is at a minimum. This can be accomplished by simply setting  $H$  to zero, and then incrementing it by an interval such that none of the resultant parameters change by more than a specified amount (this ensures a slower but smoother convergence to the final solution not accomplished by the Newton's technique in Section 3.3.3). Error is computed for each value of  $H$  and minimized by performing a simple interval halving routine on  $H$ . The old parameters are replaced by using the optimal step size  $H$  and if the convergence criterion is not met, the gradient is reevaluated and the procedure is repeated. This technique is also programmed on a digital computer and Tables 3.3 and 3.4 contain examples using five data points from actual oblique ionograms.

TABLE 3.3(a). Inversion of an Actual Ionogram

Data points scaled from oblique ionogram (Range = 1421.5 km):

i	1	2	3	4	5
$f_i$ (MHz)	14.	16.	18.	20.	22.
$P_i^*$ (km)	1536	1536.5	1540.5	1545.3	1555.5

Inversion results:

Iteration#	$f_c$ (MHz)	$h_0$ (MHz)	$y_m$ (km)	D(km)	Error = $\sum_{i=1}^5 (\Delta P_i^*)^2$
0	22.00	252.2	50.0	0.0	290.1
1	18.28	254.5	51.6	342.2	133.8
2	12.67	250.0	55.5	-797.7	14.5
3	12.47	249.9	55.5	-836.7	12.5
4	12.71	249.6	55.5	-831.4	12.3
.					
.					
.					
10	12.63	249.0	55.6	-803.6	11.1

The final individual group path errors (in km):

$$\Delta P_1^* = 1.17, \quad \Delta P_2^* = -1.46, \quad \Delta P_3^* = -1.00, \quad \Delta P_4^* = -1.11,$$

$$\Delta P_5^* = 2.30$$

TABLE 3.3(b) Inversion of an Actual Ionogram

Data points scaled from oblique ionogram: (Range = 1421.5 km):

i	1	2	3	4	5
$f_i$ (MHz)	14.	16.	18.	20.	22.
$P'_i$ (km)	1533	1539.0	1546.2	1555.8	1566.0

Inversion results:

Iteration #	$f_c$ (MHz)	$h_o$ (km)	$y_m$ (km)	D (km)	Error = $\sum_{i=1}^5 (\Delta P'_i)^2$
0	22.0	220.0	80.0	0.0	5838.5
1	12.58	227.9	88.5	1237.3	20.6
2	12.60	227.9	88.6	1239.1	20.5
3	12.59	227.9	88.5	1239.3	20.4

The final individual group path errors (in km):

$$\Delta P'_1 = .49, \quad \Delta P'_2 = 1.6, \quad \Delta P'_3 = 2.3, \quad \Delta P'_4 = 2.5,$$

$$\Delta P'_5 = -2.3$$

### 3.4 Inversion of Backscatter Leading Edge

The most important task of this project is to develop a technique of inversion of the sweep frequency backscatter leading edge data for various azimuthal directions, to an ionosphere varying in three dimensions, which can then be applied for the purpose of other ray path computations. In this section, we report our work on this problem. Several of the results can be found in the various progress reports but not in the order presented here. Here we discuss the solution of the problem in a step-by-step manner and its eventual application to the important problem of finding the ground range for a measured group path for reflection from a target.

#### 3.4.1 Basic Inversion Technique

In a paper by Rao (1974), it has been demonstrated that three data points taken from the leading edge of a backscatter ionogram can be used to obtain the quasi-parabolic layer parameters  $f_c$ ,  $r_b$ , and  $r_m$ , corresponding to those three points. Briefly, this method consists of starting with an initial estimate of the layer parameters and then calculating the minimum group paths,  $P'_{C_i}$ , corresponding to the three frequencies at which data points are taken from the leading edge. The differences between these computed minimum group path values and the actual minimum group path values,  $P'_i$ , from the leading edge are then used in an iterative procedure to obtain a final solution for the quasi-parabolic layer parameters. This final solution is such that the differences between  $P'_i$  and  $P'_{C_i}$  are less than a certain specified value (theoretically zero).

When the above described procedure was applied to synthesized leading edge data polluted intentionally by adding or subtracting a few kilometers from each of the  $P'_i$  values, thereby simulating the actual data case, it was found that in order for the differences between  $P'_i$  and  $P'_{C_i}$  to go down to less than a small specified value, one or more of the layer parameters often got incremented to physically unrealizable values. The reason for this was found to be that the backscatter leading edges corresponding to quasi-parabolic layer profiles have certain shapes and it is not in general possible to fit a synthesized leading edge exactly through three points on an experimental ionogram. In view of this, the method was modified for use in this work.

The modification involves the minimization of the following sum-squared error function:

$$E(r_b, r_m, f_c) = \sum_{i=1}^3 [P'_{C_i}(r_b, r_m, f_c) - P'_i]^2 \quad (3.17)$$

Fig. 3.16 depicts the strategy graphically. Assume that  $(f_1, P'_1)$ ,  $(f_2, P'_2)$ , and  $(f_3, P'_3)$  are the points we have chosen from the backscatter leading edge. As before, we start the procedure with an initial set of layer parameters, which are denoted by  $(r_b, r_m, f_c)_0$ . Corresponding to these starting parameters is a unique backscatter ionogram leading edge trace  $[P'(f)]_0$ . We note that the error function  $E$  is simply the sum of the squared distances between the ordinates of the  $[P'(f)]_0$  curve corresponding to the frequencies  $f_1$ ,  $f_2$ , and  $f_3$ , and the chosen backscatter ionogram minimum group paths  $P'_1$ ,  $P'_2$ , and  $P'_3$ . As  $r_b$ ,  $r_m$ , and  $f_c$

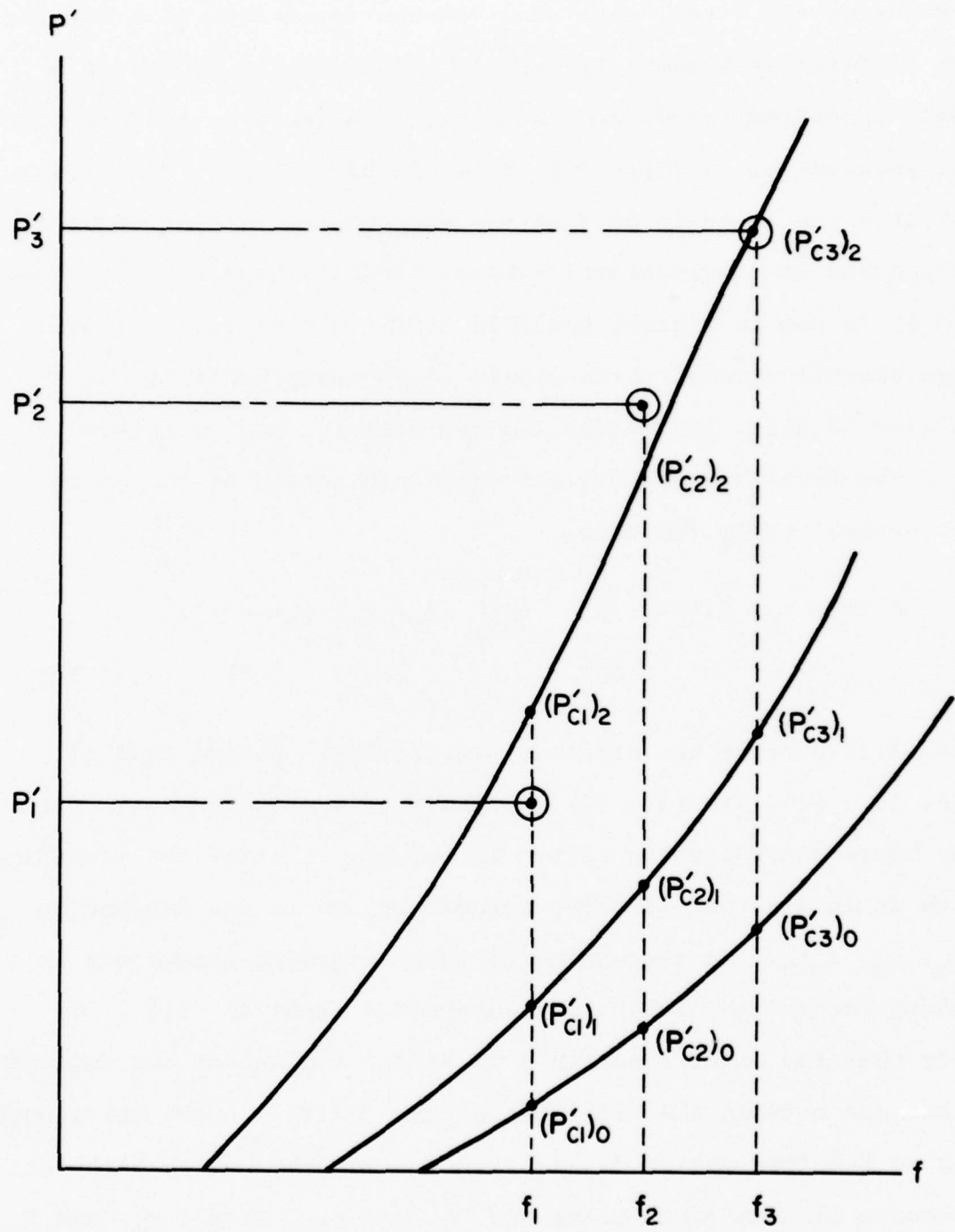


Figure 3.16. Graphical illustration of the least sum-squared error method of backscatter ionogram leading-edge inversion for a Q-P ionosphere.

are varied to minimize  $E$ , we see that we are effectively fitting the  $P'(f)$  curve to the three data points in the least-squared error sense. Furthermore, the magnitude of the minimum of  $E$  provides an indication of the noisiness of the data with reference to a synthetic leading edge. If the data points are from a synthetic curve, computed by assuming the Q-P model, the error  $E$  will then be zero.

The error  $E$  is in general a nonlinear function of  $r_b$ ,  $r_m$ , and  $f_c$  and an iterative method is required to seek its minimum. Numerical minimization techniques are available which seek a local minimum for a given starting point in parameter space. The nonlinear minimization algorithm employed in this study is described by Fletcher and Powell (1963) and is supplied in IBM's scientific subroutine package as subroutine DFMFP. This routine was modified for use with our computer. The Fletcher-Powell method performs, for each iteration step, a linear minimization along a direction determined by the current gradient and an updated estimate of the Hessian. The size of the steps taken through the parameter space as the minimum is sought is proportional to the difference between the current value of the function to be minimized ( $e$ ), and the user-supplied minimum value (EST), typically taken to be  $0.001 \text{ km}^2$ , and inversely proportional to the current magnitude of the function gradient ( $|\vec{\nabla}E|$ ). In this manner, rapid convergence is assured. The minimization procedure is terminated when the function value has not changed by more than a user-specified value (EPS), or if  $|\vec{\nabla}E|$  has become less

than EPS. This routine requires an external function subprogram, which supplies DFMFP with  $E$  and  $\nabla E$  as the parameters  $r_b$ ,  $r_m$ , and  $f_c$  are varied. The components of  $\nabla E$ , which involve derivatives of  $P'$  with respect to the layer parameters are calculated using the expressions provided by Rao (1974) and repeated here in the appendix.

Thus far we have discussed the procedure for the inversion of three data points on a backscatter leading edge to Q-P layer parameters. Since each point on the leading edge corresponds to a different ground range, it is obvious that the three points must be chosen fairly close together if horizontal gradients are present. The three data points must correspond to three ionospheric propagation paths which are in such horizontal proximity as to validate the assumption of a locally horizontally uniform ionosphere. These considerations give rise to a method of deriving the horizontal ionization gradients from the leading edge. Three closely spaced points on the leading edge just above the critical frequency at the backscatter sounder site can be used to determine the layer parameters of the ionosphere at a range which is in close proximity to the site. Next, three closely spaced points further up the leading edge can be used to obtain the layer parameters at a greater range than that corresponding to the previous set of data points. In obtaining these layer parameters, the solution for the first set of three data points can be used as the starting solution. A repetition of this process continuously along the leading edge for successive sets of three data points yields the layer parameters as a function

of distance away from the sounder site. This is the technique we employ in the following sections.

### 3.4.2. Inversion of Synthesized QP Layer Data

The basic technique of inversion of points on the backscatter leading edge for quasi-parabolic layer parameters is tested by simulating the leading edge for assumed QP layer parameters and then polluting the simulated data by adding a few kilometers to one or more of the points. The assumed values of the layer parameters are  $r_b = 6570$  km,  $r_m = 6720$  km, and  $f_c = 5.0$  MHz. Minimum group paths for frequencies of 10, 11, and 12 MHz are synthesized to be  $P'_1 = 1866.1$  km,  $P'_2 = 2133.8$  km, and  $P'_3 = 2441.3$  km, respectively.

Table 3.4 shows the results of the test by indicating the errors introduced in  $P'_1$ ,  $P'_2$ , and  $P'_3$  and the corresponding solution obtained by inverting the polluted data. For each case, starting values of layer parameters used are  $r_b = 6500$  km,  $r_m = 6650$  km, and  $f_c = 4.0$  MHz. From Table 3.4, it can be seen that even small measurement errors seem to appreciably affect the results of inversion of the leading edge data.

To investigate further the sensitivity of the inversion process to measurement errors, the procedure has been generalized to permit the use of a variable number ( $N$ ) of data points in the inversion technique, that is, for minimizing the error function  $E$ . Leading edge data are synthesized for an earth-concentric QP layer having the parameters  $r_b = 6570$  km,  $r_m = 6720$  km, and  $f_c = 7.0$  MHz and at increments of 0.25 MHz throughout the frequency range of 10.0 to 13.0 MHz. These data are then made noisy by the addition of samples of a random variable uniformly distributed over the interval

TABLE 3.4

SYNTHESIZED NOISY BACKSCATTER IONOGram LEADING EDGE DATA INVERSION  
ASSUMING A SPHERICAL EARTH-CONCENTRIC QUASI-PARABOLIC IONOSPHERE MODEL

Synthesized points on backscatter ionogram leading edge:

Point Number	Frequency (MHz)	Minimum Group Path km
(1)	10.0	1866.1
(2)	11.0	2133.8
(3)	12.0	2441.3

Layer parameters used in synthesis:

$$r_b = 6570.0 \text{ km} \quad r_m = 6720.0 \text{ km} \quad f_c = 5.0 \text{ MHz}$$

Starting values of layer parameters:

$$r_b = 6500.0 \text{ km} \quad r_m = 6650.0 \text{ km} \quad f_c = 4.0 \text{ MHz}$$

Estimated Minimum Sum-Squared Error (EST) = .001 km<sup>2</sup>  
Specified Absolute Error (EPS) = .001 km

Error introduced in $P'_1$ (km)	Error introduced in $P'_2$ (km)	Error introduced in $P'_3$ (km)	Resulting inverted layer parameter $r_m$ (km)	Resulting inverted layer parameter $f_c$ (MHz)	Value of E (km) <sup>2</sup> Minimum
0	0	0	6570.6	4.993	.00023
+1	-1	+1	6621.7	4.743	.838
-1	0	-1	6550.2	5.324	.240
-1	0	0	6543.9	5.444	.00593
-1	-1	0	6564.0	5.0311	.09162
0	0	+1	6566.6	5.0105	.0844
+2	0	0	6625.4	4.782	.109
0	+2	0	6555.0	5.248	1.83
0	+2	+1	6535.7	5.772	.411
0	4	0	6533.7	5.966	6.01

-1.0 km to +1.0 km, as illustrated in Table 3.5. These random noise values were chosen to be the rightmost three digits from consecutive entries on a page of the local telephone directory. Using an initial estimate of layer parameters  $r_b = 6600$  km,  $r_m = 6700$  km, and  $f_c = 9.0$  MHz. These data are inverted by using different sets of points, as shown in Table 3.6. It can be seen that the percent error in determining the actual parameters of the QP layer decreases as the number of noisy data points used in the inversion process is increased.

Table 3.5. Noisy Backscatter Leading  
 Edge Synthesis -- Assuming Earth-  
 Centered Q-P Ionosphere  $r_b = 6570$  km,  
 $r_m = 6720$  km, and  $f_c = 7.0$  MHz

Point No.	$f_i$ (MHz)	Precise $P'_{M_i}$ (km)	Additive Noise (km)	Noisy $P'_{M_i}$ (km)
1	10.00	1233.388	.114	1233.502
2	10.25	1268.959	-.096	1268.863
3	10.50	1304.946	-.257	1304.689
4	10.75	1341.369	-.332	1341.037
5	11.00	1378.250	-.576	1377.674
6	11.25	1415.611	.945	1416.556
7	11.50	1453.475	-.988	1452.487
8	11.75	1491.867	.062	1491.929
9	12.00	1530.814	-.600	1530.214
10	12.25	1570.344	-.760	1569.584
11	12.50	1610.486	-.271	1610.215
12	12.75	1651.272	+.931	1652.203

Table 3.6. Results of Inversion of the Data in  
Table 3.4, Using Various Numbers of Points in E.

Number of leading edge pts used	Optimized value of E ( $\text{km}^2$ )	% error in $r_b$	% error in $r_m$	% error in $f_c$
N=3 using points 1, 6, 12	.17203	.1040	.155	<b>1.77</b>
N=6 using points 1,3,5, 7,9,12	1.8730	.052	.0327	.659
N=9 using points 1,2,4,5, 7,8,10, 11,12	2.3943	.0472	.0193	.129

### 3.4.3 Inversion of Synthesized Data Involving Horizontal Gradients

To investigate the technique of inversion of successive sets of three data points on the leading edge for the horizontal gradients, the eccentric QP layer model discussed in Sec. 3.2.2 is employed. First, for assumed layer parameters of  $r_b = 6570$  km,  $r_m = 6720$  km,  $f_c = 5.0$  MHz,  $D = 1000$  km, and  $\omega_T = 0$ , data points on the leading edge trace are computed for every 0.5 MHz from 7.0 to 11.0 MHz. Next, the points are grouped in four sets of three, starting with (7.0, 7.5, 8.0), then (8.0, 8.5, 9.0), etc. Each group of three data points is then inverted for the parameters of a concentric QP layer. The first group is inverted by using an arbitrary starting set of layer parameters ( $r_b = 6500$  km,  $r_m = 6650$  km, and  $f_c = 4.0$  MHz). Succeeding groups of data are inverted by starting with the layer parameters obtained for the previous group of data points. The synthesized data as well as the computed layer parameter values are shown in Table 3.7. It can be seen from this table that inverted layer parameters indeed exhibit horizontal gradient. When the magnitude of the gradient in  $r_b$  or  $r_m$  is compared with that predicted from the model, with the use of Fig. 3.5, they are found to be in good agreement.

For a practical example of the backscatter ionogram leading edge for horizontal gradients, we consider the data supplied by the contract sponsor. These data of minimum group paths are simulated by 3-D ray tracing for models of the ionosphere, derived from ITS-78 predictions by applying various linear tilts and gradients to a median profile. This median profile, shown in

TABLE 3.7.  
 INVERSION OF SYNTHESIZED BACKSCATTER LEADING EDGE DATA  
 FOR AN ECCENTRIC QUASIPARABOLIC LAYER

Frequency MHz	$P'$ (km)	Synthesized Data Range (km)	Computed Layer Parameters	$E^2$ (km <sup>2</sup> )
			$r_b$ (km) $r_m$ (km) $f_c$ (MHz)	
7.0	1219.238	1004.889	6531.6    6660.3    4.1614	.00064
7.5	1323.839	1120.756		
8.0	1433.133	1238.934	6529.7    6659.3    4.1445	.00311
8.5	1547.939	1360.683		
9.0	1669.278	1487.355	6526.9    6657.3    4.1159	.01730
9.5	1798.458	1620.455		
10.0	1937.207	1761.826	6623.1    6652.5    4.0570	.120
10.5	2087.893	1913.875		
11.0	2253.933	2079.975		

Fig. 3.17, is assumed to represent the vertical profile at a range of 3500 km from a backscatter sounder site. A linear increase or decrease of the layer parameters along the sounder boresight is then introduced as follows:

$$(i) \text{ Gradients: } f_o F2 = (f_o F2)_{\text{median}} \pm na$$

$$h_m F2 = (h_m F2)_{\text{median}}$$

$$(ii) \text{ Tilts: } f_o F2 = (f_o F2)_{\text{median}}$$

$$h_m F2 = (h_m F2)_{\text{median}} \pm pb$$

where  $n, p=0,1,2,3$  and  $a=1 \text{ MHz}/3500 \text{ km}$ , and  $b=10 \text{ km}/3500 \text{ km}$ .

The simulated minimum group values are shown in Table 3.8. The numbers in each box corresponding to one leading edge. Thus we have 31 leading edges.

Each set of leading edge data in table 3.8 are inverted for QP layer profiles along the boresight by considering overlapping sets of the three data points. Thus a set of five data points for the minimum group path yield three sets of QP layer parameters corresponding to different ranges from the sounder location. The inversion results are shown in Tables 3.9 through 3.12, which correspond to the ground range, peak height of the layer, base height of the layer, and the critical frequency of the layer, respectively. These results indicate that while it is difficult to compare quantitatively the gradients with those of the original model in view of the differences in the two vertical profiles, the directions of the gradients are generally determined correctly by this procedure.

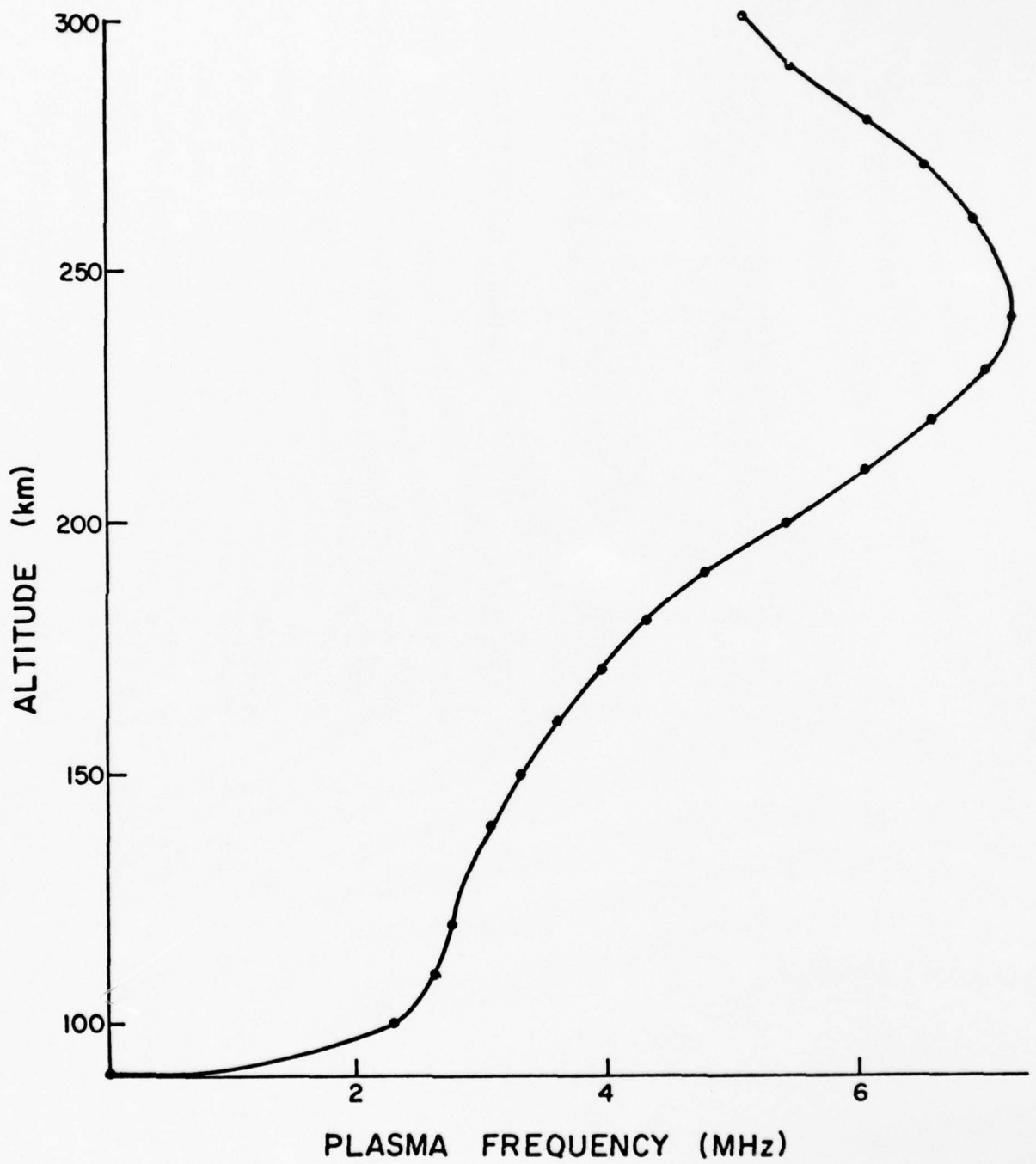


Figure 3.17. Nominal electron density profile.

Table 3.8

Group Path (km) to Leading Edge of Backscatter Ionogram for Various Linear Tilts and Gradients.

n	P	-3	-2	-1	0	1	2	3
	f=11 MHz	1036	1038	1041	1044			
	14	1388	1395	1402	1409			
-3	17	1815	1828	1838	1852			
	20	2398	2423	2459	2499			
	23	--	--	--	--			
	11	1025	1028	1031	1033			
	14	1364	1370	1377	1384			
-2	17	1766	1777	1788	1802			
	20	2288	2312	2334	2372			
	23	3128	3216	3305	3395			
	11	1015	1017	1021	1023			
	14	1343	1349	1354	1361			
-1	17	1724	1736	1743	1755			
	20	2194	2215	2235	2264			
	23	2855	2925	2992	3044			
	11	1005	1008	1011	1014	1017	1019	1021
0	14	1322	1328	1334	1338	1345	1351	1357
	17	1685	1674	1704	1715	1725	1743	1761
	20	2114	2132	2152	2184	2209	2232	2254
	23	2698	2735	2785	2848	2875	2905	2930
	11				1004	1006	1009	1012
	14				1320	1324	1330	1336
1	17				1677	1688	1705	1713
	20				2110	2133	2155	2176
	23				2679	2717	2751	2787
	11				995	998	1000	1003
	14				1302	1307	1312	1317
2	17				1643	1654	1668	1682
	20				2049	2069	2088	2107
	23				2550	2584	2617	2647
	11				987	989	992	994
	14				1284	1289	1294	1299
3	17				1611	1622	1636	1648
	20				1993	2012	2029	2047
	23				2449	2475	2503	2531

123  
Table 3.9

Ground Range (km)

		p	-3	-2	-1	0	1	2	3
n									
	f=14 MHz		1291	1302	1310	1320			
-3	17		1722	1738	1751	1768			
	14	1245	1256	1268	1282				
-2	17	1658	1671	1684	1706				
	20	2182	2208	2229	2278				
	14	1200	1218	1221	1237				
-1	17	1597	1616	1622	1641				
	20	2071	2099	2113	2157				
	14	1145	1104	1173	1184	1198	1220	1358	
0	17	1530	1539	1563	1580	1595	1625	1755	
	20	1969	2006	2018	2061	2085	2113	2251	
	14				1132	1150	1178	1193	
1	17				1517	1537	1569	1585	
	20				1966	1993	2024	2046	
	14				1061	1083	1122	1145	
2	17				1450	1471	1508	1528	
	20				1878	1902	1937	1957	
	14				958	1006	1052	1084	
3	17				1381	1404	1443	1466	
	20				1795	1816	1849	1871	

Table 3.10

Height of Maximum Plasma Frequency  
 $(h_m F_2)$   
(kilometers)

n	P	-3	-2	-1	0	1	2	3
		f=14 MHz	235	236	239	239		
-3	17	230	232	220	214			
	14	244	243	247	249			
	20	245	239	238	238			
-2	17	245	245	239	238			
	14	244	243	247	249			
	20	245	239	236	238			
-1	17	274	282	258	250			
	14	264	262	260	262			
	20	276	262	258	256			
0	17	303	276	290	266	260	263	268
	14	289	347	283	270	269	249	234
	20	290	278	277	268	277	307	319
1	17				305	288	269	259
	14				292	281	286	280
	20				292	290	311	311
2	17				340	324	302	283
	14				321	311	305	306
	20				320	315	328	332
3	17				391	364	336	315
	14				351	339	330	324
	20				346	344	356	358

Table 3.11

## Base Height of Ionosphere (km)

	p	-3	-2	-1	0	1	2	3
n								
	f=14 MHz	136.7	129.4	126.4	122.1			
-3	17	142.6	135.1	142.2	139.1			
	14	164.5	156.8	147.7	136.6			
-2	17	161.3	163.2	159.9	151.1			
	20	160.9	163.3	169.9	135.4			
	14	186.7	169.5	174.7	158.9			
-1	17	174.7	159.1	179.5	173.2			
	20	174.7	177.8	202.0	156.1			
	14	215.9	224.1	196.3	201.1	189.3	181.7	175.7
0	17	207.6	211.8	187.0	204.2	205.2	165.5	157.3
	20	225.1	169.4	213.5	182.5	167.0	148.7	150.5
	14				215.4	212.3	198.9	195.5
1	17				228.1	222.4	178.9	177.0
	20				205.4	194.2	168.6	166.8
	14				248.9	245.0	222.4	216.1
2	17				262.3	256.4	205.3	191.3
	20				231.4	226.2	191.0	187.1
	14				291.4	274.2	258.1	247.7
3	17				286.7	283.6	233.4	221.0
	20				258.0	251.0	218.3	210.7

Table 3.12

Critical Frequency ( $f_0 F_2$ )  
(in MHz.)

		p	-3	-2	-1	0	1	2	3
n									
-3	f=14 MHz	14	6.237	6.207	6.224	6.156			
		17	6.140	6.158	5.872	5.725			
-2	14	6.568	6.523	6.567	6.530				
	17	6.610	6.448	6.386	6.198				
	20	6.613	6.447	6.334	6.316				
-1	14	7.148	7.061	7.002	7.005				
	17	7.378	7.466	6.943	6.740				
	20	7.413	7.072	6.873	6.856				
0	14	7.804	9.232	7.644	7.272	7.251	6.732	6.322	
	17	8.173	7.488	7.816	7.146	6.937	7.078	7.118	
	20	7.814	7.614	7.444	7.265	7.400	7.830	7.990	
1	14				8.235	7.784	7.274	7.001	
	17				7.853	7.546	7.706	7.538	
	20				7.937	7.868	8.184	8.125	
2	14				9.193	8.739	8.176	7.679	
	17				8.558	8.262	8.288	8.264	
	20				8.713	8.547	8.763	8.782	
3	14				10.537	9.831	9.072	8.481	
	17				9.414	9.037	9.020	8.814	
	20				9.450	9.378	9.595	9.559	

### 3.4.4 Inversion of Synthesized Data for Three-Dimensional Ionosphere

For nonzero value of the parameter  $\omega_t$ , that is, when the transmitter is not situated along the line joining the Earth's center to the center of the ionosphere, the eccentric quasi-parabolic layer provides a three-dimensional variation of the electron density with respect to the transmitter location. Hence when backscatter leading edge data are synthesized for various azimuthal directions from the transmitter, they will all be different. To test the inversion of synthesized data for a three-dimensional ionosphere, leading edges are synthesized by assuming eccentric QP layer parameters of  $r_b = 6570$  km,  $r_m = 6720$  km,  $f_c = 7.00$  MHz,  $D = 500$  km, and  $\omega_T = 5^\circ$ , and for azimuthal beam headings from  $0^\circ$  to  $70^\circ$  in steps of  $10^\circ$ . The leading edge data for each azimuth is then inverted in the usual manner. The resulting concentric QP layer parameters as a function of range from the transmitter and azimuth are shown in Table 3.13. The entries in each box of this table correspond to values of  $r_b$ ,  $r_m$ , and  $f_c$ , respectively. It can be seen that the inversion results do indicate the three dimensional variability of the assumed ionospheric model.

As a further test of the inversion technique, the three-dimensional ionospheric model supplied by the contract sponsor is used and by three-dimensional ray tracing including magnetic field backscatter leading edges are generated for two azimuths ( $330^\circ$  and  $358^\circ$ ) with the transmitter located at the geographic coordinates of  $40^\circ\text{N}$  lat. and  $175^\circ$  long. The generated minimum group path values and other propagation parameters versus fre-

Table 3.13. Results of Inversion of Simulated Backscatter Ionogram Data

Approx. Gnd Range km	Azimuthal Beam Heading °	Q-P parameters:		$r_b = 6570$ km	$r_m = 6720$ km	$f_c = 7.00$ MHz
		Eccentricity: $ \vec{D}  = 500$ km	$\omega_T = 5^\circ$			
6.30	6586.5	6586.1	6583.7	6580.1	6575.0	6568.8
	6727.7	6727.5	6726.2	6724.4	6721.9	6719.5
7.1851	7.1794	7.1471	7.0998	7.0339	6.9592	6.8845
						6.8024
11.50	6564.3	6563.9	6562.7	6560.8	6558.4	6555.0
	6716.8	6716.6	6716.1	6715.3	6714.3	6714.4
6.9146	6.9087	6.8921	6.8659	6.8314	6.8065	6.7601
						6.7716
20.20	6553.7	6553.5	6552.8	6551.5	6550.0	6548.0
	6711.2	6711.1	6710.8	6710.2	6709.6	6708.4
6.7816	6.7773	6.7651	6.7447	6.7178	6.6825	6.6457
						6.6059
21.70	6545.8	6545.7	6545.1	6544.4	6543.2	6542.4
	6701.1	6701.1	6700.7	6699.6	6698.8	6690.7
6.6046	6.6006	6.5888	6.5640	6.5383	6.4940	6.4580
						6.4383

quency are shown in Tables 3.14 and 3.15. To invert these leading edge data, a QP layer is fitted to the actual vertical electron density profile existing above the transmitter location. By using these QP layer parameters as the starting solution, overlapping sets of three data points along the leading edge are inverted for QP layer parameters. In inverting a given set other than the first one, the solution found for the previous set is used as the starting solution. For each set of data inverted, the corresponding ground range is computed and the QP layer parameters are assigned to a location half that distance from the transmitter and along the pertinent azimuth. The layer parameters and the corresponding ranges generated in this manner are listed in Tables 3.16 and 3.17. It can be seen that in this manner, actual experimental backscatter leading edge data for various azimuthal directions from the transmitter location can be inverted for a three dimensional ionosphere specified by QP layer parameters at a set of grid points located along the azimuthal directions.

Table 3.14. Computed minimum group path data and other propagation parameters for transmitter location of 40°N, 175°W, and 330° azimuth.

Frequency, MHz	Minimum Group path, km	Ground range, km	Apogee height, km
10	798.35	468.81	220.26
11	884.79	590.29	222.25
12	972.60	708.63	222.02
13	1062.92	826.38	220.63
14	1155.56	929.67	223.15
15	1251.66	1041.29	222.89
16	1349.12	1150.64	222.91
17	1450.55	1261.44	223.20
18	1555.26	1370.37	225.13
19	1665.43	1483.68	227.10
20	1780.63	1604.12	227.60

Table 3.15. Same as Table 3.14 except for 358° azimuth

Frequency, MHz	Minimum Group path, km	Ground range, km	Apogee height, km
10	805.04	474.50	222.20
11	894.16	598.72	224.30
12	984.55	719.84	224.14
13	1077.68	840.37	222.70
14	1173.13	954.99	222.23
15	1273.45	1062.07	225.29
16	1376.13	1172.57	227.20
17	1483.70	1293.45	225.99
18	1596.70	1417.13	224.96
19	1714.86	1531.40	230.46

Table 3.16. Computed QP layer parameter values and the corresponding ground ranges for 330° azimuth

Range, km	$f_c$ , MHz	$r_b$ , km	$r_m$ , km
327.56	9.2406	6556.4	6676.2
377.18	9.3493	6561.9	6679.5
431.21	9.3344	6561.2	6679.1
486.87	9.2511	6557.4	6676.4
531.07	9.7489	6565.8	6694.9
577.99	10.0895	6573.9	6707.4
632.21	10.1063	6574.6	6708.0
689.80	10.0427	6572.1	6705.8
749.46	9.9592	6568.2	6702.9

Table 3.17. Same as Table 3.16 except for 358° azimuth

Range, km	$f_c$ , MHz	$r_b$ , km	$r_m$ , km
373.28	8.3981	6509.2	6661.6
414.73	8.9054	6519.1	6680.1
461.30	9.0253	6526.2	6681.9
515.75	8.9677	6522.8	6680.9
568.43	8.9757	6523.2	6681.1
619.54	9.0693	6529.0	6682.8
676.62	9.0482	6527.7	6682.4
732.96	9.2278	6528.4	6690.8

### 3.4.5 Application of the Backscatter Inversion Technique

It has been pointed out in Sec. 3.1, that while the backscatter leading edge is not capable of providing the ionospheric vertical profiles above certain heights, this is not a limitation in so far as the application of the inversion technique is concerned. In this section, we shall prove this point and provide an explanation for the applicability of the inversion technique despite the limitation for obtaining the complete ionospheric structure. To do this, we consider an important application, which consists of finding the ground range for a given group path (not a minimum group path) at a known frequency, and compare the applicability of the deduced three-dimensional ionosphere by inversion of the leading edge data, relative to that of the originally assumed three-dimensional model.

Referring back to Sec. 3.4.4 in which we presented the result of inversion of synthesized leading edges for two azimuths for the Air Force supplied model, we now trace rays at one frequency (16 MHz) in the original as well as the computed ionospheres for an azimuth of  $340^\circ$  (lying between  $330^\circ$  and  $358^\circ$  corresponding to the inverted backscatter data) and for several elevation angles of transmission. For tracing rays in the computed ionosphere, it should be noted that the rectangular grid of the originally assumed model is uniformly spaced, whereas the grid generated by the inversion of the leading edge data is nonuniformly spaced, in addition to being in azimuth-range space, rather than in the latitude-longitude space. Hence it has become necessary to generate vertical profiles at the uniformly spaced

rectangular grid of points by applying an interpolation procedure to the QP profiles at the grid point in the azimuth-range space. The result of these ray tracings are shown in Tables 3.18 and 3.19, which correspond to the originally assumed model and the computed ionosphere, respectively. The quantity ( $P' - R$ ) is shown plotted versus  $P'$  for the two cases in Fig. 3.18. A comparison of the two curves indicates that the computed ionosphere gives the correct range to within  $\pm 2$  km for a wide range of group path values. The discrepancies greater than  $\pm 2$  km toward the low end of the curves are attributable to the fact that the region is close to the minimum group path, whereas the discrepancies greater than  $\pm 2$  km toward the high end of the curves are attributable to the fact that the region is beyond the range corresponding to the inverted backscatter data.

We shall now provide a simple explanation for the success of the technique in finding the range for a given group path to a good accuracy, despite the fact that the minimum group path rays all reflect from below a certain apogee height, as can be seen from Tables 3.14 and 3.15 and hence cannot yield the vertical profiles above those apogee heights. To do this, we refer to Fig. 3.19 which illustrates the fact that the backscatter ionogram is a continuum of oblique ionograms corresponding to successively increasing values of ground range away from the transmitter. Let us suppose we have found the range corresponding to a particular point A ( $f_1, P_1'$ ) on the leading edge. Then a point B, corresponding to the same group path as that of A but to a frequency  $f_2 < f_1$ , corresponds to a range greater than that of A. Alternatively, it corresponds to a range corresponding to

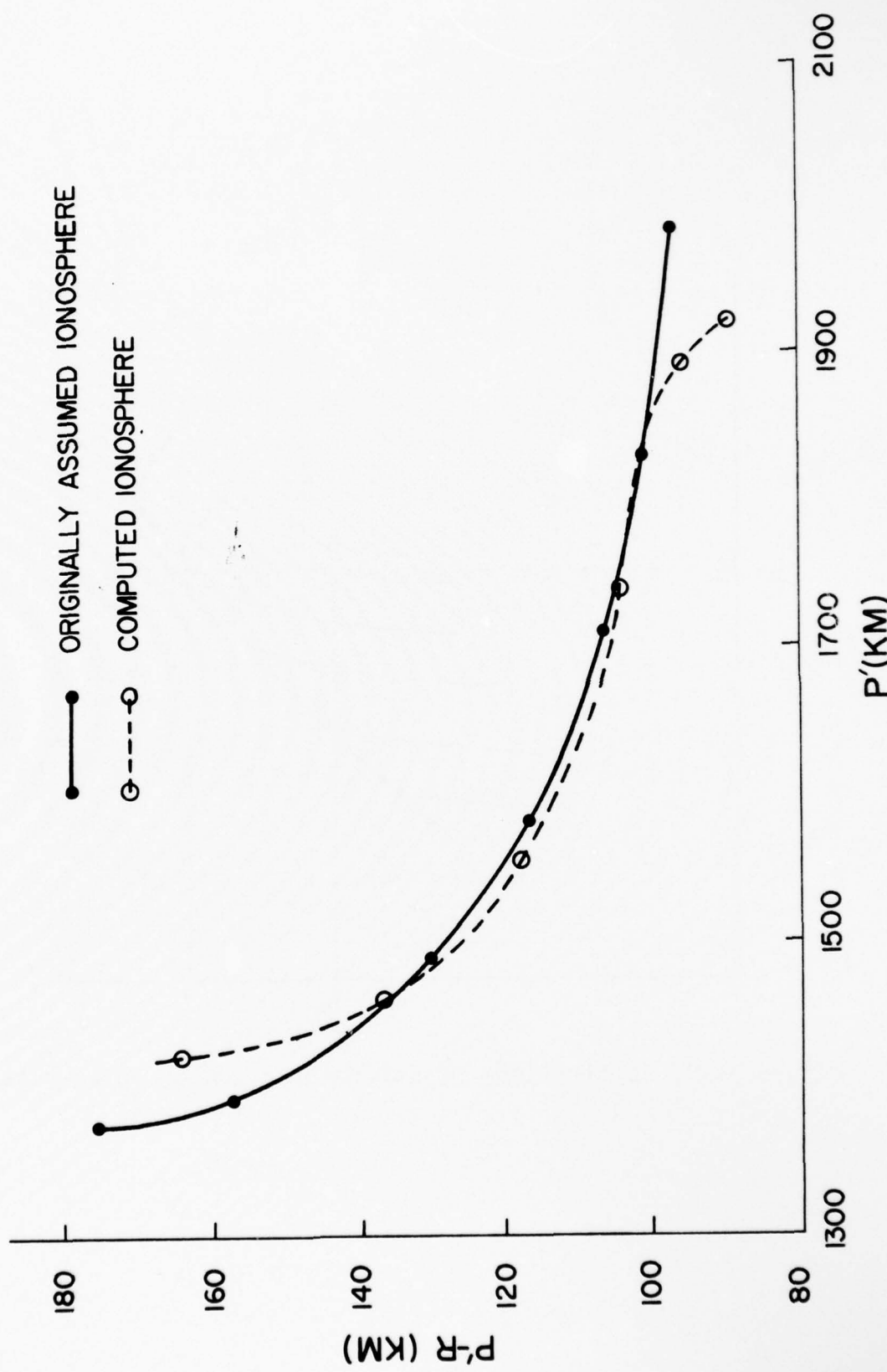


Figure 3.18. Reconstruction of ground range

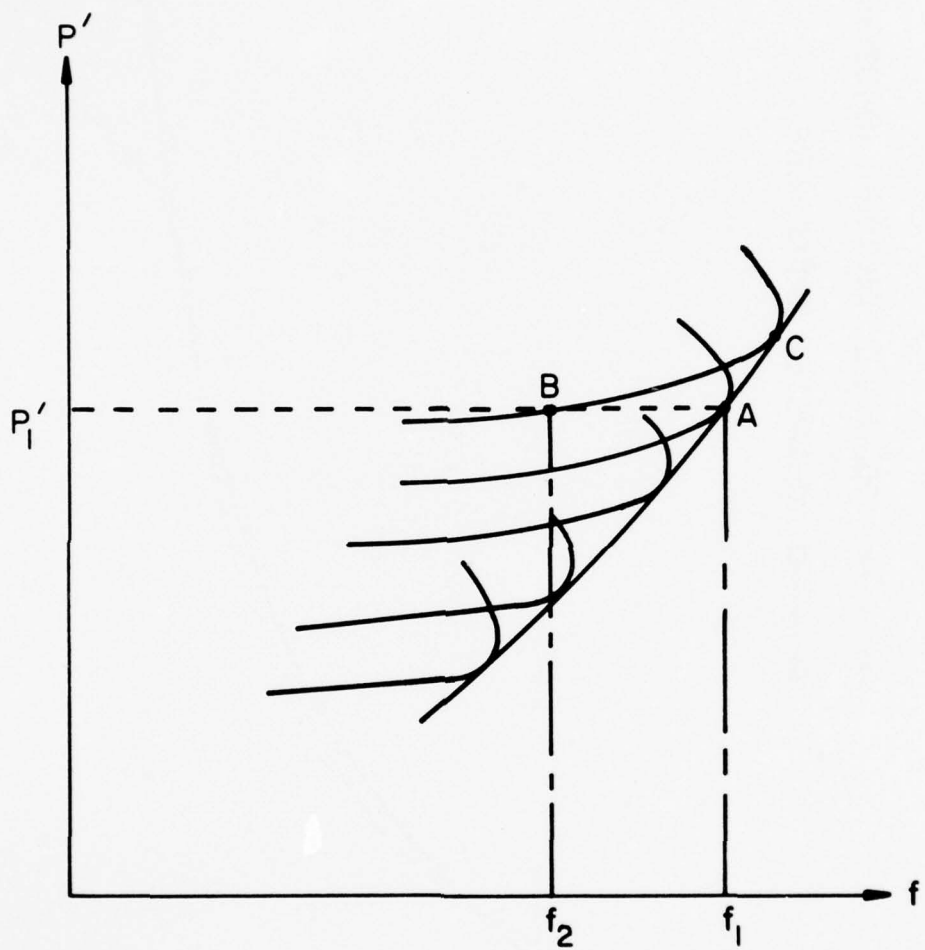


Figure 3.19. Limitations of information contained in data.

Table 3.18. Group path and ground range versus elevation angle for 16 MHz and for 340° azimuth, using the originally assumed model.

Elevation angle, deg.	Group path P', km	Ground range R, km	(P' - R) km
10	1985.06	1888.14	96.92
12	1795.51	1693.76	101.76
14	1661.89	1552.97	108.92
16	1563.03	1444.75	118.28
18	1490.80	1361.39	129.41
20	1435.69	1293.32	142.37
22	1393.93	1236.40	157.53
24	1371.43	1196.75	174.68

Table 3.19. Same as Table 3.18 except using the computed ionosphere

Elevation angle, deg.	Group path P', km	Ground range R, km	(P' - R) km
14	1921.58	1833.31	88.27
16	1892.55	1796.50	96.05
18	1725.20	1619.59	105.61
20	1555.49	1437.47	118.02
22	1458.60	1321.65	136.95
24	1422.14	1257.31	176.83

that of a point C on the leading edge, lying above the point A. Hence the ray of frequency  $f_2$  and group path  $P'_1$  reflects below the apogee height corresponding to the point C. Since this argument is true for any point on the low-ray portions of the oblique ionograms, it follows that one can always find the range corresponding to such a point, although the backscatter leading edge is not capable of yielding the ionospheric profile above the apogee heights corresponding to the minimum group path rays.

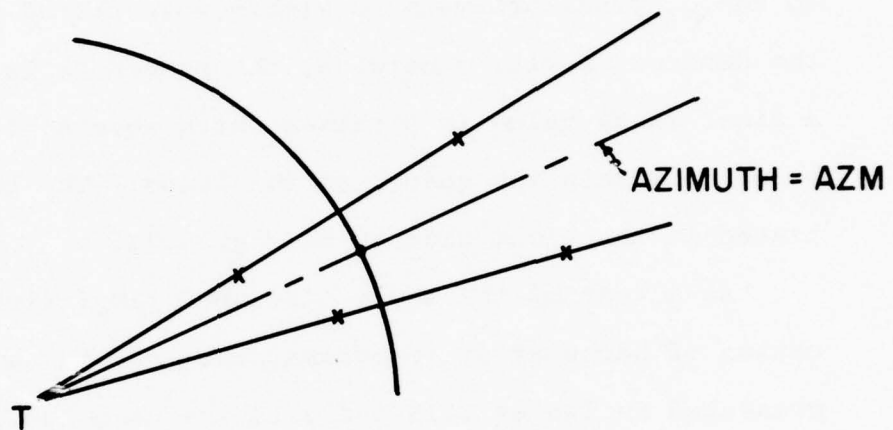
Spurred by the success of the application of the backscatter leading edge inversion technique in the determination of the ground range for a given group path, we decided to combine the inversion problem and the subsequent range determination into one computer program. Thus, provided with the input of backscatter leading edge data for several azimuths and the group path values (non-minimum) at several frequencies for a different azimuth, the program computes the ground ranges. To carry out the range computation, we decided to employ a simple homing technique in conjunction with the exact ray path computation for the concentric QP layer rather than the elaborate three-dimensional ray tracing including the Earth's magnetic field. The details of the entire program are presented in the appendix.

To describe the procedure briefly, first each backscatter leading edge is inverted for a series of QP layer profiles along the corresponding azimuth, in the usual manner. For each specified group path value ( $P'$ ) for which the ground range is to be determined, the program then computes a rough estimate of the range, based on specular reflection at an assumed value of base

height of the ionosphere. By an interpolation procedure involving two azimuths and two ranges along each azimuth as shown in Fig. 3.20, the program then computes the QP layer parameters at half the estimated ground range along the azimuth ( $\alpha$ ) corresponding to the group path data. Using analytical expressions for ray path parameters and the interpolated QP layer parameters, a ground range value is computed for the specified group path, employing an iterative technique. If this range value is close to the original estimate to within a specified tolerance, it is the desired result; otherwise, the procedure is repeated until a final range value is obtained which agrees with the previous value to within the specified tolerance. The technique is illustrated in the block diagram of Fig. 3.21.

As a test of the above discussed simplified method of application of backscatter ionograms, the leading edge inversion results presented in Tables 3.16 and 3.17 are used to compute the ground ranges for various values of group path for  $f=16$  MHz and azimuthal angle of  $340^\circ$ . The results are shown in Table 3.20, which indicates larger errors in  $(P'-R)$  than in Table 3.19, but still less than 15 percent of the actual values of  $(P'-R)$  given in Table 3.18.

TWO AZIMUTHAL DIRECTIONS  
IN WHICH IONOSPHERE HAS  
BEEN PROBED BY BSI



x DENOTES POINTS ON SURFACE OF EARTH  
FOR WHICH QPP HAVE BEEN DETERMINED  
IN ORDER TO DESCRIBE OVERHEAD IONOSPHERE

Figure 3.20. Interpolation procedure.

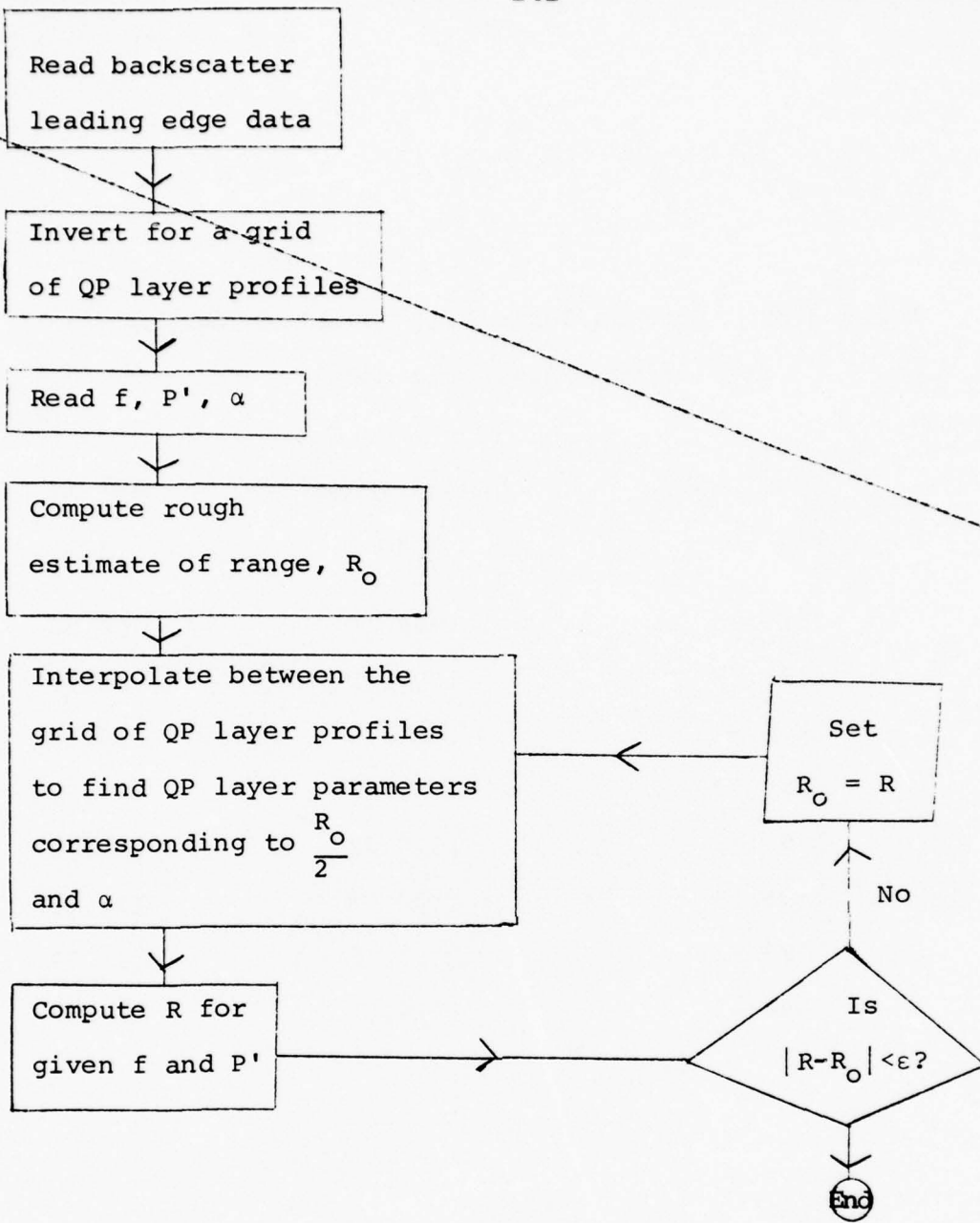


Figure 3.21. Block diagram of steps involved in backscatter leading edge inversion and application.

Table 3.20. Same as Table 3.18 except using the  
Simplified Ionospheric Model

Group path $P'$ , km	Ground range R km	$(P' - R)$ km
1985.06	1904.16	80.50
1795.51	1707.41	88.10
1661.89	1565.75	96.14
1563.03	1457.76	105.27
1490.80	1375.62	115.18
1435.69	1308.68	127.01
1393.93	1252.20	141.73
1371.43	1216.52	154.91

### 3.4.6 Uniqueness of the Application of the Inversion Technique

In this section we will consider the effect of the initial estimate of QPP (QP layer parameters) upon the inversion of group delay into ground range. The motivation for this simulation was to determine the possible effects of the nonuniqueness of the inversion of backscatter ionogram data into ionospheric refractive index. Also we were interested in the reliability of the present technique in providing a reasonably consistent inversion between group delay and ground range, despite the uncertainty involved in the initial estimate of QPP.

The results of this analysis, to date, are presented in the following set of tables. The procedure used in generating these tables was to vary one of the three initial QPP while keeping the other two parameters fixed, and observe the effect of this variation upon the inversion of a fixed value of group path into a computed value of ground range. For our present purposes, we will consider the QPP to consist of the semithickness of the layer ( $y_m$ ), the height of the base of the ionosphere ( $h_b$ ), and the critical, or maximum, plasma frequency ( $f_0 F_2$ ). Other parameters such as  $r_b(h_b + 6370 \text{ km})$  and  $r_m(y_m + h_b + 6370 \text{ km})$  may be obtained easily once  $y_m$  and  $h_b$  are specified. Table 3.21 specifically indicates the effect of varying  $r_b$  which is equivalent to varying  $h_b$ . The last column illustrates the small variation in the computed ground range thereby induced in the case of an untilted (no horizontal gradient) ionosphere. Table 3.22 demonstrates the effect of varying the initial estimate of the maximum plasma frequency (or critical frequency), and again we

## UNTILTED IONOSPHERE

Table 3.21: The Effect of Varying  $r_b$  Initial Estimate Upon Inversion of Group Path into Ground Range.

Theoretical Grp. Path (km)	Initial Est. of $r_b$	Computed Grnd. Range (km)
1700	6510	1591.89
	6520	1591.26
	6530	1591.93
	6540	1590.95
	6550	1590.53
1900	6510	1809.76
	6520	1809.26
	6530	1809.79
	6540	1808.96
	6550	1808.65
2100	6510	2020.76
	6520	2020.43
	6530	2020.79
	6540	2020.15
	6550	2019.98

see that the effect upon the computed ground range is small.

Table 3.23 demonstrates the effect of variations in the initial estimate of  $r_m$  while keeping  $r_b$  fixed. This corresponds to expansion and contraction of the vertical dimensions of the ionosphere through the variation of  $y_m$ . The variation in the computed ground range is somewhat larger than the variation obtained in the previous two tables. Nevertheless, it should be noted that even though  $r_m$  is varying by less than 1% from its nominal value of 6610 km, the really significant parameter is the semi-thickness ( $y_m$ ) of the ionospheric layer, and this latter parameter is varying over a proportionately larger range--i.e.  $r_m = 6600$  km corresponds to a 70 km semithickness, while  $r_m = 6620$  km corresponds to a 90 km semithickness.

This type of analysis has also been performed for a tilted ionosphere (an ionosphere with a horizontal gradient). Tables 3.24, 3.25, and 3.26 correspond to Tables 3.21, 3.22, and 3.23 respectively, and in comparing these two sets of tables, it would appear that the inversion of group path into ground range is more sensitive to the variability of the initial QPP in a tilted ionosphere. This effect would seem to be most pronounced in the case of variations of  $r_m$ .

We therefore decided to consider the possible causes of the relatively large variation in ground range resulting from the simulated uncertainty in the initial value of  $r_m$ . By narrowing the uncertainty in the initial estimate of  $r_m$  by a factor of 2, it can be seen that the variability of the ground range

## UNTILTED IONOSPHERE

Table 3.22: The Effect of Varying the Initial Estimate of Critical Frequency Upon Inversion of Group Path Into Ground Range.

Theoretical Grp. Path (km)	Initial Est. of $r_b$ (km)	Computed Grnd. Range (km)
1700	6.75	1592.09
	7.00	1591.35
	7.25	1591.93
	7.50	1591.17
	7.75	1591.04
1900	6.75	1809.92
	7.00	1809.33
	7.25	1809.79
	7.50	1809.19
	7.75	1809.11
2100	6.75	2020.28
	7.00	2020.46
	7.25	2020.79
	7.50	2020.39
	7.75	2020.35

## UNTILTED IONOSPHERE

Table 3.23: The Effect of Varying Layer Semithickness  
Upon Inversion of Group Path to Ground Range.

Theoretical Grp. Path (km)	Initial Est. of $r_m$ (km) $y_m$ (km)	Computed Grnd. Range (km)
1700	6600              70	1590.60
	6605              75	1590.56
	6610              80	1591.93
	6615              85	1592.26
	6620              90	1591.96
1900	6600              70	1808.73
	6605              75	1808.67
	6610              80	1809.79
	6615              85	1810.06
	6620              90	1809.81
2100	6600              70	2020.08
	6605              75	2020.14
	6610              80	2020.79
	6615              85	2020.98
	6620              90	2020.80

## TILTED IONOSPHERE

Table 3.24: The Effect of the Initial Estimate of  $r_b$  (Radius to Ionospheric Base) Upon the Inversion of Group Path into Ground Range.

Theoretical Grp. Path (km)	Initial Est. of $r_b$ (km)	Computed Grnd. Range (km)
1700	6510	1584.67
	6520	1583.57
	6530	1586.57
	6540	1586.86
	6550	1583.67
1900	6510	1798.66
	6520	1792.39
	6530	1794.79
	6540	1795.77
	6550	1792.42
2100	6510	1996.30
	6520	1994.87
	6530	1996.97
	6540	1998.44
	6550	1994.96

## TILTED IONOSPHERE

Table 3.25: The Effect of Initial Estimate of Critical Frequency ( $f_c$ ) Upon Inversion.

Theoretical Grp. Path (km)	Initial Est. of $f_c$	Computed Grnd. Range (km)
1700	6.75	1586.41
	7.00	1586.89
	7.25	1586.57
	7.50	1587.24
	7.75	1586.37
1900	6.75	1795.11
	7.00	1796.12
	7.25	1794.79
	7.50	1796.61
	7.75	1795.26
2100	6.75	1997.62
	7.00	1999.02
	7.25	1996.97
	7.50	1999.62
	7.75	1997.90

## TILTED IONOSPHERE

Table 3.26: The Effect of Initial Estimate of  $r_m$  Upon  
Inversion of Group Path into Ground Range.  
Program was allowed to go 40 Iterations

Theoretical Grp. Path (km)	Initial Est. of $r_m$ (km)	$y_m$ (km)	Computed Grnd. Range (km)
1700	6590	60	1578.35
	6600	70	1582.48
	6610	80	1586.57
	6620	90	1586.67
	6630	100	1590.76
1900	6590	60	1786.76
	6600	70	1790.84
	6610	80	1794.79
	6620	90	1798.14
	6630	100	1801.60
2100	6590	60	1988.81
	6600	70	1992.96
	6610	80	1996.97
	6620	90	2001.28
	6630	100	2005.76

## TILTED IONOSPHERE

Table 3.27: The Effect of Varying the Layer Semithickness Upon the Inversion of Group Path to Ground Range.

Theoretical Grp. Path (km)	Initial Est. of $r_m$ (km)	$y_m$	Computed Grnd. Range (km)
1700	6600	70	1582.48
	6605	75	1582.13
	6610	80	1586.57
	6615	85	1587.62
	6620	90	1588.67
1900	6600	70	1790.84
	6605	75	1790.62
	6010	80	1794.79
	6615	85	1797.08
	6620	90	1798.14
2100	6600	70	1992.96
	6605	75	1992.82
	6610	80	1996.97
	6615	85	2000.16
	6620	90	2001.28

is also reduced, as shown in Table 3.27. In order to consider the effect of allowing the program to perform a greater number of iterations, we have repeated the calculation of Table 3.26 by doubling the number of iterations which the program uses in computing a final set of QPP. The result is shown in Table 3.28. Although this increase in the number of iterations generally improves the result, this is not always the case, as can be seen in Table 3.29. The significant quantity,  $\sigma$ , denotes the standard deviation of the ground range values from their respective means. For the smaller values of simulated group path, increased iterations produce a smaller standard deviation. For the largest value of group path (2100 km) the standard deviation is actually larger in the case of 80 iterations, as opposed to the case of 40 iterations.

## TILTED IONOSPHERE

Table 3.28: The Effect of Initial Estimate of  $r_m$  Upon  
Inversion of Group Path into Ground Range.  
Program was allowed to go 80 Iterations  
in Fitting QPP.

Theoretical Grp. Path (km)	Initial Est. of $r_m$ (km)	$y_m$ (km)	Computed Grnd. Range (km)
1700	6590	60	1580.18
	6600	70	1582.72
	6610	80	1586.97
	6620	90	1587.40
	6630	100	1588.40
1900	6590	60	1778.40
	6600	70	1781.92
	6610	80	1788.25
	6620	90	1789.21
	6630	100	1790.48
2100	6590	60	1973.34
	6600	70	1977.90
	6610	80	1986.09
	6620	90	1987.49
	6630	100	1989.10

## TILTED IONOSPHERE

Table 3.29: Variance Resulting from Different Values of  
 $r_m$  as Affected by Number of Iterations (IT).

Theoretical Grp. Path (km)	IT	$\bar{D}$	$\sigma$
1700	40	1585.37	4.45
	80	1585.13	3.15
1900	40	1794.43	5.23
	80	1785.65	4.39
2100	40	1997.16	5.97
	80	1982.78	6.10

## 3.5 General Consideration of the Inversion Problem

In the past two sections of this chapter we have presented several techniques that can be applied to deduce the ionospheric structure by using point-to-point oblique ionograms (section 3.3) or backscatter leading edges (section 3.4). In both cases our computations have been carried out for quasi-parabolic profiles. Recently an inversion technique developed in connection with geo-physical problems has shown great promise. This technique, known as Backus-Gilbert technique, can be adapted to inverting oblique ionograms of both kinds. The problem has been formulated in a paper "A Method for Inverting Oblique Sounding Data in the Ionosphere" which is attached as Appendix 4. Initial application to the vertical incidence data demonstrates its rapid convergence. The technique has yet to be applied to inverting oblique ionograms. It is desirable to carry out many computations in order to understand the capability, the characteristics and the limitation of this inversion technique. So far the problem has been formulated for inverting either the backscatter leading edge or the oblique ionogram. In both cases spherical stratification is assumed. Details can be found in Appendix 4.

## 3.6 Conclusions

In conclusion, we have in this section discussed our efforts to devise techniques for the determination of ionospheric structure from oblique radio propagation data. Particular attention was devoted to the problem of obtaining the horizontal gradients. The major findings of the effort are: a) point-to-point oblique ionograms, by themselves, are not very useful for obtaining the horizontal gradients, while b) backscatter leading edge data are capable of providing information concerning the horizontal gradients.

We have provided several examples of inversion of the oblique radio propagation data and even investigated the application of the backscatter technique. We have demonstrated that despite the fact that the inversion technique does not necessarily yield a unique solution for the ionospheric structure, this uncertainty is not an important factor in the application.

#### 4. Recommendations for Future Work

Based on the efforts of our work reported in sections 2 and 3 and the conclusions reached therein, we make the following recommendations for continuing work on this project:

1. Since the backscatter data and the corresponding inversion results involve a grid of points in the azimuth-range space, it is desirable that the electron density model employed in the three-dimensional ray tracing be specified in the azimuth-range space rather than in the latitude-longitude space.
2. The basic inversion techniques of backscatter leading edge data need to be tested by employing simulated data for progressively complicated ionospheres. In this connection, it is necessary that the simulated data points be closely spaced in range, in view of the fact that successive data points correspond to successively increasing values of range away from the transmitter. Hence for the derivation of local horizontal gradients, it is necessary to consider sets of data points, closely spaced in range, and hence in frequency.
3. In addition to the inversion of backscatter leading edge for ionospheric structure, further tests are necessary with regard to the application of the inversion results for computing the ranges for non-minimum group paths. In this connection, it is necessary to have simulated ray tracing data for non-minimum group path rays for the same model ionospheres for which the backscatter leading edges are simulated.
4. The dependence of the inversion result upon the choice of the initial set of layer parameters should be further investigated

with a view to determining how in actual practice, the initial set of layer parameters must be chosen in order to minimize the uncertainty of the inversion technique.

5. The present scheme for homing the ray after one reflection from the ionosphere is very successful as demonstrated by several examples in this report. However, in extending the present scheme to multi-hop modes some difficulties are encountered. Some of these difficulties have been identified: the coarseness of the grid points at which the electron density is given, and inflexibility in the computer program to handle mixed and complex modes. To remove these difficulties requires further refinement of the ray tracing program.

6. Preliminary analysis shows promise in applying the Backus-Gilbert technique to inversion of the oblique propagation data. This technique has been applied to the vertical ionogram and very rapid convergence is obtained. Even though the mathematical formulation for the inversion of oblique data has been carried out, its application to data has yet to be made. One possibility is to choose a model profile (such as piece-wise parabolic profile) for which analytic expressions are available so as to reduce the computation time. Another area of interest is to generalize the Backus-Gilbert technique by including the horizontal gradient. In this latter case the Bouguer's rule is no longer valid, one must reformulate the problem anew.

## APPENDIX 1

The computer programs for ray homing are listed in the following pages. These programs are discussed in section 2.5.

```

C           DECIDES WHICH RAYS ARE TO BE TRACED AND SETS THE IN      0002
CONDITIONS FOR EACH RAY BEFORE CALLING TRACE, WHICH CALCULATES THE RAY  0003
DIMENSION TYPE(3),TYPE2(3)                                         0004
DIMENSION MODEIT(4)
COMMON /CCNST/ EI,PIT2,PID2,DEGS,RAD,K,C,LCGTEN                  0005
COMMON /FK/ N,STEER,MODE,E1MAX,E1MIN,E2MAX,E2MIN,FACT,RSTART        0006
COMMON /FIN/ N2,MUX,PN2(8),ECLAF(4),SPACE,CCIL,FIELD                0007
COMMON /PLG/ NTYP,RNEWW,FNEWW,RAYBEG,RAYSET,LINES,IHOP,NUIEST,APHT   0008
COMMON /MODELS/ MCDEL(4)                                         0009
COMMON /XX/ X,PXPE,PXPTH,PXPPH,FXPT,HMAX                         0010
COMMON F(12),T,STE,ERDT(12) /WW/ ID(10),W0,W(400)                   0011
COMMON /VPRN1/ VN(250),VNPR(250),VNPTH(250),VNFEH(250)             11 KV 1
COMMON /VPRN2/ VRANGE(250),VHT(250)                                 11 KV 2
COMMON /NDOPT/ NPRINT,KCPT,MPRT                                     11 KV 3
COMMON /DENS/ EUM2(683),NDUM(2),JFLAG,NSOL,EBMIN(21),JTEMP          UOFI 1
EQUIVALENCE (P,W(3)),(PLCN,W(13)),(LCN,W(14)),(PLAT,W(15)),       0012
1 (LAT,W(16)),(BETA,W(17)),(AZ1,W(18)),(EARTH,W(19)),            0013
2 (XMTRH,W(20)),(INTYP,W(41)),(MAXERE,W(42)),(ERATIO,W(43)),     0014
3 (STEP1,W(44)),(STPMAX,W(45)),(STPMIN,W(46)),(FACTR,W(47)),     0015
4 (RAY,W(67)),(MAXSTE,W(93)),(SKIP,W(180)),(HCP,W(254)),        0016
5 (ELBEG,W(255)),(ELEND,W(256)),(ELSTEP,W(257)),(FBEG,W(258)),   0017
6 (FEND,W(259)),(FSTEE,W(260)),(AZBEG,W(263)),(AZEND,W(264)),    0018
7 (AZSTEE,W(265)),(PIT,W(272)),(CNLY,W(279)),(WN,W(299))         0019
EQUIVALENCE (RC,W(375)),(ALPHA,W(376)),(THO,W(377)),(PEO,W(378)) UOFI 2
REAL LCGTEN,K,N2,MUX,MAXSTE,INTYP,MAXERE,MU,ION,LAT               0020
DATA MODELT,KOLL1,KCIL2/2*1H,4HCIEC,1H,4HWITH,4H NO/
DATA TYPE,TYPE2/4HX-CR,4HNCR,4HORDI,4HNARY,2*1H /
DATA MCBEW/0/                                                 UOFI 2A
SECCND(A)=10.0
C      CALL QSEXUN                                              0023
C      NDATE=IDATE(0)                                           0024
C      SECCND=KICK(C)*.C01                                     0025
TIME=SECCND(A)
LINES=0
NPAGE=0
DC 5 I=1,400
5 W(I)=0.0
FIELD=1.0
COLL=0.0
KOLL=KCIL2
NDATE=C
IF(CCII.NE.0.0) KCLI=KOLL1
C      CONSTANTS                                              0029
PI=3.1415926536                                             0030
PIT2=2.*EI                                              0031
PID2=PI/2.                                              0032
DEGS=180./PI                                              0033
RAD=PI/180.                                              0034
K=80.6E-6                                              0035
C=2.997925E5                                             0036
LOGTEN=AIOG(10.)
DO 2 I=1,4
2 MODELI(I)=MODELT(I)
C      INITIALIZE SOME VARIABLES IN THE W ARRAY                 0038
FLCN=0.                                              0039
FLAT=PIE2                                              0040
EARTH=6370.                                              0041
INTYP=3.                                              0042
INTYP=3.                                              0043

```

```

MAXFRR=1.E-8          0044
ERATIO=50.            0045
STEEL=1.              0046
STPMAX=100.           0047
STPMIN=1.E-4          0048
FACTR=0.5             0049
MAXSTP=1000.          0050
HCP=1.                0051
ELT=0.                0052
C                           0053
1 CALL READ W          0054
C
C     MPRT = C          KV 054
C
C     F=0.0
C     BETA=0.0
C     AZ1=0.0
C     IF (WN.LT.7.) WN=7.          0056
C     IF (WN.GT.12.) WN=12.         0057
C     IF (SKIF.EQ.0.) SKIF=MAXSTP  0058
C     NTYF=2.+FIELD*RAY+0.01       0059
C     PRINT 7, ID, RDATE, MODEL, TYPE(NTYF), TYPE2(NTYF), KOLL
7    FORMAT(1E1,10A4,2CX,I8/5X,4(1X,A4),2X,2A4,' COLLISIONS')
C     PRINT 8
8    FORMAT (85H INITIAL VALUES FOR THE W ARRAY -- ALL ANGLES IN RADIAN 0063
1S, CNLY NCNZFC VALUES PRINTF/)
DO 10 I=1,400           0064
  IF (W(I).NE.0.) PRINT 9, I,W(I)      0065
9    FORMAT (I4,E19.11)                 0066
10 CONTINUE               0067
C     LET SUBROUTINES PRINTR AND RAYPIT KNOW THERE IS A NEW W ARRAY 0068
C     PNEWW=1.0
C     RNEWW=1.0
C
C     INITIALIZE PARAMETERS FOR INTEGRATION SUBROUTINE FKAM          0069
N=WN+0.01               0070
MODE=INTYP +0.01         0071
STEP=STEEL              0072
STEP=STEEL              0073
STEP=STEEL              0074
STEP=STEEL              0075
STEP=STEEL              0076
STEP=STEEL              1/26/71
E1MAX=MAXERR            0077
E1MIN=MAXERR/ERATIO     0078
E2MAX=STEPMAX           0079
E2MIN=STEPMIN           0080
FACTR=FACTR              0081
C
C     DETERMINE TRANSMITTER LOCATION IN COMPUTATIONAL COORDINATE SYST 0082
C     (GEOMAGNETIC COORDINATES IF DIPOLE FIELD IS USED)            0083
C
RC=FARIBR+XMTRH          0084
SP=SIN(EIAT)              0085
CP=SIN(EI2-PIAT)          0086
SINCPH=SIN(LON-ELCN)       0087
COSCPH=SIN(EL2-(ION-PLCN)) 0088
SL=SIN(IAT)                0089
CL=SIN(EI2-IAT)            0090
ALPHA=ATAN2(-SINCPH*CP,-COSCPH*CP*SI+SP*CL) 0091
TH0=ARCCS(COSIEE*CP*CL+SP*SL) 0092
PH0=ATAN2(SINCPH*CL,COSCPH*SP*CI-CP*SL) 0093
THIS PORTION IS ADDED FOR THE HAVING FEATURE. IT READS THE DENSITYUOFI 3 0094
C PROFILE FROM ELECTX          UOFI 4
IF(W(380).EQ.0.0) GC TO 555  UOFI 5
IF(MOREW.EQ.1) GC TO 555    UOFI 5A

```

```

MOREW=1 UCFI 5B
CALL ELECTX UCFI 5C
C 0095
C
C      LCCE ON FREQUENCY, AZIMUTH ANGLE, AND ELEVATION ANGLE 0096
C      NFFEQ=1 UOFI 5D
555      IF (FSTEE.NE.0.) NFFEQ=(FFND-FBEG)/FSTEP+1.5 0098
      NAZ=1 0099
      IF (AZSTEP.NE.0.) NAZ=(AZEND-AZBEG)/AZSTEP+1.5 0100
      NBETA=1 0101
      IF (ELSTEP.NE.0.) NBETA=(ELEND-ELBEG)/ELSTEP+1.5 0102
      DO 50 NF=1,NFFEQ 0103
      F=FBEG+(NF-1)*FSTEP 0104
      IF(W(380).EQ.0.0) GC TO 55 UCFI 6
      CALL FCME UOFI 7
55      DO 45 J=1,NAZ UCFI 9
      IF(W(380).NE.0.0) GC TO 60 UOFI 10
      AZ1=AZBEG+(J-1)*AZSTEP 0106
      60      AZA=AZ1*DEGS UCFI 11
      GAMMA=PI-AZ1+ALEHA 0108
      SGAMMA=SIN(GAMMA) 0109
      CGAMMA=SIN(PID2-GAMMA) 0110
      DO 40 I=1,NBETA 0111
      IF(W(380).NE.0.0) GC TO 70 UCFI 12
      EETA=ELBEG+(I-1)*ELSTEP 0112
      70      CEETA=SIN(PID2-EETA) UCFI 13
      C THIS IS USED FOR THE HOMING FEATURE ONLY UOFI 14
      IF(W(380).EQ.0.0) GC TO 32 UCFI 15
      CALL AJJUST UOFI 16
      MPFT=0 UCFI 17
      GC TO 50 UOFI 18
      32      R(1)=RC UCFI 19
      R(2)=TRO 0115
      R(3)=PEC 0116
      R(4)=SIN(EETA) 0117
      R(5)=CEETA*CGAMMA 0118
      R(6)=CEETA*SGAMMA 0119
      T=0. 0120
      RSTART=1. 0121
      CALL RINDEX 0122
      EL=EETA*DEGS 0123
      IF (I.NE.1.AND.NEAGE.LT.3.AND.LINES.LE.17) GC TO 18 0124
      NPAGE=0
      LINES=0
      PRINT 7, ID(1),ID,NCODEL,TYPE(NTYP),TYPE2(NTYP),KCLL 0126
      PRINT 17, F,AZA 0127
      17 FORMAT (18X,11HFRQUENCY =,F12.6,37H MHZ, AZIMUTH ANGLE OF TRANSMI 0128
      1SSION =,F12.6,4H DEG) 0129
      18 NPAGE=NEAGE+1 0130
      PRINT 19, EL 0131
      19 FORMAT (/31X,33HELEVATION ANGLE OF TRANSMISSION =,F12.6,4H DEG/) 0132
      IF (N2.GT.0.) GC TO 25 0133
      CALL ELECTX 0134
      FN=SIGN(SQRT(ABS(X))*F,X) 0135
      PRINT 21, FN 0136
      21 FORMAT (58HOTRANSMITTER IN EVANESCENT REGION, TRANSMISSION IMECSSI 0137
      1BLE/20ECEIASMA FREQUENCY = ,F17.10) 0138
      GC TO 44 0139
      25 MU=SQRT(N2) 0140
      R(4)=MU*F(4) 0141
      R(5)=MU*F(5) 0142
      R(6)=MU*F(6) 0143

```

```

DO 28 NN=7,N          0144
28 R(NN)=0.           0145
      CAII TRACE      0146
C     SECND=KICK(0)*.C01 0148
      CSEC=TIME
      TIME=SECCND(A)
      DIFF=TIME-OSEC
      PRINT 30, DIFF
      30 FORMAT(34X,26HTHIS RAY CALCULATION TOOK ,F8.3,4H SEC ) 0150
      150 KV 1

C
C      NPRINT IS THE OPTION FOR PRINTING ELEC. DENSITY AND DERIVATIVES
C
C      IF(NPRINT.EQ.0) GC TO 370
C
C      PRINT ELECTRON DENSITY PROFILE AND THE DERIVATIVES      151 KV 1
C      USING APPLETION - HARTREE FORMULA      151 KV 2
C
C      PRINT 331
331 FORMAT (1H1, 48H ELECTRON DENSITY PROFILE AND ITS DERIVATIVES , 151 KV 5
      1 40H CCUSERY ARCCN CORE. K.VANGURI // , 151 KV 7
      2 60H N = C * X, C = 12400*F**2 F IN MHZ, N = EL. PER CC , 151 KV 8
      3 40H AEEIETCN-HARTREE FORMULA / , 151 KV 9
      4 60H DN/ER = C * PXER      IN EL/CC/KM , 151 KV10
      5 60H DN/ETH = C * PXETH * RAD IN EL/CC/DEG , 151 KV11
      6 60H DN/EPH = C * PXEPH * RAD IN EL/CC/DEG , 151 KV12
      7 6X,5HRANGE,5X,6HHEIGHT,1CX,1HN,9X,5HDN/DR,7X,6HDN/DTH,7X, 151 KV13
      8 6HDN/EPH,7X,4BSTEP/ 9X,2HKM,8X,2HKM,8X,5HEL/CC / , 151 KV14
      151 KV15

C      DC 365 MJ = 1,MPFT      151 KV25
      PRINT 345, VRANGE(MJ),VBT(MJ),      151 KV26
      2          VN(MJ),VNPF(MJ),VNPTH(MJ),VNPPH(MJ),MJ      151 KV27
345 FORMAT (1X,F10.4,2X,F10.4,4(2X,F11.4),2X,I5)      151 KV28
365 CONTINUE      151 KV28
370 CONTINUE      151 KV29
      MPFT = 0      151 KV29

C      IF (NUTEST.EQ.1.AND.CONLY.NE.0..AND.IHOP.EQ.1) GC TO 44      0152
40 CONTINUE      0153
44 IF (F17.NE.0.) CALL ENDPLT      0154
45 CONTINUE      0155
50 CONTINUE      0156
      GO TO 1      0157
      END      0158

```

```

SUEFOUTINE TRACE 0186
DIMENSION ROLD(12),TROLD(12) 0187
COMMON /FK/ N,STEEL,MCODE,E1MAX,E1MIN,E2MAX,E2MIN,FACT,RESTART 0188
COMMON /FIN/ N2,PA2(R),TFCIAR,FLCLAR,SPACE,CCLI,FIFLD 0189
COMMON /TRAC/ GRCUND,PERIGE,THERE,MINDIS,UNDER 0190
COMMON /FIG/ NTYF,BNEWW,FNEWW,RAYBEG,RAYSET,LINES,IHOP,NUTEST,APHT 0191
COMMON /XX/ X,XPXF,XPXTH,XPFPH,XPXT,HMAX 0192
COMMON/FLAGS/IFIAG
COMMON E(12),T,SIP,DELT(12) /WW/ ID(10),WC,W(400) 0193
EQUIVALENCE (FARTH,R,W(19)),(HS,W(40)),(MAXSTE,W(93)),(SKIP,W(180)) 0194
1,(HCP,W(254)),(PIT,W(272)) 0195
EQUIVALENCE (CNIY,W(371)),(STEP1,W(44)) UOFI 1
REAI MAXSTP 0196
CCMFILEY N2,TFCIAR,RFCLAR 0197
LOGICAL SPACE,HCME,WASNT,PASSED,UNDERGE,GROUND,PERIGE,THERE, 0198
1 MINDIS,UNDER 0199
CNIY=C.C UOFI 2
STEEL=STEEL1 UOFI 3
STEP=STEEL1 UOFI 4
NHCE=HCE+0.01 0200
MAX=MAXSTE+C.01 0201
NSKIE=SKIE+C.01 0202
RSTART=1. 0203
CALL HASFL 0204
IF(IFLAG.NE.0) GO TO 50
H=R(1)-FARTH 0205
HCME=DELT(1)*(H-HS).GF.0. 0206
RAYEFG=1. 0207
RAYSET=C. 0208
CALL PRINTR (EHXMTR ) 0209
IF (PIT.NE.0.) CALL FAYFIT 0210
RAYEFG=C. 0211
C 0212
C ICCF ON NUMBER OF HCP 0213
DO 45 JHOP=1,NHCP
IHCF=JHCF
RAYSET=C.
NUTEST=C
APHT=HS
TFCIAR=FLCLAR
C 0215
C ICCF ON MAXIMUM NUMBER OF STEPS PER HCP 0220
DO 28 J=1,MAX 0221
IF (ABS(E-HS).GT.AES(APHT-HS)) APHT=H 0222
IF (.NOT.SPACE) GC TO 12 0223
CALL REACH 0224
IF(IFLAG.NE.0) GO TO 50
RSTART=1.
IF (IHCE*J.EQ.1) TPOIAR=RFCLAR 0225
IF (GRCUND) GC TO 22 0226
IF (PFFIGE) CAII PRINTR (EHERRIGEE ) 0227
IF (THEBE) GO TO 40 0228
IF (MINDIS) GC TO 32 0229
IF (PIT.NE.0.) CALL RAYPLT 0230
12 DO 13 I=1,N 0231
ROLD(I)=F(L) 0232
13 DRCIE(L)=DBDT(L) 0233
TCLD=I 0234
CALL RKAM 0235
IF(IFLAG.NE.0) GC TO 50 0236

```

```

H=R(1)-EARTH
WASNT=.NCT.HOME
HCME=DFDT(1)*(H-HS).GE.0.
X=(DRCI(1)-DRCII(1))*(T-TCID)
SMT=0.
IF (X.NE.0.) SMT=0.5*(R(1)-FOLD(1)+C.5*X)**2/ABS(X) 0237
UNDRGD=H.LT.0..CR.DRET(1).GT.0..AND.DRCI(1).LT.0..AND.SMT.GT.H 0238
PASSED=(H-HS)*(FOLD(1)-EARTH-HS).LT.0. 0239
IF (PASSED.AND.(.NOT.UNDRGD.OR.HS.GT.0.)) GC TO 35 0240
IF (HS.FC.ROIL(1)-EARTH.AND.DRCI(1)*DRET(1).LT.0..AND.HCME) 0241
1 GC TO 39 0242
IF (HCME.AND.WASNT.AND.(.NCT.UNDRGD.CR.FS.GT.0.)) GO TC 17 0243
IF (UNDRGD) GC TO 18 0244
GC TO 23 0245
C
C      RAY MAY HAVE MADE A CLOSEST APPROACH 0246
17 IF (SMT.GT.ABS(H-ES)) GO TC 36 0247
NUTEST=4 0248
IF (R(5).NE.0..CR.R(6).NE.0.) CALL GFAZE(HS) 0249
IF (UNDEF) GO TC 19 0250
IF (NUTEST.EQ.0.) GO TO 36 0251
GO TO 32 0252
C
C      RAY WENT UNDERGROUND 0253
18 IF (DRET(1).LT.0.) GC TO 21 0254
19 UNDRG=.FALSE. 0255
C      CALL PRINTR(&HUNDERGRD) 0256
DO 20 L=1,N 0257
R(L)=RCLE(L) 0258
20 DFDT(L)=TCLE(L) 0259
T=TCLE 0260
CALL RINDEX 0261
IF (IFLAG.NE.0) GO TC 50 0262
21 CALL EACK UP(0.) 0263
22 R(1)=EARTH 0264
R(4)=AES(R(4)) 0265
DFDT(1)=ABS(DRET(1)) 0266
RSTART=1. 0267
CALL PRINTR(8FGFND FFF) 0268
IF (HS.FC.0.) GC TO 41 0269
H=0. 0270
GO TC 25 0271
C
23 IF (DRCI(1).LT.0..AND.DFDT(1).GT.0.) CALL FFINTR(8HPFFIGEE ) 0272
IF (DRCI(1).GT.0..AND.DRET(1).LT.0.) CALL PRINTR(8HAPCGEE ) 0273
IF (DRCII(2)*DFDT(2).LT.0.) CALL PRINTF(8HMAX LAT ) 0274
IF (DRCII(3)*DRET(3).LT.0.) CALL PRINTF(8HMAX LONG) 0275
DO 24 I=4,6 0276
IF (ROIL(I)*R(I).LT.0.) CALL PRINTR(8HWAVE REV) 0277
24 CONTINUE 0278
25 IF (PIT.NE.0.) CALL RAYFLT 0279
IF (IFLAG.NE.0) GC TO 50 0280
IF (F.GT.HMAX.AND.H.GT.HS.AND.DFDT(1).GT.0.) GO TO 30 0281
IF (MCD(J,NSKIE).EQ.0) CALL PRINTR(&H ) 0282
28 CONTINUE 0283
C
C      EXCEEDED MAXIMUM NUMBER OF STEPS 0284
NUTEST=2 0285
RAYSP=1. 0286
CALL PFINTR(8HMAX STEP) 0287
RETURN 0288
0289
0290
0291
0292
0293
0294
0295

```

```

C          RAY PENETRATED          0296
C          30 NUTEST=1           0297
          RAYSET=1.               0298
          ONLY=1.0                0299
          CALL FFINTR(8HFFINETFAT) UOFI 5
          RETURN                   0300
C          RAY MADE A CLOSEST APPROXIMAC 0301
C          32 NUTEST=4           0302
          DRDT(1)=C.              0303
          RAYSET=1.               0304
          CALL FRINTR(8HMIN DIST) 0305
          IF (FIT.NE.0.) CALL RAYPLT 0306
          IF (IHCF.GE.NHCF) GC TO 45 0307
          IHCF=IHCF+1             0308
          CALL FFINTR (8HMIN DIST) 0309
          GO TO 45                 0310
C          RAY CROSSED RECEIVER HEIGHT 0311
C          35 IP (HCME) GO TO 39      0312
          36 CCNTINC               0313
C          CALL FFINTR(8HFCVRFHT)   0314
          DC 37 I=1,N               0315
          R(L)=FCIE(L)             0316
          37 DRDT(L)=IROID(L)       0317
          T=TCID                   0318
          CALL RINDEX               0319
          RSTART=1.                 0320
          39 CALL EACK UP(HS)        0321
          40 R(1)=EARTH+HS          0322
          41 RAYSET=1.               0323
          CALL FRINTR(8HFCVF )      0324
          IF (FLT.NE.0.) CALL RAYPLT 0325
          45 HCMP=.TFUF.            0326
          RETURN                   0327
          50 NUTEST=1               0328
          FYTEST=1.0                0329
          CALL FFINTR(8H CUT ICN )  0330
          IFLAG=C
          RETURN
          END

```

0331

167

SUBROUTINE BACK UP(HS)	0332
DIMENSION NWORD1(2),NWORD2(2),NWCRD(2)	
COMMON /FR/ NN,STEP,MCDE,F1MAX,F1MIN,E2MAX,E2MIN,FACT,RSTART	0333
COMMON /IFAC/ GRCUNE,FFIGF,THEFE,MIDDIS,UNDER	0334
COMMON /FIG/ ITYP,RNEWW,ENEWW,RAYBEG,RAYSET,LINES,IHOP,NUTEST,APHT	0335
COMMON F(12),T,STP,CRDT(12)/SW/ ID(10),W0,W(400)	0336
EQUIVALENCE (EAFTHR,W(19)),(INTYF,W(41)),(STEP1,W(44))	0337
SEAL INTYF	0338
LOGICAL UNDER	0339
DATA NWCRD1,NWCDF2/4HBACK,4EUF ,4HGFAZ,4HE /	
STPS=STE	
NWORD(1)=NWORD1(1)	
NWORD(2)=NWORD1(2)	
DO 1 I=1,10	0340
IF (DRIT(1).EQ.C.) GC TO 5	0341
STEPP=- (R(1)-EARTH-RS)/DRIT(1)	0342
STP=SIGN(AMIN1(AES(STP),ABS(STEP)),STEPP)	
IF (ABS(R(1)-EARTH-RS).LT..5E-4.AND.STEP.LT.1.) GC TO 5	0344
CALL ERINTR(SBECMING )	0345
MCDE=1	0346
CALL RKAM	0348
1 CCNTINUE	0350
C	0351
ENTRY GR#2E	
STPS=STE	
NWORD(1)=NWORD2(1)	
NWORD(2)=NWORD2(2)	
DO 2 I=1,10	0352
IF (DRIT(4).EQ.C.) GO TO 5	0353
STEPP=- R(4)/DRIT(4)	0354
STP=SIGN(AMIN1(AES(STP),AES(STEP)),STEPP)	
IF (ABS(R(4)).LE.1.E-6.AND.STEP.LT.1.) GC TO 5	0356
CALL ERINTR(SBHCMING )	0357
ROLE=R(1)	0358
MCDE=1	0359
CALL RKAM	0361
IF (R(1)-EARTH.R.LT.C.) GC TO 4	0363
IF ((R(1)-EARTH-RS)*(ROLE-EARTH-RS).LT.C.) GC TO 3	0364
2 CONTINUE	0365
GC TC 5	0366
3 NUTEST=0	0367
GO TO 5	0368
4 UNDER=.TRUE.	0369
5 MODE=INTYF+C.C1	0370
STEPP=STEPP1	0371
STP=STPS	
RSTART=1.0	
CALL FFIMTR(NWCFI)	
RETURN	0372
END	0373

168

SUBROUTINE RKAM		0888
C NUMERICAL INTEGRATION OF DIFFERENTIAL EQUATIONS		0889
COMMON /FK/ NN, SFACE, MODE, F1MAX, F1MIN, E2MAX, E2MIN, FACT, RSTART		0890
COMMON Y(12), T, STEP, DYDT(12) /WW/ ID(1C), WC, W(400)		
DIMENSION DELY(4,12), BET(4), XV(5), FV(4,12), YU(5,12)		0892
REAL*8 YU		
EQUIVALENCE (EASTER,W(19)), (HMIN,W(390)), (HMAX,W(391))		
DATA XMM/1.0E-6/		
IF (RSTART.EQ.0.) GO TO 1000		0894
LL=1		0895
MM=1		0896
IF (MODE.EQ.1) MM=4		0897
ALPHA=1		0898
EPM=0.C		0899
BET(1)=C.5		0900
BET(2)=0.5		0901
BET(3)=1.0		0902
BET(4)=0.0		0903
R=19.0/270.0		0905
XV(MM)=T		0906
IF (F1MIN.LE.C.) F1MIN=F1MAX/55.		0907
IF (FACT.LE.0.) FACT=.5		0908
CALL HASEL		0909
IF(MODE.NE.1) STEP=SPACE		1/28/71
IF(IPIAG.NE.0) GO TO 100		
DO 320 I=1,NN		0910
FV(MM,I)=DYDT(I)		0911
320 YU(MM,I)=Y(I)		0912
RSTART=0.		0913
GO TO 1001		0914
1000 IF (MODE.NE.1) GO TO 2000		0915
C		0916
C FUNGE-KUTIA		0917
DR1=DYDT(1)*STEP		
DR2=HMIN+EARTH-B-Y(1)		
IF((DR1.LT.DR2).AND.(DR2.LT.0.C)) STEP=DR2/DYDT(1)+XMM		
DR3=HMAX+EARTH-B-Y(1)		
IF((DR1.GT.DR3).AND.(DR3.GT.0.C)) STEP=DR3/DYDT(1)+XMM		
1001 DO 1034 K=1,4		0918
DO 1350 I=1,NN		0919
DELY(K,I)=STEP*FV(MM,I)		0920
Z=YU(MM,I)		0921
1350 Y(I)=Z+EFT(K)*DELY(K,I)		0922
T=BET(K)*STEP+XV(MM)		0923
CALL HASEL		0924
IF(IPIAG.NE.0) GO TO 100		
DO 1034 I=1,NN		0925
1034 FV(MM,I)=DYDT(I)		0926
DO 1035 I=1,NN		0927
DEL=(DELY(1,I)+2.0*DELY(2,I)+2.0*DELY(3,I)+DELY(4,I))/6.0		0928
1039 YU(MM+1,I)=YU(MM,I)+DEL		0929
MM=MM+1		0930
XV(MM)=IV(MM-1)+STEP		0931
DO 1400 I=1,NN		0932
1400 Y(I)=YU(MM,I)		0933
T=XV(MM)		0934
CALL HASEL		0935
IF(IPIAG.NE.0) GO TO 100		
IF (MCDF.EQ.1) GO TO 42		0936

```

DO 150 I=1,NN          0937
150 FV(MM,I)=LYCT(I)  0938
IF (MM.LE.3) GC TC 1001 0939
C
C      ACAMS-MCULTON  0940
2000 DO 2048 I=1,NN    0941
  DEL=STEP*(55.*FV(4,I)-59.*FV(3,I)+37.*FV(2,I)-9.*FV(1,I))/24. 0942
  Y(I)=YU(4,I)+DEL  0943
2048 DEIY(1,I)=Y(I)   0944
  T=XV(4)+STEP  0945
  CALL HASEI  0946
  IF(IFLAG.NE.0) GC TC 100 0947
  XV(5)=T  0948
  DO 2051 I=1,NN    0949
  DEL=STEP*(9.*DYET(I)+19.*FV(4,I)-5.*FV(3,I)+FV(2,I))/24. 0950
  YU(5,I)=YU(4,I)+DEL  0951
2051 Y(I)=YU(5,I)   0952
  CALL HASEL  0953
  IF(IFLAG.NE.0) GC TC 100 0954
  IF (MCDF.LE.2) GO TO 42 0955
C
C      EERRCR ANALYSIS 0955
SSE=0.C  0956
DO 3033 I=1,NN    0957
EPSIL=R*ABS(Y(I)-DEIY(1,I))  0958
IF (MODE.EQ.3.AND.Y(I).NE.C.) EPSIL=EPSIL/AES(Y(I))  0959
IF (SSE.IT.EPSIL) SSE=EPSIL  0960
3033 CONTINUE  0961
IF (E1MAX.GT.SSE) GC TC 3035  0962
IF (ABS(STEP).LE.E2MIN) GC TC 42  0963
LL=1  0964
MM=1  0965
STEE=STEE*FACT  0966
GC TC 1001  0967
3035 IF (LL.LE.1.OR.SSE.GE.E1MIN.CE.E2MAX.LE.ABS(STEP)) GC TO 42  0968
LL=2  0969
MM=3  0970
XV(2)=XV(3)  0971
XV(3)=XV(5)  0972
DO 5363 I=1,NN    0973
FV(2,I)=FV(3,I)  0974
FV(3,I)=LYDT(I)  0975
YU(2,I)=YU(3,I)  0976
5363 YU(3,I)=YU(5,I)  0977
STEE=2.C*STEP  0978
GO TC 1001  0979
C
C      EXIT RUTINE  0980
42 LL=2  0981
MM=4  0982
DO 12 K=1,3    0983
XV(K)=XV(K+1)  0984
DO 12 I=1,NN    0985
FV(K,I)=FV(K+1,I)  0986
12 YU(K,I)=YU(K+1,I)  0987
XV(4)=XV(5)  0988
DO 52 I=1,NN    0989
FV(4,I)=LYDT(I)  0990
52 YU(4,I)=YU(5,I)  0991
IF (MODE.LE.2) RETURN  0992
E=AES(XV(4)-ALPHA)  0993
                                0994
                                0995

```

IF (E.LE.EPM) GC TO 2000  
EPM=F  
100 RETURN  
END

0996  
0997  
0999

```

C      SUBROUTINE PRINTER(NWHT)
C          PRINTS A LINE EACH TIME IT IS CALLED          0493
C          DIMENSION G(3,3),C1(3,3),A1(3),E1(3),C1(3)          0494
C          1,TITLE1(10),TITLE2(10),UNIT(10)          0496
C          DIMENSION NWHT(2),IBINK(2)
C          COMMON /CCNST/ FI,PIT2,PIT2,E2GS,RAT,DUM(3)          0497
C          COMMON /ER/ N,STEP,MODE,E1MAX,E1MIN,E2MAX,E2MIN,FACT,RESTART          0498
C          COMMON /FIN/ N2,MUX,FN2(8),TECLAF(2),FOLAR(2),SPACF,COIL,FIFL          0499
C          COMMON /FLG/ NTYP,RNEWW,ENEWW,RAYBEG,RAYSET,IINES,IHOP,NUTEST,APHT          0500
C          COMMON B(12),T /WW/ ID(10),FC,W(400)          0501
C          COMMON /XX/ X,EXEF,EXETH,EXFFH,EXPT,EMAX          501 KV 1
C          COMMON /VERN1/ VN(250),VNFF(250),VNETH(250),VNEPH(250)          501 KV 2
C          COMMON /VERN2/ VRANGE(250),VHT(250)          501 KV 3
C          COMMON /NDOPT/ NPRINT,KOPT,MPBT          501 KV 5
C          COMMON /EPLI/ SIEEG          501*KV 4
C          EQUIVALENCE (THETA,B(2)),(FHI,R(3))          0502
C          EQUIVALENCE (P,W(3)),(PLCN,W(13)),(LCN,W(14)),(PLAT,W(15)),          0503
C          1,(LAT,W(16)),(PITA,W(17)),(AZ1,W(18)),(EARTHE,W(19)),(XMTRH,W(20))          0504
C          2,(P7,W(280)),(E8,W(281)),(E9,W(282))          0505
C          EQUIVALENCE (RANGE,W(384)),(AZDEV,W(379)),(H,W(383))
C          EQUIVALENCE (E2IT,W(372)),(E3IT,W(373)),(AZA,W(374))          UOFI 1
C          REAI N2,ICN,LAT,MUX          0506
C          DATA A1,E1,C1/1EE,1HN,1HO,1HX,1HF,1HB,1ET,1HI,1HD/
C          DATA TITLE1(7),TITLE2(7),UNIT(7)/4H EH.,4H PATH,4H KM/
C          DATA TITLE1(8),TITLE2(8),UNIT(8)/4H ABS,4H ECREN,4H DB/
C          DATA TITLE1(9),TITLE2(9),UNIT(9)/4H COE,4H HELER,4H C/S/
C          DATA IBINK/2*4H
C          P7=C.0
C          E8=C.0
C          E9=C.0
C          IF (PNEWW.EQ.C.) GO TO 8          0512
C
C          NEW W ARRAY -- REINITIALIZE          0513
C          CNEWW=C.          0514
C          SPL=SIN(FION-LON)          0515
C          CPL=SIN(FID2-(PICK-ICN))          0516
C          SP=SIN(FIAT)          0517
C          CP=SIN(FID2-PLAT)          0518
C          SL=SIN(LAT)          0519
C          CL=SIN(FID2-LAT)          0520
C          G(1,1)=CFI*SP*CI-CP*SI          0521
C          G(1,2)=SEL*SP          0522
C          G(1,3)=-SI*SP*CFL-CL*CP          0523
C          G(2,1)=-SPL*CL          0524
C          G(2,2)=CFI          0525
C          G(2,3)=S1*SPL          0526
C          G(3,1)=CI*CP*CFI+SP*SL          0527
C          G(3,2)=CF*SPI          0528
C          G(3,3)=-SL*CP*CFL+SP*CL          0529
C          DENM=G(1,1)*G(2,2)*G(3,3)+G(1,2)*G(3,1)*G(2,3)+G(2,1)*G(3,2)*G(1,3)          0530
C          1)-G(2,2)*G(3,1)*G(1,3)-G(1,2)*G(2,1)*G(3,3)-G(1,1)*G(3,2)*G(2,3)          0531
C          G1(1,1)=(G(2,2)*G(3,3)-G(3,2)*G(2,3))/DENM          0532
C          G1(1,2)=(G(3,2)*G(1,3)-G(1,2)*G(3,3))/DENM          0533
C          G1(1,3)=(G(1,2)*G(2,3)-G(2,2)*G(1,3))/DENM          0534
C          G1(2,1)=(G(3,1)*G(2,3)-G(2,1)*G(3,3))/DENM          0535
C          G1(2,2)=(G(1,1)*G(3,3)-G(3,1)*G(1,3))/DENM          0536
C          G1(2,3)=(G(2,1)*G(1,3)-G(1,1)*G(2,3))/DENM          0537
C          G1(3,1)=(G(2,1)*G(3,2)-G(3,1)*G(2,2))/DENM          0538
C          G1(3,2)=(G(3,1)*G(1,2)-G(1,1)*G(3,2))/DENM          0539
C          G1(3,3)=(G(1,1)*G(2,2)-G(2,1)*G(1,2))/DENM          0540
C

```

```

RC=EARTHE+XMTSH          0542
XR=EO*G(1,1)              0543
YR=EO*G(2,1)              0544
ZR=EO*G(3,1)              0545
COSTHR=G(3,1)             0546
SINTHR=SIN(ARCCS(COSTHR)) 0547
PHIE=ATAN2(YR,XR)         0548
ALEH=ATAN2(G(3,2),G(3,3)) 0549
IF (P8.NE.0.) PUNCH 5, E1(NTYPE),ID 0550
5 FORMAT (F1,9A8,A7)      0551
IF (P9.NE.0.) FUNCH 5, C1(NTYPE),ID 0552
IF (E7.NE.0.) FUNCH 6, A1(NTYPE),ID 0553
6 FORMAT (A1,1X,9A8,A6)    0554
C
8 IF (RAYEEG.EQ.C.) GC TO 12 0555
NN=MINC(N,9)               0556
PRINT 10, (TITLE1(NR),TITLE2(NR),NR=7,NN) 0557
10 FORMAT (6IX,7HAZIMUTH/60X,9HDEVIATION,7X,9HELEVATION/20X,15HHEIGHT
1   RANGE,3X,3HESI,3X,           11HCOLAT 1CNG,2(5X,12HXMTF  LCCAL), 560 KV
2   2X,12HDECLARIZATION,2X,8H GR.PATH,4A4) 561 KV
PRINT 11, (UNIT(NR),NR=7,NN) 0562
11 FORMAT (16X,2(7X,2HKM),4X,
2   3HDEG, 6(5X,3HDEG),3Y,4HREAL,4X,4HIMAG, 563 KV
1   1 5X,2HKM,1X,2(A6,2X)) 564 KV
12 V=0.                      0565
IF (N2.NE.0.) V=(R(4)**2+R(5)**2+R(6)**2)/N2-1. 0566
H=F(1)-EARTHE              0567
SINTH=SIN(THETA)            0568
COSTH=SIN(PID2-THETA)       0569
XP=F(1)*SINTH*SIN(PID2-PHI)-XR 0570
YP=F(1)*SINTH*SIN(PHI)-YR 0571
ZP=F(1)*COSTH-ZF 0572
EPS=XP*G1(1,1)+YP*G1(1,2)+ZP*G1(1,3) 0573
ETA=XP*G1(2,1)+YE*G1(2,2)+ZP*G1(2,3) 0574
ZETA=XP*G1(3,1)+YE*G1(3,2)+ZP*G1(3,3) 0575
RCE2 = ETA**2 + ZETA**2 0576
RCE=SQRT(RCE2)              0577
RANGE=EC*ATAN2(RCE,EO+EPS)  UCPI 2
ANGDEG=ATAN2(R(4),SQRT(R(5)**2+R(6)**2))*DEGS 0579
SR=SQRT(RCE2+EPS**2)        0580
C
C CHANGES MADE BY ARCCN CCRP. BY K.VANGURI 580 KV 1
C
C STORE THE ELECTRON DENSITY PROFILE AND THE DERIVATIVES 580 KV 2
C CALCULATE N THE ELECTRON DENSITY IN APPLETICK - HARTREE FORMULA 580 KV 3
C N = 12400*F**2 * X ELECTRONS/CUBIC CM. 580 KV 4
C   EN/CR - EI/CC/KM.
C   EN/DTH - EI/CC/DEG
C   F = FREQUENCY IN MHZ 580 KV 5
C   EN/CEH - EI/CC/DEG
C DERIVATIVES OF EI. DEN. W.R.T. R,TH,PH ARE COMPUTED BY
C   MULTIPLYING PXPR, PXPTH, PXEH WITH THE CONSTANT C.
C
C = 12400.0 * F ** 2 580 KV10
MPRT = MERT + 1 580 KV11
CALL ELECTR 580 KV12
VN(MEFT) = 12400.0*F**2 *X 580 KV13
VNPH(MEFT) = C * PXPR 580 KV14
VNPTH(MEFT) = C * PXPTH * RAD 580 KV15
VNPEH(MEFT) = C * PXEPH * RAD 580 KV16
VRANGE(MEFT) = RANGE 580 KV17

```

```

VHT(MPFT) = H                                     580 KV18
IF(KOFT.EQ.0.AND.NWHY(1).EQ.IBINK(1).AND.NWHY(2).EQ.IBINK(2)) RETU
1RN
C   PRINT CCIATITUDE AND LCNGITUDE               580 KV21
C   R2LT IS COLATITUDE    AND R3LT IS LCNGITUDE   580 KV22
C   R2LT = F(2) * DEGS                           580 KV23
C   R3LT = F(3) * DEGS                           580 KV24
C
C   COMPUTE SIDEGL - ANGLE BETWEEN WAVE NCFMAI AND THE MAGNETIC FIELD580KV27
C   ** CALL MAGY FCE OPTICNS 1 + 3. ** CALL TRUFDC FOR OPTION 2. ** 583 V28
C   CALL TRUFDC                                     OPTION 2
C
C   IF (SR.GE.1.E-2) GC TO 20                      0581
C   PRINT 15, V,NWHY,H,RANGE, SIDEGL,R2LT,R3LT,
C   1          ANGDEG,ECLAE,T,(R(I),I=7,NN)        582 KV 1
15 FORMAT (1X,E8.1,1X,2A4,F8.2,1X,F8.2,3F7.1, 23X, 6F8.2,F6.1) 582 KV 2
GO TO 4C
20 ANGE=ATAN2(FES,FCE)
EL=ANGE*DEGS
IF (FCE.GE.1.E-2) GC TO 30                      0584
PRINT 25, V,NWHY,H,RANGE, SIDEGL,F2LT,R3LT,
1          FL,ANGLEEG,ECLAE,T,(R(I),I=7,NN)        0585
25 FFORMAT (1X,E8.1,1X,2A4,F8.2,1X,F8.2,3F7.1, 15X, 7F8.2,F6.1) 0586
GO TO 4C
30 ANGA=ATAN2(ETA,ZETA)
ANA=ANGA-ALPH
SINANA=SIN(ANA)
SINPHI=SINANA*SINTHE/SINTH
COSPHI=-SIN(PII2-ANA)*SIN(FID2-(EHI-EHIR))+SINANA*SIN(EHI-PHIR)*
1 COSTH
AZDEV=180.-AMCD(540.-(AZ1-ANGA)*DEGS,360.)
IF (R(5).NE.0..CR.R(6).NE.0.) GC TO 34          0597
PRINT 33, V,NWHY,H,RANGE, SIDEGL,R2LT,R3LT,
1          AZDEV,FL,ANGDEG,POLAR,T,(R(I),I=7,NN) 599 KV 2
33 FORMAT (1X,E8.1,1X,2A4,F8.2,1X,F8.2,3F7.1,F8.2,7X, 7F8.2,F6.1)
GC TO 4C
34 AZA=180.-AMCD(540.-(ATAN2(SINPHI,COSPHI)-ATAN2(F(6),R(5)))*DEGS,
1 360.)
PRINT 35, V,NWHY,H,RANGE, SIDEGL,R2LT,R3LT,
1          AZDEV,AZA,EL,ANGDEG,POLAR,T,(R(I),I=7,NN) 604 KV 2
35 FFORMAT (1X,E8.1,1X,2A4,F8.2,1X,F8.2,4F7.1, 8F8.2, F6.1)

C
C
40 LINES=IINES+1                                 0606
IF (N.IE.9) GC TO 45                           0607
PRINT 42, (R(I),I=10,N)                         0608
42 FFORMAT (110X,3F8.2)                         609 KV
LINES=LINES+1                                 0610
45 IF (RAISET.EQ.0.) RETURN                     0611
ELA=BETA*DEGS                                0612
IF (H.IE.1.) ANGDEG=ABS(ANGLEEG)              0613
C
C   3-D RAYSETS
IF (P8.EQ.0.) GC TO 55                         0614
TLCN=LCN*DEGS                                0615
IF (TLCN.LT.0.) TICN=TLCH+360.                 0616
TLAT=LAT*DEGS                                0617
IF (TLAT.LT.0.) TLAT=TLAT+360.                 0618
AZ=ANGA*DEGS                                0619
IF (AZDEV.LE.-100.) AZDEV=AZDEV+360.           0620
IF (AZA.IE.-100.) AZA=AZA+360.                 0621
                                         0622
                                         0623

```

PUNCH 50, B1(NTYP), IC(1), XMTRR, TLAT, TICN, H, RANGE, AZ, F, IHOP,	0624
1 AZDEV, A2A, ELA, ANGDEG, TECIAR, ECIAR, NUTEST	0625
50 FORMAT (A1, A3, 2FF6.0, 1P2F4.0, 2PF6.0, 1FF6.0, F5.0, 3PF7.0, I1, 2P4F5.0,	0626
1 1E4F4.0, I1)	0627
C	0628
C        SUEE. EAYSFTS	0629
55 IF (F9.NE.0.) PUNCH 60, C1(NTYP), ID(1), F, IHCF, ELA, (R(I), I=7,10),	0630
1 T, NUTEST	0631
60 FCRRMAT (A1, A3, 3PF7.0, I1, 2PF5.0, CP5P12.4, I3)	0632
C	0633
C        2-D EAYSFTS	0634
IF (NUTEST.NE.0) APET=H	0635
IF (P7.NE.0.) PUNCH 70, A1(NTYP), ID(1), F, IHCF, ELA, ANGDEG, T, R(7),	0636
1 RANGE, AEHT, NUTEST	0637
70 FORMAT ( A1, 1X, A3, 3PF7.0, I2, 0FF10.5, F9.5, 3F11.4, F12.5, 1X, I1)	0638
RETURN	0639
END	0640

```

SUBFCUTINE ADJUST
C A SUBRCUTINE TO ADJUST THE ELEVATION ANGLE BETA
C AZIMUTH TOLERANCE IS SPECIFIED IN KM THEN CCNVERTED TO RADIANS
C DIMFNSICK A1(3,3),B1(3),C1(3),DUM1(5)
C CCPFCN/CCNST/ EI, EIT2, FIE2, DEGS, RAD, DUM (3)
C COMMON Y(12), T /W/ ID(10), W0, W(400)
C COMMCM/CCNSC/ IENS(52), HEIT(52), ELRANJ(91,3,2), APPROX(8,2,2), FRATIO
1, NMAX, NSTART, JFIAG, NSCL, DBMIN(21), JJJM1
C COMMCM/ER/ N, STEE, MCDE, DUMY(5), FSTAFT
C CCPFCN/FIN/ N2, MUX, EN2(8), FOLAR(4), SPACE, CCIL, FIELD
C COMMCM /NEOPT/ NPINT, KCET, MEFT
RFAT N2, MUX, MU
EQUIVALENCE (GRANGE,W(385)), (GRANGE,W(384)), (BETA,W(17)),
1(CCNTRE,W(386)), (TOLERE,W(387)), (AZ1,W(18)), (RC,W(375)),
2(ALPHA,W(376)), (THO,W(377)), (PHC,W(378)), (AZIEV,W(379)),
3(AZA,W(374)), (BETAT,W(389)), (H,W(383)), (P2IT,W(372)),
4(RBIT,W(373)), (FASTER,W(19))
DATA A1(1,1), A1(2,1), A1(3,1)/3*1.0/
C SET UP THE MAXIMUM HEIGHT FOR GECUND - SATELLITE CASE
IF(NSOI.EQ.0) FEIUFN
NHCE=W(254)+0.1
KCNTRL=CCNTRL
RADIUS=EARTH+R(40)
IF(GRANGE.NE.C.0) GC TO 806
AZTCL=TCIURE/RADIUS
GC TO EC7
806 AZTCL=TCIURE/(RADIUS*SIN(GRANGE/RADIUS))
807 DAZTOI=AZTOI*IEGS
PRINT 808, TOLERE, DAZTOL
808 FORMAT(1X, 16FFGRANGE TOLERANCE=, F12.6, 3H KM, 3X, 18HAZIMUTH TOLERANCE=
1, F12.6, 6E DEGREES)
A22=A21
DC 800 IIL=1, NSCI
INCR=0
CONT=0.0
PRINT EC5
805 FORMAT(1E1)
IF(W(38C).NE.1.0) GC TO 249
PRINT 252, LIL
252 FORMAT(2X, 26HECMING FOR SCITION NUMEFF, I3)
C SET UP AN INITIAL SICPE EASEL UEN PIANE GECPTBY CCNSIDERATION
C FOR SATELLITE TO GROUND OF GECUND TO SATELLITE CASES
249 DINCF=-GRANGE/(SIN(AEBCX(IIL,1,1))*CCS(APRCX(IIL,1,1)))
IF(W(38C).NE.1.0) GC TO 253
DINCR=C.0
INDEX=AEBCX(LIL,2,1)
DO 254 I=1,NHCE
DINCR=DINCR+(ELFANJ(INDEX,2,I)-ELRANJ(INDEX-1,2,I))/1
(ELFANJ(INDEX,1,I)-ELFANJ(INDEX-1,1,I))
254 CONTINUE
COUNT=C.0
BETA=AEBCX(LIL,1,1)
IF(W(38C).NE.1.0.CR.NHCE.NE.1) GC TO 300
DO 260 I=1,JJJM1
IF(BETA.GT.DBMIN(I+1)) GC TO 260
JJK=I
LEFT=DEMIN(JJK)
BRIGHT=DEMIN(JJK+1)
GO TO 300
CONTINUE
260

```

```

C      FRRCR IN COMPUTING HAVING ANGLE
PRINT 261
261 FORMAT(2X,39H***FRRCR IN COMPUTING HAVING ANGLE ***)
GO TO 800
300 CALL RAYINT(AZ1,EETA)
EL=EETA*DEGS
AZ3=AZ1*DEGS
PRINT 55,EL,AZ3
IF(W(380).NE.1.C.R.NHCE.NE.1) GO TO 301
IF(EETA.IT.BLEFT.CR.EETA.GT.BRIGHT) GO TO 700
301 CALL TRACE
PRINT 75,B2LT,B3LT,AZDEV,AZA
75 FORMAT(1X,10FRAY COORD=,F12.5,2X,9HFAY LONG=,F12.5,2X,
114HF.AZDEV AT T.=,F12.5,2X,16HLCAL AZDEV AT E.=,F12.5)
IF(W(394).NE.0.C.C) CRANGE=1
IF(ABS(GRANGE-CRANGE).LE.TCLFRE) GO TO 500
IF(E.GT.(W(40)+0.1).CR .H.IT.(W(40)-0.1)) GC TO 780
MPRT=0
E1(1)=CRANGE
A1(1,2)=EETA
A1(1,3)=A1(1,2)**2
IF(INCR.EQ.0) GC TO 310
DINCR= (E1(1)-E1(2))/(A1(1,2)-A1(2,2))
C INTERPOLATE LINEARLY IF POSSIBLE
IF(E1(1).LT.GRANGE.AND.B1(2).LT.GRANGE) GC TO 310
IF(E1(1).GT.GRANGE.AND.B1(2).GT.GRANGE) GC TO 310
E=(E1(1)-B1(2))/(A1(1,2)-A1(2,2))
A=B1(1)-E*A1(1,2)
EETA=(GRANGE-A)/B
GO TO 590
C INCREMENT OR DECREMENT THE APPROXIMATE ELEVATION UTILIZING THE
C SLOPE OF THE I-E CURVE
310 DIFFR=GRANGE-CRANGE
EETA=EETA+DIFFR/DINCR
IF(EETA.GT.0.0.CR.W(380).NE.1.0) GC TO 312
IF(CCNT.EQ.1.0) GO TO 2100
EETA=0.0
CCNT=1.C
312 CALL RAYINT(AZ1,BETA)
EL=EETA*DEGS
AZ3=AZ1*DEGS
PRINT 55,EL,AZ3
IF(W(380).NE.1.C.R.NHCE.NE.1) GC TO 311
IF(EETA.IT.BLEFT.CR.EETA.GT.BRIGHT) GC TO 700
311 CALL TRACE
PRINT 75,B2LT,B3LT,AZDEV,AZA
IF(W(394).NE.0.C.C) CRANGE=1
IF(ABS(GRANGE-CRANGE).LE.TCLFRE) GO TO 500
IF(H.GT.(W(40)+C.1).CR .H.IT.(W(40)-0.1)) GC TO 780
MPRT=0
E1(2)=CRANGE
A1(2,2)=EETA
A1(2,3)=A1(2,2)**2
DINCR= (E1(1)-E1(2))/(A1(1,2)-A1(2,2))
INCFL=INCFL+1
C IF THE GIVEN RANGE IS BETWEEN THE FIRST AND SECOND RANGE THUS
C COMPUTE , INTERPOLATE LINEARLY ON EETA.
IF(E1(1).LT.GRANGE.AND.E1(2).LT.GRANGE) GC TO 580
IF(E1(1).GT.GRANGE.AND.B1(2).GT.GRANGE) GC TO 580
C INTERPOLATE USING RANGE=A+E*BETA
E=(E1(1)-E1(2))/(A1(1,2)-A1(2,2))

```

```

A=E1(1)-E*A1(1,2)
BETA=(GRANGE-A)/B
GO TO 590
C      INCREMENT OR DECREMENT THE APPROXIMATE ELEVATION UTILIZING THE
C      SLOPE OF THE I-B CURVE
580  DIFFR=GRANGE-GRANGE
      BETA=BETA+DIFFR/DINCR
      IF(FETA.GT.0.0.CE.W(380).NE.1.0)  GC TO 581
      IF(CCNT.EQ.1.0)  GO TO 2100
      FETA=0.0
      COUNT=1.0
581  IF(INCE.GT.KOMBL)  GC TO 2000
      GO TO 300
590  CALL RAYINT(AZ1,EETA)
      EL=FETA*DEGS
      AZ3=AZ1*DEGS
      PRINT 55,EL,AZ3
      IF(W(380).NE.1.0.CE.NHOF.NE.1)  GC TO 591
      IF(EETA.IT.BLEFT.CR.BETA.GT.BRIGHT)  GO TO 700
591  CALL TBACE
      PRINT 75,R2LT,R3LT,AZDEV,AZA
      IF(W(394).NE.0.0)  GRANGE=T
      IF(AES(GRANGE-GRANGE).IE.TCLEFE)  GC TO 500
      IF(E.GT.(W(40)+0.1).CR.H.IT.(W(40)-0.1))  GC TO 780
      MPFT=0
      E1(3)=GRANGE
      A1(3,2)=EETA
      A1(3,3)=A1(3,2)**2
      CALL EQSCLV(B1,A1,3,3,1,C1,DUM1,1.CF-8,IFR)
      C      USE QUADRATIC FORMULA TO COMPUTE EETA
      C      C1(3)*BETA**2+C1(2)*BETA+C1(1)-GRANGE=0
      ARG=C1(2)**2-4.0*C1(3)*(C1(1)-GRANGE)
      IF(ARG) 200,210,210
      C      THE ARGUMENT IS NEGATIVE , NO SOLUTION
200  IF(W(380).EQ.2.0)  GC TO 611
      PRINT 2010,III
      PRINT 610
      GO TO 1000
611  PRINT 2011
      PRINT 612
612  FORMAT(6X,53HDISCONTINUITY IN THE RAY TRACE RANGE-ELEVATION CURVE
      1 )
      GO TO 1000
210  BETAP=(-C1(2)+SQRT(ARG))/(2.0*C1(3))
      BETAM=(-C1(2)-SQRT(ARG))/(2.0*C1(3))
      C      FINI THE CLOSEST RANGE
      C      FINI THE CLOSEST ANGLE TO THE GIVEN RANGE
      DIFF1=ABS(GRANGE-E1(1))
      DIFF2=AES(GRANGE-E1(2))
      DIFF3=AES(GRANGE-E1(3))
      IF(DIFF1.LT.DIFF2.AND.DIFF1.LT.DIFF3)  ANG=A1(1,2)
      IF(DIFF2.LT.DIFF1.AND.DIFF2.LT.DIFF3)  ANG=A1(2,2)
      IF(DIFF3.LT.DIFF1.AND.DIFF3.LT.DIFF2)  ANG=A1(3,2)
      EETA=EETAM
      IF(ABS(ANG-BETAE).LT.ABS(ANG-BETAM))  BETA=BETAP
650  EL=EETA*DEGS
      AZ3=AZ1*DEGS
      PRINT 55,EL,AZ3
55   FORMAT(/ 5X,33HELEVATION ANGLE OF TRANSMISSION =,F12.6,4H DEG,5X,3
      1HAZIMUTH ANGLE OF TRANSMISSION =,F12.6,4H DEG/)
100  COUNT=COUNT+1.0

```

AD-A038 299

ILLINOIS UNIV AT URBANA-CHAMPAIGN DEPT OF ELECTRICAL --ETC F/6 17/2.1  
TECHNIQUES OF DETERMINING IONOSPHERIC STRUCTURE FROM OBLIQUE RA--ETC(U)

DEC 76 N N RAO, K C YEH, M Y YOUAKIM

F19628-75-C-0088

UNCLASSIFIED

UILU-ENG-76-2559

RADC-TR-76-401

NL

3 OF 3  
AD  
A038 299



END

DATE  
FILMED  
10 - 77

3 OF 3  
AD  
A038 299



```

IF(CCNT.GT.CCNIFI) GC TO 2000
CALL RAYINT(AZ1,EETA)
IF(W(38C).NE.1.0.CR.NHCE.NE.1) GC TO 101
IF(FETA.IT.BLEFT.CR.EETA.GT.BRIGHT) GO TO 700
101 CALL TFACE
PRINT 75,R2LT,R3LT,AZDFV,AZA
IF(W(394).NE.0.C) CRANGE=1
C USE THE I-P CURVE TO ADJUST EETA
DIFFR=CRANGE-CRANGE
IF(ABS(DIFFR).LE.TOLERE) GC TO 500
IF(F.GT.(W(40)+C.1).CR .H.IT.(W(40)-0.1)) GC TO 780
MPRT=0
C SELECT THE CLOSEST RANGE TO THE GIVEN RANGE
DIFF1=CRANGE-B1(1)
DIFF2=CRANGE-E1(2)
DIFF3=CRANGF-B1(3)
IF(ABS(DIFF1)-AES(DIFF2)) 10,20,20
10 IF(ABS(DIFF2)-AES(DIFF3)) 50,60,60
C REPLACE THE SECOND RANGE AND ELEVATION ANGLE
60 B1(2)=CRANGE
A1(2,2)=EETA
A1(2,3)=B1(2,2)**2
GO TO 150
20 IF(ABS(DIFF1)-AES(DIFF3)) 50,30,30
C REPLACE THE FIRST RANGE AND ELEVATION ANGLE
30 B1(1)=CRANGE
A1(1,2)=EETA
A1(1,3)=A1(1,2)**2
GO TO 150
C REPLACE THE THIRD RANGE AND ELEVATION ANGLE
50 B1(3)=CRANGE
A1(3,2)=EETA
A1(3,3)=A1(3,2)**2
150 CALL EQSCIV(B1,A1,3,3,1,C1,DUM1,1.0E-8,IFF)
C USE QUADRATIC TO COMPUTE BETA
ARG=C1(2)**2-4.0*C1(3)*(C1(1)-CRANGE)
IF(ARG) 160,170,170
C THE ARGUMENT IS NEGATIVE , THERE IS NO SOLUTION
160 IF(W(38C).EQ.2.0) GO TO 162
PRINT 2C1G,ILL
PRINT 61C
GO TO 1000
162 PRINT 2011
PRINT 612
GO TO 1000
170 BETAE=(-C1(2)+SQRT(ARG))/(2.0*C1(3))
BETAM=(-C1(2)-SQRT(ARG))/(2.0*C1(3))
C FIND THE CLOSEST RANGE
C FIND THE CLOSEST ANGLE TO THE GIVEN RANGE
DIFF1=ABS(CRANGE-B1(1))
DIFF2=ABS(CRANGE-E1(2))
DIFF3=ABS(CRANGE-E1(3))
IF(DIFF1.LT.DIFF2.AND.DIFF1.LT.DIFF3) ANG=A1(1,2)
IF(DIFF2.LT.DIFF1.AND.DIFF2.LT.DIFF3) ANG=A1(2,2)
IF(DIFF3.LT.DIFF1.AND.DIFF3.LT.DIFF2) ANG=A1(3,2)
BETA=EETAP
IF(ABS(ANG-BETAE).LT.ABS(ANG-BETAM)) BETA=EETAP
180 EL=EETA*EEGS
AZ3=AZ1*EEGS
PRINT 55,EL,AZ3
GO TO 100

```

```

C CORRECT FOR AZIMUTHAI DEVIATION
500 IF(H.LE.(W(4C)+C.1).AND.H.GE.(W(40)-C.1)) GC TO 502
GO TO 780
502 A24=A21-AZDEV*RAD
IF(ABS(A24-AZ2).LE.PZTCI) GO TO 3000
INCF=0
MPRT=0
A25=A21+AZDEV*RAD
A21=A25
IF(ABS(A25-AZ2).GT.PES(A24-AZ2)) A21=A24
COUNT=0.C
GO TO 300
2000 IF(W(380).EQ.1.C) FFINT 2C10,LII
IF(W(380).EQ.2.C) FFINT 2011
2010 FORMAT(/// 2X,62H*** HOMING CANNOT BE ACHIEVED FOR APPROXIMATE SOL
UTION NUMBER , I3)
2011 FORMAT(/// 2X,25H*** HOMING CANNOT BE ACHIEVED )
PRINT 2C20,CNTFI
2020 FORMAT(6X,35HXCEEDE NUMBER OF SPECIFIED TRIES , F5.0)
GO TO 1000
2100 PRINT 2C10,LII
PRINT 2110
2110 FORMAT(6X,49HTHE RANGE IS HIGHER THAN THE ZFC ELEVATION RANGE )
GO TO 1000
C CHECK IF THE DIAGNOSTIC IS FOR A HIGH RAY
700 JKRD2=JKR/2
JKR=JKF-JKRD2*2
IF(JKRF.FQ.0) GO TO 750
C IT IS NOT A HIGH RAY
PRINT 2C10,LII
PRINT 610
610 PRINT(6X,8EHDISCONTINUITY IN THE RAY TRACE RANGE-BETA CURVE OR R
ANGE TOO CLOSE TO THE SKID DISTANCE)
GC TO 1000
C IT IS A HIGH ANGLE RAY
750 PRINT 2C10,LII
PRINT 755
755 PRINT(6X,14HFHIGH ANGLE RAY )
GO TO 1000
780 IF(W(380).EQ.1.C) FFINT 2C10,LII
IF(W(380).EQ.2.0) FFINT 2011
PRINT 790
790 PRINT(6X,52HRAY MISSED THE EARTH OR CANNOT REACH RECEIVER HEIGHT)
GC TO 1000
C WE FOUND AN EXACT SOLUTION
3000 IF(W(380).EQ.1.C) FFINT 3C10,LII
IF(W(380).EQ.2.C) FFINT 3C11
3010 FORMAT(/// 2X,35H*** HOMING ACHIEVED FOR SOLUTION NUMBER , I3)
3011 FORMAT(/// 2X,15H*** HOMING ACHIEVED )
PRINT 3C20,EL
3020 FORMAT(6X,11HELEVATION =, F12.6,2X,7HDEGREES)
PRINT 3C30,AZ3
3030 FORMAT(6X,10HAZIMUTH =, F12.6,2X,7HDEGREES )
IF(W(394).EQ.0.C) GC TO 3034
PRINT 3C31,CRANGE
3031 FORMAT(6X,21HHCMEI IN GEOF CPATH =, F12.2,2X,2HKM)
GO TO 3C39
3034 PRINT 3C35,CRANGE
3035 FORMAT(6X,16HHCMEI IN RANGE =, F12.2,2X,2HKM)
IF(W(380).EQ.1.C) GC TO 3C39
PRINT 3C36,W(20)

```

```
3036 FORMAT(6X,20HTRANSMITTER HEIGHT =, F9.2,2X,2HKM )
PRINT 3037,W(40)
3037 FORMAT(6X,17HRECEIVES FEIGHT =, F9.2,2X,2HKM )
3039 PRINT 3040,R2I7
3040 FORMAT(6X,33HHOMFL IN GEOMAGNETIC CCIATITUDE =, F12.5,2X,7HDEGREES
1)
      EPRINT 3050,R3LT
3050 FORMAT(6X,32HHOMFL IN GEOMAGNETIC LCNGITUDE =, F12.5,2X,7HDEGREES)
1000 W(18)=A22
800 CCNTINUF
      RETURN
      END
```

```

SUBROUTINE HCMES
COMMON/CCNSI/ EI,PIC2,PID2,DEGS,RAD,DUM(3)
COMMON/DENSC/ DENS(52),HEII(52),FLRANJ(51,3,2),APROX(8,2,2),FRATIO
1,NMAX,NSTART,JFLAG,NSCI,LEMIN(21),JJJM1
COMMON Y(6) /WW/ ID(10),WC,W(400)
COMMON/DENX/ FH(19,52,5),THFTA(19),FGT(52),FHI(5),FRS(4),HI
COMMON/FCN/ FG2, LCNMX,IHTMX
EQUIVALENCE(EAFIHR,W(19)),(TLCN,W(14)),(FLCN,W(381)),(ILAT,W(16)),
1(RLAT,W(382)),(BETA,W(17)),(TFREQ,W(3)),(AZ1,W(18)),(XMTRH,W(20))
EQUIVALENCE (TFANGE,W(385)),(BETAT,W(385)),(PHC,W(378)),(THO,W(377
1))
EQUIVALENCE (PICN,W(13)),(FIAT,W(15)),(BCE,W(254))
C SET NMAX TO CNE
NMAX=1
SP=SIN(FIAT)
CP=SIN(FIC2-PLAT)
C TRANSFORM THE RECEIVER COORDINATES TO GEOMAGNETIC COORDINATES
SINIPH=SIN(RICN-PICK)
COSIPH=SIN(PID2-(RICB-FLCN))
SI=SIN(FIAT)
CL=SIN(FIC2-RLAT)
GRICN=ATAN2(SINIPH*CL,COSIPH*SP*CL-CP*SI)
GRLAT=ARCCOS(COSIPH*CP*CL+SP*SI)
GRICN=GRICN*DEGS
GRIAT=GRIAT*DEGS
ANGL=AES(TLCN-RICN)
ANGT=FIC2-TIAT
ANGR=PID2-RLAT
C USE THE COSINE LAW TO FIND THE ANGLE SUBTENDED AT THE EARTH CENTER
COSTHE=CCS(ANGT)*COS(ANGR)+SIN(ANGT)*SIN(ANGE)*COS(ANGI)
C COMPUTE THE RANGE
ANGTR=ACCS(CCSTHE)
TRANSC=EARTHr+XMTRH
TRANGE=TFANSC*ANGTR
C COMPUTE TRANSMITTER COORDINATES
COLAT=FIC2-ILAT
XT=TRANSC*COS(TLCN)*SIN(CCOLAT)
YT=TRANSC*SIN(TLCN)*SIN(CCOLAT)
ZT=TRANSC*COS(CCOLAT)
C COMPUTE RECEIVER COORDINATES
RECEIC=EARTHr+W(400)
COLAT=PID2-RLAT
XR=RECEIC*COS(RICB)*SIN(CCOLAT)
YR=RECEIC*SIN(RICB)*SIN(CCOLAT)
ZR=RECEIC*COS(CCOLAT)
C COMPUTE THE MAGNITUDES OF CR, CT AND TR
CT=SQRT(XT*XT+YT*YT+ZT*ZT)
CR=SQRT(XR*Xr+YR*YR+ZR*ZR)
TR=SQRT((XR-XT)**2+(YR-YT)**2+(ZR-ZT)**2)
C CALCULATE THE AZIMUTHAL ANGLE
IF(ANGTR.NE.0.0) GC TO 120
AZ1=0.0
IF(ILAT.GT.RLAT) AZ1=PI
GO TO 55
120 SINRNM=SIN(ANGI)*SIN(ANGE)/SIN(ANGTR)
COSFTN=(COS(ANGE)-COS(ANGT)*COS(ANGI))/(SIN(ANGT)*SIN(ANGTR))
AZ1=ARCSIN(SINFTN)
IF(SINFTN.LT.0.0) GO TO 45
IF(COSFTN.LT.0.0) AZ1=PI-AZ1
GO TO 50

```

```

45      IF(CCSETN.LT.C.C) AZ1=-EI-AZ1
50      IF(TLCN.GT.RLCN) AZ1=PIE2-AZ1
C      COMPUTE THE ELEVATION ANGLE FOR TRIANGLE TCR
55      ARGUM= (TE**2+CT**2-CR**2)/(2.*TB*CT)
IF(ARGUM.GT.1.0) ARGUM=1.0
IF(ARGUM.LT.-1.0) ARGUM=-1.0
BETA=ARCCS(ARGUM)-PIE2
75      NSOI=1
APRCX(1,1,1)=EFTA
TLATE=TLAT*DEGS
TLCNE=TLCN*DEGS
BLATD=BLAT*DEGS
RLATD=RLAT*DEGS
RCLND=EICB*DEGS
PHO1=PHO*DEGS
THO1=THC*DEGS
PRINT 27
27      FORMAT(1E1)
PRINT 30,TLATE,TLCNE,XMTSH
30      FCRMAT(11,44)THE TRANSMITTER GEOGRAPHIC COORDINATES ARE : ,4X,
14HLAT=,F8.3,2X,5HIONG=,F8.3,2X,7HHEIGHT=,F8.2,3H KM)
PRINT 31,RLATE,RLCNE,W(40)
31      FORMAT(11,41)THE RECEIVER GEOGRAPHIC COORDINATES ARE : ,4X,
14HLAT=,F8.3,2X,5HIONG=,F8.3,2X,7HHEIGHT=,F8.2,3H KM)
PRINT 19,EHC1,THO1
19      FORMAT(1X,44)THE TRANSMITTER GEOMAGNETIC COORDINATES ARE:,2X,5HLCN
1G=,F12.5,3X,6HCOLAT=,F12.5)
PRINT 21,GRBLON,GRLAT
21      FORMAT(1X,41)THE RECEIVER GEOMAGNETIC COORDINATES ARE:,2X,5HLONG=,
1P12.5,3X,6HCOLAT=,P12.5)
PRINT 32,TRANGE,TFREQ
32      FORMAT(1X,29)TRANSMITTER RADIUS = ,F12.2,2X,2BKm,5X,
127HFREQUENCY OF TRANSMISSION = , F10.4,2X,3MHZ)
DEETA=EE1A*DEGS
AZMTH=AZ1*DEGS
PRINT 37,DBETA,AZETH
37      FORMAT(1X,28)THE INITIAL ELEVATION ANGLE=,F8.3,2X,7HDEGREES,5X,
125RAZIMUTH OF TRANSMISSION = , F12.6,2X,7HDEGREES)
RETURN
END

```

SUBROUTINE HCME  
C JFLAG=0 MEANS WE CAN FIND AN APPROXIMATE ELEVATION ANGLE.  
C =1 MEANS WE CANNOT FIND AN APPROXIMATE ELEVATION ANGLE.  
C DIMENSION DDMIN(21)  
C DIMENSION JSOL(2), TEMPR(91,2), NECINT(2), JTENE(21)  
REAL\*8 A,B,C,EFIT,DANS(52), HAIT , F1,F2,R3,R4,R5,R6, RE, RI, RJ, DET  
FEAI\*8 P1,E1,C1  
CCMPCN/CCNST/ EI, FIT2, PIL2, DEGS, FAE, EUM(3)  
CCMON/DENSC/ DENS(52), HEIT(52), ELRANJ(91,3,2), APRCX(8,2,2), FRATIO  
1, NMAX, NSTART, JFIAG, NSCI, DDMIN(21), JJJM1  
CCMON Y(6) /WW/ ID(1C), WC, W(40C)  
CCMON/DENX/ FB(19,52,5), THETA(19), HGT(52), EHI(5), FRES(4), HL  
CCMPCN/FG2/ LATMX, LCNMX, IFTMX  
CCMPCN/CCEFF/ A1(52), B1(52), C1(52), HAIT(52), FAEOGE, RAPCGM  
EQUIVALENCE (EARTH, W(19)), (ILCN, W(14)), (EICK, W(381)), (ILAT, W(16)),  
1 (RLAT, W(382)), (EETA, W(17)), (TFFFC, W(2)), (AZ1, W(18))  
EQUIVALENCE (TRANGE, W(385)), (BETAT, W(389)), (IIFG, W(387))  
EQUIVALENCE (PEC, W(378)), (THO, W(377))  
EQUIVALENCE (ILCN, W(13)), (FLAT, W(15)), (FCF, W(254)), (GRCPUP, W(394))  
DATA INTERV/5C/  
C W(380)=1 MEANS COMING GFCUND TO GRCPUND.  
C W(380)=2 MEANS COMING GRCPUND TO SATELLITE OR SATELLITE TO GFCUND  
C W(380)=3 MEANS FIND THE MINIMUM GRCUE PATH  
NNN=W(380)+.1  
GO TO (1200, 1300, 1400), NNN  
C THE MINIMUM GRCUE PATH FCUTINE  
1400 CALL GRCPUM  
RETURN  
1300 CALL HCMS  
RETURN  
1200 RE=EARTH  
C SETUP THE NUMBER OF HCFS  
NHCF=HCF+0.1  
C SETUP THE FACTORS FOR THE MIDPOINT LOCATION OF EACH HOP DIVISION  
HOFF=1.0/(2.0\*HCP)  
HOFI=-1.C  
DO 1 I=1,91  
DO 1 J=1,3  
DO 1 K=1,2  
1 ELRANJ(I,J,K)=C.0  
DO 2 I=1,8  
DO 2 J=1,2  
DO 2 K=1,2  
2 APRCX(I,J,K)=C.0  
DO 3 I=1, NHOE  
3 JSCI(I)=C  
C SET UP THE NUMBER OF INTERVALS FOR THE ELEVATION ANGLE.  
FRATIO=TREQ\*\*2  
C CHECK IF GROUP PATH COMING IS NEEDED  
IF(W(394).EQ.0.0) GO TO 111  
ANGT=PI/2-TLAT  
ANGTR=GFCUP/EARTH  
TRANGE=GFCUF  
RANGE=TRANGE/HOF  
AZ1=W(263)  
GO TO 500C  
C CALCULATE THE RANGE BETWEEN TRANSMITTER AND RECEIVER  
111 ANGL=ABS(ILCN-EICK)  
ANGT=PI/2-TLAT  
ANGR=PI/2-RLAT

```

C      USE THE CCSINF LAW TO FIND ANGLE SUBTENDED AT EARTH CENTER
CCSSTH=CCS(ANGT)*COS(ANGR)+SIN(ANGT)*SIN(ANGR)*COS(ANGI)
ANGTR=ARCCS(CCSSTH)
TRANGE=ANGTR*(EARTH+R(2C))
C      DIVIDE THE TOTAL RANGE BY THE NUMBER OF HCS NEEDED.
RANGE=TRANGE/ECE

C      THIS SECTION OF THE CODE SELECTS A HCSFILE THAT IS CLOSEST
C      TO THE MID POINT BETWEEN THE TRANSMITTER AND RECEIVER(AVLON,AVLAT)
C      COORDINATES
IF(ANGTF.NE.0.0)  GC TO 4225
RTN=0.C
IF(TLAT.GT.PLAT)  RTN=PI
GO TO 5000
4225  SINFIN=SIN(ANGI)*SIN(ANGR)/SIN(ANGTF)
COSFTN=(COS(ANGR)-CCS(ANGT)*CCS(ANGTF)),(SIN(ANGT)*SIN(ANGTR))
RTN=ARCSIN(SINRTN)
IF(SINRTN.LT.0.C)  GC TO 4500
IF(COSFTN.LT.0.C)  FIN=PI-RTN
GO TO 5000
4500  IF(COSFTN.LT.0.C)  FIN=-PI-RTN
5000  DC 8000 JHOP=1,NHCP
NSOI=0
HOEI=HCEI+2.0
COSANG=CCS(HOEI*HCPF*ANGTR)
SINANG=SIN(HCEI*HCPF*ANGTF)
C      THIS SECTION IS FOR GROUP PATH FINDING
IF(W(394).EQ.0.C)  GC TO 5005
AZT=AZ1
IF(AZT.GT.PI)  AZT=PI/2-AZT
CCSNM=CCS(ANGT)*CCSANG+SIN(ANGT)*SINANG*COS(AZT)
AVLATG=EIE2-ARCCS(CCSNM)
TNM=ARCSIN(SIN(AZT)*SINANG/SIN(ARCCS(CCSNM)))
AVICNG=TICN+TNM
IF(AZ1.GT.PI)  AVICNG=TICN-TNM
GO TO 9
5005  COSNM=CCS(ANGT)*CCSANG          +SIN(ANGT)*SINANG          *COS(RTN)
AVLATG=EIE2-ARCCS(CCSNM)
TNM=ARCSIN(SIN(RTN)*SINANG          /SIN(ARCCS(CCSNM)))
IF(TLCK-FICN)  4,4,5
4    AVICNG=TICN+TNM
AZ1=RTN
GO TO 6
5    AVICNG=TICN-TNM
AZ1=PI/2-RTN
6    CONTINUE

C      TRANSFORM THE MIDPOINT TO GEOMAGNETIC COORDINATES
9    SP=SIN(FIAT)
CF=SIN(EIE2-PIAT)
SINEPH=SIN(AVICNG-PICN)
COSEPH=SIN(PID2-(AVICNG-ELCN))
SL=SIN(AVLATG)
CL=SIN(EIE2-AVLATG)
AVLCN=ATAN2(SINEPH*CL,COSEPH*SP*CL-CF*SI)
AVCLAT=ARCCS(COSEPH*CE*CI+SF*SL)
IF(W(394).NE.0.C)  GC TO 91
C      TRANSFORM THE RECEIVER COORDINATES TO GEOMETRIC COORDINATES
SINEPH=SIN(BICN-PICN)
CCSEPH=SIN(PID2-(ELCN-PICN))
SI=SIN(FIAT)

```

```

CL=SIN(FIC2-RIAT)
GRLCN=ATAN2(SINIPH*CI,CCSEFH*SF*CL-CF*SI)
GRLAT=ARCCS(CCSEFH*CP*CI+SF*SI)
GRICN=GRLCN*DEGS
GRLAT=GRLAT*DEGS
C TEMPORARY PRINTING OF THE MID POINT
91 GCLCNG=AVICNG*IEGS
GOLATG=AVIATG*DEGS
AVICND=AVLCN*DEGS
AVLATD=AVCLAT*IEGS
PRINT 9911
9911 FFORMAT(2X,'MID POINT COORDINATES, GEOMAGNETIC AND GEOFGRAPHIC /')
PRINT 9912,GCICNG,GCIATG,AVICND,AVIATC
9912 FORMAT(2X,'GEOGRAPHIC:',2X,'LONG=',F8.2,2X,'LATIT=',F8.2,7X,'GEOMA
1GNETIC:',2X,'LNG=',F8.2,2X,'CLAT=',F8.2)
DPHI=ABS(EHI(2)-EHI(1))
KK=ICKMX
DO 610 K=1,ICKMX
DIFF1=AES(AVLCN-EHI(K))
IF(DIFF1>DPHI) 620,615,610
615 KK=K
GO TO 630
620 KK=K
IF(K.GE.ICKMX) GC TO 630
DIFF2=AES(AVLCN-EHI(K+1))
IF(DIFF2.LT.DIFF1) KK=K+1
GO TO 630
610 CCNTINUE
C WE CANNOT FIND A LONGITUDE CLOSE ENOUGH TO THE MID POINT.
WRITE(6,625)
625 FORMAT(1X,82HTHE GIVEN DENSITY PROFILE DOES NOT INCLUDE THE MID PO
1INT LONGITUDE BETWEEN T AND F)
GC TO 630
630 DTHETA=AES(THETA(2)-THETA(1))
IL=IATMX
DO 635 I=1,LATMX
DIFF1=AES(AVCIAT-THETA(I))
IF(DIFF1>DTHETA) 645,640,635
640 LL=L
GO TO 660
645 LL=L
IF(L.GE.IATMX) GC TO 660
DIFF2=AES(AVCLAT-THETA(I+1))
IF(DIFF2.LT.DIFF1) II=I+1
GO TO 660
635 CCNTINUE
C CAN NOT FIND A LATITUDE CLOSE ENOUGH TO THE MID POINT
WRITE(6,650)
650 FORMAT(1X,83HTHE GIVEN DENSITY PROFILE DOES NOT INCLUDE THE MID
1POINT LATITUDE BETWEEN T AND F)
GO TO 630
C EXTRACT THE DENSITY AT THE MID POINT AND THE CORRESPONDING HEIGHT
660 DC 665 I=1,IATMX
DENS(I)=FH(LL,I,KK)**2
DENS(L)=DENS(I)
HAIT(I)=EGT(L)
HEIT(L)=EGT(L)
665 HAIT(L)=EGT(L)
C FIND THE HEIGHT ON WHICH THE MAXIMUM DENSITY OCCURS
DHEIT=HAIT(2)-HAIT(1)
TEMP=DENS(1)
KMAX=1

```

```

DC 670 I=2,LHTEX
IF(LENS(I).LE.TIME) GO TO 670
NMAX=L
TIME=LENS(L)
670 CONTINUE
HMAX=HEIT(NMAX)
FVMAX=SQRT(LENS(NMAX))
C ASSUME AN INITIAL ELEVATION ANGLE OF ZEFC
BETAF=C.C
IF(TFREQ-FVMAX) 330,320,320
330 BETAT=FIR2
GO TO 340
C COMPUTE THE ELEVATION ANGLE FOR A TRAPPED FAY
320 TEMEA=(EARTH+HMAX)*SQRT(1.0-(FVMAX**2/FRATIC))/EARTH
IF(TEMEA-1.0) 321,321,400
321 BETAT=AFCSS(TEMEA)
340 TLATE=TLAT*DEGS
TLCNE=TICN*DEGS
RLATD=RLAT*DEGS
RLCND=FICN*DEGS
PHC1=PHC*DEGS
THO1=TEC*DEGS
PRINT 29
29 FORMAT(1H1)
PRINT 30,TLATE,TICN,W(20)
30 FORMAT(1X,4HTHE TRANSMITTER GEOPHYSICAL COORDINATES ARE : ,4X,
14HLAT=,F8.3,2X,5HICKG=,F8.3,2X,7HHEIGHT=,F8.2,3H KM)
IF(W(394).NE.0.0) GO TO 301
PRINT 31,RLATE,FICN,W(40)
31 FORMAT(1X,4HTHE RECEIVER GEOPHYSICAL COORDINATES ARE : ,4X,
14HLAT=,F8.3,2X,5HLONG=,F8.3,2X,7HHEIGHT=,F8.2,3H KM)
301 PRINT 19,PHC1,THC1
19 FORMAT(1X,4HTHE TRANSMITTER GEOMAGNETIC COORDINATES ARE :,2X,5HLCN
1G=,F12.5,3X,6HCCLAT=,F12.5)
IF(W(394).NE.0.0) GO TO 3211
PRINT 21,GRLCN,GRLAT
21 FORMAT(1X,4HTHE RECEIVER GEOMAGNETIC COORDINATES ARE :,2X,5HICNG=,
1F12.5,3X,6HCOIAT=,F12.5)
3211 PRINT 32,IRANGE,IFREQ
32 FORMAT(1X,2SHRANGE AT TRANSMITTER RADIUS = ,F12.2,2X,2HKM,5X,
127HFREQUENCY OF TRANSMISSION = , F10.4,2X,3HMHZ)
NSTART=1
C CALCULATE COEFFICIENTS AND STORE THEM IN ARRAYS A1,E1,C1
87 I=NSTART
J=NSTART+1
K=NSTART+2
L=NSTART+3
IF(NMAX-3) 1000,1000,10
C THERE ARE MORE THAN THREE POINTS
10 R1=RE +HAIT(I)
R2=RE +HAIT(J)
R3=RE +HAIT(K)
R4=F3-F2
R5=F3-R1
R6=R1-F2
ED2=2.0D0
C CALCULATE THE COEFFICIENT FOR THE FIRST THREE POINTS
DET=R4*R5*R6/(F1*F2*F3)
A=(-R1*R1*R4*DANS(I)+R2*R2*R5*DANS(J)+R3*R3*R6*DANS(K))/(DET*F1*R2
1*R3)
B=(F1*R1*(R3*R3-R2*R2)*DANS(I)-F2*R2*(R3*R3-R1*R1)*DANS(J)-R3*R3*(

```

```

1R1*R1-B2*R2)*DANS(K))/(EE1*R1*R2*R3)
C=(-R1*R4*DANS(I)+R2*R5*DANS(J)+R3*R6*DANS(K))/DET
DELT=-E/(R3*R3)-EE2*C/(R3**3)
A1(1)=A
E1(1)=E
C1(1)=C
M=1
DO 73 I=I,NMAX
M=M+1
RJ=FE      +HAIT(I)
RI=FE      +HAIT(I-1)
C CALCULATE THE COEFFICIENT A,E,C
DET=(RJ-RI)**2/((RI**2)*EJ)
A=(EI*RI*(RI-RJ)*DELT+RI*(RI-EE2*RJ)*DANS(I-1)+RJ*EJ*DANS(I))/(DET
1*RI**2)
B=(EI*(EJ*RJ-RI*RI)*DELT-EE2*EJ*RJ*(DANS(I)-DANS(I-1)))/(DET*RI*RJ
1)
C=(EI*(RI-RJ)*DELT+EJ*(DANS(I)-DANS(I-1)))/DET
DELT=-E/(EJ*RJ)-EE2*C/(RJ**3)
A1(M)=A
E1(M)=E
C1(M)=C
73 CONTINUE
C CALCULATE THE RANGE AND GROUP PATH
CALL FITT(CRF,CGPF,EFTAF)
86 CALL FITT(CRT,CGPT,EFTAT)
IF(JFLAG.EQ.0) GO TO 88
C DECREMENT THE ELEVATION ANGLE.
BETAT=EFTAT-0.4C*FAD
GO TO 86
C CHECK IF THE TRANSMISSION FREQUENCY IS GREATER THAN FC
88 IF(TFREQ>FVMAX) 92,92,89
C CORRECT THE TRAPPING ANGLE EFTAT
89 CRT1=CRT
CGPT1=CGPT
EFTAT1=EFTAT
C INCREMENT THE ANGLE EFTAT BY C.1 DEGREE AND CHECK THE SLOPE.
BETAT=EFTAT+0.10*FAD
CALL FITT(CRT,CGPT,EFTAT)
IF(JFLAG.EQ.0) GO TO 95
EFTAT=EFTAT1
CRT1=CRT1
CGPT1=CGPT1
GO TO 92
95 IP(CRT,LT,CRT1) GO TO 89
C WE HAVE THE MAXIMUM AND MINIMUM ELEVATION ANGLES AND CORRESPONDING
C RANGES. DIVIDE THE ELEVATION ANGLE RANGE INTO INTERVALS, THE NUMBER
C OF INTERVALS.
92 KINT=INTERV+1
ELRANJ(1,1,JHCE)=EFTAF
ELRANJ(1,2,JHCE)=CRF
ELRANJ(1,3,JHOP)=CGPF
ELFAKJ(KINT,1,JHCE)=BETAT
ELRANJ(KINT,2,JHCE)=CRT
ELRANJ(KINT,3,JHCE)=CGPT
DINT=(EFTAT-BETAF)/INTERV
C GENERATE THE RANGES CORRESPONDING TO THE INTERVAL VALUES OF THE
C ELEVATION ANGLES.
DO 110 I=2,INTERV
BETAI=(I-1)*DINT

```

```

CALL FITT(CR,CGE,EETAI)
ELRANJ(I,1,JHCE)=EETAI
ELFANJ(I,2,JHCE)=CR
EIFANJ(I,3,JHCE)=CGE
110  CONTINUE
C   LOCATE THE MAXIMA AND MINIMA OF THE ELEVATION-FANGE CURVE
C   INITIALIZE THE VECTOR DEMIN
DO 1110 I=1,21
1110 DBMIN(I)=C.O
TEME=ELFFNJ(1,2,JHOP)**
JJJ=1
JJ=1
DBMIN(JJJ)=ELRANJ(1,1,JHCE)
JTEMP(1)=1
DO 1111 I=2,KINI
GO TO(1112,1113),JJ
1112 IF(ELRANJ(I,2,JHCE).LT.TEME)  GC TO 1118
C   REPLACE AND STORE THE ELEVATION ANGLE VALUES
JJ=2
JJJ=JJJ+1
DBMIN(JJJ)=ELRANJ(I-1,1,JHCE)
JTEMP(JJJ)=I-1
GO TO 1118
1113 IF(EIFANJ(I,2,JHCE).GT.TEME)  GC TO 1118
C   REPLACE THE INDEX VALUE
JJ=1
JJJ=JJJ+1
DBMIN(JJJ)=ELRANJ(I-1,1,JHCE)
JTEMP(JJJ)=I-1
1118 TEME=EIFANJ(I,2,JHOP)
1111  CONTINUE
JJJ=JJJ+1
DBMIN(JJJ)=BETAI
JTEMP(JJJ)=KINI
DO 1147 KQ=1,JJJ
1147 DDMIN(KQ)=DBMIN(KQ)*TEGS
PRINT 8733, (DEMIN(KQ),KQ=1,JJJ)
C   REMOVE SMALL OSCILLATIONS FROM THE LAYERS OF THE D-E CURVE
C   ASSUME 150 KM OSCILLATIONS OR LESS TO BE REMOVED
JJR=1
JJ=1
DO 1130 I=2,JJJ
C   RETRIEVE THE INDICES FOR CMEABISCN
J1=JTEMP(JJB)
J2=JTEMP(I)
DIFFR=EIFANJ(J1,2,JHCE)-EIFANJ(J2,2,JHCE)
GO TO (1135,1140),JJ
C   D-E CURVE SLOPING DOWNWARDS
1135 IF(DIFFR.GT.0.C)  GC TO 1137
IF(ELRANJ(J2,2,JHCP).LT.ELRANJ(J1,2,JHCE))  GO TO 1130
DBMIN(JJR)=DEMIN(I)
JTEMP(JJF)=JTEMP(I)
GO TO 1130
1137 IF(ABS(DIFFR).LT.150.0)  GC TO 1130
JJ=2
JJR=JJR+1
DBMIN(JJB)=DBMIN(I)
JTEMP(JJB)=JTEMP(I)
GO TO 1130
C   D-E CURVE SLOPING UPWARDS
1140 IF(DIFFR.LT.0.C)  GC TO 1143

```

```

IF (ELRANJ(J2,2,JHCP).GT.EIFANJ(J1,2,JHCE))  GC TO 1130
DBMIN(JJF)=DBMIN(I)
JTEMP(JJF)=JTEMP(I)
GC TC 1130
1143 IF(ABS(DIFFR).LT.150.0)  GC TC 1130
JJ=1
JJR=JJR+1
DBMIN(JJF)=DBMIN(I)
JTEMP(JJF)=JTEMP(I)
1130 CCNTINUE
DO 1146 KQ=1,JJR
1146 DDMIN(KQ)=DMIN(KQ)*DEGS
PRINT 8733, (DMIN(KQ),KQ=1,JJR)
JJJM1=JJF-1
PRINT 114
114 FORMAT(2X,21HTHE RANGE-BETA VALUES)
PRINT 115
115 FORMAT(1X,9HPCINT NC.,10X,6H&L DEG,10X,E RANGE KM,10X,9HG.PATH KM)
L=2
K=3
IF(W(394).EQ.0.C)  GC TO 118
L=3
K=2
118 DO 116 I=1,KINT
BETAD=ELRANJ(I,1,JHCE)*DEGS
116 PRINT 117,I,BETAD,ELRANJ(I,L,JHCP),ELRANJ(I,K,JHCP)
117 FORMAT(1X,I6,8X,F12.3,5X,F12.3,7X,F12.3)
C CHECK THE GIVEN RANGE AGAINST THE CALCULATED RANGES TO FIND THE
C NUMBER OF SOLUTIONS.
KFLAG=0
C SET A FLAG EQUAL TO ZERO SO THAT IF THE INTERPOLATION DOES NOT
C CONVERGE WITHIN TEN TRIES, THERE IS NO SOLUTION FOR THAT ANGLE
C (MFLAG)
IF(ELRANJ(1,2,JEOF).LT.RANGE)  KFLAG=1
DO 120 I=2,KINT
IF(KFLAG.EQ.1)  GC TC 180
C CHECK THE NEXT RANGE IF LARGER THAN GIVEN RANGE
IF(ELRANJ(I,2,JEOF).GT.RANGE)  GC TC 120
C INCREMENT NSOL AND HOME THE SOLUTION TO FIND THE APPROXIMATE
C ELEVATION ANGLE.
156 LB=(ELRANJ(I,1,JHCP)-ELRANJ(I-1,1,JHCE))/9.0
BETAI=EIFANJ(I-1,1,JHCP)
CR=ELRANJ(I-1,2,JEOF)
MFLAG=C
DO 127 J=1,10
IF(KFLAG.EQ.1)  GC TC 129
IF(CR.LT.RANGE)  GC TO 128
125 ELRANJ(I-1,1,JHCP)=BETAI
ELRANJ(I-1,2,JHCP)=CR
BETAI=EFTAI+DB
CALL FIII(CR,CGE,EFTAI)
GO TO 127
128 ELRANJ(I,1,JHCE)=BETAI
ELRANJ(I,2,JHCP)=CR
GO TO 126
129 IF(CR.GT.RANGE)  GC TC 128
GO TO 125
127 CCNTINUE
C WE CANNOT FIND A SOLUTION
175 DO 1275 JK=1,JJJM1
JK=JK

```

```

1275 IF(BETAI.GT.DBMIN(JK).AND.EETAI.LE.EMIN(JK+1)) GC TO 1280
CONTINUE
1280 GO TO (1281,1283,1285,1287,1289,1291,1293,1295),JK
1281 PRINT 12E2
1282 FORMAT(2X,62HCANNOT FIND APPROXIMATE SOLUTION FOR FIRST LAYER LOW
1 ANGLE )
GO TC 171
1283 PRINT 12E4
1284 FORMAT(2X,62HCANNOT FIND APPROXIMATE SOLUTION FOR FIRST LAYER HIGH
1 ANGLE )
GC TC 171
1285 PRINT 12E6
1286 FORMAT(2X,62HCANNOT FIND APPROXIMATE SOLUTION FOR SECOND LAYER LOW
1 ANGLE )
GO TC 171
1287 PRINT 12E8
1288 FORMAT(2X,62HCANNOT FIND APPROXIMATE SOLUTION FOR SECOND LAYER HIGH
1H ANGLE )
GO TO 171
1289 PRINT 12E0
1290 FORMAT(2X,62HCANNOT FIND APPROXIMATE SOLUTION FOR THIPE LAYER LOW
1 ANGLE )
GO TC 171
1291 PRINT 12E2
1292 FORMAT(2X,62HCANNOT FIND APPROXIMATE SOLUTION FOR THIPE LAYER HIGH
1 ANGLE )
GO TO 171
1293 PRINT 12E4
1294 FORMAT(2X,62HCANNOT FIND APPROXIMATE SOLUTION FOR FOURTH LAYER LOW
1 ANGLE )
GO TO 171
1295 PRINT 12E6
1296 FORMAT(2X,62HCANNOT FIND APPROXIMATE SOLUTION FOR FOURTH LAYER HIGH
1H ANGLE )
GC TC 171
C USE LINEAR INTEGRATION RANGE=F+Q*BETA
126 IF(ELRANJ(I-1,1,JHCE).EQ.ELRANJ(I,1,JHCE)) GC TO 175
Q=(ELRANJ(I-1,2,JHCP)-ELRANJ(I,2,JHCE))/(ELRANJ(I-1,1,JHCP)-
1ELRANJ(I,1,JHCE))
IF(Q.EQ.0.0) GC TC 175
P=ELRANJ(I-1,2,JHCP)-Q*ELRANJ(I-1,1,JHCE)
BETAI=(RANGE-F)/Q
CALL FITT(CR,CFF,EETAI)
IF(JFLAG) 130,130,175
130 DIFF=RANGE-CR
IF(DIFF) 135,160,145
135 IF(DIFF+IIFG) 140,160,160
140 IF(KFLAG.EQ.1) GC TC 146
136 ELRANJ(I-1,1,JHCE)=EETAI
ELRANJ(I-1,2,JHCP)=CR
MFLAG=MFLAG+1
IF(MFLAG.GE.10) GC TO 175
GO TO 126
145 IF(DIFF-IIFG) 160,160,150
150 IF(RFLAG.EQ.1) GC TC 136
146 ELRANJ(I,1,JHCE)=EETAI
ELRANJ(I,2,JHCE)=CR
MFLAG=MFLAG+1
IF(MFLAG.GE.10) GC TO 175
GO TC 126
C WE HAVE FOUND THE APPROXIMATE ANGLE

```

```

160  NSCI=NSCI+1
      JSOL(JHCE)=NSCI
      APRCX(NSCI,1,JHCP)=EETAI
      APRCX(NSCI,2,JHCP)=I
      DEETA=EETAI*DEGS
      DO 1160 JK=1,JJJM1
      JJK=JK
      IF(EETAI.GT.EBMIN(JK).AND.EETAI.LT.EMIN(JK+1)) GC TC 1170
1160  CONTINUE
1170  GO TO(1171,1173,1175,1177,1179,1181,1183,1185),JJK
1171  PRINT 1172,NSCI,DEETA,CR,CGP
1172  FORMAT(2X,28HAFFRCXIMATE SCLUTION NUMBER=,I3,2X,22HFIRST LAYER LO
1W ANGLE , 10H,EL.ANGLE=,F8.3,2X,6HRANGE=,F8.3,2X,7HG.PATH=,F8.3)
      GO TO 171
1173  PRINT 1174,NSCI,DEETA,CF,CGP
1174  FORMAT(2X,28HAFFRCXIMATE SCLUTION NUMBER=,I3,2X,23HFIRST LAYER HI
1GH ANGLE , 10H,EL.ANGLE=,F8.3,2X,6HRANGE=,F8.3,2X,7HG.PATH=,F8.3)
      GO TO 171
1175  PRINT 1176,NSCI,DEETA,CF,CGP
1176  FORMAT(2X,28HAFFRCXIMATE SCLUTION NUMBER=,I3,2X,23HSECCND LAYER L
1OW ANGLE , 10H,EL.ANGLE=,F8.3,2X,6HRANGE=,F8.3,2X,7HG.PATH=,F8.3)
      GC TC 171
1177  PRINT 1178,NSCI,DEETA,CR,CGP
1178  FORMAT(2X,28HAFFRCXIMATE SCLUTION NUMBER=,I3,2X,24HSECCND LAYER HI
1GH ANGLE , 10H,EL.ANGLE=,F8.3,2X,6HRANGE=,F8.3,2X,7HG.PATH=,F8.3)
      GO TO 171
1179  PRINT 1180,NSCI,DEETA,CR,CGP
1180  FORMAT(2X,28HAFFRCXIMATE SCLUTION NUMBER=,I3,2X,22HTHIRD LAYER LO
1W ANGLE , 10H,EL.ANGLE=,F8.3,2X,6HRANGE=,F8.3,2X,7HG.PATH=,F8.3)
      GO TO 171
1181  PRINT 1182,NSCI,DEETA,CF,CGP
1182  FORMAT(2X,28HAFFRCXIMATE SCLUTION NUMBER=,I3,2X,23HTHIRD LAYER HI
1GH ANGLE , 10H,EL.ANGLE=,F8.3,2X,6HRANGE=,F8.3,2X,7HG.PATH=,F8.3)
      GC TC 171
1183  PRINT 1184,NSCI,DEETA,CR,CGP
1184  FORMAT(2X,28HAFFRCXIMATE SCLUTION NUMBER=,I3,2X,23HFOURTH LAYER L
1OW ANGLE , 10H,EL.ANGLE=,F8.3,2X,6HRANGE=,F8.3,2X,7HG.PATH=,F8.3)
      GC TC 171
1185  PRINT 1186,NSCI,DEETA,CF,CGP
1186  FORMAT(2X,28HAFFRCXIMATE SCLUTION NUMBER=,I3,2X,24HFOURTH LAYER HI
1GH ANGLE , 10H,EL.ANGLE=,F8.3,2X,6HRANGE=,F8.3,2X,7HG.PATH=,F8.3)
171  IF(KFLAG.EQ.0) III=1
      IF(KFLAG.EQ.1) III=C
      KFLAG=III
      GO TO 120
C     CHECK IF THE NEXT RANGE IS SMALLER THAN GIVEN RANGE
180  IF(FLRANJ(I,2,JEOP).LT.RANGE) GC TC 120
      GC TC 156
120  CONTINUE
280  IF(NSCI.GT.0) GO TO 300
      PRINT 2805
2805 FORMAT(2X,34HTHERE ARE NC APPROXIMATE SCLUTICNS )
      GC TC 300
1000  PRINT 1005
1005 FORMAT(1X,47HTHERE ARE LESS THAN THREEE FCINTS IN THE DENSITY)
      GC TC 300
400  PRINT 410
410  FORMAT(1X,25HTHE FREQUENCY IS TCC HIGH)
300  CONTINUE
8000  CONTINUE
C     CHECK TC SEE IF IT IS ONE BCE MODE

```

```

      IF(NHOF.EQ.1) GC TO 12000
C   CHECK IF THE HOFS ARE SYMMETRIC WITHIN A CERTAIN TOLERANCE
      DO 8050 I=1,NHCE
      IF(JSOI(I).EQ.0) GC TO 8050
C   THERE ARE SOLUTIONS
      GO TO 8060
8050 CONTINUE
C   SET THE CONTROL NSOI TO ZERO DRAFTING NC SOLUTIONS
      NSOI=0
      GO TO 12000
C   CHECK FOR SYMMETRIC ECFS
8060 NHCE=NHCE-1
      DO 8070 I=1,NECE
      IF(JSOI(I).EQ.JSOI(I+1)) GC TO 8070
C   THE HOFS ARE NOT SYMMETRICAL
      GO TO 8100
8070 CONTINUE
C   CHECK IF THE ELEVATION ANGLES ARE CLOSE TO EACH OTHER
      KECINT=JSCL(1)
C   ONE DEGREE SEPARATION MAXIMUM
      XXJ=1.0*FAD
      DO 8080 I=1,RECINT
      HTEMP=AEFCX(I,1,1)
      DO 8085 J=2,NHCE
      IF(ABS(FTEMP-AEFCX(I,1,J)).LE.XXJ) GO TO 8085
C   THE HOFS ARE NOT SYMMETRIC SINCE THE ELEVATION ANGLES ARE NOT
C   CLOSE TO EACH OTHER
      GC TO 8100
8085 CONTINUE
8080 CONTINUE
C   THE HOFS ARE SYMMETRIC
      NSOI=JSCL(1)
      GC TO 12000
8100 DO 8120 J=1,NHCE
      JJ=1
      TEMER(JJ,J)=ELRANJ(1,2,J)
      XJ=JJ*RAD
      DO 8110 I=2,KINT
      IF(ELRANJ(I,1,J).LT.XJ) GC TO 8110
C   INTERPOLATE LINEARLY ON THE RANGE
      SLCFF=(ELRANJ(I-1,2,J)-ELRANJ(I,2,J))/(ELRANJ(I-1,1,J)-
      1*ELRANJ(I,1,J))
      CRSS=ELRANJ(I-1,2,J)-SLCFF*ELRANJ(I-1,1,J)
      TEMPF(JJ+1,J)=SLOPE*XJ+CRSS
      JJ=JJ+1
      XJ=JJ*RAD
      GC TO 8110
8110 CONTINUE
      NPOINT(J)=JJ
8120 CONTINUE
C   FIND THE NUMBER OF SOLUTIONS BY COMPARING THE SUM OF THE RANGES/
C   HOFS WITH THE GIVEN RANGE
      ITEMP=RECINT(1)
      DO 8130 I=2,NECE
      IF(NPCINT(I).GT.ITEMP) GC TO 8130
      ITEMP=RECINT(I)
8130 CONTINUE
C   RECOPY THE TEMPORARY ARRAYS INTO THE PERMANENT ONES
      DO 8140 I=1,ITEMP
      DO 8140 J=1,NHCE
      ELRANJ(I,1,J)=(I-1)*RAD

```

```

8140  EIFANJ(I,2,J)=TEMER(I,J)
      NSCI=0
      SUM1=0.0
      DO 8145 J=1,NECE
8145  SUM1=SUM1+TEMER(1,J)
      DO 8150 I=2,IITEMP
      SUM=0.0
      DC 8160 J=1,NHCE
8160  SUM=SUM+TEMER(I,J)
      IF(SUM.LT.TRANGE.ANI.SUM1.LT.TRANGF)  GC TC 8149
      IF(SUM.GT.TRANGE.ANI.SUM1.GT.TRANGE)  GC TC 8149
C      WE FOUND A SCIUTICN
      NSCI=NSCI+1
C      INTERECIATE TO FIND THE APPROXIMATE ELEVATION ANGLE
      SLCFF=(SUM-SUM1)/(EIFANJ(I,1,J)-FLRANJ(I-1,1,J))
      CROSS=SUM1-SLCFF*FLFANJ(I-1,1,J)
      APRCX(NSCI,1,1)=(TRANGE-CROSS)/SLCFF
      APRCX(NSCI,2,1)=I
8149  SUM1=SUM
8150  CCNTINUE
      DO 8771 KQ=1,91
      PR1=EIFANJ(KQ,1,1)*DEGS
      PR2=EIFANJ(KQ,1,2)*DEGS
      PRINT 8734,PR1,FLFANJ(KQ,2,1),PR2,EIFANJ(KQ,2,2)
8734  FORMAT(1X,2F12.3,12X,2F12.3)
8771  CONTINUE
8733  FORMAT(1X,12F8.3)
12000 RETURN
      END

```

```

SUBROUTINE PITT(RANG,GFCUF,ANG)
REAL*8 EARTH,R,PF,AA,EB,CC,FF,A1,E1,C1,HAIT,ARGUM,X1,X2,X3,R1,R2,X,
1R3,XI,FI,XJ,RJ,EETA, CR,CR1,CR2,CR3,CGF,CGF1,CGF2,CGP3
CCFMCN/CCNST/ FI,FI12,PIC2,DEGS,FAC,LUM(3)
CCMMCN/DENSC/ DENS(52),HEIT(52),FLRABJ(91,3,2),APRCX(8,2,2),FRATIO
1,NMAX,NSTART,JFLAG,NSCL,LEMIN(21),JJM1
COMMNC/CCEFF/ I1(52),E1(52),C1(52),FAIT(52),FAFCGF,FAFCGM
COMMNC Y(6)/WW, ID(10),WC,W(400)
EQUIVALENCE (EARTH,W(19))
C CR IS THE CALCULATED RANGE
C NMAX IS THE NUMBER OF POINTS UP TO THE HEIGHT OF MAXIMUM DENSITY
C HEIT IS THE HEIGHT INCREMENTS CORRESPONDING TO THE DENSITY
C DENS IS THE NORMALIZED DENSITY
C CGF IS THE CALCULATED GFCUF PATH
C FRATIO IS THE TRANSMISSION FREQUENCY, F, SQUARED.
C BETA IS THE ELEVATION ANGLE
C NSTART IS THE INDEX AT WHICH THE DENSITY HAS A VALUE
SQRT(X)=ISQRT(X)
ALOG(X)=ILOG(X)
ARSIN(X)=DARSIN(X)
ARCCS(X)=DARCCS(X)
CCS(X)=ICCS(X)
SIN(X)=ISIN(X)
AES(X)=IAES(X)
DD1=1.0IC
ID2=2.0IC
ID4=4.0IC
BETA=ANG
FF=FRATIO
EARTH=EARTH
JFLAG=0
RE=EARTH**2
M=NSTART
C CALCULATE THE RANGE AND GFCUF PATH FROM EARTH SURFACE TO THE
BOTTOM OF THE IONOSPHERE
CR=ABS(EARTH*CCS(BETA)/(FAIT(M)+EARTH))
CR=ID2*EARTH*(ARCCS(CR)-EETA)
CGF=ID2*(SQRT((EARTH+HAIT(M))**2-(EARTH*CCS(BETA))**2)-EARTH*
1SIN(BETA))
C SET UP THE CONSTANTS AA,EE,CC FOR THE FIRST THREE POINTS
JJ=1
AA=DD1-A1(JJ)/FF
BB=-B1(JJ)/FF
CC=-C1(JJ)/FF-(EARTH*CCS(BETA))**2
ARGUM=EE*EE-DD4*AA*CC
I=M+3
R1=EARTH+HAIT(M)
R2=EARTH+HAIT(M+1)
R3=EARTH+HAIT(M+2)
X1=AA*E1*R1+BB*E1+CC
X2=AA*E2*R2+BB*E2+CC
X3=AA*E3*R3+BB*E3+CC
IF(X1) 400,52
52 IF(X2) 55,55,56
C THE RAY REFLECTED
55 XI=X1
RI=R1
GO TO 305
56 IF(X3) 57,57,75
57 XI=X1

```

```

RI=F1
GO TO 305
C CALCULATE THE RANGE
75 IF(CC) 70,60,60
70 CR1=DD2*EE*CCS(EETA)/SQRT(-CC)
CR2=(EE*E3+DD2*CC)/(ABS(F3)*SQRT(ARGUM))
CR3=(EE*E1+DD2*CC)/(ABS(R1)*SQRT(ARGUM))
CR=CR+CF1*(ARSIN(CR2)-ARSIN(CR3))
GO TO 80
60 CR1=-DD2*EE*CCS(EETA)/SQRT(CC)
CR2=AES(DD2*SQRT(CC*X3)/R3+DD2*CC/R3+EE)
CR3=ABS(DD2*SQRT(CC*X1)/R1+DD2*CC/R1+EE)
CR=CR+CE1* ALOG(CR2/CR3)
80 CGF1=DD2*(SQRT(X3)-SQRT(X1))/AA
C CALCULATE THE GROUP PATH
IF(AA) 90,100,100
90 CGF2=(DD2*AA*R3+EE)/(SQRT(ARGUM))
CGP3=(DD2*AA*R1+EE)/(SQRT(ARGUM))
CGP=CGF+CGP1+BB*(ARSIN(CGF2)-ARSIN(CGE3))/(AA*SQRT(-AA))
GO TO 110
100 CGP2=AES(DD2*SQRT(AA*X3)+DD2*AA*E3+EE)
CGP3=AES(DD2*SQRT(AA*X1)+DD2*AA*R1+EE)
CGP=CGF+CGP1-EE*ALOG(CGP2/CGE3)/(AA**1.5)
C START THE CALCULATION FOR THE REST OF THE LENSITY FILE
110 DO 20 I=1,NMAX
JJ=JJ+1
C SET UP THE CONSTANTS AA,BB,CC
120 AA=DD1-A1(JJ)/FF
FB=-F1(JJ)/FF
CC=-C1(JJ)/FF-(EARTH*CCS(EETA))**2
ARGUM=EE*EB-DD4*AA*CC
RJ=EARTH+HAIT(I)
RI=EARTH+HAIT(I-1)
XJ=AA*RJ*PJ+EE*FJ+CC
XI=AA*FI*RI+BB*FI+CC
IF(XI) 300,300,172
172 IF(XJ) 300,300,171
171 IF(CC) 170,160,160
C CALCULATE THE RANGE OF THE REFLECTION HEIGHT
170 CR1=DD2*EE*CCS(EETA)/SQRT(-CC)
CR2=(EE*FJ+DD2*CC)/(ABS(FJ)*SQRT(ARGUM))
CR3=(EE*FI+DD2*CC)/(ABS(FI)*SQRT(ARGUM))
CR=CR+CF1*(ARSIN(CR2)-ARSIN(CR3))
GO TO 180
160 CR1=-DD2*EE*CCS(EETA)/SQRT(CC)
CR2=AES(DD2*SQRT(CC*XJ)/RJ+DD2*CC/RJ+EE)
CR3=ABS(DD2*SQRT(CC*XI)/RI+DD2*CC/RI+EE)
CR=CR+CF1* ALOG(CR2/CR3)
180 CGP1=DD2*(SQRT(XJ)-SQRT(XI))/AA
C CALCULATE THE GROUP PATH OF THE REFLECTION HEIGHT
IF(AA) 190,200,200
190 CGP2=(DD2*AA*RJ+EE)/(SQRT(ARGUM))
CGE3=(DD2*AA*RI+BB)/(SQRT(ARGUM))
CGP=CGF+CGP1+EE*(ARSIN(CGE2)-ARSIN(CGP3))/(AA*SQRT(-AA))
GO TO 200
200 CGP2=AES(DD2*SQRT(AA*XJ)+DD2*AA*FJ+EE)
CGP3=AES(DD2*SQRT(AA*XI)+DD2*AA*RI+EE)
CGP=CGF+CGP1-EE*ALOG(CGP2/CGP3)/(AA**1.5)
20 CONTINUE
130 JFLAG=3
GO TO 400

```

```

300  CONTINUE
      RAFCGF=(-BB+SQRT(ARGUM))/ (DD2*AA)
      RAFCGM=(-BB-SQRT(ARGUM))/ (DD2*AA)
305  IF(CC) 310,320,32C
310  CR1=DD2*EE*COS(EETA)/SQRT(-CC)
      CR2=ETD2
      CR3=(EE*RI+DD2*CC)/(ABS(RI)*SQRT(ARGUM))
      CR=CR+CR1*(CR2-ARCSIN(CR3))
      GO TO 350
320  CR1=-DD2*EE*COS(EETA)/SQRT(CC)
      CR2=ABS(SQRT(ARGUM))
      CR3=ABS(DD2*SQRT(CC*XI)/RI+DD2*CC/RI+EE)
      CR=CR+CR1* ALOG(CR2/CR3)
350  CGE1=-DD2*SQRT(XI)/EE
      IF(FA) 360,370,37C
360  CGE2=-ETD2
      CGE3=(DD2*AA*RI+BB)/(SQRT(ARGUM))
      CGP=CGE+CGP1+EE*(CGE2-ARCSIN(CGE3))/(AA*SQRT(-AA))
      GO TO 400
370  CGE2=ABS(SQRT(ARGUM))
      CGP3=AEE(DD2*SQRT(AA*XI)+DD2*AA*FI+EE)
      CGP=CGE+CGP1-EE*ALOG(CGE2/CGE3)/(AA**1.5)
400  RANG=CF
      GRCUF=CGE
      IF(W(394).EQ.C.C)  GC TO 500
      RANG=CGE
      GROUP=CR
500  RETCEN
      END

```

```

SUBROUTINE GRCEM
C   A SUBROUTINE TO COMPUTE THE MINIMUM GRCUE PATH
C   FIRST WE FIND THE PENETRATION ANGLE AND THEN USE CHECKING
C   AND CHOOING TECHNIQUE TO LOCATE THE MINIMUM WITHIN A GIVEN
C   TOLERANCE IN GRCUE PATH
COMMON/CCNST/ EI, FIT2, FILE2, EIGS, FAD, IUM(3)
COMMON/FIAGS/ IFIAG, IGRT
COMMON Y(12), I, WW/II(10), LC, W(400)
COMMON/DENSC/ DENS(52), HEIT(52), ELRANJ(91,3,2), APPROX(8,2,2), FRATIO
1, NMAX, NSTART, JFLAG, DSCI, DPMIN(21), JJM1
COMMON/DENT/ EH(19,52,5), TEETA(19), EGT(52), EEI(5), FRES(4), HI
COMMON/EG2/ LATEX, LCRMX, IHMX
COMMON/ER/N, SIEE, PCIE, ICMY(5), ESTART
COMMON/FIN/XN2, XMUX, FN2(8), ECLAE(4), SEACE, CCIL, FIELD
COMMON/NICFI/ NEFINI, RCET, MEFT
EQUIVALENCE (EAEETH, W(19)), (F, W(2)), (AZ1, W(18)), (BETA, W(17)),
1 (ONLY, W(371)), (AZ1, W(263))
EQUIVALENCE (EEO, W(378)), (THO, W(377))
NSCI=0
C   SELECT THE LONGITUDE COORDINATE OF DENSITY
DFHI=AES(EHI(2)-EHI(1))
KK=ICNEX
DO 110 K=1,LCNEX
DIFF1=AES(PHO-EHI(K))
IF(DIFF1-DPHI) 120,115,110
115
KK=K
GO TO 130
120
KK=K
IF(K.GE.ICNMX) GO TO 130
DIFF2=AES(PHO-PHI(K+1))
IF(DIFF2.LT.DIFF1) KK=K+1
GO TO 130
110
CONTINUE
C   PRINT THE ERROR MESSAGE
PRINT 125
125
FORMAT(2X,'CANNOT FIND A LONGITUDE CLOSE TO THE TRANSMITTER')
GO TO 400
C   SELECT THE COLATITUDE COORDINATE OF DENSITY
130
ITHETA=AES(THETA(2)-THETA(1))
IL=LATEX
DO 135 I=1,LATMX
DIFF1=AES(THO-THETA(I))
IF(DIFF1-ITHETA) 145,140,135
140
II=I
GO TO 160
145
LL=L
IF(I.GE.IATMX) GO TO 160
DIFF2=AES(THO-TEETA(I+1))
IF(DIFF2.LT.DIFF1) II=I+1
GO TO 160
135
CONTINUE
C   PRINT THE ERROR MESSAGE
PRINT 150
150
FORMAT(2X,'CANNOT FIND A COLATITUDE CLOSE TO THE TRANSMITTER')
GO TO 400
C   EXTRACT THE DENSITY
160
DC 165 I=1,IHMX
165
DENS(I)=FH(LL,I,KK)
TEMP=DEKS(1)
DO 170 I=2,IHMX

```

```

IF(TENS(I).LE.TFME)  GC TC 170
NMAX=L
TEMP=CDENS(L)
170  CONTINUE
HMAX=FGT(NMAX)
FC=CDENS(NMAX)
WRITE(6,24) F
24  FORMAT(1X,'THE TRANSMISSION FREQUENCY=',F12.5,' MHZ')
TOIGRF=1.0
C  TEMECAEAY ALICCATICK CF AZIMUTH IN W(263)
AZ1=AZA
C  COMPUTE THE ELEVATION ANGLE FOR A TRAPPED RAY
TEMFA=(EARTH+HMAX)*SQRT(1.0-(FC/F)**2)/EARTH
IF(TFMPA-1.0) 1C,1C,9CC
1C  BETAR=ACOS(TEMFA)
2C  EETAR=EETAR
C  INITIALIZE THE RAY PARAMETERS AND TRACE THE RAY
CALI RAYINT(AZ1,EETAR)
BETA=BETA1
EL=EETA*LEGS
AZM=AZ1*LEGS
WRITE(6,25) EL,AZM
25  PCFPAT(1X,'ELEVATION ANGLE OF TRANSMISSION=',F12.6,' DEG',5X,
1'AZIMUTH ANGLE OF TRANSMISSION=',F12.6,' DEG')
CALI TRACE
MPRT=0
IF(IGRT.NE.0)  GC TC 950
C  CHECK FOR PENETRATION
IF(CNLY.EQ.0.0)  GC TC 30
BETAF=C.55*EETAF
GC TC 20
C  STORE THE VALUES
30  GROUP1=1
C  TAKE 95% OF INITIAL TRAPPING ANGLE
BETAF=C.95*BETAR
CALI RAYINT(AZ1,BETAF)
BETA=BETAF
EL=EETA*LEGS
WRITE(6,25) EL,AZM
CALI TRACE
MPRT=0
IF(IGRT.NE.0)  GC TC 950
GROUP2=1
C  TAKE 90% OF INITIAL TRAPPING ANGLE
BETAF=C.90*BETAF
EETAI=EETAF
CALI RAYINT(AZ1,BETAF)
BETA=BETAF
EL=BETA*LEGS
WRITE(6,25) EL,AZM
CALI TRACE
MPRT=0
IF(IGRT.NE.0)  GO TC 950
GRCUP3=1
C  CHECK FOR THE SCAFF OF THE CURVE
40  IF(GROUP3.LT.GRCUP2)  GC TC 80
C  SLCFING TOWARDS THE RIGHT TO GRCUP 2
50  IF(GRCUP2.LT.GRCUP1)  GC TC 200
C  SLCFING TOWARDS THE RIGHT; FINE A NEW PENETRATION ANGLE
C  INCREMENT EETAF BY 5%
BETAF=1.05*EETAF

```

```

60      CALL RAYINT(AZ1,EETAB)
BETA=BETAR
EL=EETA*DEGS
WRITE(6,25) EL,AZM
CALL TRACE
MPRT=0
IF(IGRT.NE.0)  GC TC 950
C     CHECK FOR PENETRATION
IF(CNIY.GT.0.0) GC TC 70
C     INTERCHANGE THE VALUES
EETA3=EETA2
EETA2=EETA1
EETA1=EETAR
GROUFB=GFCUP2
GROUFA=GFCUP1
GRCUE1=T
GC TO 50
C     RAY PENETRATED INCREMENT THE ANGLE BY 1%
70      EETAR=C.99*BETAR
GC TC 60
C     SLICING TOWARDS THE LEFT
80      EETAL=0.95*EETAI
CALL RAYINT(AZ1,BETAI)
BETA=BETAL
EL=EETA*DEGS
WRITE(6,25) EL,AZM
CALL TRACE
MPRT=0
IF(IGRT.NE.0)  GO TC 950
EETA1=EETA2
EETA2=EETA3
EETA3=EETAL
GRCUE1=GFCUE2
GROUFB=GFCUP3
GRCUE3=T
GO TC 40
C     WE FOUND A SMALL VALUE GFCUE2 INCLUDED BETWEEN TWO LARGER VALUES
C     GROUFB AND GRCUE3
C     USE THE CHOP METHOD ON EITHER SIDE OF GFCUE2
200    BETA5=BETA3+0.5*(EETA2-EETA3)
BETA4=EETA2+0.5*(EETA1-EETA2)
CALL RAYINT(AZ1,BETA4)
BETA=BETA4
EL=BETA*DEGS
WRITE(6,25) EL,AZM
CALL TRACE
MPRT=0
IF(IGRT.NE.0)  GC TC 950
GRCUE4=T
CALL RAYINT(AZ1,EETAS)
EETP=EETAS
EL=BETA*DEGS
WRITE(6,25) EL,AZM
CALL TRACE
MPRT=0
IF(IGRT.NE.0)  GC TC 950
GRCUE5=T
C     CHECK IF IT IS WITHIN THE TOLERANCE
IF(ABS(GROUFB-GROUFB).GT.TCLGRF) GO TO 210
IF(GROUFB.LT.GRCUE5)  GO TO 350
GO TO 300

```

```

C      CHECK THE LEFT SIDE
210    IF(GROUE5.GT.GRCUE2) GO TO 220
C      REPLACE THE LEFT SIDE VALUES
EETA1=EETA2
EETA2=EETA5
GROUE1=GFCUF2
GRCUF2=GRCUE5
GO TO 200
C      CHECK IF IT IS WITHIN THE TOLERANCE
220    IF(ABS(GFOUP4-GFOUP2).LE.TCLGRF) GO TO 350
C      CHECK THE RIGHT SIDE
IF(GROUE4.GT.GFCUF2) GO TO 240
C      REPLACE THE RIGET SIDE VALUES
BETA3=BETA2
BFTA2=EFTA4
GROUE3=GFCUF2
GROUE2=GFOUP4
GO TO 200
C      REPIACE THE MIDDLE ECFTION
240    BFTA3=EFTA5
EETA1=EETA4
GROUE3=GFCUF5
GROUE1=GFCUF4
GO TO 200
C      WE FOUND THE LEFT SIDE MINIMUM VALUE OF GRCUF PATH
300    IF(GROUE5.GT.GRCUE2)  GC TC 305
GROUE2=GFCUF5
EETA2=EETA5
305    WRITE(6,307)
307    FORMAT(//1X,'****//)
WRITE(6,310)
310    FORMAT(1X,'THE LEFT SIDE      ,MINIMUM GRCUF PATH AND ITS ANGLE ARE
1.')
BETAD=EFTA2*DEGS
WRITE(6,320) BETAD,GFCUF2
320    FORMAT(1X,'ELEVATION ANGLE=',F9.4,2X,'MINIMUM GROUP PATH=',F9.4)
WRITE(6,307)
GO TO 400
C      WE FOUND THE RIGHT SIDE MINIMUM VALUE GFCUF PATH
350    IF(GFOUE4.GT.GFCUE2)  GO TO 355
GROUE2=GFCUF4
BETA2=EFTA4
355    WRITE(6,307)
WRITE(6,360)
360    FORMAT(1X,'THE RIGHT SIDE      ,MINIMUM GFCUF PATH AND ITS ANGLE ARE
1.')
BETAD=EFTA2*DEGS
WRITE(6,320) BETAD,GFCUF2
WRITE(6,307)
400    RETURN
900    WRITE(6,910)
910    FORMAT(1X,'THE ARGUMENT OF ARCCOS IS GREATER THAN CNE')
GO TO 400
950    IGRM=0
GO TO 400
END

```

```

C      SUBROUTINE PROFIL
C      A RUTINE TO GENERATE A NEW DENSITY PROFILE
      DIMENSION AZT(5),REMFC(20,5,4),RR(2,3),R(3),NE(5)
      COMMON /LENX/ FF(19, 52, 5),THETA(19),HGT( 52),PHI( 5),FRES(4),HL
      COMMON /EG1/ ETB(2),EPH(2),DTH(2),LTH,LIPF,LIFT,THZC,PHIZC,HIZC
      COMMON /EG2/ LATMX,LCNMX,LHTMX
      COMMON /CCNST/ PI,PIT2,PII2,DEGS,RAI,DUM(3)
      COMMON Y(12),T,STE,CDFT(12) /WW/ ID(10),W0,W(400)
      EQUIVALENCE (EARTH,W(19)),(FLOB,W(13)),(FLAT,W(15)),(TLON,W(14)),
      1(TLAT,W(16)),(AIPH,W(376)),(TCLAT,W(377)),(TLONG,W(378))
C      AZIMUTH TOLERANCE
      AZTCL=10.*RAD
C      CONVERT THE ANGLES TO RADIANS
      DO 40 I=1,LATMX
      40 THETA(I)=THETA(I)*RAD
      DC 50 I=1,LCNMX
      50 PHI(I)=PHI(I)*RAD
C      READ THE NUMBER OF AZIMUTH AND THE NUMBER OF POINTS IN EACH
C      AZIMUTH
      READ(5,100) N,(NE(I),I=1,N)
 100 FORMAT(6I10)
C      READ THE AZIMUTHAL ANGLES
      READ(5,110) (AZT(I),I=1,N)
 110 FORMAT(8F10.0)
C      READ RR,FM,PC,AND E FOR EACH AZIMUTH
      DC 130 J=1,N
      NP1=NP(J)
      READ(5,120) ((FEMFC(I,J,K),K=1,4),I=1,NE1)
 120 FORMAT(4F10.0)
 130 CONTINUE
C      LOCATE THE CLOSEST RANGE TO THE TRANSMITTER
      TEST=REMFC(1,1,4)
      K1=1
      K2=1
      DO 160 I=1,N
      NE1=NP(I)
      DO 165 I1=1,NE1
      IF(FBMFC(I1,I,4).GE.TEST) GO TO 165
      K1=I1
      K2=I
      TEST=REMFC(I1,I,4)
 165 CONTINUE
 160 CONTINUE
C      GENERATE THE NEW DENSITY FILE IN ALL THE SPACE
      RB=FBMFC(K1,K2,1)
      RM=FEMFC(K1,K2,2)
      FC=FEMFC(K1,K2,3)
      YM=FM-BE
      DO 170 K=1,LCNMX
      DO 170 J=1,LATMX
      DO 170 I=1,LHTMX
      FH(J,I,K)=0.0
      RT=EARTH+HGT(I)
      FACT=((RT-RM)*BE/(YM*RT))**2
      IF(FACT.GT.1.0) GO TO 170
      FH(J,I,K)=SQRT(FC**2*(1.0-FACT))
 170 CONTINUE
C      FIND THE MAXIMUM RANGE AND SET THE LIMIT
      TEST=REMFC(1,1,4)
      DO 145 I=1,N

```

```

NP1=NP(I)
DO 140 I1=1,NE1
IF (RBMFCD(I1,I,4).LE.TEST) GC TC 140
TEST=REMFC(I1,I,4)
140 CONTINUE
145 CCONTINUE
RANGEI=TEST+100.0
C PRINT INPUT DATA
PRINT 1230,N,(NE(I),I=1,N)
1230 FORMAT(1X,'N=',I3,5(' NE=',I4))
PRINT 1231,(AZT(I),I=1,N)
1231 FORMAT(1X,'AZIMUTES=',E(F8.2,3X))
DO 1233 J=1,N
NP1=NP(J)
PRINT 1232,AZT(J)
1232 FORMAT(1X,'AZIMUTH=',F8.2)
PRINT 1234,((REMFC(I,J,K),K=1,4),I=1,NE1)
1234 FORMAT(1X,'RE=',F8.2,' EM=',F8.2,' FC=',F8.2,' D=',F8.2)
1233 CONTINUE
PRINT 1235, RANGEI,AIEH
1235 FORMAT(1X,'MAXIMUM RANGE=',F8.2,' AIEH=',F14.7)
C GO THROUG THE GRID POINTS AND TRY TO INTERPOLATE THE GIVEN DATA
DO 400 K=1,LONMX
TNE=ABS(TLNGH-PHI(K))
DO 380 J=1,LATMX
C FIND THE AZIMUTH OF ONE POINT P(J,K)
ANGTC=CCS(TCLAT)*CCS(THETA(J))+SIN(TCIP)*SIN(THETA(J))*CCS(TNF)
ALPFA=ARCCS(ANGTC)
SINPTN=SIN(TNE)*SIN(THETA(J))/SIN(AIEHA)
COSFTN=(COS(THETA(J))-CCS(TCLAT)*COS(AIEHA))/(SIN(TCLAT)*
1SIN(AIEHA))
AZE=ARSIN(SINPTN)
IF (SINPTN.LT.0.0) GC TC 210
IF (COSFTN.LT.0.0) AZE=PI-AZE
GO TO 220
210 IF (CCSFN.LT.0.0) AZE=-PI-AZE
220 IF (TLNGH.GT.PHI(K)) AZE=PI/2-AZE
RANGEF=TAUHR*AIEHA
P1=PHI(K)*DEGS
P2=THETA(J)*DEGS
E3=AZE*DEGS
PRINT 1450,RANGEF,P3,F2,E1
1450 FORMAT(1X,'RANGE=',F8.2,' AZIMUTH=',F8.2,' COLAT=',F8.2,
1' LONG=',F8.2)
C CHECK IF THE AZIMUTH AZE OF P IS WITHIN THE LIMITS OF GIVEN
C AZIMUTES PLUS TOLERANCE
AZ1=AZT(1)*RAD-AIEH-AZTCI
AZN=AZT(N)*RAD-AIEH+A2TCI
IF (AZP.GE.AZ1.AND.AZE.LE.AZN) GC TC 240
C THE AZIMUTH OF P IS OUT OF RANGE
GO TO 380
C CHECK IF THE RANGE IS OUTSIDE THE MAXIMUM GIVEN RANGE + TOLERANCE
C OF 100M
240 IF (RANGEF.GT.RANGEI) GO TC 380
C LOCATE TWO AZIMUTHAL ANGLES FOR P
KK=N
DO 260 I=1,N
AZT1=AZT(I)*RAD-AIEH
IF (AZE.GT.AZT1) GO TC 260
KK=I
GC TC 265

```

```

260  CCNTINUE
265  KKK=KK-1
      IF(KK.EQ.1) KKK=KK+1
C       COMPUTE THE GEOMAGNETIC AZIMUTHS
      AZT1= A2T(KK)*RAD-AIPH
      AZT2= A2T(KKK)*RAD-AIPH
C       SEARCH FOR THE CLOSEST TWO VALUES OF GROUND RANGES TO GROUND
C       RANGE OF E
      II=1
      TEST=RANGEP
      I=KK
270  NE1=NE(I)
      K1=NE1
      DO 290 II=1,NE1
      IF(EMFC(I1,I,4).LT.TEST) GC TO 290
      K1=II
      GO TO 295
290  CONTINUE
C       INTERPOLATE LINEARLY FOR THE VALUES OF EE, EM, EC
295  K2=K1-1
      IF(K1.EQ.1) K2=K1+1
      DO 300 M=1,3
      SLOPE=(EMFC(K1,I,M)-EMFC(K2,I,M))/(EMFC(K1,I,4)-
      1EMFC(K2,I,4))
      CROS=EMFC(K1,I,M)-SLOPE*EMFC(K1,I,4)
      PR(II,M)=CROS+SLOPE*RANGE
300  CCNTINUE
      IL=IL+1
      I=KK
      IF(IL.LE.2) GC TO 270
C       FIND THE DIFFERENCE IN AZIMUTHAL ANGLES AND COMPUTE THE VALUES OF
C       EB, RM, EC AT THE POINT E
      ANG1P=AZT1-AZE
      ANG2P=AZE-AZT2
      ANG12=AZT1-AZT2
      DO 310 M=1,3
310  R(M)=(ANG2P*RR(1,M)+ANG1P*RR(2,M))/ANG12
C       R(1) CONTAINS EE, R(2) CONTAINS EM, R(3) CONTAINS EC
C       COMPUTE VALUES OF EC AT DIFFERENT HEIGHTS
      YM=R(2)-R(1)
      DO 340 I=1,LHTMX
      FH(J,I,M)=0.0
      RT=EARTH+HGT(I)
      FACT=((RT-R(2))*R(1)/(YM*RT))**2
      IF(FACT.GT.1.0) GO TO 340
      FH(J,I,M)=SQRT(R(3)**2*(1.0-FACT))
340  CCNTINUE
380  CCNTINUE
400  CCNTINUE
C       PREPARE ANGLES IN DEGREES FOR PRINTING
      DO 420 I=1,LOKRY
      PHI(I)=EHI(I)*DEGS
      DO 440 I=1,LATMX
      THETA(I)=THETA(I)*DEGS
      RETURN
      END

```

SUBROUTINE ELECTY

C C COMPUTES THE ELECTRON DENSITY AND ITS DERIVATIVES AT ANY POINT  
(R,PEI,TH) ALONG THE RAY IN A THREE DIMENSIONAL IONOSPHERE .

C DESCRIPTION OF PARAMETERS

C GRID PARAMETERS CARD: FCFMAT (315,A5,6F10.3)

C ICMX - MAXIMUM = OF LONGITUDE PLANES ELE 1  
C LATMX - MAXIMUM = OF LATITUDE SECTORS ELE 2  
C IHTMX - MAXIMUM = OF HEIGHT LAYERS ELE 3  
C NAME - I.E. (ONLY) OF THE DATA GRID ELE 4  
C THZC - LEAST COLATITUDE SECTOR IN DEG. ELE 5  
C PHIZO - LEAST LONGITUDE PLANE IN DEG. (WESTMOST) ELE 6  
C HTZC - LEAST HEIGHT LAYER ELE 7  
C DLTH - INTERVAL IN THETA DIRECTION ELE 8  
C DLPH - INTERVAL IN PHI DIRECTION ELE 9  
C DLHT - INTERVAL IN HEIGHT ELE 10  
C FH - GRID DATA OF PLASMA FREQ. ARRANGED IN (TH,HT) PLANES. ELE 11  
C SUBROUTINE REQUIRED : INTER(LI,KK,JJ) ELE 12  
C FRES - OUTPUT RETURNED BY SUBROUTINE INTER ELE 13  
C COMMON /FLAGS, IFLAG, IGRT

C NOTE:

C WHEN CHANGING TO DIFFERENT SIZE GRID CHECK PROPER DIMENSIONS.

C ARCCN CORP., WAKEFIELD, MASS., 01880 KRISHNA VANGURI.

C COMMON /XX/ X,PYER,PFETH,PFEEH,EXPT,HMAX ELE 31  
COMMON /DENX/ FH(19, 52, 5),THETA(19),HGT( 52),PHI( 5),FRES(4),HL ELE 32  
COMMON /EG1/ DTE(2),DPH(2),DHT(2),DLTH,DLPH,DLHT,THZO,PHIZO,HTZO ELE 33  
COMMON /EG2/ LATMX,ICMX,IHTMX ELE 34  
COMMON /CCNST/ EI,PIT2,PIC2,DEGS,RAI,DUM(3) ELE 35  
COMMON F(12),T,SIE,DRDT(12),WW, ID(10),WC,W(40C) ELE 36  
EQUIVALENCE(T,F(2)),(PF,F(3)) ELE 37  
EQUIVALENCE(F,W(3)),(FAFTHR,W(19)) ELE 38  
DATA IREAD / 0 / ELE 39

C -----

C IF(IREAD-1) 100,300,100 ELE 40  
100 IFLAG = 0 ELE 41  
IGRT=0 ELE 42  
IREAD = 1 ELE 43

C I/O TAPE DESIGNATIONS: IX=INPUT UNIT, IY=OUTPUT TAPE UNIT. ELE 44

C IX = 5 ELE 45  
IY = 6 ELE 46

C READ GRID PARAMETERS. SIZE AND INITIAL VALUES. ELE 47

C READ(IX,120) ICMX,LATMX,IHTMX,NAME,PHIZC,THZC,HTZC,DLFH,DLTH,DLHT ELE 48

C 120 FORMAT (315,A4,6F10.3) ELE 49

```

C      EXIT IF IIMITS EXCEED.          ELE   61
C
C      IF (LCNMX - 5) 125,125,135      ELE   62
C      125 IF (LATMX - 19) 130,130,135  ELE***63
C      130 IF (LHTMX - 52) 150,150,135  ELE***64
C      135 WRITE (IY,140) ICMX,LATMX,LHTMX  ELE   65
C      140 FCFORMAT (1X,35E PARAMETERS OUTSIDE THE IIMITS:    ,/
C      1 10X,41E MAXIMUM NUMBER OF LONGITUDE PLANES = ,15 , /  ELE   66
C      2 10X,41E MAXIMUM NUMBER OF LATITUDE SECTORS = ,15 , /  ELE   67
C      3 10X,41E MAXIMUM NUMBER OF HEIGHT LAYERS = ,15 //)  ELE   68
C      STCE
C      150 CCNTINUE
C
C      SETUP UNIFORM SPHERICAL GRID.     ELE   69
C
C      DO 151 J = 1,IATMX             ELE   70
C      151 HGT(J) = HTZC + FLCAT(J-1) * DLHT  ELE   71
C      DO 152 L = 1,LHTMX             ELE   72
C      152 THETA(L) = THZC + FLCAT(L-1) * DLTH  ELE   73
C
C      READ FILEQ. DATA PLANES OF SIZE=(IATMX X LHTMX) FOR EACH LONGITUDE ELE   74
C
C      DO 169 KEH= 1,ICNEX            ELE   75
C      PHI(KPH) = PHIZC + FLCAT(KPH-1) * DLPH  ELE   76
C
C      REAL(IY,160) ((FH(I,J,KEH),I=1,IATMX),J=1,LHTMX)  ELE   77
C      160 FORMAT(15E5.2,5X)           ELE   78
C      169 CCNTINUE
C      IF(W(393).GT.0.0) CALL PRCFIL  ELE   79
C
C      WRITE OUT DATA PLANES: (ICNOSPEERE GRID MCFL)  ELE   80
C
C      WRITE (IY,202)                 ELE   81
C      202 FCFORMAT( 1H1,47H PREPARED BY ARCCN CORE. WAKEFIELD, MASS. 01880, ELE   82
C      4 3Y, 21HTEL: (E17) 245-3404 , ' AUG. 1973. '/')  NC5   83
C      WRITE(IY,203) ICMX,LATMX,LHTMX,NAME,PHIZC,THZC,DLH,DLTE,DLHTE  ELE   84
C      203 FCFORMAT (/1X,48E UNIFORM GRID PARAMETERS : ,/ ELE   85
C      11X,8HLCMX = ,16,4X,8HLATMX = ,16,4X,8HLHTMX = ,16,4X,5HNAME=,A5,/ ELE   86
C      21X,8HPHIZC = ,F9.2,1X,8HTHZC = ,F9.2,1X,8HTTZC = ,F9.2,/ ELE   87
C      31X,8HDLPEC = ,F9.2,1X,8HDLTH = ,F9.2,1X,8HDLHT = ,F9.2,/ )  ELE   88
C      WRITE (IY,202)
C      WRITE (IY,210) (THETA(I),I=1,IATMX)  ELE   89
C      210 FCFORMAT ( 2Y, 12HICNG. HGT. , 20F6.1 //)
C      WRITE (IY,235)  ELE   90
C
C      DO 240 K = 1,LCNMX            ELE   91
C      DO 230 J = 1,LHTMX            ELE   92
C      WRITE (IY,220) PHI(K), HGT(J) , (FH(L,J,K),I=1,LATMX)  ELE   93
C      220 FCFORMAT (1X, 2F6.1, 1X, 2CF6.2)  ELE   94
C      230 CCNTINUE
C      WRITE (IY,235)  ELE   95
C      235 FORMAT (1X)               ELE   96
C      240 CCNTINUE
C
C      CONVEET ALL ANGLES INTO RADIANS  ELE   97
C
C      DO 245 K = 1,LCNMX            ELE   98
C      245 PHI(K) = PHI(K) * RAD  ELE   99
C

```

```

    DO 250 L = 1,LATMX          ELE 120
  250 THETA(L) = THETA(I) * RAD          ELE 121
C
C      DIPH = DIPH * RAD          ELE 122
C      DLTH = DLTH * RAD          ELE 123
C      PHIZO = PHIZO * RAD          ELE 124
C      THZO = THZO * RAD          ELE 125
C
C      CALCULATE PHI,THETA,HEIGHT DIFFERENCES          ELE 126
C
C      DTH(1) = 0.5 / (DLTH*DIPH)          ELE 127
C      DPH(1) = 0.5 / (DLTH*DIPH)          ELE 128
C      DHT(1) = 0.5 / (DLTH*DIPH)          ELE 129
C      DTH(2) = -2.0 * DTH(1)          ELE 130
C      DPH(2) = -2.0 * DPH(1)          ELE 131
C      DHT(2) = -2.0 * DHT(1)          ELE 132
C
C      ADDED FOR THE HOMING FEATURE ONLY          ELE 133
C      IF(W(380).NE.C.C) RETURN          ELE 134
  300 CONTINUE          ELE 135
C
C      HL = R(1) - EARTH          ELE 136
C      FREQS = E * F          ELE 137
C      X = C.0          ELE 138
C      PYFF = C.0          ELE 139
C      PYFH = C.0          ELE 140
C      PXFH = C.0          ELE 141
C
C      FIND THETA SECTOR AND INDEX LL          ELE 142
C
C      LL = IFIX (((TF - THZO) / DLTH) + 1.00001)          ELE 143
C      IF((TH.LT.(THZO-1.E-06)).OR.(TH.GT.(THETA(LATMX)+1.E-06)))GOTO320          ELE 144
C      IF (LL - 1) 320,310,310          ELE 145
  310 IF (LL - LATMX) 330,325,320          ELE 146
  320 CONTINUE          ELE 147
C
C      LL = LL+100          ELE 148
C      GO TO 4000          ELE 149
  325 LL = LATMX - 1          ELE 150
  330 CONTINUE          ELE 151
C
C      FIND EPI PLANE AND INDEX KK          ELE 152
C
C      KK = IFIX (((FF - PHIZO) / DIPH) + 1.00001)          ELE 153
C      IF((PH.LT.(PHIZO-1.E-06)).OR.(PH.GT.(PHI(LCNMX)+1.E-06)))GOTO350          ELE 154
C      IF (KK - 1) 350,340,340          ELE 155
  340 IF (KK - LCNMX) 360,355,350          ELE 156
  350 CONTINUE          ELE 157
C
C      KK = KK+100          ELE 158
C      GO TO 4000          ELE 159
  355 KK = LCNMX - 1          ELE 160
  360 CONTINUE          ELE 161
C
C      FIND HEIGHT LAYER AND INDEX JJ          ELE 162
C
C      JJ = IFIX (((HI - HTZO) / DLTH) + 1.00001)          ELE 163
C      IF (JJ - 1) 380,370,370          ELE 164
  370 IF (JJ - LATMX) 510,380,380          ELE 165
  380 CONTINUE          ELE 166
C

```

```

HMAX = EGT(IHTMX)
GO TO 999
C      PRINT EEECCR MESSAGES EEEFCRF EXIT.
C
4000C ANG1 = TF * DEGS
ANG2 = FF * DEGS
X     = 1.0
EXFF = 1.0
EXFTH = 1.0
HMAX=EGT(LHTMX)
R(1)=EAFTHR+HMAX
IFLAG = 1
IGFT=1
WRITE (IY,4444) ANG1,ANG2,LI,KK,IFLAG
4444  FFORMAT (//1X,36HANGLES CUTTING RANGE OF ICNCSPHERE /16X,
16HTPPRA=,F7.1,3X,4HEHI=, F7.1, / 1Y,
2 15INDICES AEE ,6H LI = ,I7,3X,4H KK=,I7,6HIFLAG=, I5)
C      GO TO 999
C      510 CCNTINUE
C      INTERPARE E(TH,BL,PH) USING THE INDICES LI,KK,JJ
C      CALL INTER(IL,KK,JJ)
C      CCMPUTE X EPCM   X=(ELASMA EEEQS/E) **2, EL. DEN.= 12400 (X)
C
X     = FRE(1) / EEEQS
EXFF = FRE(2) / EEEQS
EXFTH = FRE(3) / EEEQS
EXFFF = FRE(4) / EEEQS
C      IFLAG = 0
C
999 RETURN
END

```

ELE	179
PLE	180
ELE	181
ELF	182
ZLE	183
EIE	184
ELE	185
EIE	186
ELF	187
ELE	188
EIE**	189
ELE**	190
EIE	191
EIE	192
ELE	193
ELE	194
EIE	195
ZLE	196
EIE	197
EIE	198
ZLE	199
EIE	200
EIE	201
EIE	202
EIE	203
EIE	204
EIE	205
ELE	206
EIE	207
EIE	208
EIE	209
EIE	210
ELE	211
EIE	212
ELE	213
ELE	214
ELE	215

## APPENDIX 2

This appendix contains expressions for the partial derivatives of the ground range ( $R$ ) and the group path ( $P'$ ) with respect to the elevation angle of transmission ( $\beta$ ) and the quasi-parabolic layer parameters ( $f_c, r_m, r_b$ ), required in the inversion of point-to-point oblique ionograms and backscatter leading edges:

$$\begin{aligned} \frac{\partial R}{\partial \beta} = & 2r_o \left( \frac{r_o \sin \beta}{r_b \sin \gamma} - 1 \right) \\ & + \frac{Fr_o^2 \cos \beta}{\sqrt{C}} \left[ \frac{4\sqrt{C} F r_o \sin \beta \cot \gamma}{W} + F^2 r_o^2 \sin 2\beta \left( \frac{4}{W} + G \right) \right. \\ & \left. + \tan \beta \ln \left( \frac{Ur_b^2}{W^2} \right) \right] \end{aligned} \quad (\text{A.1})$$

$$\begin{aligned} \frac{\partial R}{\partial f_c} = & \frac{F^2 r_o^2 \cos \beta}{\sqrt{C} f_c} \left[ 2 F r_o^2 \cos^2 \beta \left( \frac{4}{W} + G \right) - \frac{8CF}{U} \right. \\ & \left. + \frac{1}{F} \ln \left( \frac{Ur_b^2}{W^2} \right) - \frac{4\sqrt{C} r_b \sin \gamma}{W} \right] \end{aligned} \quad (\text{A.2})$$

$$\frac{\partial R}{\partial r_m} = \frac{F r_o^2 \cos \beta}{\sqrt{C} r_m y_m} \left[ B r_b r_m G - 2 B y_m \left( \frac{B}{U} - \frac{r_b}{W} \right) + \frac{4B}{U} (Br_m + C) \right] \quad (\text{A.3})$$

$$\begin{aligned}
 \frac{\partial R}{\partial r_b} = & \frac{2r_o^2 \cos \beta}{r_b^2 \sin \gamma} \\
 + & \frac{Fr_o^2 \cos \beta}{\sqrt{C} r_b y_m} \left[ \frac{4\sqrt{C} F r_b y_m \operatorname{cosec} \gamma}{W} - \frac{4B}{U} (Br_m + C) \right. \\
 & \left. - \frac{2By_m}{W} (r_m + y_m) - Br_m^2 G - 2y_m \right] \quad (A.4)
 \end{aligned}$$

In Eqs. (A.1) - (A.4),

$$\begin{aligned}
 W &= 2\sqrt{C} Fr_b \sin \gamma + 2C + Br_b \\
 G &= \frac{4A}{U} + \frac{1}{2C} \ln \left( \frac{Ur_b^2}{W^2} \right) + \frac{2Fr_b \sin \gamma}{\sqrt{C} W}
 \end{aligned}$$

$$\begin{aligned}
 \frac{\partial P'}{\partial f_c} = & \left[ 4 - \frac{4F^2}{A} - \frac{2B(F^2 + A)}{AV} \right] \frac{F^2 r_b \sin \gamma}{A f_c} \\
 + & \frac{BF}{f_c A^{3/2}} \left[ \frac{1}{2} \left( 1 - \frac{3F^2}{A} \right) \ln \frac{U}{V^2} \right. \\
 & \left. - \frac{4F^2 (C - A r_o^2 \cos^2 \beta)}{U} - \frac{4F^2 r_b}{V} \right] \quad (A.5)
 \end{aligned}$$

$$\begin{aligned}
 \frac{\partial P'}{\partial r_m} = & \frac{BF}{r_m y_m A^{3/2}} \left[ \left( 2 + \frac{B}{V} \right) \frac{F r_b \sin \gamma}{\sqrt{A}} \right. \\
 & + B \left( \frac{3}{4A} \ln \frac{U}{V^2} + \frac{2(A r_m r_b + C)}{U} + \frac{2 r_b}{V} \right) \\
 & \left. + (r_m + r_b) \left( \frac{1}{2} \ln \frac{U}{V^2} + \frac{B^2}{U} - \frac{B}{V} \right) \right] \quad (A.6)
 \end{aligned}$$

$$\begin{aligned}
 \frac{\partial P'}{\partial r_b} = & 2 \left( 1 - \frac{F^2}{A} + \frac{BF^2}{AV} \right) \cosec \gamma \\
 & - \frac{BF}{r_b y_m A^{3/2}} \left[ \left( 2 + \frac{B}{V} \right) \frac{F r_b \sin \gamma}{\sqrt{A}} + \left( r_m + \frac{3B}{4A} \right) \ln \frac{U}{V^2} \right. \\
 & \left. + \frac{2B(A r_m^2 + B r_m + C)}{U} - \frac{2y_m (Ar_b + B)}{V} \right] \quad (A.7)
 \end{aligned}$$

## APPENDIX 3

The computer program for the inversion of backscatter ionograms by utilizing the quasi-parabolic model is listed in the subsequent pages. In addition, this appendix contains a complete set of flow charts (with the exception of subroutine FMFP, which was written from the standard IBM scientific subroutine package), and a description of the input/output formats.

```
        NAME MAIN
        EQUIP=CARDRE,PRINTE,CARDPU
        DIMENSION F(20),RBC(20),RMC(20),FCC(20),RANGE(20),GPATHC(20),
        1FC(5,2),RR(5,20),RM(5,20),RANGE(5,20),GPATH(5,20),N(5),AZ(10)
        DIMENSION FMID(20)
202 CONTINUE
        READ 1 ,TLAT,TLONG,FCS,H0,YM,NAZ,IND
10 FORMAT(5F10.2,I1,9X,I1)
40 FORMAT(10X,6F10.2)
        R0=637 .
        RBS=R0+H0
        RMS=RBS+YM
        I=1
25 FORMAT(I2)
50 READ 2 ,AZ(I),NUMTOT,NPTS
20 FORMAT(F10.2,I2,8X,I2)
        CALL BACKS3(NUMTOT,NPTS,RBS,RMS,FCS,RBC,RMC,FCC,FMID,RANGE,
        1GPATHC,NC,1)
30 FORMAT(5F10.2)
        PRINT 35,(FCC(J),RRC(J),RMC(J),RANGE(J),GPATHC(J),J=1,NC)
35 FORMAT(5X,5F10.4)
        N(I)=NC
        DO 60 J=1,NC
        FC(I,J)=FCC(J)
        RB(I,J)=RBC(J)
        RM(I,J)=RMC(J)
        RANGE(I,J)=RANGE(J)
60 GPATH(I,J)=GPATHC(J)
        I=I+1
        IF (I-NAZ) 70,70,80
70 FCC=FCC(1)
        RBS=RBC(1)
        RMS=RMC(1)
        GO TO 50
80 IF(IND)180,85,180
85 READ 1 ,FW,AZM,GPM
        IF(FW)201,202,203
203 CONTINUE
        CALP=(6370.*6370.+6470.*6470-GPM*GPM/4.)/(2.*6370.*6470.)
        DEST=AROSF(CALP)*6370.*2.
        PRINT 41,FW,AZM,GPM,DEST
        IF(NAZ-1)204,204,205
205 CONTINUE
        DO 100 K=1,NAZ
        IF (AZM-AZ(K)) 110,110,100
100 CONTINUE
110 FACTOR=(AZM-AZ(K-1))/(AZ(K)-AZ(K-1))
        N1=N(K)
        N2=N(K-1)
112 DO 120 J=1,N1
        IF (DEST-RANGE(K,J)) 130,130,120
120 CONTINUE
130 FACT=(DEST-RANGE(K,J-1))/(RANGE(K,J)-RANGE(K,J-1))
        FC1=FC(K,J-1)+FACT*(FC(K,J)-FC(K,J-1))
        RB1=RB(K,J-1)+FACT*(RB(K,J)-RB(K,J-1))
        RM1=RM(K,J-1)+FACT*(RM(K,J)-RM(K,J-1))
        PRINT 42,FC1,RB1,RM1
        DO 140 J=1,N2
```

```
IF (DEST-RANGE(K-1,J)) 150.150.140
140 CONTINUE
150 FACT=(DEST-RANGE(K-1,J-1))/(RANGE(K-1,J)-RANGE(K-1,J-1))
FC2=FC(K-1,J-1)+FACT*(FC(K-1,J)-FC(K-1,J-1))
RB2=RB(K-1,J-1)+FACT*(RB(K-1,J)-RB(K-1,J-1))
RM2=RM(K-1,J-1)+FACT*(RM(K-1,J)-RM(K-1,J-1))
PRINT 41,FC2,RB2,RM2
FC1=FC2+FACTOR*(FC1-FC2)
RBI=RBI+FACTOR*(RBI-RB2)
RMI=RMI+FACTOR*(RMI-RM2)
208 CONTINUE
PRINT 41,FC1,RBI,RMI
DTOL=1.
GPTOL=.1
CALL DCAL(FC1,RBI,RMI,FW,GPM,D,GRTOL)
PRINT 40,FW,AZM,GPM,DEST,D
IF (ABSF(D-DEST)-DTOL) 170.170.160
160 DEST=D
IF(NAZ-1)204,204,112
170 PRINT 40,FW,AZM,GPM,D
GO TO 81
180 CONTINUE
READ 200, KGO
200 FORMAT(I10)
IF(KGO)201,202,201
201 CALL EXIT
204 N1=N(NAZ)
DO 206 J=1,N1
IF(DEST-RANGE(1,J))207,207,206
206 CONTINUE
207 FACT=(DEST-RANGE(1,J-1))/(RANGE(1,J)-RANGE(1,J-1))
FC1=FC(1,J-1)+FACT*(FC(1,J)-FC(1,J-1))
RB1=RB(1,J-1)+FACT*(RB(1,J)-RB(1,J-1))
RMI=RM(1,J-1)+FACT*(RM(1,J)-RM(1,J-1))
GO TO 208
END
```

```
H      NAME A2
H      EQUIP=CARDRE,PRINTE,CARDPU
H      FUNCTION FOGX(ARG)
C*****SURE FOGX CHECKS TO MAKE SURE WE ARE NOT TAKING THE NATURAL LOG OF A
C*****NEG NUMBER...IF WE ARE IT FLAGS THE ERROR BY SETTING FOGX = 9999.
C*****THE INVALID ARGUMENT IS PRINTED OUT WITH AN ERROR MSG.
      IF(ARG)>10,20,20
10    CONTINUE
      PRINT 15,ARG
15    FORMAT(29H LOGF ENTERED WITH NEG ARG = , E13.7)
      FOGX=9999.
      GO TO 30
20    FOGX=LOGF(ARG)
30    RETURN
      END
```

```

4      NAME AS
4      EQUIP=CARDRE,PRINTE,CARDPU!
5      SUBROUTINE FSTDFS(FW,FC,RB,YM,DGRT,GP,DGPDFC,DGPDRC,DGPDRC,RANGE,
5      $BDEG)
*****THIS SUBR COMPUTES THE MIN TIME DELAY TRACE(MIN GROUP PATH VS FREQ) OF A
*****EARTH-PONCENTRIC Q-P IONOSPHERE LAYER AS WELL AS THE DERIVATIVES OF THE
*****THE GROUP PATH WRT RB,RM,AND FC. IT IS A HOPEFULLY MORE RAPID VERSION OF
*****SUBR DIFFS, WHICH DID NOT USE NEWTONS METHOD TO FIND THE ELEVATION ANGLE B
*****BETA WHICH MINIMIZES THE GROUP PATH FUNCTION
C
*****CALLING SEQUENCE
C      FW=(INPUT) FREQ OF TRANSMISSION (MHZ)
C      FC=(INPUT) CRITICAL FREQUENCY OF Q-P LAYER (IN MHZ)
C      RB=(INPUT) BASE HEIGHT OF Q-P LAYER (IN KM)
C      YM=(INPUT) SEMITHICKNESS OF Q-P LAYER (KM)
C      DGPT=(INPUT) TOLERANCE OF GROUP PATH WRT ELEVATION ANGLE , BETA USED IN
C      FINDING MINIMUM GROUP PATH IN KM/RAD
C      GP=(OUTPUT) MIN GROUP PATH (KM)
C      DGPDFC=(OUTPUT) DERIV OF MIN GROUP PATH WRT FC
C      DGPDRC=(OUTPUT) DERIV MIN GROUP PATH WRT RM
C      DGPDRC=(OUTPUT) DERIV MIN GROUP PATH WRT RB
C      RANGE=(OUTPUT) GROUND RANGE OF BACKSCATTER PT OF MIN GROUP RAY
C
      R0=6370.
      R02=R0*R0
      RB=R0+WB
      RB2=RB*RB
      RM=R0+YM
      RM2=RM*RM
      YM2=YM*YM
      F=FW/FC
      F2=F*F
      RBYM2=RB2/YM2
      A=F2-1.+RBYM2
      SQA=SQR00(A)
      IF(SQA=9999.)50,950,50
*****
950  NERPT=1
*****
      GO TO 900
50  CONTINUE
      B=2.*RM*RBYM2
*****NOW SET SOME CONSTANTS UP FOR FURTHER USE IN THE ITERATION LOOP
*****THESE CONSTS HAVE NO SIGNIFICANCE IN THE 1974 PAPER BY NNR
      CON1=2.*A*RB+B
      CON2=2.*RB+F*SQA
      B2=B*B
      F2A=F2/A
      CON3=2.*R0*(1.-F2A )
      CON4=(B*F2A )*2.*R0
      CON5=4.*B*F2*F*R02/SQA
      CON6=R0/RB
      CON7=8.*A*F2*R02
*****BETPEN IS THE PENETRATION ELEVATION ANGLE (BETA MUST BE BETWEEN 0
*****AND BETPEN)
      SQR00X=SQR00(RM2*RBYM2-B2/(4.*A))
      IF(SQR00X=9999.)75,960,75
*****

```

```

960 NERPT=2
*****+
    GO TC 900
75  CONTINUE
    BETPEN= ((1./(F+R0))*S0R00X)
    BETPEN = ACOSCK(BETPEN)
    IF(BETPEN=9999.)90,970,90
*****
970 NERPT=3
*****+
    GO TC 900
90  CONTINUE
*****INITIALIZE BETA, THE ELEVATION ANGLE OF THE GROUP RAY PUT THE INITIAL GUES
*****RIGHT IN THE MIDDLE OF THE RANGE OF POSSIBLE BETA VALUES.
    BETA=BETPEN*.5
*****ITERATE HERE FOR NEW VALUES OF BETA (AT STATEMENT 100, WHICH MINIMIZE
*****THE GROUP PATH AT A GIVEN OPERATING FREQ FW (USING NEWTONS METHOD)
    NTRY=100
    ITERCT=0
100 SINBET=SIN(BETA)
    ITERCT=ITERCT+1
*****IF WE HAVE TRIED TO FIND BETA SUCH THAT GP IS MINIMIZED TO WITHIN
*****DGPT OF ZERO 100 TIMES LETS GIVE UP
    IF(ITERCT=NTRY)150,150,140
140 PRINT 145,DGPT,NTRY
145 FORMAT(//,4H FSTDIF ROUTINE CANNOT MINIMIZE DGPDB TO WITHIN ,
$F5.3,1H KM AFTER ,I3,6H TRIES ,//)
    PRINT 147,BETA,DGPDB
147 FORMAT(8H BETA = ,F5.2,9H DGPDB = ,F10.5)
    RETURN
150 CONTINUE
    COSBET=COS(BETA)
    COSBE2=COSBET*COSBET
    CRBYM2=RM2=F2*R02*COSBE2
    COSGAM=R0*COSBET/RB
    GAMMA=ACOSCK(COSGAM)
    IF(GAMMA=9999.)165,971,165
*****
971 NERPT=4
*****+
    PRINT 972,BETA,BETPEN,ITERCT
972 FORMAT(8H BETA = ,E12.5,5X,10H BETPEN = ,E12.5,5X,10H ITERCT = ,I4)
    $)
    GO TC 900
165 CONTINUE
    SINGAM=SINF(GAMMA)
    COTGAM=COSGAM/SINGAM
    V=CON1*CON2*SINGAM
    V2=V*V
    U=82=4.*A*C
    U2=U*U
    F1=(CON3*CON4/V)
    G2=2.*R0*CON5*SINBET/U
    DGDB=F1*SINBET*COTGAM-G2*COSBET
*****BRANCH OUT OF NEWTON ITERATION LOOP HERE WHEN BETA IS FOUND WHICH
*****MINIMIZES DGPDB TO WIWIN TOLERANCE DGPT (IN KM/RAD )
    IF(ABS(DGPDB)-DGPT)<000,350,350
350 CONTINUE

```

```

SQROOY=SQR00(1.-(CON6*COSBFT)**2.)
IF(SQR00Y=9999.)375,973,375
*****973 NERPT=5
***** PRINT 072,BETA,BETPEN,ITERCT
GO TO 900
375 CONTINUE
DGAMDB=SINBET*CON6/SQROOY
DCOTDB=-DGAMDB/(SINGAM*SINGAM)
DVDB=CON2*COSGAM*DGMDB
DF1DB=-(CON4/V2)*DVDB
DUDB=-CON7*COSBET*SINBET
DF2DB=-CON5*(COSBET/U-(SINBET/U2)*DUDB)
DGPDB2=DF1DB*SINBET*COTGAM+F1*(COSBET*COTGAM+SINBET*DCOTDB)
S=DF2DB*COSBET+G2*SINBET
BETA=BETA-DGPDB/DGPDB2
***** IF BETA HAS BEEN INCREMENTED TO A NEG VALUE BY NEWTONS METHOD WE BETTER SE
***** BETTER SET BETA BACK TO A LITTLE ABOVE 0 OR WE MIGHT HAVE TROUBLES LATER 0
IF(BETA)400,400,500
400 BETA=.0001
500 IF(BETPEN-BETA)600,600,700
600 BETA=BETPEN-.0001
***** CHECK TO ENSURE NEWTONS METHOD IS NOT CAUSING US TO OVERSTEP THE
***** PENETRATION ELEVATION ANGLE BOUNDARY. IF SO SET BETA BACK TO LITTLE BELOW
***** BETPEN
700 GO TO 100
800 CONTINUE
***** AT STATEMENT 800 THE ELEVATION ANGLE BETA CORRESPONDING TO THE MINIMUM GRO
***** GRUP PATH HAS BEEN COMPUTED BY SOLVING FOR THE VALUE OF BETA WHICH FORCES
***** DGPDB2 TO 0. NOW WE CAN COMPUTE THE MINIMUM GROUP PATH GPM
UV2LOG=FOGX(U/V2)
IF(UV2LOG=9999.)850,974,850
*****974 NERPT=6
***** GO TC 930
930 CONTINUE
BFA32=P*F/(A*SQA)
GPM=CON3/CON6*SINGAM-2.*R0*SINBET
S=(BFA32+.5)*UV2LOG
GP=GPM
DPDFC1=2.*CON3/R0-2.*B*(F2+A)/(A*V)
DPDFC2=F2*RB*SINGAM/(A*FC)
DPDFC3=BFA32/FC
DPDFC4=.5*(1.-3.*F2A)*UV2LOG-4.*F2*(C=A*R02*COSBE2)/U
S=4.*F2*RB/V
DGPDFC=DPDFC1*DPDFC2*DPDFC3*DPDFC4
DPDRM2=.75/A*UV2LOG+2.*((A*RM+RB+C)/U+2.*RB/V
DPDRM1=BFA32/(RM*YM)
DPDRM3=(2.+B/V)*F*RB*SINGAM/SQA+B*DPDRM2+(RM+RB)*(1.5*UV2LOG+B2/U-B/V)
S/V)
DGPDRM=DPDFC1*DPDFC2*DPDFC3*DPDFC4
DPDRB1=(CON3+CON4/V)/(R0*SINGAM)
DPDRB2=-BFA32/(RB*YM)*((2.+B/V)*F*RB*SINGAM/SQA+(RM+.75*B/A)*UV2LO
SG+.2.*R*(A*RM2+B*RM+C)/U=.2.*YM*(A*RB+B)/V)
DGPDRB=DPDFC1*DPDFC2
SQC=SQR00(C)

```

```
IF(SCC.9999.1875,975,875
=====
975 NERPT=7
=====
GO TO 900
975 CONTINUE
R1=2.*SQC*RB*F*SINGAM+2.*C+B*RB
R12=R1+R1
W=FOGX(U*R02/R12)
R3=.5*P*R0*COSBET*W/SQC
RANGE=2.*R0*(GAMMA-BETA+R3)
BDEG=BETA*57.2985
RETURN
900 FC=-ABSF(FC)
PRINT 980,NERPT
980 FORMAT(1X,100(1H*),/,3nH FQTDFS ERROR AT POINT NUMBER ,I2,/,1X,
$100(1H*))
PRINT 985,FH,FC,H8,YM,DGPT
985 FORMAT(1X,5E15.7)
RETURN
END
```

```

H      NAME A4
H      EQUIP=CARDRE,PRINTE,CARDPU,
H      SUBROUTINE FUNCT(N,ARG,VAL,GRAD)
H      DIMENSION ARG(3),GRAD(3),FBSMES(50),PBSMES(50),GPC(50),DGPC(50,3)
H      DIMENSION RAN(50),BTA(50)
H      COMMON FBSMES,PBSMES,DT,NPTS,RAN,BTA,GPCTID
C
C*****SUBROUTINE FUNCT TO BE USED BY BACKS3 BACKSCATTER IONOGRAM INVERSION
C*****ROUTINE. IT EVALUATES THE SUM SQUARED ERROR AND ITS GRADIENT AS A
C*****FUNCTION OF Q-P LAYER PARAMETERS RB, RM, FC.
C
C*****CALLING SEQUENCE.....
C*****N=(INPUT) CONTROL PARAMETER
C***** IF N=3 FUNCTION NORMALLY, RETURN VALUE OF ERROR FUNCTION AND ITS
C***** GRADIENT
C*****ARG=(INPUT) 3 ELEMENT ARRAY OF LAYER PARAMETERS
C***** ARG(1)=RB
C***** ARG(2)=RM
C***** ARG(3)=FC
C*****VAL=(OUTPUT) VALUE OF ERROR FUNCTION E CORRESPONDING TO CURRENT VALUE OF
C***** ARG
C*****GRAD=(OUTPUT) 3 ELEMENT ARRAY WITH
C***** GRAD(1)=DE/DRB
C***** GRAD(2)=DE/DRM
C***** GRAD(3)=DE/DFC
C*****END OF INPUT SEQUENCE*****+
C
C      FC=ARG(3)
C      HB=ARG(1)-6370.
C      YM=ARG(2)-ARG(1)
C*****HERE N=3 AND WE WILL EVALUATE E AND GRAD OF E
C*****FIRST INITIALIZE VALUES FOR SUBSEQUENT SUMMING OPERATION
40    SUMF=0
      SUMDRB=0
      SUMDRM=0
      SUMDFC=0
      NMID=NPTS/2+1
      DO 50 I=1,NPTS
C*****FSTDFS CALLED TO EVALUATE MIN GROUP PATH AND ITS DERIVS WRT RB,RM,FC AS A
C*****FUNCTION OF FBSTMES(I), THE ITH TRANSMISSION FREQ
      FBSTM=FBSMES(I)
      ITRY=0
      CALL FSTDFS(FBSTM,FC,HB,YM,DT,GPC(I),DGPC(I,1),DGPC(I,2),
      SDGPC(I,3),RA,BT)
      RAN(I)=RA
      BTA(I)=BT
C*****CATCH AND STORE THE FINAL VALUE OF THE GROUP PATH CORRESPONDING TO THE MID
C*****BACKSCATTER LEADING EDGE POINT
      IF(I-NMID)46,47,46
47    GPCMID=GPC(I)
46    CONTINUE
C      NUMERICAL ERROR FLAGGED IF FC NEGATIVE . IF SO ABORT JOB BY MAKING N
C      NEGATIVE AND RETURNING TO MAINLINE VIA SUBR FMFP
      IF(FC)42,45,45
42    N=-3
      ARG(1)=A1SV
      ARG(2)=A2SV
      ARG(3)=A3SV

```

```
VAL=VALSV
G1SV=GRAD(1)
G2SV=GRAD(2)
G3SV=GRAD(3)
RETURN
45 CONTINUE
ERR=GPC(I)-PBSMES(1)
ERSQ=ERR*ERR
SUMF=SUMF+ERSQ
SUMDRB=SUMDRB+ERR*DGPC(I,3)
SUMDRM=SUMDRM+ERR*DGPC(I,2)
50 SUMDFC=SUMDFC+ERR*DGPC(I,1)
C****NOTE SUMF NOW CONTAINS SUM SQUARED ERROR
C****GRAD CONTAINS THE GRADIENT OF THE SUM SQUARED ERROR
VAL=SUMF
GRAD(1)=2.*SUMDRB
GRAD(2)=2.*SUMDRM
GRAD(3)=2.*SUMDFC
C
C**** NOTE THAT AT THIS POINT IT MEAY BE DESIRABLE TO INSERT PRINT OUT STATEMENT
C****TO OUTPUT ARG, VAL,GRAD,RANGE, AND BDEG TO OBSERVE CONVERGENCE OF THE ERROR
C****FUNCTION TO A MINIMUM AS FMFP DOES ITS STUFF.....
C****ALSO PRINTING OUT RANGE AND BDEG GIVES US SOME INDICATION OF WHERE WE ARE
C****SAMPLING THE IONOSPHERE IN THE CASE OF HORIZONTAL GRADIENTS
C****

A1SV=ARG(1)
A2SV=ARG(2)
A3SV=ARG(3)
VALSV=VAL
G1SV=GRAD(1)
G2SV=GRAD(2)
G3SV=GRAD(3)
200 RETURN
END
```

```

H      NAME A4
H      EQUIP=CARDDR,PRINTE,CARDPU,
H      SUBROUTINE FMFP(N,X,F,G,EST,EPS,LIMIT,IER,H)          FMFP 20
C
C      DIMENSIONED DUMMY VARIABLES                         FMFP 30
C      DIMENSION H(1),X(1),G(1)                           FMFP 40
C
C      COMPUTE FUNCTION VALUE AND GRADIENT VECTOR FOR INITIAL ARGUMENTFMFP 60
C      CALL FUNCT(N,X,F,G)
C      IF(N)56,100,100
100    CONTINUE
C
C      RESET ITERATION COUNTER AND GENERATE IDENTITY MATRIX   FMFP 80
C      IER=0
C      KOUNT=1
C      N2=N+N
C      N3=N2+N
C      N31=N3+1
1      K=N31
DO 4 J=1,N
H(K)=1.
NJ=N-J
IF(NJ)5,5,2
2      DO 3 L=1,NJ
KL=K+L
3      H(KL)= .
4      K=KL+1
C
C      START ITERATION LOOP
5      KOUNT=KOUNT +1
C
C      SAVE FUNCTION VALUE, ARGUMENT VECTOR AND GRADIENT VECTOR   FMFP 250
C      OLDF=F
DO 9 J=1,N
K=N+J
H(K)=G(J)
K=K+N
H(K)=X(J)
C
C      DETERMINE DIRECTION VECTOR H
K=J+N3
T=0.
DO 8 L=1,N
T=T-G(L)*H(K)
IF(L=J)6,7,7
6      K=K+N-L
GO TO 8
7      K=K+1
8      CONTINUE
9      H(J)=T
C
C      CHECK WHETHER FUNCTION WILL DECREASE STEPPING ALONG H,
Dy=0.
HNRM=0.
GNRM=0.
C
C      CALCULATE DIRECTIONAL DERIVATIVE AND TESTVALUES FOR DIRECTION   FMFP 480
C      VECTOR H AND GRADIENT VECTOR G.                                FMFP 490
FMFP 500
FMFP 510
FMFP 520
FMFP 530
FMFP 540

```

```

DO 10 J=1,N                                FMFP 550
HNRM=HNRM+ABSF(H(J))                      FMFP 560
GNRM=GNRM+ABSF(G(J))                      FMFP 570
10 DY=DY+H(J)*G(J)                         FMFP 580
C
C      REPEAT SEARCH IN DIRECTION OF STEEPEST DESCENT IF DIRECTIONAL
C      DERIVATIVE APPEARS TO BE POSITIVE OR ZERO.
IF(DY)>11.51.51                            FMFP 590
C
C      REPEAT SEARCH IN DIRECTION OF STEEPEST DESCENT IF DIRECTION
C      VECTOR H IS SMALL COMPARED TO GRADIENT VECTOR G.
11 IF(HNRM/GNRM-EPS)>51.51.12             FMFP 600
C
C      SEARCH MINIMUM ALONG DIRECTION H       FMFP 610
C
C      SEARCH ALONG H FOR POSITIVE DIRECTIONAL DERIVATIVE   FMFP 620
12 FY=F                                     FMFP 630
ALFA=2.*(EST-F)/DY                         FMFP 640
AMBDA=1.                                    FMFP 650
FMFP 660
FMFP 670
FMFP 680
FMFP 690
FMFP 700
FMFP 710
FMFP 720
FMFP 730
FMFP 740
FMFP 750
FMFP 760
FMFP 770
FMFP 780
FMFP 790
FMFP 800
FMFP 810
FMFP 820
FMFP 830
FMFP 840
FMFP 850
FMFP 860
FMFP 870
FMFP 880
FMFP 890
FMFP 900
FMFP 910
FMFP 920
FMFP 930
FMFP 940
FMFP 950
FMFP 960
FMFP 970
FMFP 980
FMFP 990
FMFP1000
FMFP1010
FMFP1020
FMFP1030
FMFP1040
FMFP1050
FMFP1060
FMFP1070
FMFP1080
FMFP1090
FMFP1100
C
C      USE ESTIMATE FOR STEPSIZE ONLY IF IT IS POSITIVE AND LESS THAN 1.
1. OTHERWISE TAKE 1. AS STEPSIZE
IF(ALFA)<15.15.13                          FMFP 750
13 IF(ALFA-AMBDA)>14.15.15                FMFP 760
14 AMBDA=ALFA                               FMFP 770
15 ALFA=0.                                  FMFP 780
C
C      SAVE FUNCTION AND DERIVATIVE VALUES FOR OLD ARGUMENT
16 FX=F                                     FMFP 790
DX=DY                                      FMFP 800
C
C      STEP ARGUMENT ALONG H                  FMFP 810
DO 17 I=1,N                                FMFP 820
17 X(I)=X(I)+AMBDA*H(I)                   FMFP 830
C
C      COMPUTE FUNCTION VALUE AND GRADIENT FOR NEW ARGUMENT
CALL FIUNCT(N,X,F,G)                       FMFP 840
FY=F                                         FMFP 850
IF(N)>54.101.101                           FMFP 860
101 CONTINUE                                 FMFP 870
C
C      COMPUTE DIRECTIONAL DERIVATIVE DY FOR NEW ARGUMENT. TERMINATE
C      SEARCH, IF DY IS POSITIVE: IF DY IS ZERO THE MINIMUM IS FOUND
DY=0.                                         FMFP 880
DO 18 I=1,N                                FMFP 890
18 DY=DY+G(I)*H(I)                         FMFP 900
IF(DY)>19.36.22                            FMFP 910
C
C      TERMINATE SEARCH ALSO IF THE FUNCTION VALUE INDICATES THAT
C      A MINIMUM HAS BEEN PASSED
19 IF(FY-FX)>20.22.22                     FMFP 920
C
C      REPEAT SEARCH AND DOUBLE STEPSIZE FOR FURTHER SEARCHES
20 AMBDA=AMBDA+ALFA                         FMFP 930
ALFA=AMBDA                               FMFP 940
C
C      END OF SEARCH LOOP                    FMFP 950
C
C      TERMINATE IF THE CHANGE IN ARGUMENT GETS VERY LARGE

```

```

IF(HNRM*AMBDA-1.E10)16,16,21 FMP1110
C
C      LINEAR SEARCH TECHNIQUE INDICATES THAT NO MINIMUM EXISTS FMP1120
21 IER=2 FMP1130
      RETURN FMP1140
C
C      INTERPOLATE CUBICALLY IN THE INTERVAL DEFINED BY THE SEARCH FMP1150
C      ABOVE AND COMPUTE THE ARGUMENT X FOR WHICH THE INTERPOLATION FMP1160
C      POLYNOMIAL IS MINIMIZED FMP1170
22 T=0. FMP1180
23 IF(AMBDA)24,36,24 FMP1190
24 Z=3.*(FX-FY)/AMBDA+DX+DY FMP1200
      ALFA=MAX1F(ABSF(Z),ABSF(DX),ABSF(DY)) FMP1210
      DALFA=Z/ALFA FMP1220
      DALFA=BALFA+DALFA-DX/ALFA+DY/DALFA FMP1230
      IF(DALFA)51,25,25 FMP1240
25 W=ALFA+SQRT(DALFA) FMP1250
      ALFA=(DY+W-Z)*AMBDA/(DY*2.+W-DX) FMP1260
      DO 26 I=1,N FMP1270
26 X(I)=X(I)+(T-ALFA)*H(I) FMP1280
      FMFP1290
      FMFP1300
C
C      TERMINATE, IF THE VALUE OF THE ACTUAL FUNCTION AT X IS LESS FMFP1310
C      THAN THE FUNCTION VALUES AT THE INTERVAL ENDS. OTHERWISE REDUCE FMFP1320
C      THE INTERVAL BY CHOOSING ONE END-POINT EQUAL TO X AND REPEAT FMFP1330
C      THE INTERPOLATION. WHICH END-POINT IS CHOSEN DEPENDS ON THE FMFP1340
C      VALUE OF THE FUNCTION AND ITS GRADIENT AT X FMFP1350
      FMFP1360
      FMFP1370
      FMFP1380
CALL FUNCT(N,X,F,G)
IF(N) 56,102,102
102 CONTINUE
IF(F=FX)27,27,28 FMP1390
27 IF(F=FY)36,36,28 FMP1400
28 DALFA=1. FMP1410
      DO 29 I=1,N FMP1420
29 DALFA=BALFA+G(I)*H(I) FMP1430
      IF(DALFA)30,33,33 FMP1440
30 IF(F=FY)32,31,33 FMP1450
31 IF(DX=DALFA)32,36,32 FMP1460
32 FX=F F-FP1 70
      DX=DALFA FMP1480
      T=ALFA FMP1490
      AMBDA=ALFA FMP1500
      GO TO 23 FMP1510
33 IF(FY-F)35,34,35 FMP1520
34 IF(DY-DALFA)35,36,35 FMP1530
35 FY=F FMP1540
      DY=DALFA FMP1550
      AMBDA=AMBDA-ALFA FMP1560
      GO TO 22 FMP1570
      FMFP1580
C
C      COMPUTE DIFFERENCE VECTORS OF ARGUMENT AND GRADIENT FROM FMFP1590
C      TWO CONSECUTIVE ITERATIONS FMFP1600
36 DO 37 J=1,N FMP1610
      K=N+J FMP1620
      H(K)=G(J)-H(K) FMP1630
      K=N+K FMP1640
37 H(K)=X(J)-H(K) FMP1650
      FMFP1660
C

```

```

C      TERMINATE, IF FUNCTION HAS NOT DECREASED DURING LAST ITERATION FMFP1670
C      IF(OLDF-F+EPS)51,38,38                                         FMFP1680
FMFP1690
C      TEST LENGTH OF ARGUMENT DIFFERENCE VECTOR AND DIRECTION VECTOR FMFP1700
C      IF AT LEAST N ITERATIONS HAVE BEEN EXECUTED, TERMINATE, IF FMFP1710
C      BCTW ARE LESS THAN EPS                                         FMFP1720
FMFP1730
38 IER=0.                                                       FMFP1740
IF(KOUNT=N)42,39,39                                         FMFP1750
39 T=0.                                                       FMFP1760
Z=0.                                                       FMFP1770
DO 40 J=1,N                                                 FMFP1780
K=N+J                                                       FMFP1790
W=W(K)                                                       FMFP1800
K=K+1                                                       FMFP1810
T=T+ABSF(H(K))                                         FMFP1820
40 Z=Z+W*W(K)                                         FMFP1830
IF(HNRM-EPS)41,41,42
41 IF(T-EPS)55,55,42                                         FMFP1850
FMFP1860
C      TERMINATE, IF NUMBER OF ITERATIONS WOULD EXCEED LIMIT FMFP1870
42 IF(KOUNT=LIMIT)43,50,50                                         FMFP1880
FMFP1890
C      PREPARE UPDATING OF MATRIX H
43 ALFA=0.                                                       FMFP1900
DO 47 J=1,N                                                 FMFP1910
K=J+N3                                                       FMFP1920
W=0.                                                       FMFP1930
DO 46 L=1,N                                                 FMFP1940
KL=N+L                                                       FMFP1950
W=W+H(KL)*H(K)                                         FMFP1960
IF(L=J)44,45,45                                         FMFP1970
44 K=K+N-L
GO TO 46
45 K=K+1
46 CONTINUE
K=N+J
ALFA=ALFA+W*H(K)
47 H(J)=W
C      REPEAT SEARCH IN DIRECTION OF STEEPEST DESCENT IF RESULTS FMFP2050
C      ARE NOT SATISFACTORY                                         FMFP2060
IF(Z>ALFA)48,1,48                                         FMFP2070
FMFP2080
FMFP2090
C      UPDATE MATRIX H
48 K=N+1
DO 49 L=1,N
KL=N+L
DO 49 J=L,N
NJ=N+J
H(K)=H(K)+H(KL)*H(NJ)/Z=H(I)*H(J)/ALFA
49 K=K+1
GO TO 5
C      END OF ITERATION LOOP
C      NO CONVERGENCE AFTER LIMIT ITERATIONS
50 IER=1
RETURN
C

```

```

C      RESTORE OLD VALUES OF FUNCTION AND ARGUMENTS          FMFP2250
51 DO 52 J=1,N                                         FMFP2260
      K=N2+J                                         FMFP2270
52 X(J)=H(K)                                         FMFP2280
      CALL FUNCT(N,X,F,G)                           FMFP2290
      IF(N)56,103,103
103 CONTINUE
C
C      REPEAT SEARCH IN DIRECTION OF STEEPEST DESCENT IF DERIVATIVE
C      FAILS TO BE SUFFICIENTLY SMALL
      IF(GNRM-EPS)55,55,53
C
C      TEST FOR REPEATED FAILURE OF ITERATION
53 IF(IER)56,54,54
54 IER=-1
      GOTO 1
55 IER=0
      PRINT 57,KOUNT
57 FORMAT(//,22H FMFP CONVERGED AFTER ,I4,11H ITERATIONS ,//)
56 RETURN
      END

```

FMFP2300  
FMFP2310  
FMFP2320  
FMFP2330  
FMFP2340  
FMFP2350  
FMFP2360  
FMFP2370  
FMFP2380  
FMFP2390  
FMFP2400  
FMFP2410

H NAME A6  
H EQUIP=CARDRE,PRINTE,CARDPU:  
H SUBROUTINE BACKS3(NUMTOT,NPTX,RBSTRT,RMSTRT,FCSTRT,RBB,RMM,FCC,  
SFMD,RANMID,GPTHMD,NUSED,PRNTSW)  
H DIMENSION X(3),G(3),H(32)  
H DIMENSION FBSMES(50),PBSMES(50)  
H DIMENSION RAN(50),BTA(50),RBB(20),RMM(20),FCC(20),FMID(20)  
H DIMENSION RANMID(20),GPTHMD(20)  
H COMMON FBSMES,PBSMES,DT,NPTS,RAN,BTA,GPCMD

C\*\*\*\*\*  
C\*\*\*\*\*THIS IS SUBROUTINE FOR THE MIN SUM SQUARED ERROR NOISY BACKSCATTER LEADING  
C\*\*\*\*\*EDGE INVERSION PROCEDURE.  
C\*\*\*\*\*DEVELOPED IN QUARTERLY REPORTS 3,4,5 OF DR. YEH AND DR. RAD S AIR FORCE  
C\*\*\*\*\*AFCRD CONTRACT NUMBER F 19628-75-C-0088, 1975-1976

C  
C  
C SURROUNTING INPUT PARAMETERS FOLLOW.....

C NUMTOT=TOTAL NUMBER OF POINTS SCALED FROM IONOGGRAM BACKSCATTER LEADING  
C EDGE WHICH ARE TO BE INVERTED IN GROUPS OF NPTS  
C NPTS=NUMBER OF POINTS IN EACH GROUP OF DATA THAT WILL BE SUCCESSIVELY INV

C FOR EXAMPLE...TO PROCESS 12 BACKSCATTER IONOGGRAM PTS BY INVERTING  
C OVERLAPPING GROUPS OF 4 POINTS AT A TIME, WE LET NUMTOT=12 AND  
C NUMGRP=4.

C NOTE THAT THE STARTING SET OF ESTIMATED LAYER PARAMETERS IS USED  
C IN INVERTING THE FIRST SET OF BACKSCATTER LEADING EDGE POINTS. EACH  
C SUBSEQUENT SET USES THE IMMEDIATELY PRECEDING SOLUTION AS THE  
C STARTING POINT.

C RBSTRT=STARTING VALUE RB IN KM  
C RMSTRT=STARTING VALUE RM IN KM  
C FCSTRT=STARTING VALUE FC IN MHZ

C OUTPUT PARAMETER DEFNS.....  
C RBB=VECTOR OF RB PARAMETERS OBTAINED FROM THE SUCCESSIVE INVERSION OF THE  
C SETS OF NPTS POINTS  
C RMM=VECTOR OF RM PARAMETERS  
C FCC=VECTOR OF FC PARAMETERS  
C FMID=VECTOR OF THE FREQUENCIES CORRESPONDING TO THE MIDDLE BACKSCATTER  
C LEADING EDGE POINT IN THE SUCCESSIVE SETS OF NPTS POINTS  
C RANMID=VECTOR OF RANGES IN KM  
C GPTHMD=VECTOR OF GROUP PATHS IN KM  
C NUSED=NUMBER OF SETS OF NPTS POINTS SUCCESSFULLY INVERTED FROM  
C BACKSCATTER LEADING EDGE  
C PRNTSW=3=DO NOT PRINT INTERMEDIATE RESULTS  
C PRNTSW=1=PRINT INTERMEDIATE RESULTS

C  
C \*\*\*\*\*DESCRIPTION OF DATA DECK TO BE READ IN BY SUBROUTINE  
C  
C\*\*\*\*\*PARAMETER CARD DESCRIPTION IN 4F10.5 FORMAT  
C\*\*\*\*\*DT IS THE TOLERANCE IN THE DERIV OF THE MINIMUM GROUP PATH WITH RESPECT  
C\*\*\*\*\* TO BETA, TYPICALLY SET TO .05 KM/RAD.  
C\*\*\*\*\* EST = ESTIMATED MIN VALUE OF SUM-SQUARED ERROR FUNCTION E (IN SQ KM)

```

C***** UPON WHICH THE MINIMIZATION PROCEDURE BASES ITS STEPSIZE
C***** EPS=TOL TO WHICH MINIMUM IS TO BE COMPUTED (SUBR FMFP USES IT TO DETERM
C***** WHEN TO TERMINATE MINIMIZATION ITERATIONS)
C***** LIMIT=MAXIMUM NUMBER OF ITERATIONS ALLOWED IN MINIMIZATION ITERATION
C***** LOOP BEFORE GIVING UP
C
NPTS=NPTX
X(1)=RRSTRT
X(2)=RMSTRT
X(3)=FCSTRT
C***** X(1)=STARTING VALUE RB IN KM
C***** X(2)=STARTING VALUE RM IN KM
C***** X(3)=STARTING VALUE FC IN MHZ
READ 11,DT,EST,EPS,XLIMIT
10 FORMAT(4F10.5)
LIMIT=XLIMIT
NUMSET=NUMTOT-NPTS+1
NUQED=NUMSET
JARRAY=1
DO 101 ICT=1,NUMSET
C*****SAVE STARTING VALUES IN CASE WE WANT TO ABORT ATTEMPT AND TRY AGAIN
XSV1=X(1)
XSV2=X(2)
XSV3=X(3)
C*****KT=0 INDICATES FIRST ATTEMPT AT MINIMIZATION
KT=0
ESTSVE=EST
C*****FIRST INITIALIZE FUNCT BY READING IN
C*****IN AND PRINT OUT THE NUMPT POINTS SCALED OFF LEADING EDGE OF BS IONOGRAM
C*****AS WELL AS READ IN THE TOLERANCE TO WHICH THE MIN GROUP PATH IS FOUND IN
C*****SUBROUTINE FSTDIF AND THE NUMBER OF IONOGRAM PTS USED IN DEFINING THE ERRO
C*****ERROR FUNCTION E. IN SUBROUTINE FUNCT.....
IF(PRNTSW)119,121,119
119 CONTINUE
PRINT 12, DT
C*****DT IS THE TOLERANCE OF DERIV OF GROUP PATH WRT BETA (KM/RAD)
C*****FOR USE IN FSTDIF ROUTINE WHEN IT COMPUTES THE MIN GROUP PATH
12 FORMAT(1,.54H1TOLERANCE OF DERIV OF GROUP PATH WRT BETA (KM/RAD) =
$ ,F5.3//)
C*****NPTS IS THE NUMBER OF POINTS SCALED FROM LEADING EDGE OF B S IONOGRAM
C*****FOR USE IN EVALUATING THE SUM SQUARED ERROR FCN
PRINT 13,NPTS
121 CONTINUE
13 FORMAT(1, 61H NUMBER OF SCALED IONOGRAM POINTS TO BE USED IN ERROR
$ FCN = ,I2)
IF(ICK -1)130,125,130
125 READ 14,(FBSMES(I),PBSMES(I),I=1:NPTS)
C*****HERE THE LEADING EDGE POINTS ARE READ IN
16 FORMAT (2F10.5)
GO TO 150
130 DO 145 IND=2,NPTS
FBSMES(IND-1)=FBSMES(IND)
145 PBSMES(IND-1)=PBSMES(IND)
READ 14,FBSMES(NPTS),PBSMES(NPTS)
150 CONTINUE
IF (PRNTSW)151,201,151
151 CONTINUE
PRINT 17

```

```

17  FORMAT(5JH MEASURED POINT ON BACKSCATTER IONOGRAM LEADING EDGE ,
$/.9X,14HFREQUENCY (MHZ) ,AX,6X,15HGROUP PATH(KM) )
PRINT 19,(FBSMES(I),PBSMES(I),I=1,NPTS)
19  FORMAT(/,11X,F8.3,19X,F8.3./)
PRINT 20,X(1),X(2),X(3),EST,EPS,LIMIT
20  FORMAT(   26H STARTING VALUE RB (KM) = ,F8.4,8X,
$25H STARTING VALUE RM(KM) = ,F8.4,8X,
$27H STARTING VALUE FC (MHZ) = ,F8.6,/,
$37H ESTIMATE OF MIN SUM SQUARED ERROR = ,F10.5,/,
$27H EXPECTED ABSOLUTE ERROR = ,F10.8,/,
$32H MAXIMUM NUMBER OF ITERATIONS = ,I4///)
N=3
CALL FUNCT(N,X,VAL,G)
PRINT 21,VAL,G
21  FORMAT(3JH INITIAL SUM SQUARED ERROR (E) = , E12.5,/,
$9H DEDRB = ,E12.5,5X,
$9H DEDRM = ,E12.5,5X,
$9H DEDFC = ,E12.5,/)
201 CONTINUE
N=3
OLDMIN=99999.
*****THIS BUSINESS ABT OLDMIN HAS TO DO WITH NUMERICAL ERROR PROB IN FSTDF SUB
*****SEE STATEMENT 2600 TO SEE WHAT I AM TALKING ABOUT
*****FMFP IS THE NONLINEAR MINIMIZATION ROUTINE FOUND IN IBM SCIENTIFIC SUBR
*****SUBRCUTINE PACKAGE. IT INTERNALLY CALLS FUNCT TO PERFORM SUCCESSIVE
*****EVALUATIONS OF THE SUM SQUARED ERROR FUNCTION AND ITS GRADIENT
22  CALL FMFP(N,X,FMIN,G,EST,EPS,LIMIT,IER,H)
*****IF NUMERICAL ERRORS SUCH AS SQRT (NEG NUMBER), LOG(LESS THAN 0), OR
*****ACOS(GREATER THAN 1) WERE FLAGGED IN THE EVALUATION OF FUNCT, N IS
*****NEGATED AND SO WE TEST FOR THIS ERROR CONDITION UPON EXIT FROM FMFP
  IF(N)25,27,27
25  PRINT 26,KT,EST
26  FORMAT(//30H NUMERICAL ERRORS ON TRY NR = ,I2,16H WITH EST MIN =
$= ,F7.5,///)
  KT=KT+1
*****SET N BACK TO +3
N=N
CALL FUNCT(N,X,FMIN,G)
*****EVALUATE FMIN ON BASIS OF PARTIALLY ITERATED PARAMETERS JUST BEFORE NUMERI
*****NUMERICAL PROBLEMS WERE ENCOUNTERED
  IF(OLDMIN-FMIN)2610,2610,2600
2600 SOLN1=X(1)
SOLN2=X(2)
SOLN3=X(3)
SVMIN=FMIN
GSV1=G(1)
GSV2=G(2)
GSV3=G(3)
OLDMIN=FMIN
2610 CONTINUE
*****IF THIS IS 7TH TRY GIVE UP ENTIRLY
  IF(KT-7)260,270,270
*****IF NUMERICAL ERRORS, ALTER EST, WHICH WILL DECREASE THE STEP SIZE AND TRY
*****TRY AGAIN. FIRST GO BACK TO ORIGHINAL STARTING SOLUTION
260  IF(FMIN-EST)262,262,261
*****IF OUR ESTIMATE WAS TOO SMALL INCREASE IT
261  EST=EST+10.
  GO TO 263

```

C\*\*\*\*\*IF OUR ESTIMATE WAS TOO LARGE DECREASE IT  
262 EST=EST/10.  
263 CONTINUE  
X(1)=XQV1  
X(2)=XSV2  
X(3)=XQV3  
C\*\*\*\*\*NOW GO BACK TO 22 AND TRY AGAIN  
GO TO 22  
270 PRINT 271  
271 FORMAT(//,.57H WILL GIVE UP TRYING TO INVERT THIS DATA AFTER 7 ATTEMPTS,PRINT 275  
275 FORMAT(100(1HS),//,106H WILL USE LAST VALUES OF ITERATED PARAMETERS  
\$ BEFORE NUMERICAL PROBLEM OCCURRED--NOTE FMFP DID NOT CONVERGE,/  
\$,100(1HS),//)  
X(1)=SOLN1  
X(2)=SOLN2  
X(3)=SOLN3  
FMIN=SVMIN  
G(1)=GSV1  
G(2)=GSV2  
G(3)=GSV3  
GO TO 38  
27 CONTINUE  
C  
C\*\*\*\*IER=0, A VALID MINIMUM WITHIN THE SPECIFIED TOLERANCE (EPS) WAS FOUND BY FMFP  
C\*\*\*\*IER=1, A MINIMUM WAS NOT FOUND IN THE SPECIFIED (LIMIT) NUMBER OF ITERATIONS  
C\*\*\*\*IER=1, IMPLIES ERROR IN GRADIENT CALCULATION  
C\*\*\*\*IER=2, LINEAR SEARCH CANNOT FIND MINIMUM  
C  
IF(PRNTSW)301,401,301  
301 CONTINUE  
IGOTO=IER+2  
GO TO(30,32,34,36),IGOTO  
32 PRINT 33  
33 FORMAT(//,.60H VALID MINIMUM FOUND BY FMFP WITHIN SPECIFIED TOLERANCE EPS  
\$ SINCE EPS )  
GO TO 38  
30 PRINT 33  
31 FORMAT(//,.35H ERROR IN FMFP GRADIENT CALCULATION )  
GO TO 38  
34 PRINT 35,LIMIT  
35 FORMAT(//,.86H ERR FCN COULD NOT BE MINIMIZED WITHIN THE SPECIFIED  
\$ NR (LIMIT) OF ITERATIONS ! LIMIT = .15)  
GO TO 38  
36 PRINT 37  
37 FORMAT(//,.45H LINEAR SEARCH IN FMFP COULD NOT FIND MINIMUM)  
38 CONTINUE  
C\*\*\*\*\*PRINT INVERTED LAYER PARAMETERS AS WELL AS MINIMUM VALUE OF SUM-SQUARED  
C\*\*\*\*\*ERROR FUNCTION  
PRINT 40,X,FMIN ,G  
40 FORMAT(//,.29H ITERATED VALUE OF RB (KM) = ,F6.2, 5X,  
\$29H ITERATED VALUE OF RM (KM) = ,F6.2, 5X,  
\$30H ITERATED VALUE OF FC (KHZ) = ,F8.4,/)  
\$25H MIN SUM SQUARED ERROR = ,F10.5,/

\$9H DEDRB = ,E12.5,5X,9H DEDRM = ,E12.5,5X,9H DEDFC = ,E12.5)  
PRINT 51

```
50 FORMAT(//104H RANGE AND ELEVATION ANGLES CORRESPONDING TO THE NPTS &
$ BACKSCATTER LEADING EDGE POINTS USED IN INVERSION //)
60 PRINT71,(I,FBSMES(I),RAN(I),BTA(I),I=1,NPTS)
70 FORMAT(3H F(,I2,4H) = ,F7.4,4H MHZ,5X,23HMIN GROUP RANGE (KM) = ,
$F9.3,5X,30HMIN GROUP ELEV ANGLE (DEG) = ,F6.3)
401 CONTINUE
C****HERE WE SAVE THE RESULTS OF THE PRESENT NPTS INVERSION
RBB(JARRAY)=X(1)
RMM(JARRAY)=X(2)
FCC(JARRAY)=X(3)
NMIDL=NPTS/2+1
FMID(JARRAY)=FBSMES(NMIDL)
RANMID(JARRAY)=RAN(NMIDL)
GPPTHMD(JARRAY)=GPCMID
JARRAY=JARRAY+1
100 CONTINUE
EST=ESTSVE
101 CONTINUE
C****PRINT OUT SUMMARY OF THE INVERTED BACKSCATTER IONOGRAM POINTS
PRINT 700,NUSED,NPTS
700 FORMAT(1H1,/,100(1H*),/,5NH SUMMARY OF THE BACKSCATTER LEADING EDG
SGE INVERSION,/,1X,I2,8H SETS OF,I2,4H OVERLAPPING SETS WERE SUCCE
SSIVELY INVERTED,///)
PRINT 710
710 FORMAT(84H      RB (KM)      RM(KM)      FC (MHZ)      FREQ (MHZ)      RANGE (KM)
$ (KM)      MIN GROUP PATH (KM)      /)
PRINT 720,(RBB(J),RMM(J),FCC(J),FMID(J),RANMID(J),
SGPTHMD(J),J=1,NUSED)
720 FORMAT(2X,F9.3,1X,F10.3,F10.3,3X,F10.3,4X,F10.3,9X,F10.3)
RETURN
END
```

```
H NAME A7
H EQUIP=CARDRE,PRINTE,CARDPUI
H SUBROUTINE DCAL(FC,RB,RM,FW,GP,D,GPTOL)
R0=637 .
SINBET=(RB+RB-R0*R0-GP*GP/4.)/(R0*GP)
BETA=ASINF(SINRET)
BETA=0.0001
20 COSBET=COSF(BETA)
SINBET=SINF(BETA)
F=FW/FC
FF=F*F
YM=RM-RB
RB*YM2=RB*RB/(YM*YM)
A=FF=1.+RB*YM2
B=-2.*AM*RB*YM2
C=RB*YM2*RM*RM-FF*R0*R0*COSRET*COSBET
U=B-4.*A+C
GAM=ACOSF((R0/RB)*COSBET)
SINGAM=SINF(GAM)
COSGAM=COSF(GAM)
COTGAM=COSGAM/SINGAM
SQA=SQRTF(A)
V=2.*A*RB+B+2.*RB*F*SQA*SINGAM
GPC=2.*(-FF/A)*RB*SINGAM-2.*R0*SINBET-(B*F/(2.*A*SQA))*LOGF
1(U/(V*V))
IF (ABSF(GPC-GP)-GPTOL) 100,100,50
50 DGPDB=2.*(-FF/A+B*FF/(A*V))+R0*SINBET*COTGAM
1=2.*(-2.*R*F*FF*R0*SINBET)/(SQA*U)*R0*COSBET
PRINT 40,FW,GP,BETA,GPC,DGPDB,FC,RB,RM
40 FORMAT(6X,8F10.2)
BETA=BETA+(GP-GPC)/DGPDB
SINBET=SINF(BETA)
GO TO 20
100 SQC=SQRTF(C)
W=2.*SQC*F*RB*SINGAM+2.*C*A*RB
D=(GAM-BETA)-(F*R0*COSBET/(2.*SQC))*LOGF(U*RB*RB/(W*W))
D=2.*R0*D
RETURN
END
```

H NAME AR  
H EQUIP=CARDRE,PRINTE,CARDPU:  
FUNCTION SQROO(ARG)

C  
\*\*\*\*\*SUBROUTINE SQROO CHECKS TO SEE IF WE ARE TRYING TO TAKE THE SQRT OF A NEG  
\*\*\*\*\*NUMBER. IF WE SO THEN AN ERROR CONDX IS FLAGGED AND THE ARG IS PRINTED OUT  
\*\*\*\*\*WITH A MESSAGE... THE FLAGGING IS DONE BY SETTING SQROO = 9999.  
\*\*\*\*\*WITHOUT SUCH A SUBROUTINE THE G20 WILL SIGN YOU OFF IN A HURRY  
\*\*\*\*\*KEEPING US FROM GETTING TO ANY GOOD DATA

C  
10 IF(ARG)<0,20,20  
CONTINUE  
PRINT 15, ARG  
15 FORMAT(29H SQRT ENTERED WITH NEG ARG = ,E13.7)  
SQROO=9999.  
GO TO 30  
20 SQROO=SQRT(ARG)  
30 RETURN  
END

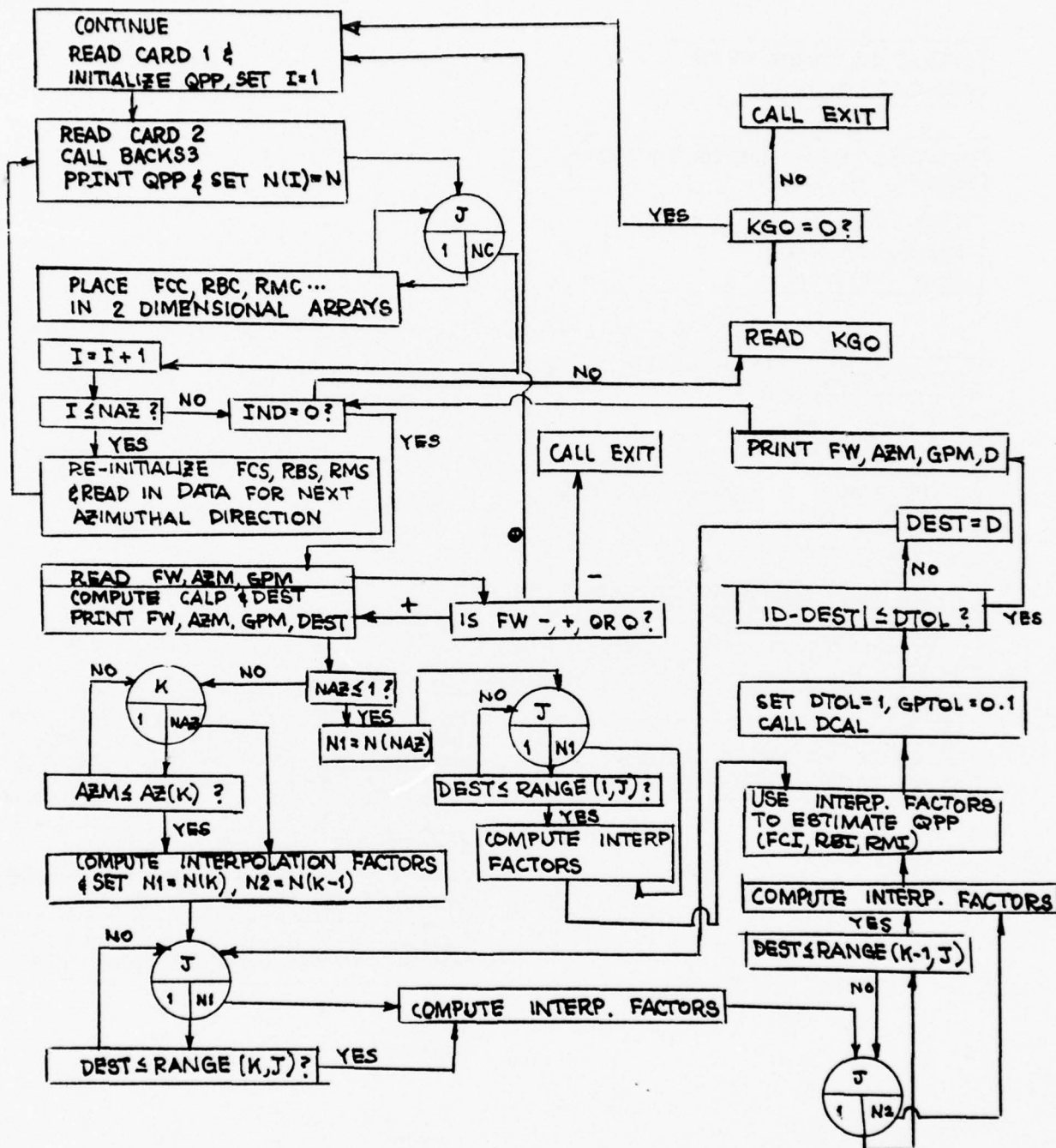


Figure A.3.1. Flow chart for main program.

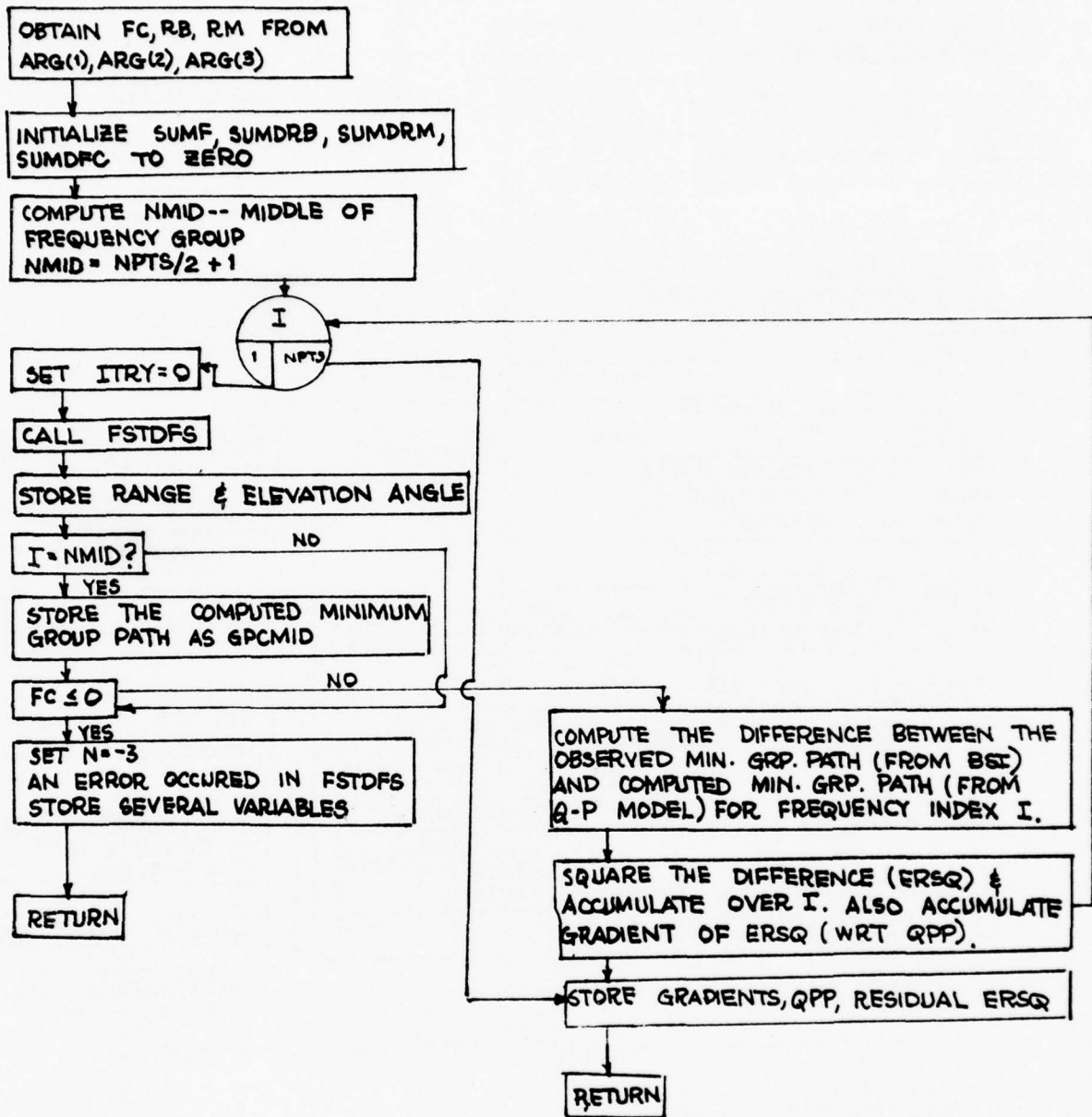


Figure A.3.2. Flow chart for subroutine FUNCT.

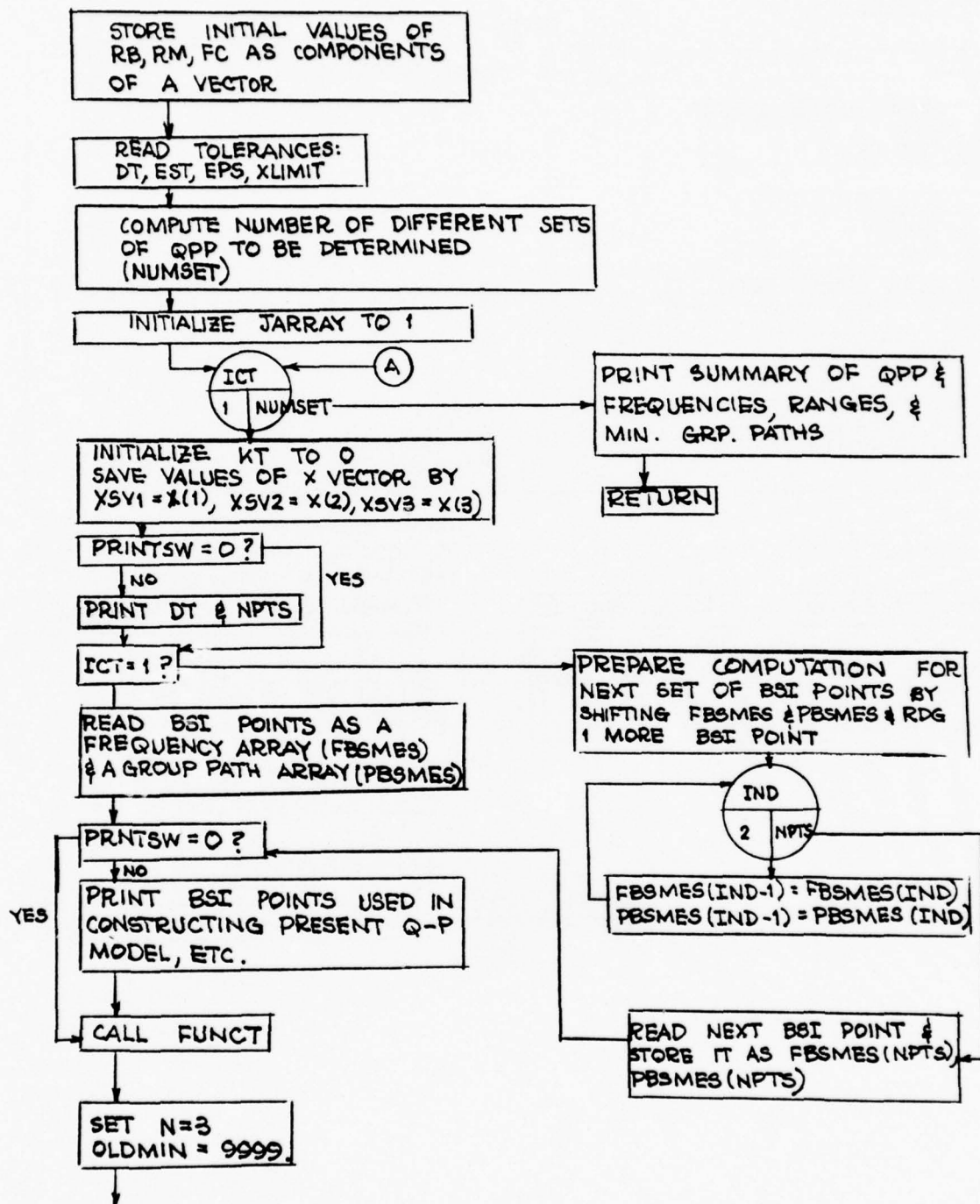


Figure A.3.3.a. Flow chart for subroutine BACKS3  
(continued on next figure).

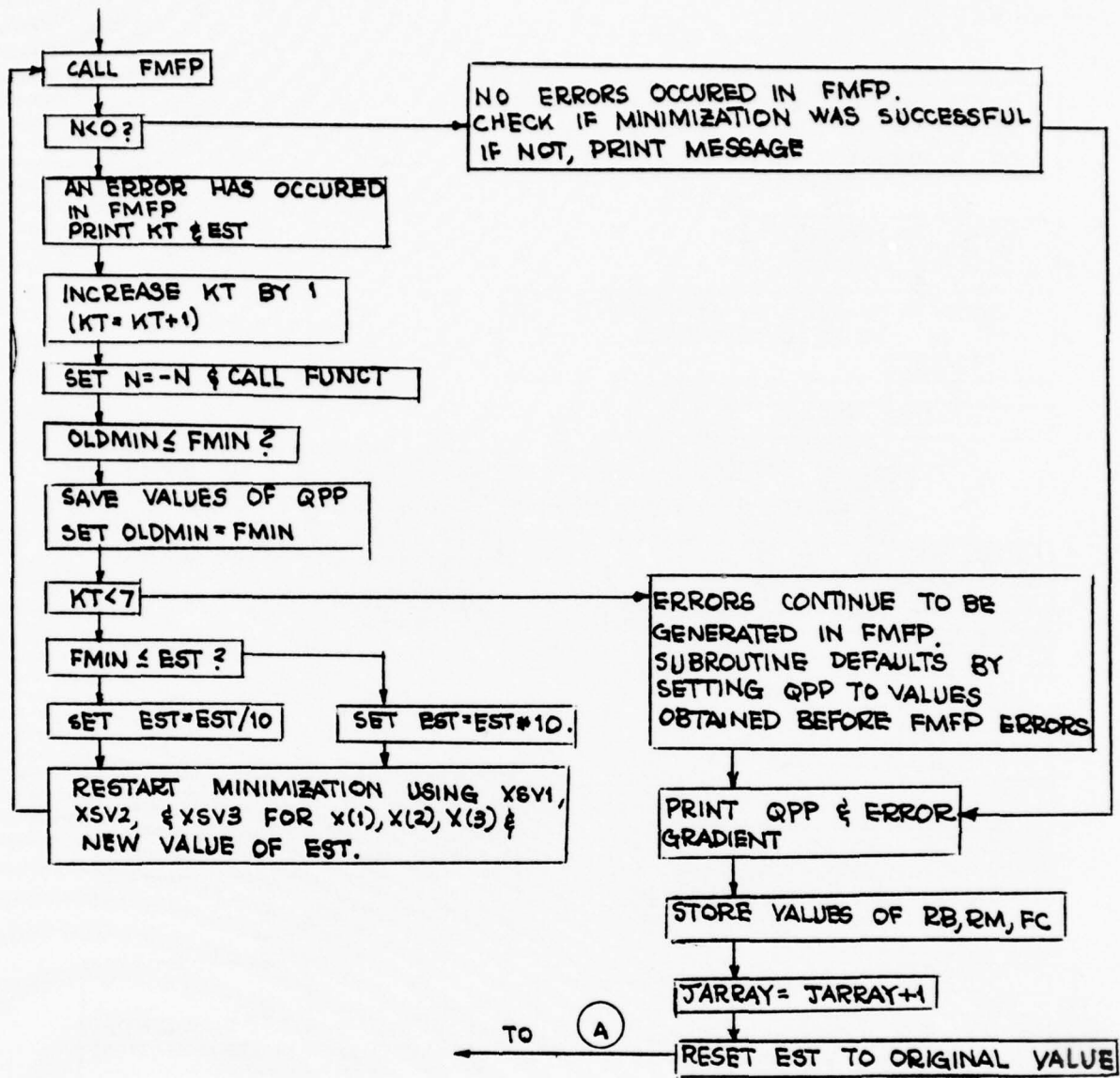


Figure A.3.3.b. Flow chart for subroutine BACKS  
continuation of Figure A.3.3.a).

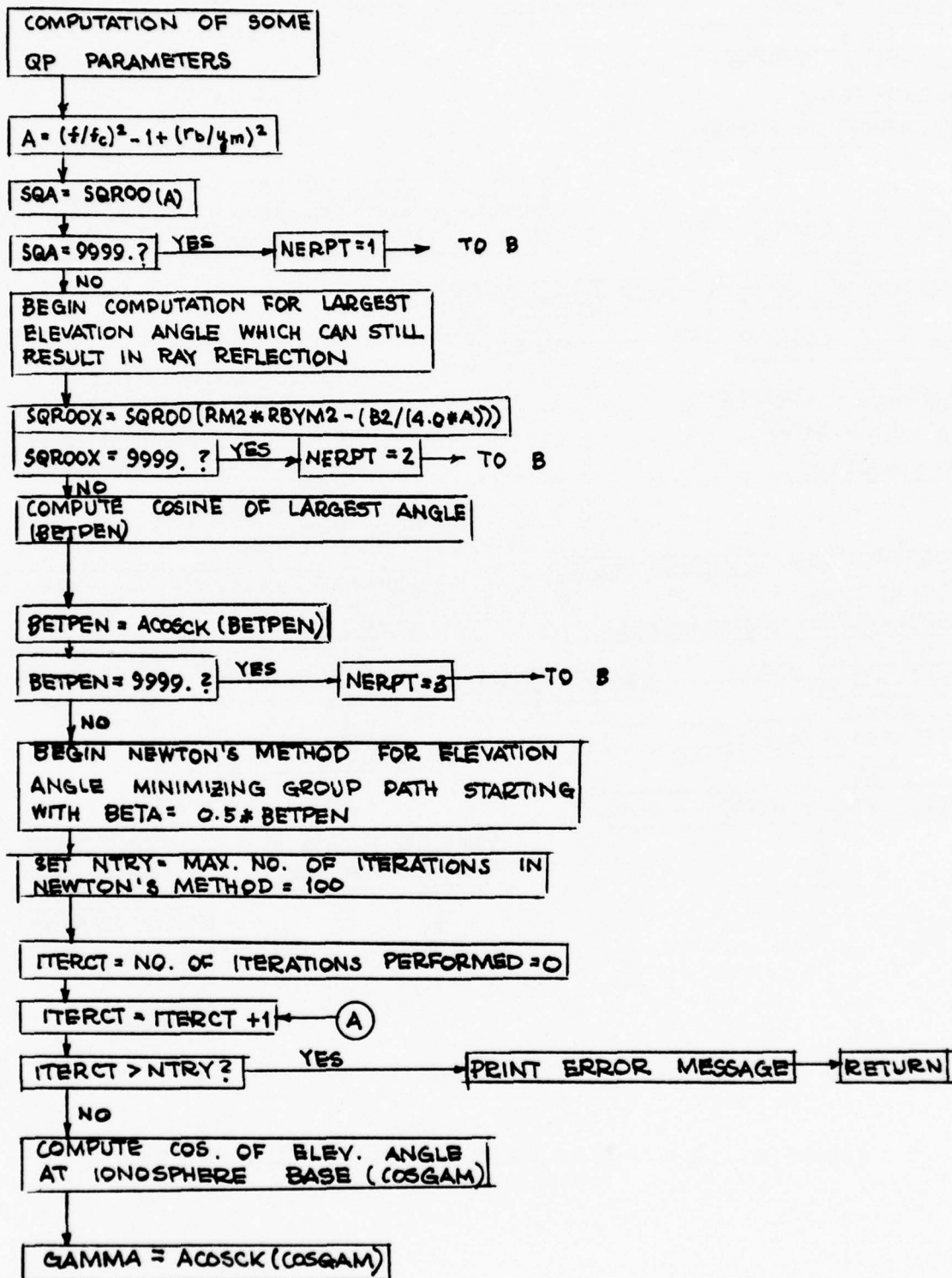


Figure A.3.4.a. Flow chart for subroutine FSTDFS  
(continued on next figure).

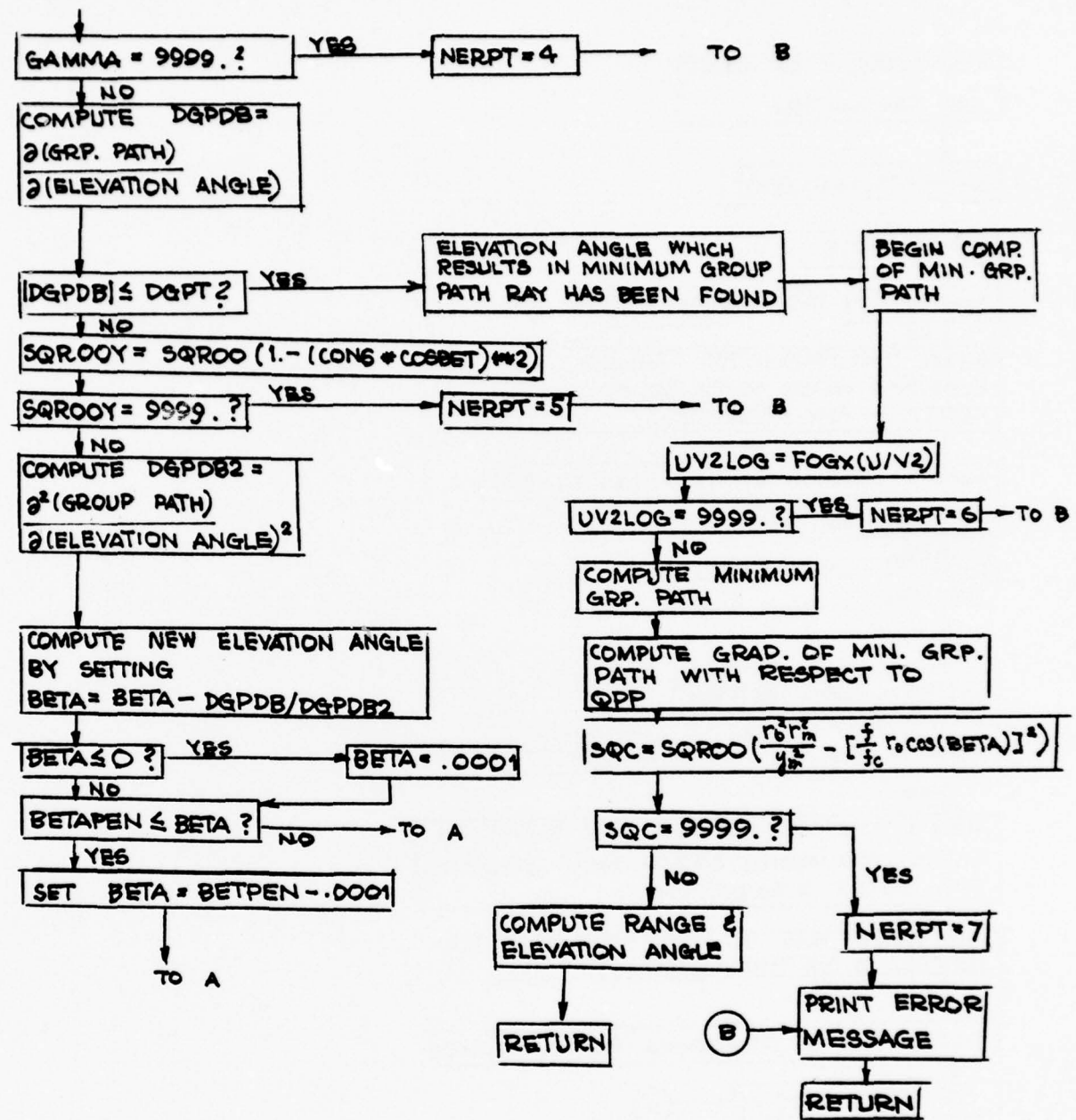


Figure A.3.4.b. Flow chart for subroutine FSTDFS  
(continuation of Figure A.3.4.a).

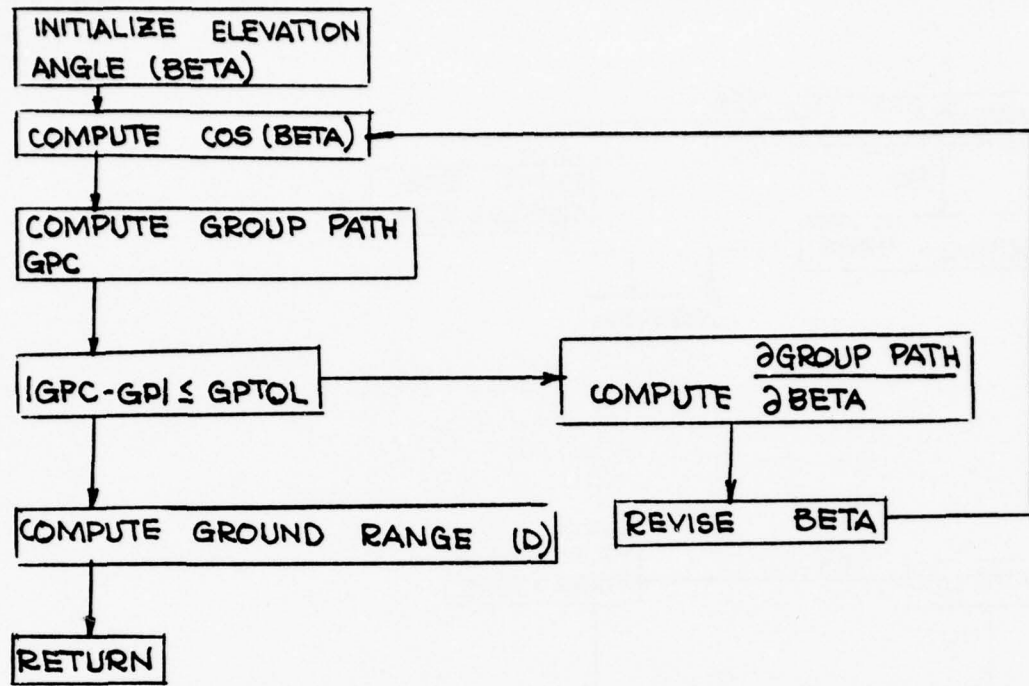


Figure A.3.5. Flow chart for subroutine DCAL.

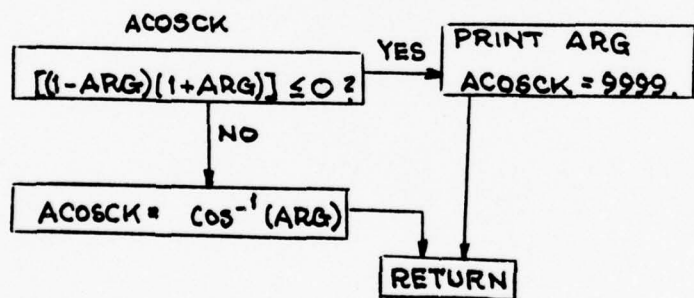
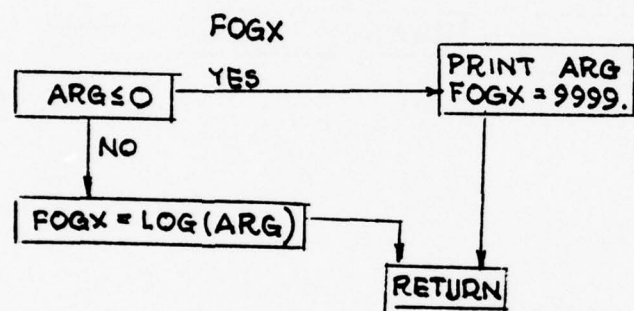
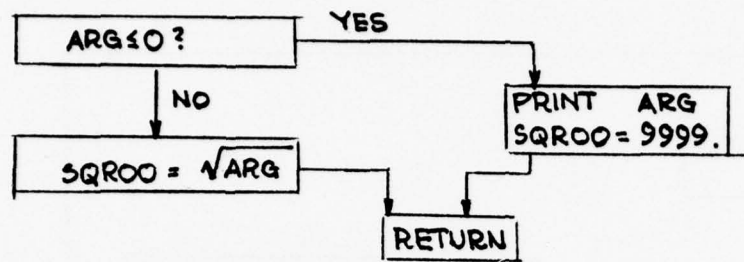


Figure A.3.6. Flow chart for special functions (square root, log, and  $\cos^{-1}$ ).

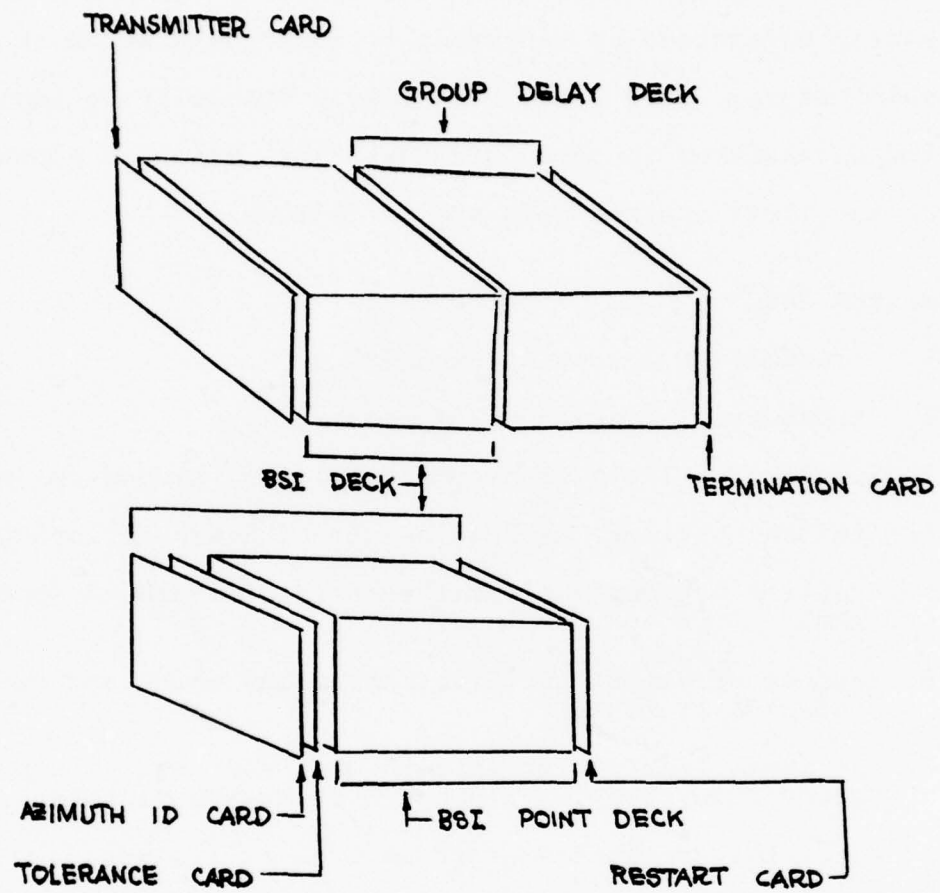


Figure A.3.7. Sequence of data cards.

The program formats are as follows

INPUT:

The input format shown in Figure A.3.7 can, perhaps, be more easily understood by referring to the flow diagram of the main program. The first card serves primarily to identify the backscatter ionogram sounder. The variables appearing on the first control card are as follows.

TRANSMITTER CARD:

1. transmitter latitude (degrees)
2. transmitter longitude (degrees)
3. initial estimate of overhead critical frequency (MHz)
4. initial estimate of base height of overhead ionosphere (km)
5. initial estimate of semithickness of overhead ionosphere (km)
6. number of azimuthal directions along which BSI are obtained (integer)
7. an index (ind) which is zero when the user is supplying group delay deck, and nonzero otherwise (integer)

The format of the transmitter card is 5F10.2, I1, 9X, I1 respectively.

The next set of cards comprise the BSI deck. The first card in this set is the azimuth identification card which contains

AZIMUTH ID CARD:

1. azimuth along which the following set of backscatter ionogram points have been obtained. (degrees)
2. the total number of backscatter ionogram points along the azimuth which will be read in. (integer)
3. the number of consecutive BSI points (less than or equal to the total number of BSI points) which will be considered simultaneously in obtaining a single net of QPP. (integer)

The format of the azimuth card is F10.2, I2, 8X, I2

TOLERANCE CARD:

1. tolerance of the deviation of the group path with respect to elevation angle (typically .05 km/rad.)
2. final step size control for minimization (typically .01)
3. desired final value of error in fitting QPP to measured BSI (typically .05 km/rad.)
4. maximum number of iterations which may be performed in fitting QPP to measured BSI (floating point)

The format of this card is 4F10.5.

BSI POINT DECK (SINGLE AZIMUTH)

There is one card for each measured point on the BSI along the given azimuthal direction. Each card contains:

1. frequency of BSI point (MHz)
2. group path of BSI point (km)

The format is 2F10.0.

USING THE RESTART CARD:

The restart card (format I10) is used only if IND $\neq$ 0. When the user sets IND $\neq$ 0 (referring to the main program flow chart) the program will not use the QPP to compute the ground range corresponding to a given group path. In fact, the program will go no further than the computation of QPP as performed by subroutine BACKS3. The only information on the restart card is the integer KGO. Setting KGO to zero (or, equivalently, using a blank card) tells the program to read in another batch of cards consisting of

1. TRANSMITTER CARD
2. AZIMUTH ID CARD
3. TOLERANCE CARD
4. BSI POINT DECK

and, if the new transmitter card has IND=0

5. GROUP DELAY DECK
6. TERMINATION CARD

Setting KGO < 0 will terminate the execution by telling the program that there is no more data to be processed.

#### NOT USING THE RESTART CARD:

The restart card should not be used when IND=0. Also, even when IND $\neq$ 0 the restart card should not be used between BSI decks corresponding to the same transmitter card, but different azimuthal angles (multi-azimuth case). In this case, the last card of the BSI point deck is followed immediately by the:

1. AZIMUTH ID CARD
2. TOLERANCE CARD
3. BST POINT DECK

corresponding to the next azimuthal direction, with the data from the first transmitter card being used for all subsequent azimuthal angles. After the BSI point deck corresponding to the last azimuthal angle, the restart card is used to signify end of data (KGO < 0), or a new transmitter card (KGO = 0).

#### GROUP DELAY DECK:

The group delay deck provides the program with a specific value of group path from which to compute the ground range.

There is one card for each group path measurement to be used in this manner. Each card in the group delay deck contains:

GROUP DELAY DECK CARD:

1. frequency at which measurement is made (MHz)
2. azimuthal angle at which measurement is made (degrees)
3. measured value of group path (km)

The format is 3F10.0.

TERMINATION CARD:

After the last group delay deck card there must be a termination card, containing the parameter FW in F10.0 format. FW < 0 signifies end of data and terminates the program. FW=0 tells the program that more data will be read in, starting from the transmitter card and continuing in order to either a restart card or a new termination card.

\*\*\*\*\*  
 SUMMARY OF THE BACKSCATTER LEADING FDF INVERSION  
 3 SETS OF 3 OVERLAPPING SETS WERE SUCCESSIVELY INVERTED

RB (KM)	RM(KM)	FC (MHZ)	FREQ (MHZ)	RANGE (KM)	MIN GROUP PATH (KM)
6618.919	6710.406	9.193	14.000	1061.038	1302.247
6632.230	6690.685	8.558	17.000	1449.758	1644.938
6601.425	6690.132	8.713	20.000	1877.891	A 2046.869
9.1927	6618.918	6710.4n62	1061.0383	1302.2466	
8.5580	6632.2304	6690.6846	1449.7578	1644.9381	B
8.7130	6601.4253	6690.1316	1877.8905	2046.8686	
		16.00	52.00	1700.00	1676.31 C
		8.64	6615.93	6690.39	
14.00	1700.00	n.00	3730.98	-12739.52	8.64 6615.93 6690.39
14.00	1700.00	n.16	2271.71	-6004.27	8.64 6615.93 6690.39
14.00	1700.00	n.25	1829.23	-3462.60	E 8.64 6615.93 6690.39
14.00	1700.00	n.29	1714.51	-2700.21	8.64 6615.93 6690.39
14.00	1700.00	n.30	1700.28	-2597.05	8.64 6615.93 6690.39
		16.00	52.00	1700.00	1676.31 1557.09 F
		8.60	6624.51	6690.55	
14.00	1700.00	n.00	3780.11	-12739.53	8.60 6624.51 6690.55
14.00	1700.00	n.16	2286.07	-6003.18	8.60 6624.51 6690.55
14.00	1700.00	n.26	1832.05	-3471.20	E 8.60 6624.51 6690.55
14.00	1700.00	n.30	1714.65	-2715.10	8.60 6624.51 6690.55
14.00	1700.00	n.30	1700.27	-2613.88	8.60 6624.51 6690.55
		16.00	52.00	1700.00	1557.09 1552.33
		8.60	6624.85	6690.55	D
14.00	1700.00	n.00	3782.03	-12739.53	8.60 6624.85 6690.55
14.00	1700.00	n.16	2286.62	-6003.28	8.60 6624.85 6690.55
14.00	1700.00	n.26	1832.14	-3471.84	E 8.60 6624.85 6690.55
14.00	1700.00	n.30	1714.65	-2716.14	8.60 6624.85 6690.55
14.00	1700.00	n.30	1700.27	-2615.06	8.60 6624.85 6690.55
		16.00	52.00	1700.00	1552.33 1552.15 F
		16.00	52.00	1700.00	G

## OUTPUT FORMAT:

Referring to the sample output which resulted from a single azimuth measurement, subroutine BACKS3 causes block A to be printed. Each row of block A contains RB, RM, FC, frequency, range, and minimum group path. Block B contains the same information as block A (except for frequency) and shows that the variables have been transferred from BACKS3 to the main program. Block C contains frequency, azimuth, measured group path and the first approximation to ground range in the subsequent attempt to compute the ground range from a given value of group path. Block D contains the interpolated values of QPP at the reflection point. Block E is printed out in subroutine DCAL and represents the progress of subroutine DCAL in homing a ray through the QP ionosphere model based upon group path. Each row of block E contains frequency, measured group path, initial elevation angle ( $\beta$ ), computed group path, the derivative of group path with respect to  $\beta$ , and the three QPP describing the ionosphere. In the last row of block E, it can be seen that the computed and measured group paths are very close, so DCAL returns to the main program. Upon returning to the main program block F is printed and contains frequency, azimuth, measured group path, estimated ground range, and ground range based upon the homed in value of the initial ray elevation angle. Since these two ground ranges are so different a new interpolation procedure is initiated in the main program to compute the values of QPP at the reflection point of the homed in ray. This interpolation is summarized in block D, and comparing the first block D with

the second block D, we can see that the QPP at the reflection point are indeed different when computed for the homed in ray. This leads to an iterative process which alternates between subroutine DCAL, and the recomputation of the interpolated QPP. The final block F shows, however that the most recent computed ground range, and the ground range from the previous iteration are very close. Thus, block G is printed in the main program and contains the frequency, azimuth, group path and final solution for the ground range.

## APPENDIX 4

A Method for Inverting Oblique Sounding Data  
in the Ionosphere

by S. I. Chuang and K. C. Yeh

This paper has been submitted to Radio Science.

A METHOD FOR INVERTING OBLIQUE  
SOUNDING DATA IN THE IONOSPHERE

S. L. Chuang and K. C. Yeh \*  
Department of Electrical Engineering  
National Taiwan University

We have developed in this paper a method of inverting backscatter leading edge ionograms and fixed distance oblique ionograms to obtain ionization profiles. The problem of ionogram inversion is first formulated in such a way that the Backus-Gilbert technique can be applied. This inversion technique starts by assuming an initial profile based on available knowledge. Oblique group paths are computed by using this initial profile and are compared with the experimental data. The discrepancy in group path is used as a basis for improving the profile and thus an iterative procedure is developed. This iteration is continued until an optimum solution is found. As is well-known, when ionograms are given at discrete frequencies there may exist an infinite number of profiles that will yield the observed group path data. Among this infinite number of solutions there is an optimum one in the sense that its fractional departure from the initially assumed profile is a minimum in terms of value at boundaries and in terms of the profile curvature. The method is then applied to the special vertical incidence case and reasonably fast convergence is obtained. This success demonstrates the promise of this method in inverting oblique sounding data.

\* Permanent address: Department of Electrical Engineering, University of Illinois.

## 1. INTRODUCTION

In ionospheric sounding one usually measures the wave parameters, such as transit time, frequency shift, polarization, power returned, etc. One wishes then to make use of these measured wave parameters to deduce the physical parameters of the ionosphere, such as electron density, temperature, motion, etc. In order to deduce these physical parameters one must make use of a theory, known as the inversion theory, to relate these desired physical parameters to wave parameters. Sometimes the inversion is quite simple; sometimes the inversion can be quite complex. A case in point is the inversion of vertical ionograms, e.g., [Budden, 1961, p. 161], where the virtual height  $h'(f)$  as a function of frequency  $f$  is measured and the true ionization profile  $N(h)$  is desired. From wave propagation studies one realizes that  $h'$  is a nonlinear functional of  $N$  and as such it is in general very difficult to solve. Fortunately for the case of vertical ionograms with magnetoionic effects ignored, the integral can be put in the form of a convolution type which can then be solved, for example, by Laplace transform, provided that  $N(h)$  increases monotonically with height. Now if one wishes to sound obliquely in order to obtain the profile some distance away from the local vertical, the integral is no longer of the convolution type. In this case, since the group delay is a nonlinear functional of  $N(h)$ , the inversion becomes very difficult. Current techniques are largely numerical and are designed to obtain a model profile that will yield data approximating the measured data.

However, ionospheric investigations have been carried out for several decades. The accumulated knowledge enables us to make a zeroth-order guess about the profile. If this zeroth-order profile does not depart appreciably from the true profile, it is possible to reformulate the problem by a linearization procedure. This reformulated problem is much simpler to deal with

because it is now linear. Many mathematical techniques applicable to linear problems can be used in order to arrive at a solution. Our approach is similar to that used in geophysics for inverting seismic data [Backus and Gilbert, 1967].

## 2. FORMULATION

For simplicity we will ignore the magnetoionic effects completely. The ionosphere is assumed to be spherically stratified so that the Bouguer's rule applies at any point along the ray, i.e.,

$$r_0 \cos \phi_0 = r n \cos \phi = r_t n_t = \text{constant} \quad (1)$$

where  $r$  is the geocentric distance of a point along the ray,  $n = n(r)$  is the refractive index and  $\phi = \phi(r)$  is the elevation angle of the ray. The earth radius is  $r_0$  at which  $\phi_0 = \phi(r_0)$ . The ray is reflected with a geocentric distance  $r_t$  at which  $n_t = n(r_t)$  and  $\phi(r_t) = 0$ . The group path of an ionospherically reflected signal is

$$P = 2 \int_{r_0}^{r_b} ds + 2 \int_{r_b}^{r_t} ds/n . \quad (2)$$

This integral is integrated along the ray from  $r_0$  to the bottom of the ionosphere at  $r_b$  in free space and then from  $r_b$  to  $r_t$  in the ionosphere. In the ionosphere the refractive index is related to the electron density profile  $N(r)$  through

$$n^2 = 1 - kN/f^2 \quad (3)$$

where  $f$  is the radio frequency and  $k = e^2/4\pi^2 m \epsilon_0$  has a numerical value 80.6 in S.I. units. It is easily seen from (2) that  $P$  is a nonlinear functional of  $N$ . We are not aware of any analytic method that can be used to solve for  $N$ .

Therefore, we will adopt a perturbation scheme to linearize the problem. Our approach is similar to that used in inverting teleseismic ray data [Johnson and Gilbert, 1972].

Perturbations in  $P$  can come from two sources: perturbations in  $n$  and perturbations in  $\phi_0$ . Taking the variation in (2) and linearizing, we obtain

$$\delta P = 2 \int_{r_b}^{r_t} \frac{-\delta n}{n^2} ds + \frac{\partial P}{\partial \phi_0} \delta \phi_0 . \quad (4)$$

In practice two kinds of oblique sounding data can be obtained: backscatter leading edge and oblique ionogram. For a thorough review on the nature of these data, the reader is referred to Davies [1965]. We discuss both of these cases for our purpose in the following.

(i) Backscatter leading edge.

The backscattered leading edge has a minimum time delay. In this case  $\partial P / \partial \phi_0 = 0$  and the variation in group path is caused entirely by variations in the refractive index. The variation in  $n$  can be related to the variation in  $N$  by using (3). Substituting (3) and (1) in (4) yields

$$\delta P = \int_{r_b}^{r_t} K'_1 x dr \quad (5)$$

where

$$x = \delta N/N \quad (6)$$

and

$$K'_1 = krN/f^2(1 - kN/f^2)[(1 - kN/f^2)r^2 - r_0^2 \cos^2 \phi_0]^{1/2} . \quad (7)$$

The kernel  $K'_1$  can be computed from the model ionosphere and is therefore known. We note in (5) that  $\delta P$  is a linear functional of  $\delta N$ .

## (ii) Oblique ionogram

The oblique ionogram gives the group path of ionospherically reflected signals as a function of frequency for a fixed ground distance D. The ground distance is

$$D = 2r_0^2 \cos \phi_0 \left[ \int_{r_0}^{r_b} \frac{dr}{r\sqrt{r^2 - r_0^2 \cos^2 \phi_0}} + \int_{r_b}^{r_t} \frac{dr}{r\sqrt{n^2 r^2 - r_0^2 \cos^2 \phi_0}} \right]. \quad (8)$$

As the ionization profile is varied by  $\delta N$ , the initial elevation angle of the ray must also be varied by  $\delta \phi_0$  in order to keep D fixed. Take the variation of (8) and set it to zero to produce

$$\delta \phi_0 = \left[ 2r_0^2 \cos \phi_0 \int_{r_b}^{r_b} \frac{-kr\delta N dr}{2n^2 f^2 r^2 (n^2 r^2 - r_0^2 \cos^2 \phi_0)^{1/2}} \right] \Bigg/ \frac{\partial D}{\partial \phi_0}. \quad (9)$$

Inserting (9) in (4), the variation in group path of an oblique ionogram is found to be

$$\delta P = \int_{r_b}^{r_t} K'_2 x dr \quad (10)$$

where the known kernel is

$$K'_2 = K'_1 \left[ 1 - \left( r_0^2 \cos \phi_0 / r^2 \right) (\partial P / \partial \phi_0) / (\partial D / \partial \phi_0) \right]. \quad (11)$$

Comparing (5) and (10), one notes that for both kinds of oblique data, the variation in group path is given by

$$\delta P(f) = \int_{r_b}^{r_t} K'(r, f, \phi_0) x(r) dr \quad (12)$$

where for backscatter leading edges  $K' = K'_1$ , and for oblique ionograms  $K' = K'_2$ .

The kernel  $K'$  is referred to as the Frechet kernel [Backus and Gilbert, 1967; Green, 1975] because  $\delta P$  is obtained by taking the Frechet differential of (2). Our objective is to obtain the optimum  $x$  in some sense. We do this by following the Backus-Gilbert approach in the following section.

### 3. OPTIMIZATION

Suppose the oblique sounding data have been measured experimentally at  $M$  frequencies  $f_i$ ,  $i = 1, 2, \dots, M$ . The corresponding group paths are  $P_{mi}$ ,  $i = 1, 2, \dots, M$ . For the purpose of obtaining the ionization profile  $N(r)$  that produces these experimental data, we make use of our knowledge based on past experience to construct a zeroth-order approximation to the true ionization profile. This approximate profile is then used to compute  $M$  group paths  $P_{ci}$ , for  $M$  frequencies  $f_i$ , and  $M$  initial elevation angles  $\phi_{oi}$ . The departure of the computed group path  $P_{ci}$  from the experimentally measured group path  $P_{mi}$  is  $y_i$ , i.e.,  $y_i = P_{ci} - P_{mi}$ . Then according to (12),

$$y_i(f_i) = \int_{r_b}^{r_p} K_i(r, f_i, \phi_{oi}) x(r) dr \quad i = 1, 2, \dots, M \quad (13)$$

where  $r_p$  is the peak height of the ionosphere. The Frechet kernel  $K_i$  is given by

$$K_i(r, f_i, \phi_{oi}) = \begin{cases} K'_1(r, f_i, \phi_{oi}) & r_b \leq r \leq r_{ti} \\ 0 & r_{ti} \leq r \end{cases}, \quad (14)$$

for backscatter leading edges, and, for oblique ionograms,

$$K_i(r, f_i, \phi_{oi}) = \begin{cases} K'_2(r, f_i, \phi_{oi}) & r_b \leq r \leq r_{ti} \\ 0 & r_{ti} \leq r \end{cases} \quad (15)$$

where  $r_{ti}$  is the geocentric distance of reflection for  $f_i$ . In later development  $K_1$  will be required to be square integrable. However, since both  $K_1'$  and  $K_2'$  have singularities at the point of reflection,  $K_i$  is obviously not square integrable. This difficulty can be remedied by integrating (13) by parts twice, as suggested by Johnson and Gilbert [1972], to produce

$$y_i = -H_i(r_b)x(r_b) - G_i(r_p)x'(r_p) + \int_{r_b}^{r_p} G_i(r)x''(r) dr \quad (16)$$

$$i = 1, 2, \dots, M$$

where

$$x'(r) = dx/dr$$

$$x''(r) = d^2x/dr^2$$

$$H_i(r) = \int_{r_p}^r K_i(r', f_i, \phi_{oi}) dr' \quad (17)$$

$$G_i(r) = \int_{r_b}^r H_i(r') dr' . \quad (17)$$

Now our original nonlinear inversion problem is reduced to the linear problem of (16) in which we have  $M$  data points to determine  $x''(r)$ . In general, the solution to (16) is nonunique. Among this infinite number of solutions is a particular one for which

$$\frac{1}{2} \left\{ x^2(r_b) + x'^2(r_p) + \int_{r_b}^{r_p} [x''(r)]^2 dr \right\} = \text{minimum} . \quad (18)$$

This solution, if it exists, is the optimum solution we seek. It is optimum in the sense that the constraint condition (18) is satisfied and that the errors in  $x(r_b)$  and  $x'(r_p)$  are minimized and the profile  $x(r)$  is very smooth since the square of its cumulative curvature over the interval  $[r_b, r_p]$  is minimized. Notice that we have chosen to deal with fractional departures of

electron density here as  $x$  is defined by (6). But it is possible to introduce any other reasonable weighting function on  $\delta N$  if so desired by modifying the definition of the Frechet kernel as done by Green [1975]. Such weighting may be desirable in cases where parts of data are known a priori more accurately than others, and hence deserve more weight.

The optimum solution can be found easily by introducing Lagrange multipliers  $v_i$ . Carrying out the process of minimization, the solutions are found to be

$$x''(r) = \sum_{i=1}^M v_i G_i(r) \quad (19a)$$

$$x'(r_p) = - \sum_{i=1}^M v_i G_i(r_p) \quad (19b)$$

$$x(r_b) = - \sum_{i=1}^M v_i H_i(r_b) . \quad (19c)$$

Insertion of (19) into (16) yields

$$y_i = \sum_{j=1}^M v_j \left[ H_i(r_b) H_j(r_b) + G_i(r_p) G_j(r_p) + \int_{r_b}^{r_p} G_i(r) G_j(r) dr \right] . \quad (20)$$

Equation (20) can be put in a very compact form if the following vector notations are used. Let the column vectors be

$$\vec{v} = \begin{bmatrix} v_1 \\ v_2 \\ \vdots \\ v_M \end{bmatrix} \quad \vec{y} = \begin{bmatrix} y_1 \\ y_2 \\ \vdots \\ y_M \end{bmatrix} \quad (21)$$

and the symmetric  $M \times M$  matrix  $A = [A_{ij}]$  have an  $ij$ th element

$$A_{ij} = H_i(r_b)H_j(r_b) + G_i(r_p)G_j(r_p) + \int_{r_b}^{r_p} G_i(r)G_j(r) dr . \quad (22)$$

Then (20) becomes simply

$$\vec{y} = A\vec{v} . \quad (23)$$

For independent data,  $\det A \neq 0$ , and (23) can be inverted to give  $\vec{v}$ . Knowing  $\vec{v}$ , (19a) reduces to

$$x''(r) = (A^{-1}\vec{y})\vec{G}(r) \quad (24)$$

where  $\vec{G}(r)$  is a column vector whose  $i$ th element is  $G_i(r)$ . Equation (24), together with the boundary conditions (19b) and (19c), enables us to compute  $x(r)$  by integrating (24) twice. Once  $x(r) = \delta N/N$  is determined, the desired correction  $\delta N$  to the zeroth-order model  $N(r)$  is known. Computations can then be started anew by using the new model,  $N(r) + \delta N(r)$ , to produce eventually a second correction. Thus an iteration procedure is established. By repeated iteration, a final optimum solution can be achieved. At each step we may check the value

$$x^2(r_b) + x'^2(r_p) + \int_{r_b}^{r_p} [x''(r)]^2 dr = \vec{v}^T A \vec{v} \quad (25)$$

When this value is less than a certain specified small value, the iteration procedure may be terminated. The final profile  $N(r)$  will be the desired optimum electron density profile for the set of data  $P_{mi}$ ,  $i = 1, 2, \dots, M$ .

#### 4. VERTICAL INCIDENCE

As mentioned earlier, the vertical ionogram can be inverted exactly if the ionization profile increases monotonically with height. However, for the sake of completeness, we will also work out our scheme for this particular

case. Since the vertical incidence case is easier to manage analytically, a numerical example will be given in the next section to illustrate the computational procedures involved.

For vertical incidence the initial elevation angle  $\phi_0$  is  $90^\circ$ . The once-integrated Frechet kernel  $H_i(r)$  no longer exists at  $r = r_{ti}$  since the singularity of  $K'_1$  at  $r_{ti}$  as given by (7) is now of higher order. Close attention must be paid in order not to allow singularities to get out of hand. This can be done by a slight modification. Taking the Frechet differential of (2) as before, except for the vertical incidence case,  $ds$  is replaced by  $dr$  and one obtains

$$y = \delta P = \int_{r_b}^{r_t} K(r)x(r) dr \quad (26)$$

with

$$x(r) = \delta n / (n + \delta n) \quad (27)$$

$$K(r) = -2/n . \quad (28)$$

Now (26) is identical in form to (13). An identical procedure can be followed by first integrating by parts twice and setting up the minimization process similar to that given in the last section to obtain  $x$ . After knowing  $x(r)$ , (27) and (3) can be used to find the perturbed ionization profile required through

$$\delta N(r) = (1 - kN/f^2)[1 - (1 - x)^{-2}]f^2/k . \quad (29)$$

If one wants, a new model  $N(r) + \delta N(r)$  can be used to replace the initial model  $N(r)$ , and the computations are repeated. Thus an iteration procedure is established as before. This iteration can be terminated when the error is smaller than some specified value.

## 5. AN EXAMPLE

For purposes of illustration, we shall assume a parabolic layer

$$N_p(z) = N_m [1 - (z - Y)^2/Y^2] \quad 0 < z < 2Y \quad (30)$$

as the true ionization profile. For simplicity the vertical coordinate  $z$  starts at the bottom of the ionosphere and the ionosphere has a semithickness  $Y$ . In this case the measured group path (equal to twice the group height) is

$$P_m = Y(f/f_c) \ln[(f_c + f)/(f_c - f)] \quad (31)$$

where  $f_c$  is the critical frequency.

Suppose as an initial guess of the profile we assume a linear profile

$$N_l(z) = az \quad 0 < z . \quad (32)$$

A signal of frequency  $f$  incident vertically is reflected at a height  $z_t = f^2/ka$ .

Its corresponding group path is

$$P_c = 4z_t . \quad (33)$$

The Frechet kernel (28) becomes, for this initial profile,

$$K(z) = -2/(1 - z/z_t)^{1/2} . \quad (34)$$

The corresponding once-integrated and twice-integrated Frechet kernels can be computed easily as

$$H(z) = \int_{z_t}^z K(z) dz = 4z_t(1 - z/z_t)^{1/2} \quad (35)$$

and

$$G(z) = \int_0^z H(z) dz = -(8z_t^2/3)[(1 - z/z_t)^{3/2} - 1] . \quad (36)$$

With (36) substituted into (19a), we obtain the solution  $x''(z)$ . Integrate the resulting expression twice, constrained by the boundary conditions (19b) and (19c), and we obtain

$$x(z) = -v(8z_t^2/3) \left[ \frac{4z_t^2}{35} \left(1 - \frac{z}{z_t}\right)^{7/2} - \frac{z^2}{2} + (z_t + 1)z + \left(\frac{3}{2z_t} - \frac{4z^2}{35}\right) \right]. \quad (37)$$

The Lagrange multiplier  $v$  in (37) is computed from

$$v = A^{-1}y \quad (38)$$

where  $y = P_c - P_m$  is the difference of time delay in a linear model profile (32) from that in a true parabolic profile (30) at frequency  $f$ , and  $A$  is computed from the expression

$$A = 16z_t^2 + (64/9)z_t^4 + (16/5)z_t^5 \quad (39)$$

by using formula (22). After knowing  $x(z)$ , it is then inserted in (29) to produce  $\delta N(z)$ . Computations can be repeated anew by using  $N(z) + \delta N(z)$  as the model profile, except now the corrected model profile is not necessarily linear so that a numerical scheme may have to be developed. One possibility is to use a piecewise linear model.

Let us now adopt some numerical values. We take, for the true (parabolic) profile  $Y = 100$  km,  $N_m \approx 10^{12}$  el/m<sup>3</sup>. Then at a frequency  $f = 8.693$  MHz, we obtain from (31)  $P_m \approx 400$  km. For the model (linear) profile, we take  $a = 1.25 \times 10^{10}$  el/m<sup>3</sup>/km, which gives  $P_c \approx 300$  km at the same frequency. This gives an error in group path of  $y = P_c - P_m = -100$  km. Substitute these numerical values in (37) to obtain  $x(z)$  which, when inserted in (29), gives us the perturbed  $\delta N(z)$  required to reduce the error. The results are shown graphically in Figure 1. It is seen that by using data only at one frequency, the once-iterated profile  $N_\ell + \delta N$  approaches the true profile  $N_p$  reasonably fast.

## 6. CONCLUSION

We have outlined in this paper a method whereby ionospheric profiles can be deduced from oblique sounding data. The method starts by assuming a guessed zeroth-order profile based on our past experience and the accumulated knowledge about the ionosphere. An iterative scheme has been worked out to enable us to improve the computed profiles until the errors are smaller than some specified value. As an illustration the method is applied to the vertical incidence case, which shows reasonably fast convergence. Encouraged by this success, we would like to suggest that more extensive numerical computations be carried out.

## ACKNOWLEDGEMENT

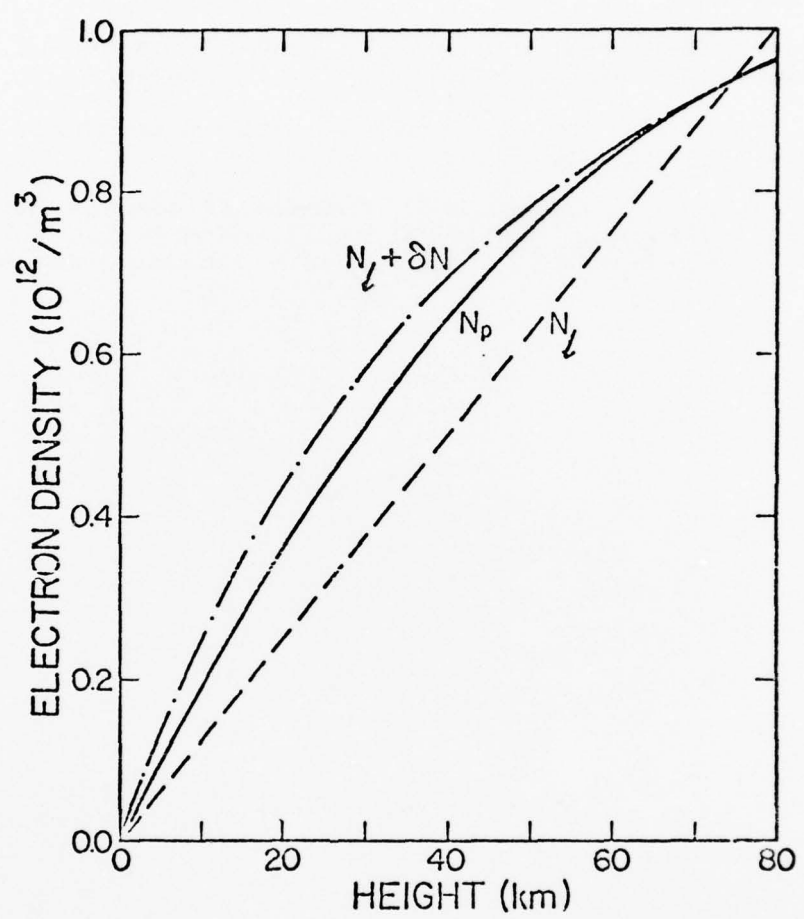
The major part of this research was carried out while K. C. Yeh was visiting the National Taiwan University with the support of the National Science Council, Republic of China. The work was finished at the University of Illinois with the support of the Deputy for Electronic Technology (RADC-ETEI), Hanscom AFB, MA, under Contract F19628-75-C-0088. Professor Yeh would like to express his appreciation to Professors T. S. Kuo and K. H. Pai of the National Taiwan University for their hospitality.

## FIGURE CAPTION

Figure 1. Illustrating convergence of the iterative procedure. The parabolic profile  $N_p$  is assumed to be the real profile. The linear profile  $N_l$  is the initial guess. The one-iterated profile is  $N_l + \delta N$ .

## REFERENCES

- Backus, G. E. and J. F. Gilbert (1967), Numerical application of a formalism for geophysical inverse problems, Geophys. J., 13, 247-276.
- Budden, K. G. (1961), Radio Waves in the Ionosphere, Cambridge University Press, New York.
- Davies, K. (1965), Ionospheric radio propagation, National Bureau of Standards Monograph 80, U.S. Government Printing Office, Washington, D. C.
- Green, W. R. (1975), Inversion of gravity profiles by use of a Backus-Gilbert approach, Geophysics, 40, 763-772.
- Johnson, L. E. and F. Gilbert (1972), Inversion and inference for teleseismic ray data, in Methods in Computational Physics, edited by B. A. Bolt, vol. 12: Seismology, Body Waves and Sources, pp. 231-266, Academic Press, New York.



## REFERENCES

- Booker, H. G., "Fifty years of the ionosphere. The early years - Electromagnetic theory", J. Atmos. Terr. Phys., 36, 2113-2136, 1974.
- Breit, G. and M. A. Tuve, "A test for the existence of the conducting layer", Phys. Rev., 28, 554-575, 1926.
- Croft, T. A. and H. Hoogasian, "Exact ray calculation in a quasi-parabolic ionosphere with no magnetic field", Radio Sci. 3, 69-74, 1968.
- Fletcher, R. and M. J. D. Powell, "A rapidly convergent descent method for minimization", Computer Journal, 6, 163-168, 1963.
- Manning, L. A., "The determination of ionospheric electron distribution", Proc. IRE, 35, 1203-1207, 1947.
- Rao, N. N., "Bearing deviation in HF transionospheric propagation, I. Exact computations for some ionospheric models with no magnetic field", Radio Sci. 3, 1113-1117, 1968.
- Rao, N. N., "Synthesis of three-dimensional oblique ionograms", Radio Sci., 8, 449-451, 1973.
- Rao, N. N., "Inversion of sweep-frequency sky wave backscatter leading edge for quasiparabolic ionospheric layer parameters", Radio Sci., 9, 845-847, 1974.
- Rao, N. N., "Analysis of discrete oblique ionogram traces in sweep-frequency sky wave high resolution backscatter", Radio Sci., 10, 149-153, 1975.
- Waynick, A. H., "Fifty years of the ionosphere: The early years--Experimental", J. Atmos. Terr. Phys., 2105-2112, 1974.